THE MODIFICATION OF SOLVENTS FOR LIQUID-LIQUID EXTRACTION PROCESSES

by

ADILAH BINTE ABDUL HAMID

A thesis submitted to
The University of Aston in Birmingham
for the degree of
Doctor of Philosophy

Department of Chemical Engineering
The University of Aston in Birmingham

January, 1983

The University of Aston in Birmingham

SUMMARY

THE MODIFICATION OF SOLVENTS FOR LIQUID-LIQUID EXTRACTION PROCESSES

Adilah binte Abdul Hamid PhD January 1983.

The ability to modify the efficiency of selected solvents in liquid-liquid extraction by the addition of small amounts of additives would offer advantages in extraction, solvent recovery and inventory costs. Therefore, the literature relating to desirable solvent properties, variations in solvent use, methods of determining, representing, interpolating, extrapolating and predicting liquid-liquid equilibria and the fundamentals of mass transfer has been critically reviewed.

The use of pro- and anti-solvents to modify the phase equilibria of ternary systems is well established but these compounds are added to influence the solubility curve. In a preliminary study of these effects, it was noticed that polar molecules affected the tie-lines more than the solubility. Therefore, in depth study of the ternary systems, namely: Acetone - Toluene - Water, Methanol - Xylene - Water and Isopropanol - Cyclohexane - Water were determined at 20°C. The Sulphuric Acid was added at 2% and 5% by weight. Significant tilting of the tie-lines was confirmed and the changes in the slopes of the distribution diagram favourably indicate solubility enhancement due to the salting effect.

The mass transfer was studied on a pilot scale Rotating Disc Contactor. The hydrodynamic behaviour of the R.D.C. was reviewed and established. The evaluated overall mass transfer coefficients suggested that the acid generally increased the values.

Key Words: Liquid-Liquid Equilibria
Polar Molecules
Rotating Disc Contactor
Overall Mass Transfer Coefficient

ACKNOWLEDGEMENTS

The author wishes to express her gratitude to Professor G. V. Jeffreys, the Head of Department of Chemical Engineering for providing the facilities for this research, for his invaluable supervision, his patience, encouragement and continued help and constructive criticism.

Sincere appreciation is felt for:

Dr. C. J. Mumford, for his interest and encouragement throughout this study,

The Laboratory and Technical Staff of the Department of Chemical Engineering for their assistance,

Ms S. Ellis and Ms S. Mehrali for their diligence in typing this thesis.

Last, but certainly not least, thanks are due to the Malaysian Public Services Department for financial aid, the University Malaya for granting the study leave and the author's mother and family for continual support throughout her studies.

CONTENTS

	Page No.
SUMMARY	i
ACKNOWLEDGEMENTS	ii
CONTENTS	iii
List of Tables	ix
List of Figures	x
CHAPTER ONE 'INTRODUCTION'	1
CHAPTER TWO 'LIQUID-LIQUID EXTRACTION'	
2.1 Introduction	5
2.2 Extraction Techniques	7
2.2.1 Ternary Systems	9
2.2.2 Special Features of Ternary Systems	14
2.2.2.1 Solutropy	14
2.2.2.2 Isopycnic	14
2.2.2.3 Isoptic	15
2.3 System Selection	18
2.4 Solvent Selection	18
2.4.1 Cost	20
2.4.2 Selectivity	21
2.4.3 Distribution Coefficient	24
2.4.4 Solvent Stability	27
2.4.5 Density	27
2.4.6 Capacity	27

Page No.

2.4.7 Recoverability 28

2.4.8 Other Physical Properties 28

Corrosiveness 28

Viscosity 28

Vapour Pressure 29

Freezing Point 29

Flammability 30

Toxicity 30

2.4.9 Specific Interactions in Solution 30

2.5 Equipment Selection 39

CHAPTER THREE 'THE MODIFICATIONS OF LIQUID-LIQUID EXTRACTION PROCESSES' 47

3.1 Use of Reflux 48

3.1.1 Methods to Provide Extract Reflux 51

3.1.2 Feasibility of Reflux 52

3.2 A Change in Pressure 53

3.3 A Change in Temperature 53

3.4 Dual Solvents 55

3.5 Mixed Solvents 57

3.5.1 Application of Mixed Solvents 58

3.6 Modified Solvents 60

3.6.1 Active Constituents

i) Salting Agents 60

ii) Anti-solvents 61

iii) Pro-solvents 63

3.6.2 Diluents 64

3.6.3 Practice and Limitations 64

Page No.

CHAPTER FOUR 'LIQUID-LIQUID EQUILIBRIA'

4.1 Introduction 66

4.2 Experimental Determination 67

4.2.1 Determination of Two Phase Equilibria 68

a) Analysis Method 69

b) Titration Method 71

4.3 Thermodynamic Basis of Liquid-Liquid Equilibria 72

4.3.1 Thermodynamic Models for LLE 75

4.3.1.1 Models for Activity Coefficients 75

4.3.1.2 Equation of State 82

4.3.2 Group Contribution Models 82

4.3.2.1 UNIFAC Group Contribution 83

4.4 Representation of LLE Data 84

4.4.1 Tie-line Correlation Methods 86

4.4.1.1 Graphical Methods 88

4.4.1.2 Empirical Methods 90

4.4.2 Estimation of Plait Points 94

4.4.3 Graphical Stagewise Analysis 95

i) Difference Point Method 95

ii) Distribution Coordinate Method 101

iii) Solvent-free Coordinate Method 102

CHAPTER FIVE 'MASS TRANSFER IN LIQUID-LIQUID EXTRACTION'

5.1 Introduction 105

5.2 Mass Transfer To and From Drops 109

5.2.1 Mass Transfer During Drop Formation 109

5.2.2 Mass Transfer During Drop Release 110

Page No.

5.2.3 Mass Transfer in the Dispersed Phase 111

5.2.4 Mass Transfer in the Continuous Phase 112

5.2.5 Mass Transfer During Coalescence 113

5.3 The Overall Mass Transfer Coefficient 114

5.4 Application of Droplet Models to Practical Extraction 115

5.5 Droplet Phenomena 116

5.5.1 Effect of Impurities or Surface Active Agents 122

5.5.2 Effect of Mass Transfer 124

CHAPTER SIX 'ROTATING DISC CONTACTOR'

6.1 Introduction 126

6.2 Construction 128

6.3 Mode of Operation 130

6.4 Modified R.D.C. 131

6.5 Hydrodynamic Characteristics 133

6.5.1 Flooding 133

6.5.2 Hold-up 135

6.5.3 Backmixing 139

6.5.4 Drop Size 142

6.5.5 Drop Size Distribution 147

6.6 Mass Transfer in R.D.C. 148

CHAPTER SEVEN 'EXPERIMENTAL INVESTIGATIONS'

7.1 Experimental Approach 154

7.2 Determination of Phase Equilibria 155

Page No.

7.2.1 Determination of Mutual Solubility Curve 151

7.2.2 Determination of Tie-lines 160

7.2.3 Analytical Techniques 162

7.2.4 Confirmatory Chemical Tests 162

7.3 Experimental Investigations on a Pilot-Scale Rotating Disc Contactor 163

7.3.1 Chemical System 172

7.3.2 Cleaning Procedure 174

7.3.3 Preparation of Fluid System 175

7.3.4 Hydrodynamic Studies 175

7.3.4.1 Flooding 176

7.3.4.2 Dispersed Phase Hold-up 178

7.3.4.3. Photography and Associated Techniques 179

7.3.5 Mass Transfer Studies 180

7.3.5.1 Operating Procedure 180

CHAPTER EIGHT 'DISCUSSION OF RESULTS'

8.1 Liquid-Liquid Equilibria Studies 182

i) Acetone-Toluene Water 183

ii) Propan-2-ol-Cyclohexane-Water 184

iii) Methanol-Xylene-Water 184

8.2 Extraction Studies of the Pilot-Scale Rotating Disc Contactor 200

8.2.1 Non-mass Transfer Studies 200

8.2.1.1 Flooding Phenomena 200

8.2.1.2 Dispersed Phase Hold-up 204

8.2.1.3 Drop Size 208

Page No.

8.2.1.4 Drop Size Distribution 210

8.2.2 Mass Transfer Studies 214

8.2.2.1 Experimental Mass Transfer Coefficient 215

8.2.2.2 Theoretical Mass Transfer Coefficient 216

8.2.2.3 Discussion of Results 220

CHAPTER NINE 'CONCLUSION' 224

CHAPTER TEN 'RECOMMENDED FUTURE WORK' 227

APPENDICES

I Physical Properties of Systems 231

II Experimental LLE Data 242

III Chemical Confirmatory Tests 286

IV (i) Sample Calculation for Approach to Equilibrium 290

(ii) Sample Calculation for Rotor Speed Requirement 292

V Sample Calculation for Thermodynamic Consistency Test 295

VI Sample Calculation for Drop Size and Drop Size Distribution 303

VIII Sample Calculation for Experimental and Theoretical Overall Mass Transfer Coefficient 315

NOMENCLATURE 323

REFERENCES 334

LIST OF TABLES

Table No.	Title	Page No.
2.1	Classification of Industrial Extraction Techniques	8
2.2	Important Solvent Properties	8
2.3	Classification of Liquids by Ewell	33
2.4	Summary of Deviations from Raoult's Law	35
2.5	Gilmont-Zudkevitch-Othmer Grouping of Field Factors	37
2.6	Solute-Solvent Group Interactions	38
4.1	Activity Coefficient Models for Correlating Liquid-Liquid Equilibria	76
7.1	R.D.C. Dimensions	165
8.1	Interpolated Data for System: Acetone-Toluene-Water	187
8.1 (contd.)	Interpolated Data for System: Propan-2-ol-Cyclohexane-Water	188
8.2	Othmer-Tobias' Correlation	189
8.3	Hand's Correlation	190
8.4	Flooding Data	204
8.5	Dispersed Hold-up	207
8.6	Mass Transfer Results (N=500 r.p.m.)	221
8.7	Mass Transfer Results (N=700 r.p.m.)	222
8.8	Experimental and Theoretical Overall Mass Transfer Coefficients.	223

LIST OF FIGURES

Figure No.	Title	Page No.
2.1	Types of Ternary Systems	11
2.2 (a)&(b)	System with and without Critical Solution Temperature	12
2.2 (c)	Conversion of Type I to Type II System	12
2.3	Analysis of Ternary Systems	16
2.4	Extraction Process	19
2.5	Effect of Different Solvents on Solute Distributions	19
2.6	Classification of Commercial Extractors	44
2.7	Selection Guide for Extraction Devices	46
3.1	Analogy between Reflux in Extraction and Rectification in Distillation	49
3.2	Comparison between Type II and Type I Systems on Application of Reflux	49
3.3	Effect of 'Opening Out' a Type I System	54
3.4	Separation of Fission Products (Use of Dual Solvents)	54
3.5	Effect of Anti-Solvent on Phase Equilibria	62
3.6	Effect of Temperature Variations on Phase Equilibria	62
4.1	Equilibrium Distribution Diagram	85
4.2	Selectivity Diagram	85
4.3	Right-Triangular Diagram	85
4.4	Janecke Diagram on Solvent-free Coordinate	87
4.5	Distribution Curve on Solute-free Basis	87
4.6	External Construction for Tie-line	89

Figure No.	Title	Page No.
4.7	Internal Construction for Tie-line Interpolation	89
4.8	Tie-line Correlation on Rectangular Diagram	89
4.9	Campbell's Correlation	91
4.10	Brancker's Correlation	91
4.11	Treybal's Method of Plait Point Estimation	96
4.12	Difference Point Method for Stagewise Analysis	96
4.13	Approximation Method for Stagewise Analysis	99
4.14	Analytic-Graphic Method for Stagewise Analysis	99
4.15	Right Triangular Diagram) Distribution) Coordinate) Method	103
4.16	Equilibrium Diagram) Method	
4.17	Solvent-free Coordinate Method	103
6.1	R.D.C. Power Input Group Operating Range	143
6.2	Typical Flow Patterns in an R.D.C.	143
7.1	Smith-Bonner Cell	156
7.2	Smith-Bonner Cell and its Ancillary Parts	158
7.3	Arrangement of the Cells and the Temperature Controlling Unit	159
7.4	Pilot Scale Rotating Disc Contactor	164
7.5	Schematic Flow Diagram of the Pilot Scale Rotating Disc Contactor	166
7.6	Constructional Details of Middle of Column	167
7.7	Constructional Details of Bottom of Column	168
7.8	Constructional Details of Top of Column	170

Figure No.	Title	Page No.
8.1	Interpolated Equilibrium Diagram for System: Acetone-Toluene-Water	191
8.2	Othmer-Tobias Correlation for Systems Acetone-Toluene-Water	192
8.3	Hand's Correlation System: Acetone-Toluene-Water	193
8.4 (a)	Distribution Diagram for System: Acetone-Toluene-Water	194
8.4 (b)	Extrapolated Distribution Diagram for System: Acetone-Toluene-Water	195
8.5	Interpolated Distribution Diagram for System: Propan-2-ol-Cyclohexane-Water	196
8.6	Othmer-Tobias Correlation for System: Propan-2-ol-Cyclohexane-Water	197
8.7	Hand's Correlation for System: Propan-2-ol-Cyclohexane-Water	198
8.8	Experimental Distribution Diagram for System: Propan- 2-ol-Cyclohexane-Water	199 199
8.9	Experimental Flooding Curves	202
8.10	Correlation of Flooding Data using Equation (8.4)	203
8.11	Experimental Dispersed Phase Hold-up and Al-Aswad's Correlation	206
8.12	Typical Photograph used for Drop Size Measurements	209
8.13	Comparison of Experimental and Predicted Upper Limit Drop Size Distribution at 500 r.p.m.	211

CHAPTER one 1

INTRODUCTION

The large scale industrial application of liquid-liquid extraction dates from the early 1930s, when it answered the need for a method of removing aromatic hydrocarbons from the kerosene fraction during oil refining. Its use spread to other industrial organic processes and since then it has found ever-increasing application in the coal-tar industry, petrochemical industry, pharmaceutical industry, metals extraction, industrial inorganic processes and waste disposal treatment.

In recent years, a number of changing factors have had a marked effect on liquid-liquid extraction processes and will continue to influence them in the future. New technological improvements are sought to produce maximum yields and overall process economy. Some excellent research of a fundamental nature which throws considerable light on the mechanism of solvent extraction has been carried out. Such work, e.g. the study of single drop mass transfer, efficiency of specific equipment designs, axial mixing models et cetera, has markedly altered our concept of what is actually accomplished by extraction;

but there is room for a considerable expansion of effort in this direction, notwithstanding the complexity and analytical difficulties of the problem. It seems highly probable that fundamental work aimed at placing the mechanism of liquid-liquid extraction on a sound scientific basis will lead to further development of the process, or the development of new processes to work in conjunction with liquid-liquid extraction for the production of improved yields and reduction in process costs. However, the economics of liquid-liquid extraction depend greatly upon the solvent properties, the inventory needed and the ease of recovery of solute and solvent from the extract and raffinate streams. Thus, any development which improves solvent selectivity or any other desirable physical properties would be of considerable industrial significance. Developments in physical chemistry, for example, have increased the knowledge of solute-solvent interactions considerably so that the selection of solvents are done scientifically instead of by trial as in the past.

Many fascinating separations are done first in laboratory for reasons of analysis and these become of interest industrially when one of the substances so separated becomes important, and engineers frequently evaluate both the technical and the economical aspects of small-scale operations for possible industrial exploitations.

In an investigation of the esterification of butanol with acetic acid, the phase equilibria of the quarternary

liquid system n-butanol, acetic acid, water and n-heptane was determined (1) and it was noticed that the presence of acetic acid or/and sulphuric acid had a marked effect on the distribution ratio of n-butanol due to the salting effect of these polar molecules. Therefore, it was considered worthwhile to investigate whether similar effect can be found in other liquid-liquid systems. Ternary systems are by far the most frequently found in industrial applications and easiest to determine and thus the systems selected were all ternary systems namely Acetone-Toluene-Water, Methanol-Xylene-Water and Isopropanol-Cyclohexane-Water. These were chosen not because of any commercial significance but as mere representations and among other advantages easy to analyse, safe to handle, relatively inexpensive and at the chosen temperature, i.e. 20^{o}C, gives a significantly large heterogeneous area under the solubility curve, thus allowing a wide range of solute concentrations to be studied.

The use of dual or mixed solvents, examples of their industrial applications, their practice and limitations are discussed in Chapter 3. However, the intention in this work was to study the effect of relatively small amounts of additives, i.e. below 5% by weight.

Methods to evaluate, represent, interpolate, extrapolate and predict liquid-liquid equilibria are reviewed in Chapter 4.

The phase equilibria results from the system Acetone-Toluene-Water was applied in the mass transfer study on a pilot scale Rotating Disc Contactor (R.D.C.) as it is a representative of the best type of continuous differential contactor for liquid-liquid extraction. The hydrodynamic behaviour of the 50 mm, 50 compartments, 125 cm high R.D.C. (2) was established and its performance compared to some of the existing empirical correlations reviewed in Chapter 6.

Fundamentals of mass transfer are reviewed in Chapter 5 and the models were used in evaluating the overall mass transfer coefficient from the mass transfer experiments.

CHAPTER two 2

LIQUID-LIQUID EXTRACTION

2.1 INTRODUCTION

Liquid-liquid extraction, commonly termed liquid extraction or solvent refining, is a widely used method of separation, both in the laboratory and on a plant scale. The operation was first used on a large scale by Edeleanu in 1908 in the removal of aromatic hydrocarbons from kerosene (3,4) and was later used on the refining of lubricating oils and waxes (5). Considerable developments have occurred in the last seventy years and liquid extraction is now one of the most important techniques for the physical separation and refining of mixtures of liquids. Most developments have taken place in the fields of petroleum refining and uranium extraction, and to a lesser extent, in the final stages of antibiotics manufacture, particularly in the extraction of penicillin (5).

Commercially, the petroleum industry is the largest user (6) of liquid-liquid extraction operations. The largest equipment, the highest number of extractors, the greatest variety of extraction processes and the largest amount of feed material are used in this industry. Nowadays, only primary separation of crudes or cracked products is

achieved by distillation. Separation of close boiling range fractions by means of chemical reaction utilizing a reagent has been found impracticable. Separation by liquid extraction, in which the solvent dissolves various compounds without chemical reaction, thus permitting complete solvent recovery, offers distinct advantages. Liquid extraction has played an important role, mainly in hydrocarbon separation, e.g. involving kerosene, lubricating oils and the lighter napthas and in desulphurization of petroleum products.

Liquid extraction is a mass transfer operation which relies upon differential solubility between the components of a mixture and a third component. It involves the partition of components between two immiscible liquid phases, one of which is added as a solvent. It differs from other separation methods in which an equilibrium distribution is created by the addition or withdrawal of heat e.g. distillation, evaporation or crystallisation. It is, therefore used for the separation of close boiling liquids, liquids of low relative volatility, as a substitute for expensive thermal processes such as evaporation, for the separation of heat sensitive materials and mixtures which form azeotropes and as a substitute for chemical process involved in the recovery of metals. In the latter example, the reduced energy consumption is one factor which makes liquid extraction attractive (7).

Among many other advantages, extraction is chosen due to the comparative simplicity of the equipment, its ease of

operation and control, and the generally wide choice of solvents available as extractive agents. The process does, of course, involve the consumption of energy since every extractive plant is invariably accompanied by stripping columns to recover the solvent from the extract and raffinate streams. This duty generally involves distillation or evaporation and this installation introduces additional capital and operating costs. Also, use of the most efficient solvent for the required separation may necessitate expensive materials of construction.

A major factor determining the success or otherwise of a liquid extraction process is the correct choice of solvent. Many considerations have to be made; in engineering, for a successful system all the relevant properties of the solvent system and ways to improve certain properties must be reviewed.

2.2 EXTRACTION TECHNIQUES

Separation of the components of a mixture by application of liquid-liquid extraction can be brought about in a variety of ways. The techniques used industrially can be classified depending upon the type of solvent system and the physical arrangement of the equipment. This is summarised in Table 2.1.

Phase equilibria may be classified according to the nature and number of the solvents, as:

i) Three component systems (Ternary): one solvent,

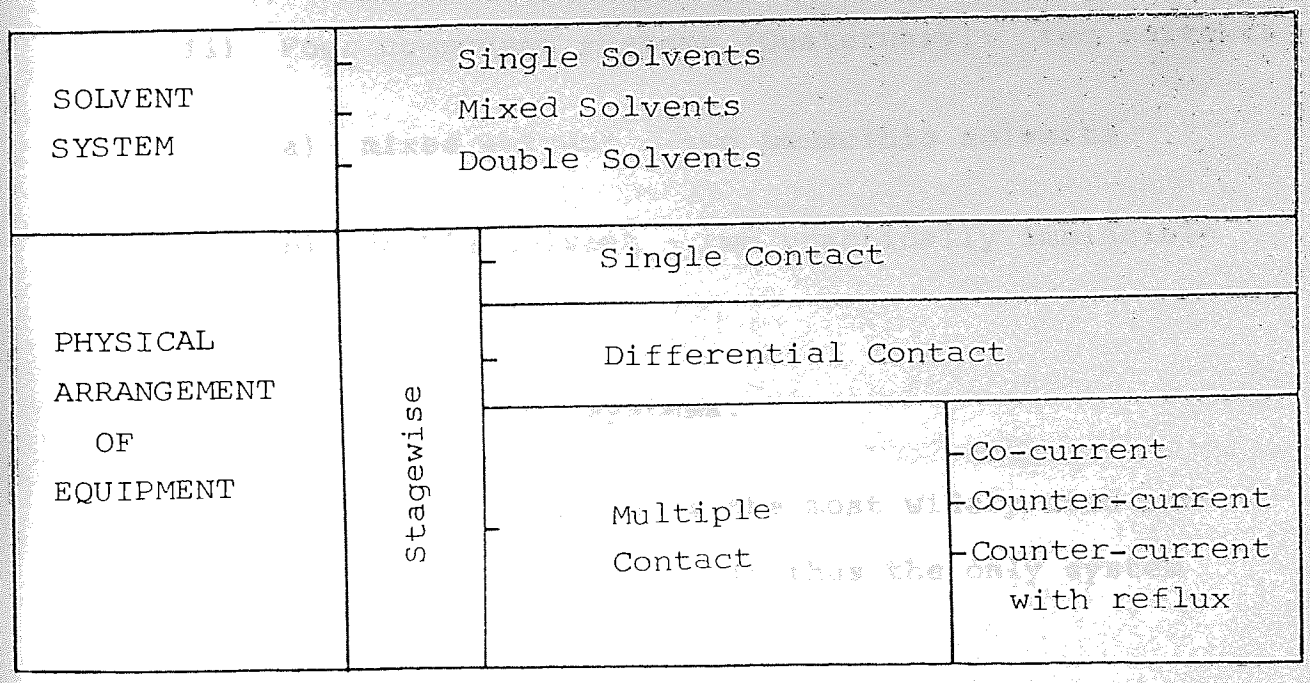

Table 2.1 : Classification of Industrial Extraction Techniques.

Cost
Equilibrium Data
Selectivity
Solubility
Loading Capacity
} Thermodynamic Data
Reaction Kinetics
Recoverability
Stability
Density, ρ : $\rho = f(C)(T)$
Interfacial Tension, σ : $\sigma = f(C)$
} Physical Data
Viscosity
Toxicity
Inflammability
Vaporisation - Losses
Pollution Hazard

Table 2.2 : Important Solvent Properties.

ii) Four component systems (Quaternary): two solvents

a) mixed solvent - two immiscible solvents

b) double solvent - two practically immiscible solvents

iii) Multicomponent systems.

The first classification is the most widely used and also the easiest to study and it is thus the only system studied in this work.

Operations with most ternary systems use a single solvent system, i.e. separation is achieved at a convenient temperature and pressure using only one solvent which may be pure or modified. Modified solvents consist of a solvent solution of at least two components, one of which is added either to increase or decrease the solubility. In processes using double solvent systems, solutes are distributed between two immiscible or partially miscible solvents. In the Duosol process, which is the outstanding example of the commercial application of double solvents, a mixture of phenol and cresylic acid is used as the selective solvent and propane acts both as a diluent to reduce the viscosity of the lubricating oils being extracted and as a precipitant of the asphaltic constituents (5).

2.2.1 TERNARY SYSTEMS

Ternary systems are classified according to the immiscibility between the components. Equilibrium data

are generally represented on triangular coordinates. Each coordinate represents the composition in terms of each component; solute, carrier liquid and solvent. Any point on or within the triangle represents a mixture of known composition. The type of equilibrium curve representing the compositions of the saturated liquid phases at equilibrium at a constant temperature is different in each system. Each triangle in Figure 2.1 illustrates the ternary systems. Type I and Type II systems are of particular relevance to liquid-liquid extraction.

The Type I system is the most common; in this system there is one partially immiscible pair. The solubility curve for this type is shown in Figure 2.1 (a). The solute C is completely miscible in solvent B and the carrier liquid A, whereas A and B are partially miscible in each other. Any mixture represented by a point below the solubility curve will form two immiscible phases which have compositions at the ends of the tie line passing through that point. In Figure 2.1 (a) the point I represents a composition which will produce two phases of compositions G and H. GH is the tie-line through I. An infinite number of tie-lines can be drawn in the area beneath the equilibrium curve; these lines are not parallel and usually have changing slopes. At the plait point, P, where the critical conditions forms, there is only one phase. Since the solubility of solute C in A and B varies as temperature changes, the shape of the curve is temperature dependant. In some cases, there is no critical solution temperature and the isotherms of the equilibrium curve are shown in Figure 2.2 (a).

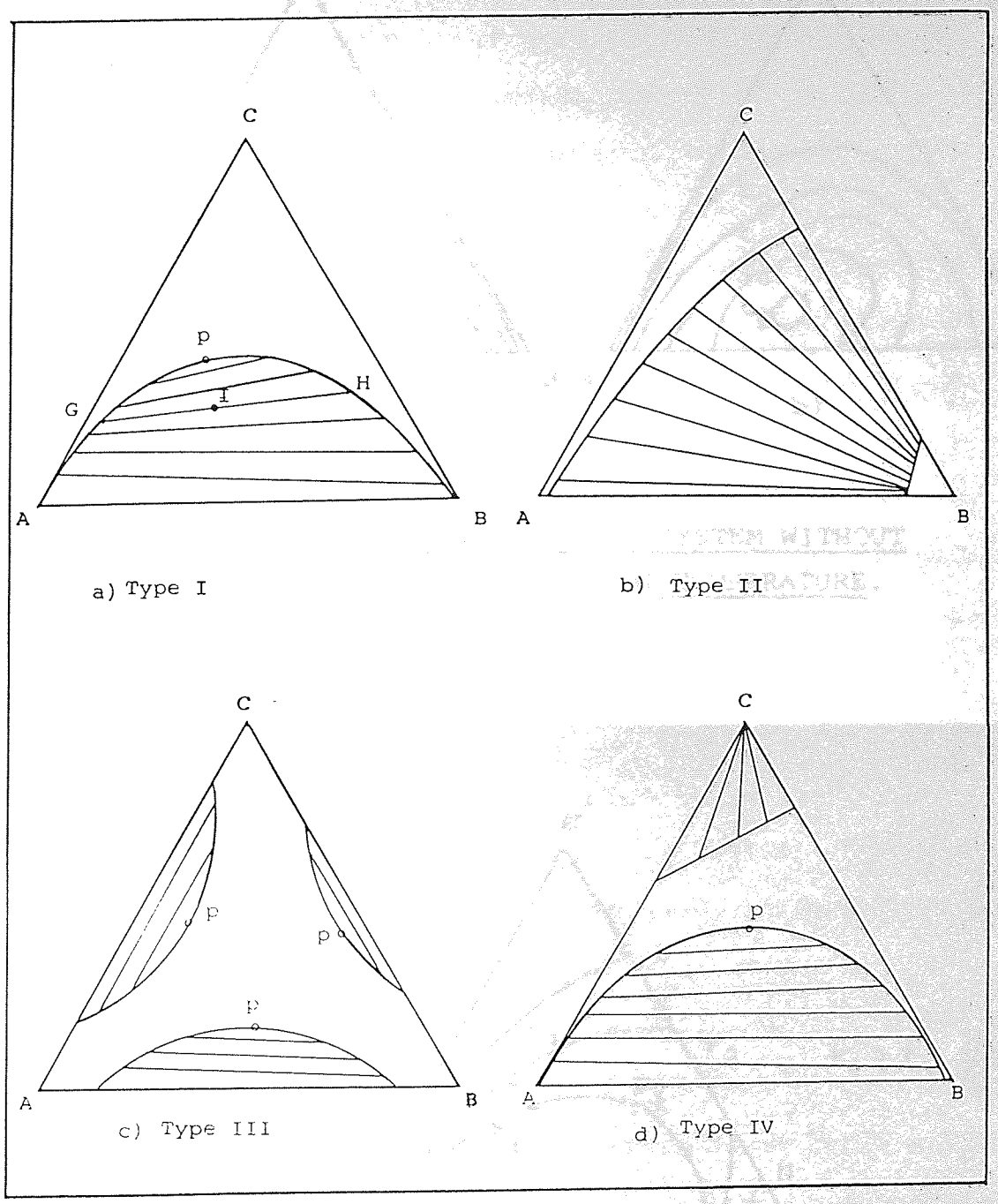

Figure 2.1 : Types of Ternary Systems.

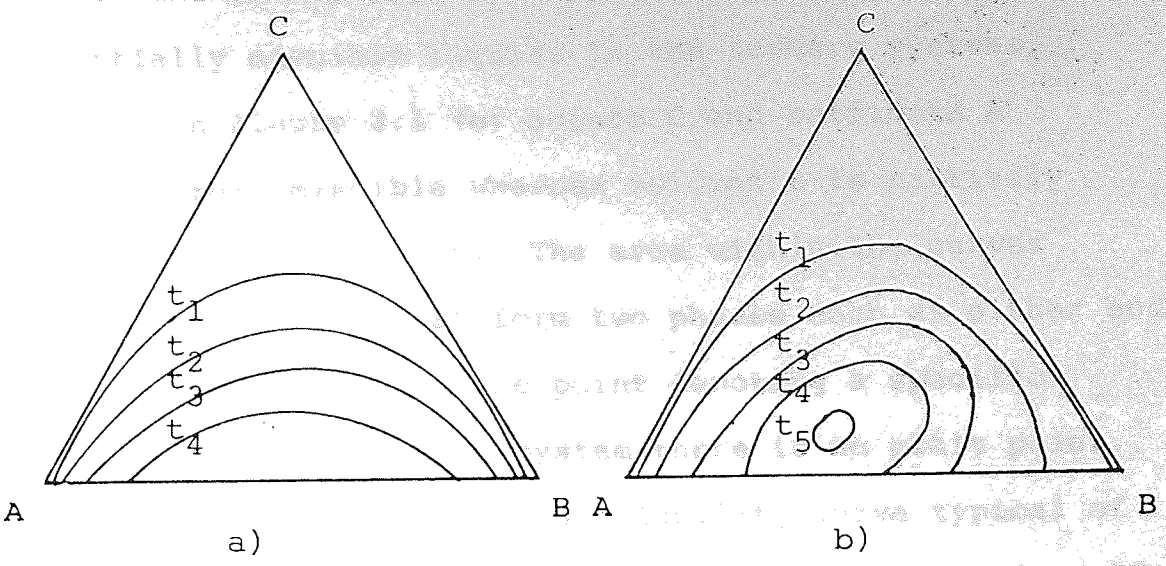

Figure 2.2 : b) SYSTEM WITH AND a) SYSTEM WITHOUT CRITICAL SOLUTION TEMPERATURE.

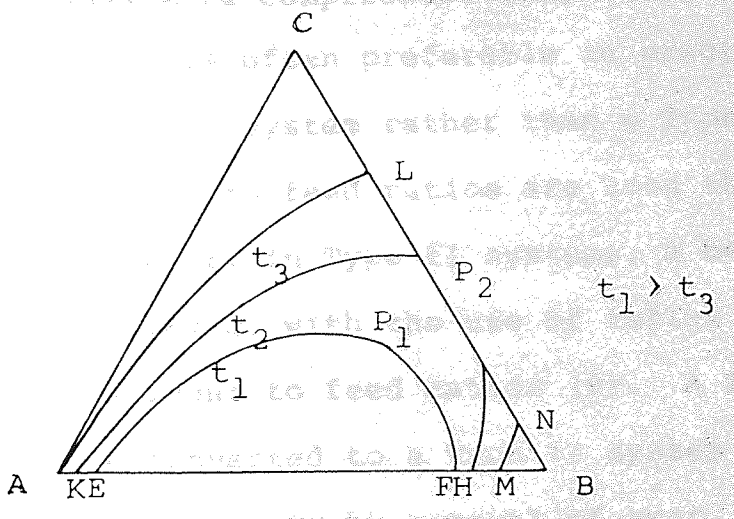

Figure 2.2 : c) CONVERSION OF TYPE I TO TYPE II SYSTEM.

Curve EP_1F represents a Type I system

Curve KL-NM represents a Type II system.

In the case of Type II system, there are two pairs of partially miscible liquids in the ternary systems. As shown in Figure 2.1 (b) solute C and raffinate A are completely miscible whereas solvent B is partially miscible in both A and C. The area within the curves represents mixtures that form two phases each at either end of the tie-line through the point denoting a specific mixture. Unlike a Type I system there is no plait point. A ternary system exhibiting a solubility curve typical of a Type I system at one temperature can change to a Type II system at another lower temperature. For example, by reference to Figure 2.2 (c), at t_3 there are two pairs of partially miscible liquids whereas at t_1 there is only one. Hence the system is converted to one characteristic of Type II system by reducing the temperature from t_1 to t_3. In some cases more complicated temperature changes occur (8). It is often preferable in practice to operate with a Type II system rather than a Type I system. Smaller solvent to feed ratios are used than in Type II systems. However, in Type II systems, a better extraction can be achieved, with the use of reflux without employing high solvent to feed ratios (9). A Type I system may also be converted to a Type II system by the addition of an anti-solvent or by removal of heat.

In Type III system, all three pairs of components in the ternary system are partially miscible in one another. This phenomena occurs very rarely. Normal extraction processes are not able to separate systems of this type.

Type IV systems are those which involve the formation of a solid phase. Only a few of this type, such as the ternary systems aniline-iso-octane-napthalene and methyl-ethyl-ketone-water-calcium carbonate, are of importance for liquid extraction (9).

2.2.2 Special Features of Ternary Systems

2.2.2.1 Solutropy

In general, the slope of the tie-lines and the magnitude of the selectivity are functions both of composition and of temperature, but in some ternary systems, the slope of the tie-lines changes sign isothermally:- this phenomena is termed solutropy (10), and a solutropic system is not necessarily an azeotropic system (11). Solutropy frequently disappears when the concentrations are computed in moles rather than in weight fractions, especially when one of the constituents is water, but not always (12).

2.2.2.2 Isopycnic Tie-lines

In the application of liquid extraction, rapid and complete separation of the raffinate and extract phases; after contacting, is highly desirable especially when mechanical agitation is employed to increase the surface available for mass transfer. This separation depends upon the density difference between the dispersed and the continuous phases, interfacial tension, viscosity, droplet size and other factors. In some systems, a tie-line connects equilibrium phases with the same density and is termed an isopycnic tie line: the separation of the phases

is then difficult and very slow (13, 14, 15).

2.2.2.3 Isoptic Tie-lines

A few ternary systems have been reported in which conjugate phases have the same refractive index, leading to some difficulty in observing the interface when determining equilibrium data (13).

2.3 SYSTEM SELECTION

Since the solvent is always recovered the analysis of an extraction system is best made by considering the solutions after solvent removal (solvent-free basis). On a three-coordinate diagram this is easily managed by carrying the composition of each layer on the diagram back along a line running from the solvent apex through the composition point to the base opposite the solvent apex. This then represents the enrichment (extract) and depletion (raffinate) obtained.

Let us consider a system with one partially immiscible pair and see what is required to make a good extraction system. In the diagrams, C is the solute, and it will be assumed that the solution to be extracted is a mixture of A and C, represented by F in Figure 2.3.

The questions are whether B is a good solvent and whether this is a practical extraction system. Two things must be considered: the maximum possible enrichment of solute in the extract and the number of stages required to affect the extraction.

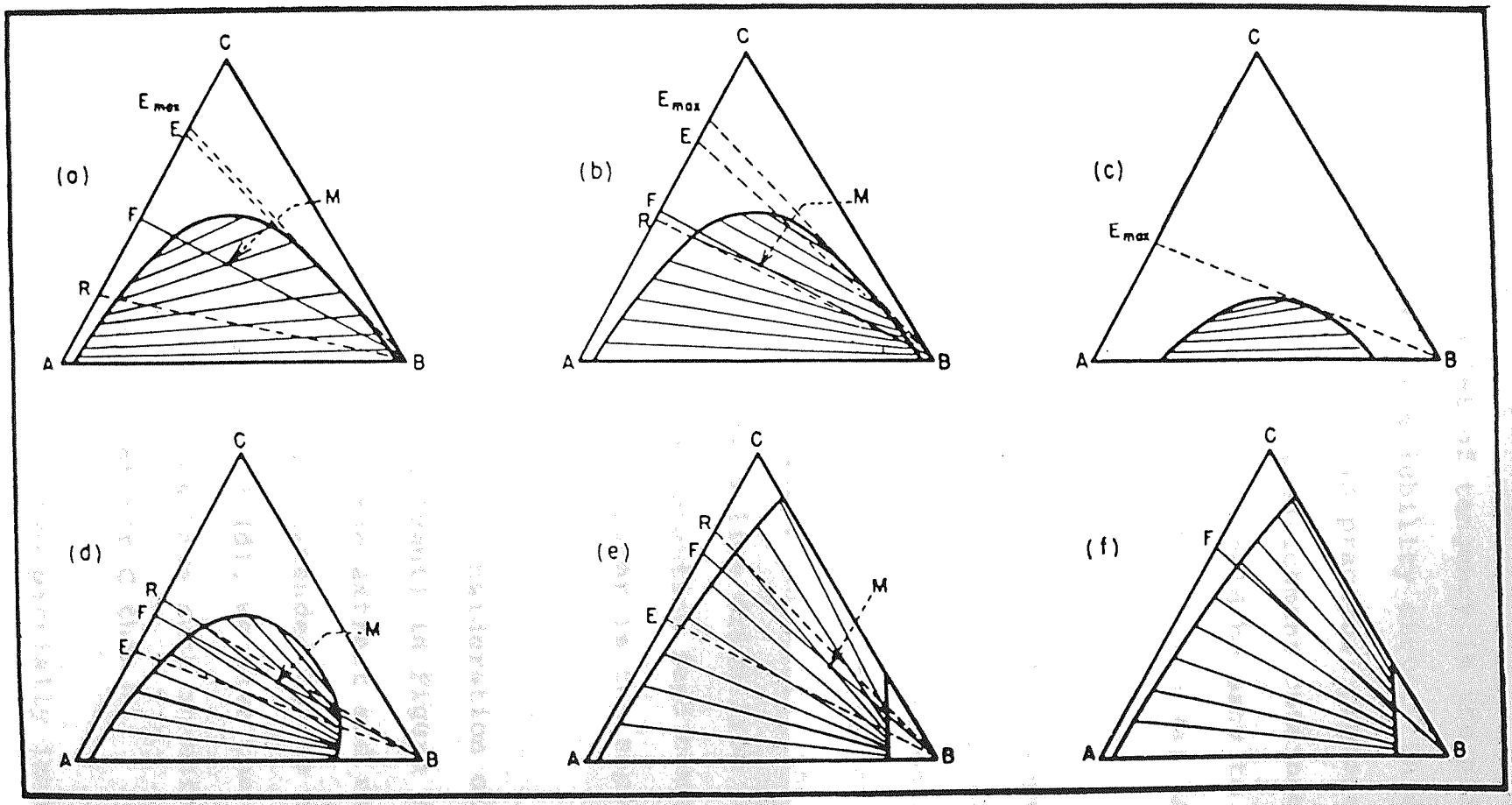

Figure 2.3 : Analysis of Ternary Systems.

The maximum enrichment of solute C can be obtained by drawing a tangent to the solubility curve from the solvent apex B. The point of tangency is the point of highest ratio of C to A on the solubility curve. This ratio may not be reached easily in practical process, but it does represent the maximum enrichment obtainable using this extraction system. It should be easy to see that a curve of the type shown in Figure 2.3 (a) is much to be preferred to that shown in Figure 2.3 (c).

The other consideration involves the slope of the tie-lines. Although most analyses are made on the basis of counter-current extraction, these systems can be judged quantatively by considering only a single contact and separation stage. In general, the larger the angle between the tie-lines and a line drawn from the solvent apex through the point representing feed composition in the two phase region, the greater is the separation of extract and raffinate.

This is illustrated by a consideration of the over-all composition M (feed plus solvent) in Figure 2.3 (a), (b) and (d). The solvent-free extract and raffinate are shown by the points E and R extended to the side of the triangle AC. In Figure 2.3 (d), we have the extreme case in which the tie-lines have such an unfavourable slope that A is a better solvent for C than B.

A system consisting of two partially immiscible pairs is shown in Figure 2.3 (e) and (f). In such a system B is the solvent for either A or C, depending on the

slopes of the tie-lines. All enrichments of A or C are theoretically possible in this system.

The system in Figure 2.3 (e) gives reasonable enrichment of A per stage. In Figure 2.3 (f), the angle between the tie-lines and a line drawn from the solvent apex through the two-phase region is very small, and is a much less satisfactory system.

Other types of systems can be analysed qualitatively using similar methods. There exist, however, many unusual liquid systems whose analyses require a more exact and quantitative approach. It should be fully understood that counter-current flow, ratio of feed to solvent, and use of reflux, all have a great influence on the exact way a liquid-liquid extraction will function. Hence, the final analysis must be made by calculating the number of the theoretical stages needed for a particular process. Such methods are demonstrated in detail by Perry (36) and Treybal (24).

2.4 SOLVENT EXTRACTION

Liquid-liquid extraction involves a minimum of two operations: extraction and solvent recovery as illustrated in Figure 2.4. Technical and economic factors both influence the choice of solvent or solvents employed to affect a particular separation and it is frequently impossible to satisfy all the desirable factors simultaneously. Therefore, in practice a compromise is necessary.

Major factors to be considered in the selection of

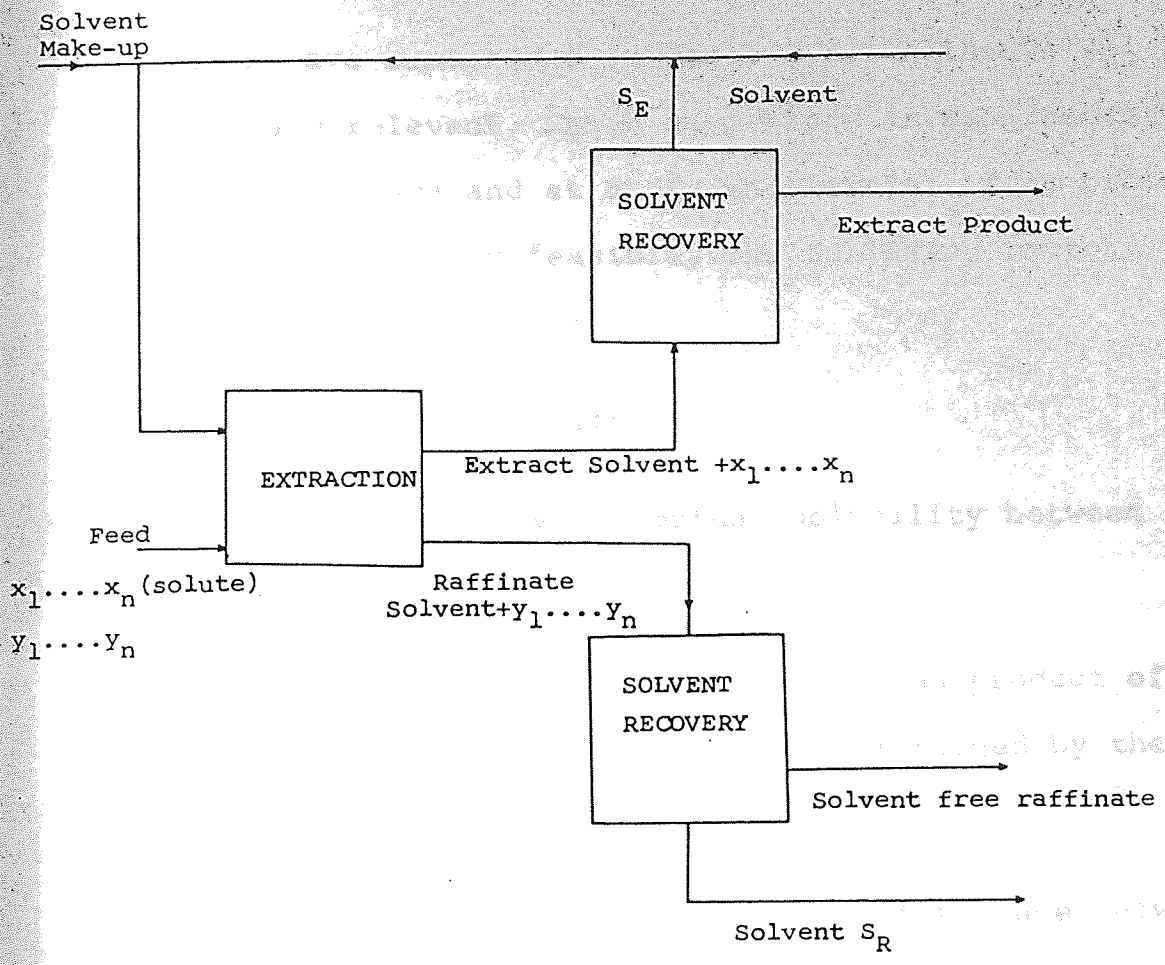

Figure 2.4 : Extraction Process.

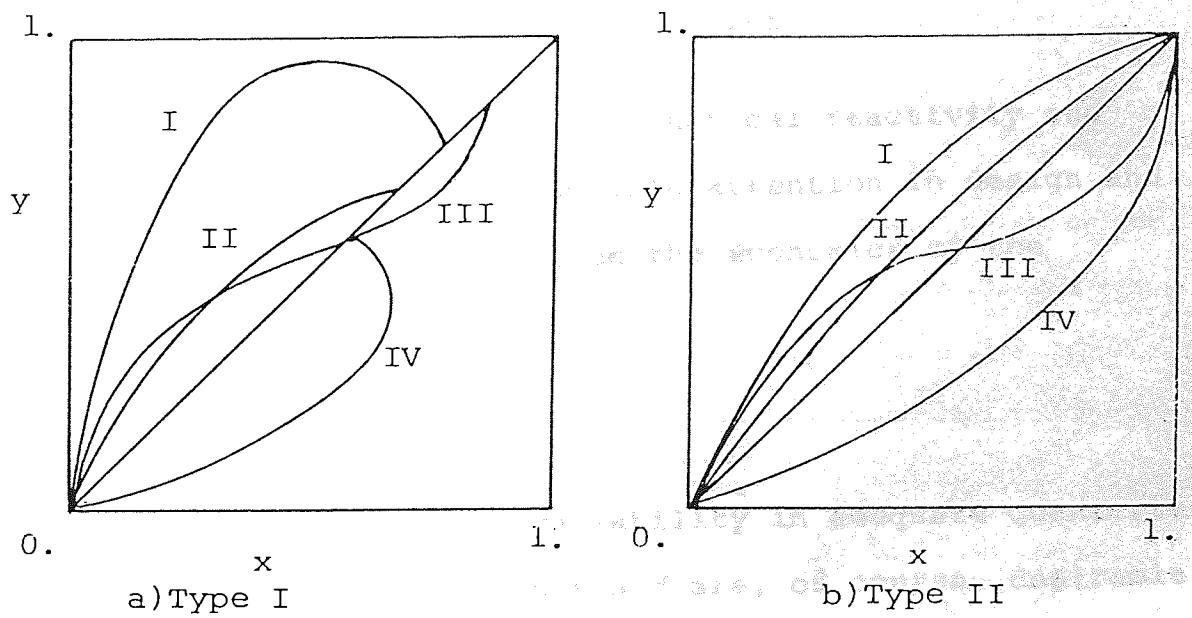

Figure 2.5 : Effect of Different Solvents on Solute Distributions.

a solvent are summarised in Table 2.2. Although all these factors are relevant, their importance is manifested in different ways and at different levels. If a process is to be technically feasible, the following factors (18) should be satisfied:

i) high selectivity,

ii) sufficiently low mutual solubility between solvents employed,

iii) easy recovery of the solvent and product of separation i.e. solute (this is often attained by the use of a high boiling solvent),

iv) a sufficiently high density difference between phases,

v) an interfacial tension allowing economic dispersion and coagulation of phases, and

vi) high rates of mass transfer.

Inflammability, toxicity, chemical reactivity and corrosiveness merit considerable attention in design and all factors have a bearing on the economics of the extraction.

2.4.1 Cost

Low cost and ready availability in adequate quantities usually parallel each other and are, of course, desirable solvent attributes. Although it is true that solvents are recovered from product solutions, nevertheless, make-up solvent to replace inevitable losses must be expected.

Furthermore, large quantities of expensive solvents that are retained in the plant represent sizeable sums invested. Interest on such money is chargeable directly to the process.

2.4.2 Selectivity

The selectivity of a solvent is probably the most important technical factor and it is certainly the first to be considered in the selection of a solvent.

In Figures 2.5 (a) and (b), curve I shows the solute distribution obtained with a selective solvent, curve III shows 'azeotropy' i.e. a reversal of selectivity and curve IV is obtained if the solute favours the raffinate or A-rich phase throughout the extraction, that is, the selectivity of A for C is greater than that of B for C. When considering a set of experimental distribution data, it must always be decided which is more selective solvent, A or B. The operating temperature has a considerable influence on the mutual solubility but its effect on the selectivity, which is a ratio of equilibrium concentrations, is much smaller and if a solvent is insufficiently selective or 'azeotropic' at one temperature, it is unlikely to be selective at a temperature 20^{o} different from the first. The selectivity of a solvent tends to increase slightly as the temperature falls and to decrease as the concentration of solute rises at constant temperature, but it is not possible to generalise quantitatively. In general, a solvent is selected to give the type of distribution shown in curve I or curve II.

Selectivity considerations is usually made on the basis of the functional group possessed by the potential solvent. Methods of selectivity prediction, based upon different limitations in the information available, is outlined by Cremer and Davies (12).

The distribution coefficients of both the solute C which is the desired product of the separation, and of the undesirable residual component or residue A may be too high, thereby giving a difficult separation or no separation at all. The selectivity is the ratio of these distribution coefficients and is the separation factor analogous to the relative volatility in distillation (16, 17).

A solvent is selective if the concentration of the desired solute is relatively higher in the extract phase (solvent rich) than in the feed and in the raffinate or residual phase;

$$\text{Selectivity, } \beta = \frac{\dfrac{\text{conc. of solute in the extract phase}}{\text{conc. of residue in the extract phase}}}{\dfrac{\text{conc. of solute in the raffinate phase}}{\text{conc. of residue in the raffinate phase}}}$$

$$= \frac{x_C^E}{x_A^E} \Big/ \frac{x_C^R}{x_A^R} = \frac{x_C^E}{x_C^R} \cdot \frac{x_A^R}{x_A^E} = \frac{K_C}{K_A} \qquad (2.1)$$

The selectivity has therefore the same value on the solvent-free basis as when the solvent is included; similarly the distribution coefficients K_C and K_A may be measured in any consistent units. Although the selectivity usually varies widely with composition (except in some

hydrocarbon - solvent systems) and with temperature to a lesser degree, it provides a true criterion of the extraction efficiency of a solvent (8, 18, 19). If the selectivity reached unity at some concentration, the extraction process would be halted at this point: this is the analogue of azeotropy in distillation.

In terms of activity coefficient:

$$\beta = \frac{\gamma_C^R \cdot \gamma_A^E}{\gamma_C^E \cdot \gamma_A^R} \qquad (2.2)$$

The use of this important relationship for correlating and predicting ternary distribution data from ternary solubility data and binary solubility, azeotropic or vapour-liquid equilibria data is discussed in sufficient detail and has been used as one of the initial procedures for screening potential solvents(20, 21, 23,24).

Practical processes require that β exceed unity, the more so the better. Selectivities close to unity will result in large plant requirement, large numbers of extraction contacts or stages, and, in general, costly investment and operation.

Selectivity may be increased with the use of reflux directly or induced. In the case of extraction with phenol, for example, induced reflux is obtained by the simple expedient of injecting water into the extract system and thereby throwing some of the extracted hydrocarbons out of solution (24).

2.4.3 Distribution Coefficient

Distribution coefficient is important since it influences selectivity; a more favourable coefficient will lead to a more favourable selectivity.

The distribution coefficient K_i for any component i distributed between the two phases conventionally denoted as R and E (for the raffinate and extract phases), is defined as the ratio of the equilibrium concentrations of i in the two phases.

$$K_i = \frac{\text{concentration of i in the E phase}}{\text{concentration of i in the R phase}} \qquad (2.3)$$

These concentrations may be expressed in any convenient , but consistent units, depending on the stoichiometry used, in the calculation of mass transfer. It is often convenient to define K_i in terms of mole fractions as:

$$K_i = \frac{x_i^E}{x_i^R} \qquad (2.4)$$

The distribution coefficient of any solute depends on the components in, and the composition of the mixture being separated and on the solvent used, and generally to a lesser extent, on the temperature. Occasionally, where association complexes of the solute are of a stoichiometrically simple nature and where the phases are practically immiscible, the distribution coefficient is independent of concentration, at least in dilute solution (24, 25). For this reason, and also because the distribution coefficient affords no measure of the solubility of the two phases, it is of practical value only for fractional or

double solvent extraction and then often only in dilute solutions.

A thermodynamic interpretation of the distribution coefficient is readily derived. The condition for the equilibrium distribution of any component between liquid phases E and R at constant temperature and pressure is the equality of the fugacities of the component in each phase (26, 27).

$$f_i^E = f_i^R \tag{2.5}$$

Now, $f_i^E = a_i^E f_i^{oE}$ and $f_i^R = a_i^R f_i^{oR}$, where 'a' represents the activity and f^o, the fugacity of the component in the standard state. If the standard state chosen is the pure component in the liquid phase at the temperature and pressure of the solution, then $f_i^{oE} = f_i^{oR}$ and the condition of phase equilibria may be rewritten as

$$a_i^E = a_i^R \tag{2.6}$$

or again,

$$\gamma_i^E x_i^E = \gamma_i^R x_i^R \tag{2.7}$$

Therefore,

$$K_i = \frac{x_i^E}{x_i^R} = \frac{\gamma_i^R}{\gamma_i^E} \tag{2.8}$$

The distribution coefficient is related to the activity coefficients (referred to pure material as standard state) of the component in each phase and thus become amenable

to more elaborate thermodynamic treatment.

In the case of a solvent that provides a poor distribution coefficient but is otherwise desirable, the coefficient may be altered by changing the pH of the solution when the extracted solute is an ionizing substance. Deliberate alteration of pH to obtain a more favourable coefficient, or addition of a buffer to maintain a favourable pH during the extraction of an acidic or basic substance, is a frequent practice; especially important in the separation of many metals (8). Another way of favourably altering the distribution coefficient, is by the addition of an unextracted salt i.e. 'salting-out' (37, 38).

Salting out agents frequently operate through a common-ion effect or by hydrolysis to produce H^+. In other areas where an electrolyte is distributed, addition of an electrolyte will frequently alter the distribution ratio in accordance with Setschenow's rule (28, 29, 30).

$$\log \frac{m_c^*}{m_c} = kX_s \qquad (2.9)$$

where m_c = the distribution ratio in the absence of salt.

m_c^* = the distribution ratio in the presence of salt at concentration X_s.

k = a constant, which permits estimating the effect of different salt concentrations.

Increase of the solubility of inorganic and organic solutes in water as the result of addition of certain salts, 'salting in' or hydrotropy, has been observed. Extraction

equilibria may thereby be profoundly altered, and useful extraction processes that are otherwise impossible may result (31).

2.4.4 Solvent stability

It is essential that the solvent is chemically stable under the operating conditions of the extraction process. It must not be degraded in any way or lose the solvency properties for which it was selected.

2.4.5 Density

A difference in densities of the contacted phases is essential and should be as great as possible. Not only is the rate of disengaging of the immiscible layers thereby enhanced, but the volumetric capacity of the contacting equipment is increased since gravity settling is accelerated. It is insufficient to examine merely the relative densities of the solution to be extracted and the pure extracting solvent, since on admixture mutual solubility of the two will alter the densiti es; for continuous contacting equipment, it is important to be certain that a satisfactory density difference for the contacted phases exists throughout the entire range of the contemplated process.

2.4.6 Capacity

It is not desirable to use a solvent of high selectivity if the quantity of the extracted solute is low. High solvent to feed ratios are required for higher capacities which may be uneconomical. The solvent to feed ratio required for a given separation is of prime importance since the

solvent rate controls the dimensions of the extractor, and the energy requirements and size of the recovery plant.

2.4.7 Recoverability

In all liquid extraction processes, it is necessary to remove the extraction solvent from the products. This is important not only to prevent contamination of the products with the solvent but also to permit reuse of the solvent. If distillation is the method to be used for solvent recovery, solvent properties such as volatility and latent heat of vaporization become important. However, other methods of solvent recovery should also be considered.

2.4.8 Other physical properties

Corrosiveness

In order to reduce the cost of equipment , the solvent should cause no severe corrosion difficulties with common materials of construction or with those ordinarily used to handle the feed to the extraction process. The modern availability of unusual materials at relatively low cost, however, has opened up possibilities that would have been out of the question several years ago. Entire commercial extraction plants have been built of plastic-lined metals, and such materials should be kept in mind if the value of the product warrants.

Viscosity

Low power requirements for pumping and agitating, rapid extraction, rapid settling of dispersions, and high heat- and mass-transfer rates are corollaries of low viscosity

and hence this is a desirable property of solvents in extraction processes. Solvents may sometimes be mixed with low-viscosity inert diluents to improve this characteristic, as in the dilution of tributyl phosphate with kerosene or even less viscous hydrocarbons for uranium extraction.

Vapour pressure

Ordinarily low vapour pressure is desired so that storage and extraction operations are possible at atmospheric or at most only moderately high pressure, so that losses of solvent are kept to a minimum. Exceptions to this requirement are frequently made in the interest of easy recovery of the solvent by volatilization and other desirable properties, however. For example, liquid propane and liquid sulphur dioxide are commonly used in the refinery of petroleum products, where their desirable selectivities are utilized, and advantage is taken of their high volatilities in solvent-recovery operations.

Freezing point

The solvent should have a sufficiently low freezing point so that it may be conveniently stored and otherwise handled at outdoor temperatures in cold weather.

Flammability

Low flammability is, of course, desirable for reasons of safety, and the flash point is frequently used as a numerical indication of the property. If the solvent can be burnt, it should have a high flash point and close concentration limits for explosive mixtures with air.

Toxicity

Highly poisonous materials are difficult to handle industrially. Unless elaborate plant-safety devices are planned, with frequent medical inspection of personnel, the more toxic substances must be avoided. Solvents that might leave toxic residues in food and pharmaceutical products must be avoided in this industry.

2.4.7 Specific Interactions in Solutions

The selectivity of a solvent B for a solvent C in A is:

$$\beta = \frac{x_C^E}{x_C^R} \cdot \frac{x_A^R}{x_A^E} = K_C \frac{x_A^R}{x_A^E} \qquad (2.10)$$

A and B are partially miscible and for any saturated composition $x_A^R > x_A^E$, thus the ratio x_A^R/x_A^E is always greater than unity, sometimes by a large factor. The selectivity of the solvent can be greater than unity even when the distribution coefficient is less than unity, and particularly at low solute concentration if A and B are nearly immiscible, but a selective solvent is one for which $K_C >> 1$

$$K_C = \frac{\gamma_C^R}{\gamma_C^E} \qquad (2.11)$$

and the nature of the interactions of the solute C with the two solvents A and B determines quantitatively the magnitudes of the activity coefficients, γ_C^R and γ_C^E ; if in the extract phase $\gamma_C^E < 1$, the solute is saturated by the solvent and the excess attractions between solute and solvent

molecule is often due to bond or hydrogen bridge. In effect, the solvent and solute form a weakly bonded associated complex, displacing the equilibrium towards the solvent phase.

In order to predict whether hydrogen bonds will be formed in a given solution, it is necessary to consider polar bonds (32). Many organic and inorganic molecules contain functional groups in which there is permanent displacement of electric charge, giving rise to the electric or dipole moment of the whole molecule and to the dielectric constant of the material. However, a classification based on electrical attraction and on dipole moments may not be adequate, because if there are several hundred functional groups present in the molecule, the dipole effects of the individual groups may tend to cancel each other, giving a low dipole moment for the whole molecule. Polar molecules tend to associate and the strong intermolecular attraction is manifested, for example in a relatively high boiling point and in a value for the latent heat of vaporisation higher than that predicted by Trouton's rule. The association in a pure material proceeds by means of the hydrogen bond, that is —Ö— , nitrogen —N̈— and flourine —F̈: are able to donate a pair of unshared electrons to an active hydrogen atom —$\overset{\delta+}{H}$ to form a bond.

In alcohols, 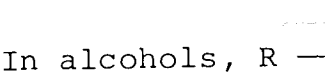 is associated thus

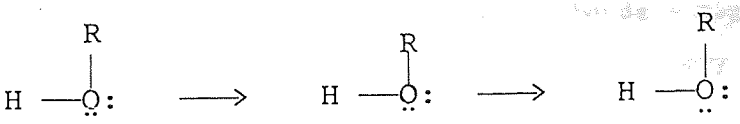

In water, the effect of the hydrogen bond is particularly marked and water has a three-dimensional network of bonds. Atoms of nitrogen, oxygen and flourine are termed 'donor atoms' and an 'active' hydrogen atom is the 'acceptor atoms'. The polarization of the C-H bond is insufficient to produce an active hydrogen atom, but groups of strong polarity include

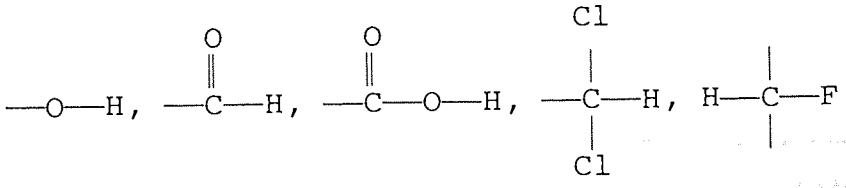

Hydrogen bonds are important in theories of solutions because they can be formed between dissimilar molecules, one containing a donor atom and the other an active hydrogen atom.

The classification of liquids according to the functional groups which may form hydrogen bonds within the same substance or with others by Ewell et al (33) represented in Table 2.3, regards the hydrogen bond as predominant, and the effects of induced dipole and dispersion forces as negligible. Equivalent of this method of classification has been given by Francis (13). Thus association of like molecules can occur only if donor atoms and an active hydrogen atom are present in the same molecules: if only one of these is present, solvation can occur in the mixture

Class I.	Liquids capable of forming three-dimensional networks of strong hydrogen bonds - e.g., water, glycerol, amino alcohols, hydroxylamine, hydroxy acids, polyphenols, amides etc. Compounds such as nitromethane and aceto-nitrile also form three-dimensional networks of hydrogen bonds, but the bonds are much weaker than those involving OH and NH groups. Therefore, these types of compounds are placed in Class II.
Class II.	Other liquids composed of molecules containing both active hydrogen atoms and donor atoms (oxygen, nitrogen, and fluorine) - e.g., alcohols, acids, phenols, primary and secondary amines, oxines, nitro compounds with α-hydrogen atoms, nitriles with α-hydrogen atoms, ammonia, hydrazine, hydrogen fluorine, hydrogen cyanide etc.
Class III.	Liquids composed of molecules containing donor atoms but no active hydrogen atoms - e.g., ethers, ketones, aldehydes, esters, tertiary amines (including pyridine type), nitro compounds and nitriles without α-hydrogen atoms etc.
Class IV.	Liquids composed of molecules containing active hydrogen atoms but no donor atoms. These are molecules having two or three chlorine atoms on the same carbon as a hydrogen atom, or one chlorine on the same carbon atom and one or more chlorine atoms on adjacent carbon atoms - eg., $CHCl_3$. CH_2Cl_2, CH_3CHCl_2, CH_2Cl-CH_2Cl, $CH_2Cl-CHCl-CH_2Cl$, $CH_2Cl-CHCl_2$, etc.
Class V.	All other liquids - i.e., liquids having no hydrogen-bond-forming capabilities - e.g., hydrocarbons, carbon disulphide, sulphides, mercaptans, halohydrocarbons not in class IV, non-metallic elements such as iodine, phosphorus, sulphur etc.

Figure 2.3 : Classification of Liquids by Ewell et al(33).

only if the complementary donor or acceptor atom is present in the second component. Because the formation of hydrogen bonds in solution is a strong solvation effect, the derivations from Raoult's law are negative: conversely, the breakdown of the hydrogen bonds in a material on the addition of a second component, gives a positive deviation and finally phase separation in the resultant solution.

These concepts may be applied to the qualitative prediction of the direction of solute distribution by estimating the distribution coefficient from $K_c = (\gamma_c{}^R/\gamma_c{}^E)$ but it is not always possible to predict which will be more selective of several possible solvents. The method, however, indicates those types of solvent which are potentially useful, and some of the additional information listed earlier may be employed to check the prediction based on hydrogen bonding. Any promising solvent would finally be tested by determining the solubility and tie-line relations. Apart from the approximate nature of the prediction, Paris (34) has indicated that when a solvent possesses more than one functional group, it is less certain whether hydrogen bond concepts will give reliable results. Saunders (35) has studied derivatives of nitriles containing a second functional group as highly selective solvents for aromatics in hydrocarbon mixtures; the interpretation of the results in terms of hydrogen bonding was not always clear and this is unfortunate because the modification of solubility and selectivity by the use of an additional functional group offers scope for improved solvents.

Classes	Deviations	Hydrogen bonding
I+V II+V	Always + deviations; I+V, frequently limited solubility	H bonds broken only
III+IV	Always - deviations	H bonds formed only
I+IV II+IV	Always + deviations; I+IV, frequently limited solubility	H bonds both broken and formed, but dissociation of Class I or II liquid is more important effect
I+I I+II I+III II+II II+III	Usually + deviations, very complicated groups, some - deviations give some max. azeotropes	H bonds both broken and formed.
III+III III+V IV+IV IV+V V+V	Quasi-ideal systems, always + deviations or ideal; azeotropes, if any, will be minima	No H bonds involved

TABLE:2.4 SUMMARY OF DEVIATIONS FROM RAOULT'S LAW.

Gilmont, Zudkevitch and Othmer (39) subdivided the five suggested classes by Ewell et al (33) in ten groups according to field factors, as in Table 2.5. Using this classification, Robbins (40) recorded the number of maximum - and minimum - boiling point azeotropes reported by Horsley (41) for each binary interaction. A positive, +, deviation was assigned to a two-group interaction which produced a preponderance of minimum-boiling point azeotropes. A negative, -, deviation was assigned for a preponderance of maximum boiling point azeotropes. A zero, O, deviation was assigned to interactions which were seldom azeotropic or produced few of each type of azeotrope. Whenever subgroups provided the same interaction profile, they were grouped together. This led to the formation of a tenth group which did not fit into any other profile.

The table of interactions, Table 2.6, can provide a preliminary guide for the selection of the best solvents for an extraction process. If a solute is to be extracted, it would be desirable to reduce the activity coefficient of the solute, giving a high distribution coefficient into the solvent. Generally, the activity coefficient of a solute will stay within a factor of 2 or 3 for one class of solvents, but it may change by two or three orders of magnitude, between classes. The relationships among classes of compounds have been correlated by Leo et al (46). Treybal (36) and Francis (45) have also provided a collection of data which can help to evaluate solvent-solute group-interactions.

Class I Liquids capable of forming strong hydrogen bonding. Liquids in this class are also capable of association and formation of networks.	
Group 1.	Organic acids, phenols, aromatic alcohols, in some cases aniline.
Group 2.	Water and alcohols.
Class II Liquids that contain a donor atom (oxygen, nitrogen) but no active hydrogen atoms.	
Group 3.	Ketones and nitriles without α-hydrogen.
Group 4.	Esters.
Group 5.	Ethers and dioxane.
Class III Liquids composed of molecules that are not capable of hydrogen bonding	
Group 6.	Aromatic compounds, icluding the halogen aromatic compounds that have no active hydrogen - e.g. chlorobenzene, dichlorobenzene, dimethylaniline.
Group 7.	Nonaromatic hydrocarbons. This group also includes the cycloparaffins with the exception of cyclohexane. Also included are the silicoparaffins, CS_2, mercaptans, and other sulfides.
Group 8.	Halogenated hydrocarbons that do not contain an active hydrogen atom attached to the same carbon atom - e.g., monochlorides or CCl_4.
Class IV Liquids composed of molecules containing an active hydrogen atom but no donor atom.	
Group 9.	Halogenated hydrocarbons that have a single hydrogen atom attached to the same carbon atom to which the halogen atoms are attached - e.g., molecules of the type CCl_3, CH_2Cl_3, $CH_2ClCHCl_2$.
Class V Miscellaneous grouping which includes those compounds which could not be classified because of the lack of sufficient data.	
Group 10.	Picolines.

Table 2.5 : GILMONT -ZUDKEVITCH -OTHMER Grouping of Field Factors.

Group	Solute	Solvent 1	2	3	4	5	6	7	8	9
1	Acid, aromatic OH (phenol)	0	-	-	-	-	0	+	+	+
2	Paraffin OH (alcohol), water, imide or amide with active-H	-	0	+	+	+	+	+	+	+
3	Ketone, aromatic nitrate, tertiary amine, pyridine, sulfone, trialkyl phosphate, or phosphine oxide	-	+	0	+	+	-	0	+	+
4	Ester, aldehyde, carbonate, phosphate, nitrite, or nitrate, amide without active-H, intramolecular bonding, e.g., o-nitrophenol	-	+	+	0	+	-	+	+	+
5	Ether, oxide, sulfide, sulfoxide, primary and secondary amine or imine	-	+	+	+	0	-	0	+	+
6	Multihalo paraffin with active H	0	+	-	-	-	0	0	+	0
7	Aromatic, halogen aromatic, olefin	+	+	0	+	0	0	0	0	0
8	Paraffin	+	+	+	+	+	+	0	0	0
9	Monohalo paraffin or olefin	+	+	+	+	+	0	0	+	0

Effect of interaction between groups on solute activity coefficient.

\+ increases activity coefficient, minimum-boiling-point azeotropic

0 mild interaction, seldom azeotropic

\- decreases activity coefficient, maximum-boiling-point azeotropic

TABLE:2.6 SOLUTE-SOLVENT GROUP INTERACTIONS.

Systems with water as one component are of great practical interest and also throw light upon the effects of polarity and the hydrogen bond (44).

2.5 EQUIPMENT SELECTION

All liquid-liquid extraction processes must include the following sequence of steps:

i) production of an intimate contact of feed mixture with solvent,

ii) separation into two liquid phases, and

iii) recovery of solute from extract phase and recovery from both phases.

Ideally, process equipment should handle with a high efficiency, the largest possible throughput in the smallest possible volume of apparatus. At the same time, it should be cheap to build and operate and should perform with constant efficiency and stability over a wide range of throughputs. Most of these criteria represent conflicting demands and much of the skill and art of the designer lies in achieving a satisfactory or reasonable compromise between them.

A single equilibrium contacting of feed mixture with solvent comprises a theoretical stage. Commercial extractions usually require a number of theoretical stages, a requirement that can be satisfied by many different types of equipment.

The intimate contacting of the two liquid phases is brought about by various devices which produce localized turbulence. This turbulence produces a dispersion of one phase in the other and provides a large surface area for mass transfer at the phase boundary. It also aids mass transfer to the phase boundary because of movement within each phase relative to this surface. The rate of mass transfer is expressed by the basic rate equation as follows:

$$N = K_c A \Delta C \qquad (2.12)$$

It is clear that high mass transfer rates can be obtained by maintaining the mass transfer coefficient, K, interfacial area, A, and the driving force, ΔC , at their highest practical values. A large interfacial area can be created by dispersing one of the phases as droplets in the other. The practical criterion is the interfacial area per volume, i.e. the number and size of the droplets in unit volume of dispersion. Therefore, for a high interfacial area appropriate means must be incorporated in extractors to promote dispersion and redispersion. The mass transfer coefficient depends upon the resistance to diffusion within the dispersed and continuous phases. By creating turbulent conditions, eddy diffusion, which is more effective than molecular diffusion, occurs; this results in higher mass transfer coefficients. Depending upon the degree of turbulence, a wide distribution of droplet size exists in practical contactors. The flow inside and outside the drops, which depends upon the drop hydrodynamics, exhibits 'stagnant', 'circulating' or 'oscillating' behaviour.

This is dependent on the Reynolds number within the drops. 'Stagnant' behaviour generally applies only to small drops. Drops larger than about 2 mm diameter for which Re < 1, exhibit laminar circulation; when Re > 1, turbulent circulation occurs. In general, all drops with Reynolds numbers above 200 tend to oscillate. Each flow pattern results in different values for the film coefficient.

In practical extractors, mass transfer to or from drops occur throughout the different stages of drops life. These stages are:

i) formation of drops either at a distributor or by agitation,

ii) release of drops,

iii) travel of formed drops throughout the continuous phase, and

iv) coalescence of drops at a phase boundary e.g. in a settler.

In agitated contactors during travel of the formed drops, mass transfer is complicated by coalescence - redispersion phenomenon which results in a loss of drop identity.

The overall mass transfer coefficient is found from the dispersed phase coefficient k_d, and the continuous phase coefficient k_c. Neglecting the interfacial resistance ,

$$\frac{1}{K_c} = \frac{1}{k_d} + \frac{m}{k_c} \qquad \text{or} \qquad \frac{1}{K_d} = \frac{1}{k_d} + \frac{1}{mk_c} \tag{2.13}$$

Preferably, equipment should form a mono-dispersion of drops which oscillate since oscillating drops have the most desirable transfer characteristics. Another aspect which should be considered for a reliable calculation of extractor efficiency is backmixing, which has an unfavourable influence on the extraction efficiency because it results in a reduction in ΔC (43).

Frequently, a compromise in the degree of mixing is necessary to permit separation of the phases. Separation is usually accomplished by gravity settling. For more difficult cases, coalescence may be promoted by special fine packings or by use of centrifugal force.

Hence, it is evident that surface and interfacial tensions, viscosities and relative densities of the phases are very important properties of any extraction system and will probably govern to a great extent the type of equipment used. The presence of emulsifying agents and solids has an even greater effect on choice of equipment.

The contacting devices used in industrial processes are of two types (41, 47) as listed in Table 2.1. These are:

1. Discrete stage contactors

and 2. Continuous differential contactors, in which there is no intermediate separation of phases.

Discrete stage contactors include the mixer-settler range of equipment in which the immiscible liquids are brought into contact and mixed to form a homogeneous dispersion in each phase which is subsequently separated in a gravity operated settler. If the operation is batchwise the same vessel serves for both mixing and settling. Continuous operation is more common with settling taking place in a separate vessel of sufficient size to allow residence time for gravity settling and coalescence. In continuous differential contactors, counter-current flow is promoted by the density difference between the fluids being contacted. In spray columns, dispersion is created simply by passage of the dispersed phase through a distributor.

Continuous differential contactors operates through continuous counter-current contact between the immiscible phases to give the equivalent of any desired number of stages. These may be further subdivided as follows:

A. Gravity Operated Extractors:

1. Non-mechanical dispersion

   a) Spray columns

   b) Baffle plate columns

   c) Packed columns

2. Mechanically agitated extractors

   a) Pulsed columns

   b) Rotary agitated columns

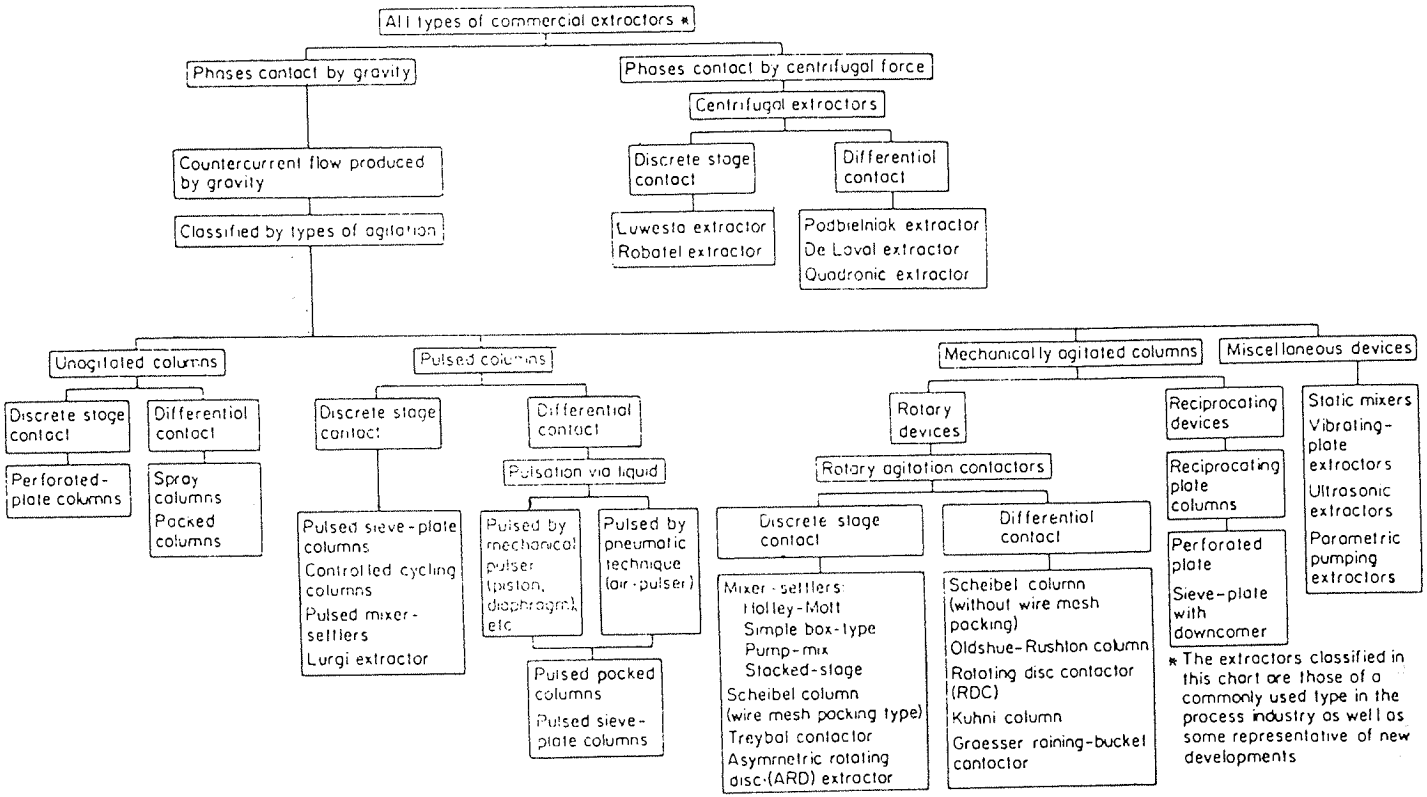

Figure 2.6 : Classification of Commercial Extractors.

B. Centrifugal Extractors:

Figure 2.6 classifies some of the commercial extractors.

Various workers (46, 47, 48, 49, 50, 51, 52) have extensively reviewed the factors to be considered in choosing an extractor for a particular application. However, there are still no general rules for the choice of an extractor for any particular mass transfer application. A simplified decision network for extraction equipment selection is shown in Figure 2.7 (53).

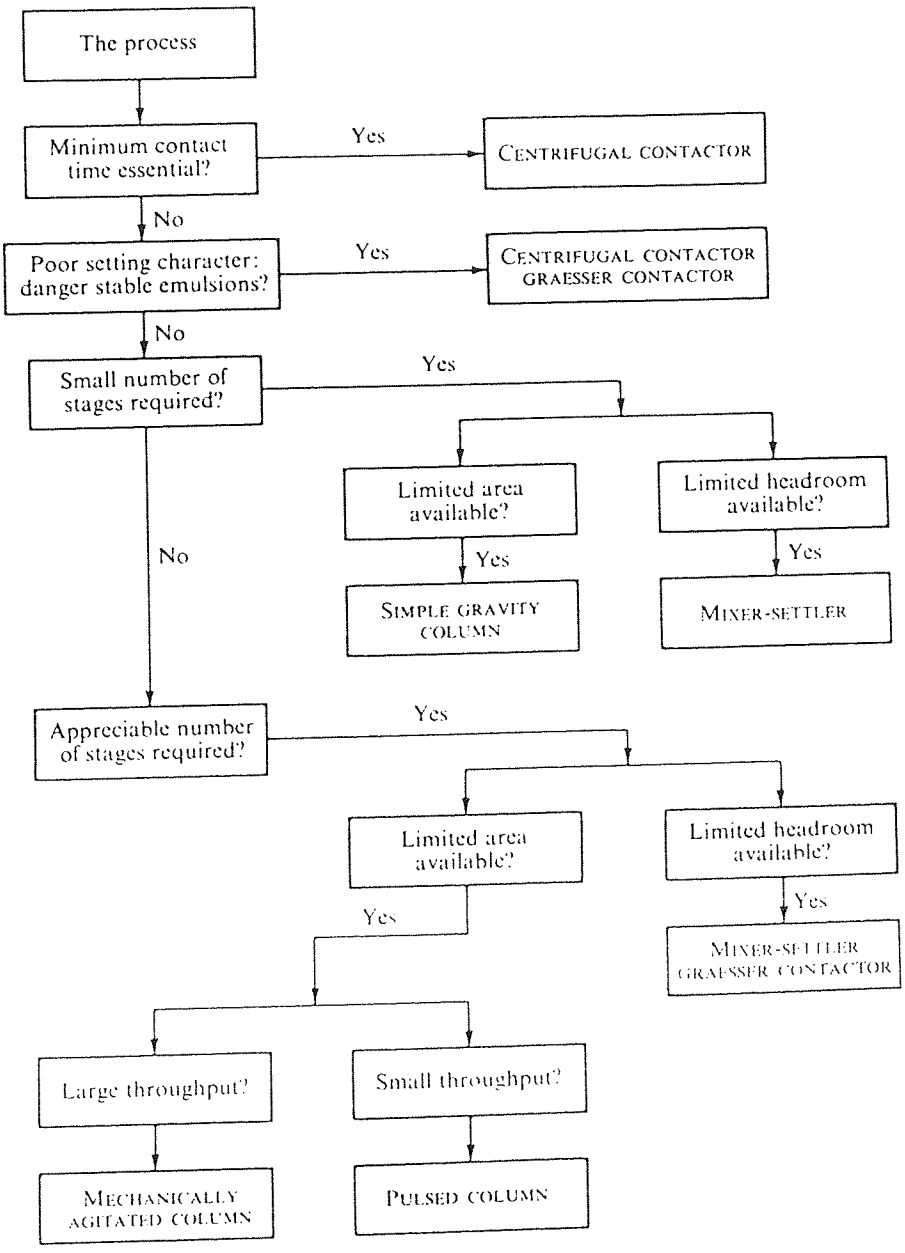

Figure 2.6 : Selection Guide for Extraction Devices.

CHAPTER three 3

THE MODIFICATION OF LIQUID-LIQUID EXTRACTION PROCESSES

In recent years, a number of factors have had a marked effect on liquid-liquid processes and will continue to influence them in the future. Shortages of high quality lubricating oil crudes, for instance, have forced refiners to process crudes of marginal quality. Extraction of such crudes must be more drastic to produce the required viscosity, and more efficient to produce maximum yield. In general, this has been accomplished by increasing the number of extraction stages and by taking full advantages of new technological improvements. Increasing demands made on lubricating oils by high temperature and heavy duty operation have been met by the introduction of a large number of additives and inhibitors for practically all types of services. This in turn has imposed a new criterion on liquid-liquid extraction, namely that of "additive response". Additive response might be broadly defined as the degree of desired improvement obtained by the addition of any given amount of additives. Such response varies with crude source and with the degree of refining to which the crude may be subjected.

It is most striking that since the early development of liquid-liquid extraction, very few improvements or modifications of a fundamental nature have been made. There is

room for a considerable expansion of effort in this direction, notwithstanding the complexity and the analytical difficulties of the problem.

It seems highly probable that fundamental work aimed at placing the mechanism of liquid-liquid extraction on a sound scientific basis will lead to further development of the process, or the development of new processes to work in conjunction with liquid-liquid extraction for the production of improved yields.

Outlined in the following sections are some of the various known modifications that have been achieved.

3.1 USE OF REFLUX

In 1933, Saal and Van Dyke (9) proposed a new process of solvent extraction, in which the feed would be introduced into the middle of the contactor and parts of the extract and raffinate streams would be returned to the contactor as extract and raffinate reflux respectively. They claimed that this process was analogous to that of complete rectification in distillation, and therefore the method should be able to completely separate the two components of a binary mixture: Figure 3.1(a) and 3.1(b) show the analogy between the two processes. The extract reflux is obtained by removal of some, or all, of the solvent from the extract; this is analogous to the removal of heat from the vapour to produce the reflux in distillation. Similarly, the solvent added to part of the raffinate to produce the raffinate reflux is analogous to the heat added to produce the vapour (i.e. the 'gaseous reflux') from the reboiler in the distillation

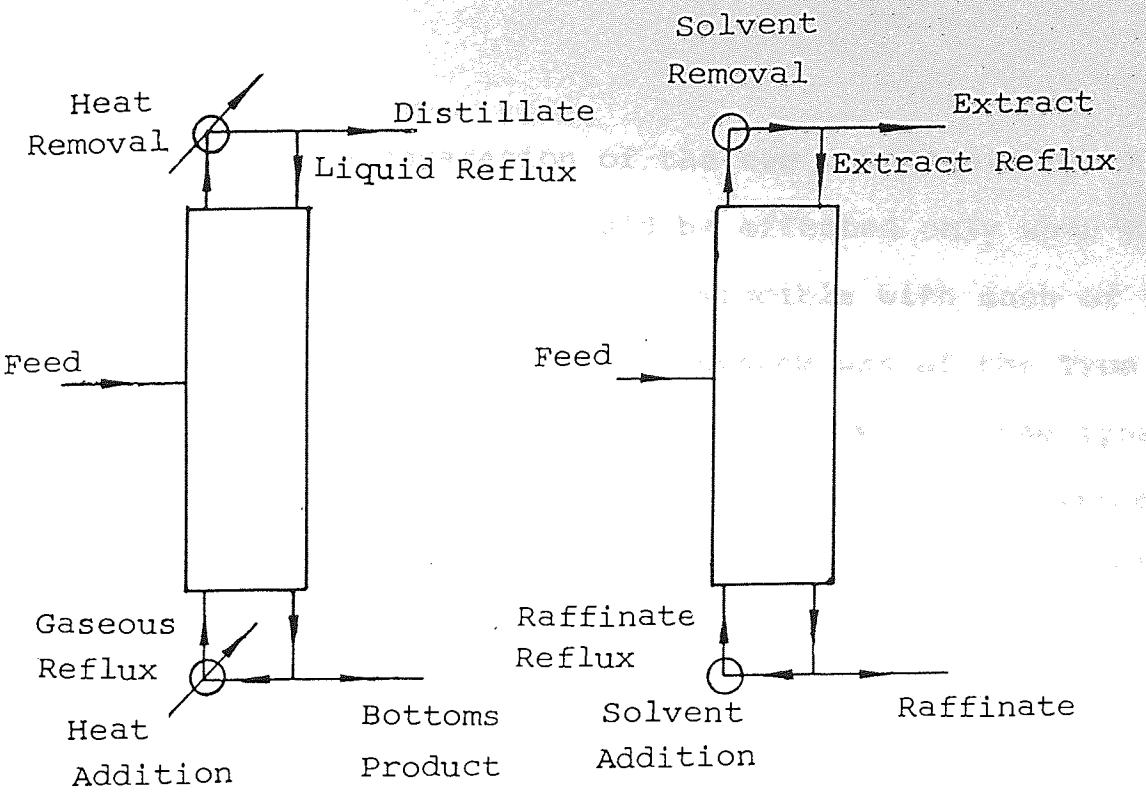

Figure 3.1 : Analogy Between Reflux in Extraction and Rectification in Distillation.

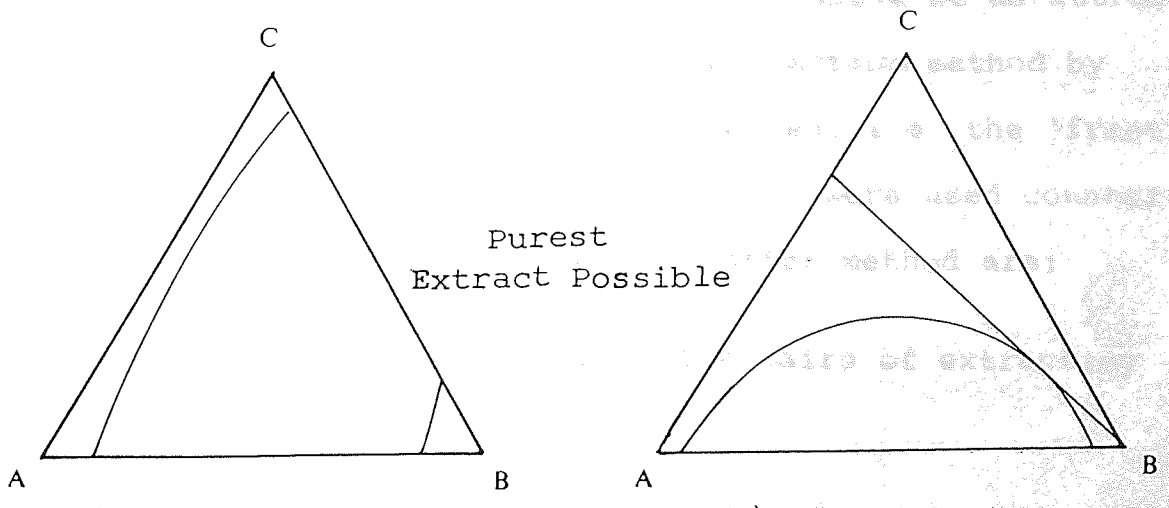

Figure 3.2 : Comparison Between Type II and Type I Systems on Application of Reflux.

system.

The complete separation of the two components by this solvent extraction process could be effected only when the extracting agent was completely immiscible with each of the components, i.e. when the ternary system was of the Type II, as shown in Figure 3.2(a). If the system was of the Type I system, as shown in Figure 3.2(b), then the use of extract reflux is superfluous, since the purest extract obtainable, with or without reflux, as determined by the tangent from B to the saturation curve. With the Type II system, there was no such limitation on the purity of the extract obtainable. With both these types, the raffinate can be obtained at any desired purity without using raffinate reflux; thus sometimes this form of reflux is unnecessary (54, 55).

This new process, in which the reflux streams would be produced from the contactor exit streams, would be an attractive alternative to the other solvent extraction method by which complete separation could be effected, i.e. the 'fractional distribution' method in which two solvents were used countercurrently. The disadvantages of the latter method are:

a) the limited choice of suitable pairs of extracting agents (i.e. solvents), and

b) the additional apparatus required to deal with two solvents.

Industrial applications are in the Duosol process for the treatment of asphaltic feed stocks, purification of vitamins (56) and in the laboratory, for the separation of quinoline bases from coal tar.

In subsequent articles (17, 57-63) other workers elaborate on the ideas of Saal and Van Dyke (9), and describe graphical techniques for the calculation of the number of theoretical stages, reflux ratios, etc. Nearly all the authors emphasised the distillation/solvent extraction analogy, and included reflux of both extract and raffinate in their diagrams and calculations, but they did not give any examples of the actual use of reflux in industrial solvent extraction processes. The same omission was noticeable in most chemical engineering textbooks which included reflux, of both extract and raffinate, in their chapters on solvent extraction.

3.1.1 Methods to provide extract reflux

Extract reflux can be provided in a number of ways. The usual method is to recover solvent from the extract leaving the contactor, by distillation or evaporation, and to return it to the column. This is termed 'external reflux'. Alternatively, reflux may be provided by the withdrawal of heat from the extract phase or by the addition of an anti-solvent to the system. These two methods are known as 'internal reflux'.

If the system is Type I and it is desired to form reflux by withdrawal of heat, in order to obtain a raffinate and an extract of high purity, it should first be converted to a Type II system. This removes limitations on the concentration of the extract. The effect of temperature on the shape of the solubility curve has been discussed in Section 2.2. In theory, extraction can be carried out at a temperature which would produce an optimum-shaped solubility curve.

However, this method is not always applicable since to obtain an equilibrium curve of Type II with some ternary systems would require the temperature to be lowered to a value below which one of the components may solidify. Also at low temperatures, other factors which directly affect operation, such as mass transfer rate and distribution coefficients, are depressed so that it would be necessary to use a large number of stages and a large solvent to feed ratio . In practice, in extraction processes using this procedure, solvent and feed are introduced into the extractor at different temperatures thereby promoting a temperature gradient along the column (62).

Formation of reflux by addition of an anti-solvent involves a similar route to that produced by reduction in temperature. An anti-solvent, which is partially or completely miscible in the extracting solvent, is added to reduce the solubility of the solute. In this way a Type I system can be converted to a Type II system. In a countercurrent extraction process in which solvent and feed are introduced at opposite ends of the extractor unit, the anti-solvent is fed in near the extract outlet. However, formation of reflux by the addition of an anti-solvent often has the disadvantages of introducing a low mass transfer rate and also low distribution coefficient. Therefore, the method is not always practicable.

3.1.2 Feasibility of reflux

Although the use of reflux in liquid extraction was known in the 1930's its industrial application has been limited due to lack of data (12). Until the 1950's, only

one process made use of extract reflux; this was the refining of vegetable oils using furfural as solvent. Lately, reflux has been incorporated into aromatic recovery processes. In the Udex process, which uses diethylene glycol as solvent for the removal of aromatics from refined naphthas, reflux has been applied to obtain a pure product (5,7). Also in the Sulfolane process, efficient recovery of aromatics makes use of reflux which is produced in a flash separator (65).

3.2 A CHANGE IN PRESSURE

The change in solubility of the relatively immiscible liquids with externally applied pressure is very small and may be ignored in most situations. The nature of the effect may be predicted from the principle of Le Chatelier; if solution of the two components is accompanied by an increase in volume, it follows that an increased pressure will favour a decreased solubility and vice versa.

3.3 A CHANGE IN TEMPERATURE

This is the method used in the furfural extraction of lube oils, a temperature gradient being maintained in one section of the extraction column by indirect water coolers (66). Most systems of Type I 'open-out', as in Figure 3.3, i.e. the mutual solubility of the components decreases, as the temperature is lowered, but exceptions are the systems in which propane is one component, for in these cases it is an increase in temperature which produces the desired effect. Hence, in the propane deasphalting of viscous petroleum

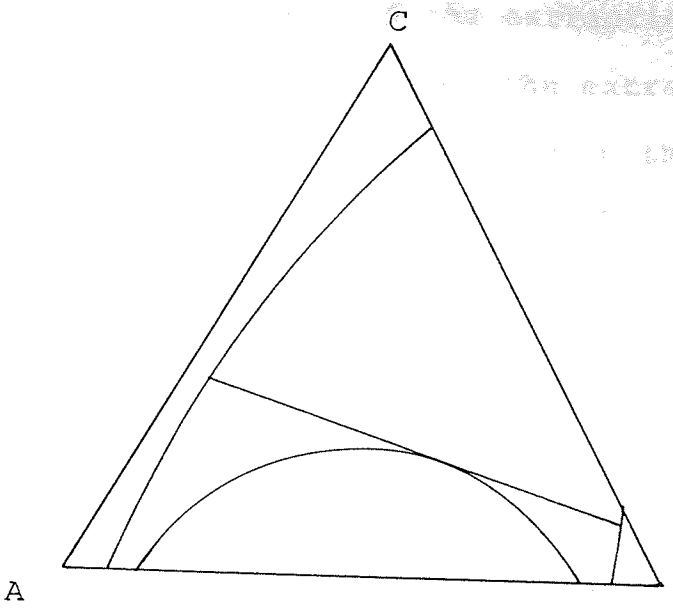

Figure 3.3 : EFFECT OF 'OPENING OUT' A TYPE I SYSTEM.

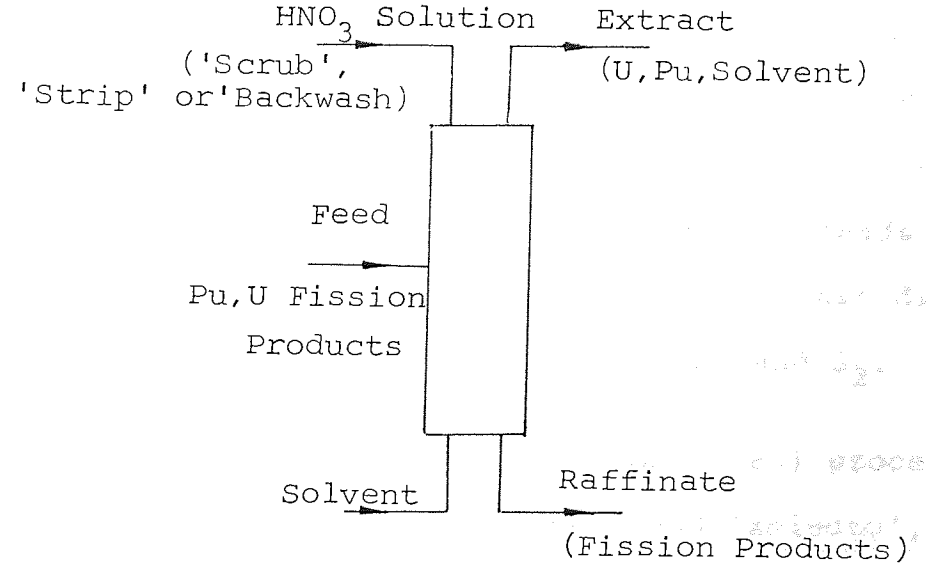

Figure 3.4 : SEPARATION OF FISSION PRODUCTS (USE OF DUAL SOLVENTS).

fractions the upper part of the extraction column contains a steam heater to produce the extract reflux (66). This method of heating is also used in the Solexol process for the refining of vegetable oils (67).

3.4 DUAL SOLVENT

The principle feature of this process is the use of two solvents whose mutual solubility is low and in either of which one of the two substances (or groups of substances) to be separated is preferentially soluble.

As a rule, the two solvents pass the entire extraction system countercurrently though other procedures are possible (64). In the normal case, therefore, the solvents S_1 and S_2 are introduced at the top and bottom of an extraction tower respectively. The mixture to be separated (the feed) can, theoretically be introduced anywhere in the tower. The mutual solubility of the two solvents used in this extraction process must be low, since this leads to a high selectivity. In general, this implies a great difference in polarity between the two solvents S_1 and S_2.

The classic example is the Duosol (66) process, in which the two solvents are propane and 'selecto', the latter being a mixture of phenol and cresols. Kirk and Othmer (68) stated that this is the only commercial application of solvent extraction with two solvents, but the 'strip' or 'back-wash' used in some processes is effectively a second

solvent, since it performs the reflux function of producing a purer extract that would be possible without an additional countercurrent stream. Figure 3.4 shows the first part of the extraction system in most atomic energy separation plants (81) in which the second 'solvent' is a solution of nitric acid, which serves to strip the extract stream of the fission products. Similar processes, using 'strip' or 'backwash' in the same way, are used to separate niobium and tantalum, and uranium from the rare earth metals (72).

Another way in which a stream flowing counter-currently to the extract phase may be produced is by the fractional distribution method, in which the second solvent is, in effect, an extract reflux. Hanson et al (68) in their example of a two-solvent process, refer to the upper solvent as 'reflux'. This process also does not have a simple distillation counterpart, although it could be argued that it is analogous to extractive distillation.

3.5 MIXED SOLVENTS

Only a very limited number of solvents possess all the properties for ideal solvents, discussed in Section 2.4. When considering the additional requirements, such as low freezing point, non-corrosiveness, non-toxicity and reasonable prices the range of suitable solvents is narrowed still further.

Investigations were therefore concentrated on solvent mixtures (71, 72) because in view of the great number of possible solvent combinations there are good prospects for finding an optimum mixture. However, only some of these properties can be improved by the combination of solvents without impairing other properties at the same time. The most promising method of combining solvents is based on the mutual relation between selectivity and capacity. By mixing a basic solvent of high capacity and low selectivity with a blending of high selectivity and low capacity, the selectivity and capacity of the mixture can be adjusted to optimum values. Hereby, a great number of suitable solvent mixtures can be prepared by the combination of different solvents which cannot be used for extraction singly.

Another advantage of solvent mixtures is that their composition can be adapted to the specific extraction problem, which is of particular importance when handling feeds of different aromatic content. When the aromatic content in the feed is low, the proportion of the high capacity component in the solvent mixture increased, and vice versa. The two components of solvent mixtures should boil in a narrow range, otherwise heat consumption for the stripper will be

higher than when using a single solvent. The component with the lowest boiling point determines the reflux ratio in the stripper column while the bottoms temperature is largely affected by the component with the higher boiling point.

3.5.1 Applications of mixed solvents (24)

i) Phenol: This popular solvent is used at relatively high temperatures (about 93°C) to permit treatment of oils of high viscosity and wax contents. Although the melting point of pure phenol is high (40.9°C), the presence of water, which is used to control selectivity and to provide reflux, and even small traces of extracted material, reduces the melting point sufficiently to cause no problem with clogging of equipment.

ii) Sulphur Dioxide - Benzene: Sulphur dioxide alone is too highly selective for aromatic hydrocarbons to produce a raffinate of high viscosity index from lubricating oil fractions, since it rejects naphthenic compounds almost completely. Benzene is added to produce a mixed solvent usually containing 15 to 25 per cent benzene, which is more versatile. The solvent has not widely been accepted however.

iii) Acetic acid recovery: It is difficult to extract/recover acetic acids from dilute aqueous solutions for reasons of poor distribution coefficients with most solvents. Common solvents are ethyl acetate for dilute solutions, or for strong solutions, mixtures of ethyl acetate with added benzene to improve the selectivity and reduce the amount of

water extracted.

iv) Udex process: A better solvent, diethylene glycol is used as a competitor of sulphur dioxide. The selectivity for aromatic extraction is improved by the addition of from 5 to 12 per cent of water to the glycol.

v) Desulphurization: In the Solutizer process, strong potassium hydroxide solutions are used, in which potassium isobutyrate has been dissolved to enhance the mercaptan's distribution coefficient. The Mercapsol process is similar and uses sodium hydroxide with added naphthenic acids and cresols. The Dualayer process is a variant of these, using potassium hydroxide solution containing potassium cresylates. The extract is freed of mercaptans by stripping, and its concentration adjusted by contacting with a potassium hydroxide-water solution (with which the cresylate solution is immiscible) before being reused. In the Unisol process, methanol is the added agent to improve caustic soda solutions. Since it dissolves in gasoline, the treated gasoline is further extracted with aqueous caustic to recover the methanol. The solutions are recovered by vapour stripping. Anhydrous hydrogen flouride, alone and in mixtures with boron triflouride, is also a desulphurizing solvent.

vi) Miscellaneous extractions: Naphthenic acids may be extracted from hydrocarbon oils by a number of solvents including aqueous solutions of the lower alcohols. Isopropyl alcohol is used to extract petroleum sulfonate from oils that have been treated with concentrated sulphuric acid

or oleum.

Several competing commercial solvents that might compare unfavourably with sulfolane have had their selectivities modified by the addition of a polar mixing component. Notable examples are: N-methyl pyrrolidone, dimethyl sulfoxide and N- formylmorpholine, where the addition of water has been shown to improve the selectivity at little expense to capacity. One advantage of this kind of mixed solvent is that the type and quantity of the mixing component can be varied to adapt the solvent to a greater range of duties. For example, if the aromatic content of the feedstock is low, then the most suitable solvent is one with a high capacity; that is, one containing less of the polar mixing component.

3.6 MODIFIED SOLVENTS

3.6.1 Active constituents

i) 'Salting' agents.

The term 'salting' applies to those electrolytes whose addition greatly enhances the extractability of complexes, particularly those encountered in oxonium extractions where the use of 'salting' agents may mean the difference between success and failure in the system.

The function of the 'salting-out' agent would, at first seem to be primarily one of providing a higher concentration of complexing anion, which by mass action, would increase the concentration of the complex and thus improve the extraction. Differences in salting agents will also depend

on their influence on the activity coefficient of the ions participating in the formation of the complex. Then, too, one of the important factors in salting-out is the binding of water by the ions of the salting agent. Water is probably bound as a shell of oriented water dipoles around the ion and thus becomes unavailable as 'free solvent'.

ii) Anti-solvent.

Low molecular weight hydrocarbons, particularly those of high polarity, such as aromatics, have high solubilities in anhydrous ammonia. Their solubility in the solvent can be decreased using an anti-solvent. There are a number of anti-solvents which can be used with ammonia such as ethylene glycol, formamide, water and ethylene diamine (75). Water is the most satisfactory of these because it is cheap, readily available, and easy to handle in a solvent recovery unit. Very low water concentrations in ammonia solvents are effective, therefore the desirable physical properties of ammonia are unaffected. Other anti-solvents have less effect on solubility when used in small amounts, so that they must be used in higher concentrations in the solvent.

The effect of water as an anti-solvent to ammonia is shown on the triangular diagram in Figure 3.5. The data represented in theis figure is analogous to that in Figure 3.6 where the solvent is anhydrous ammonia but the temperature varied for different solubilities. However,

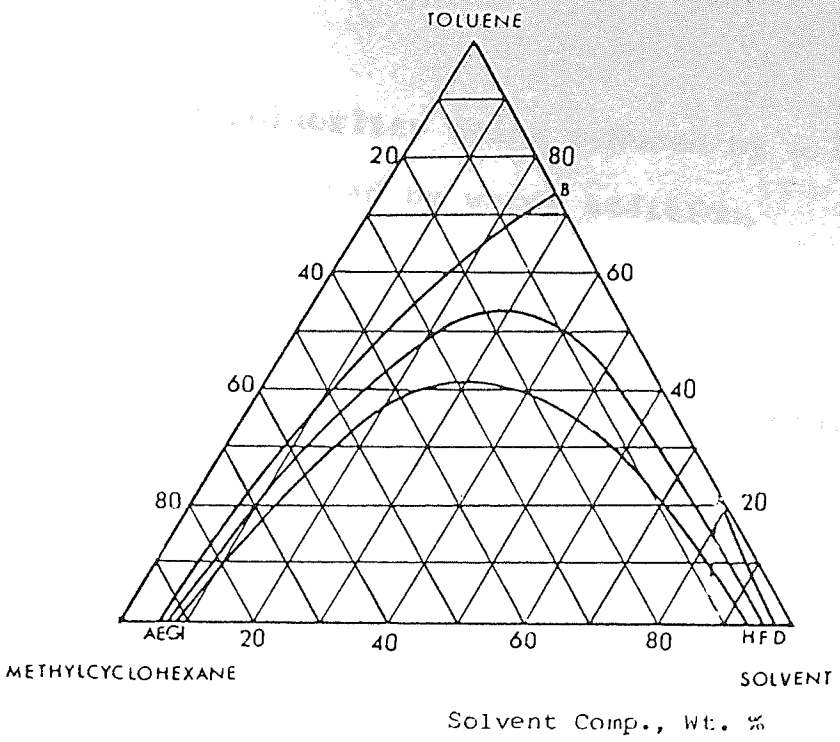

Area	NH_3	H_2O
AB-CD	86	14
EF	90	10
GH	95	5
IJ	100	0

Figure 3.5 : Effect of Anti - Solvent on Phase Equilibria.

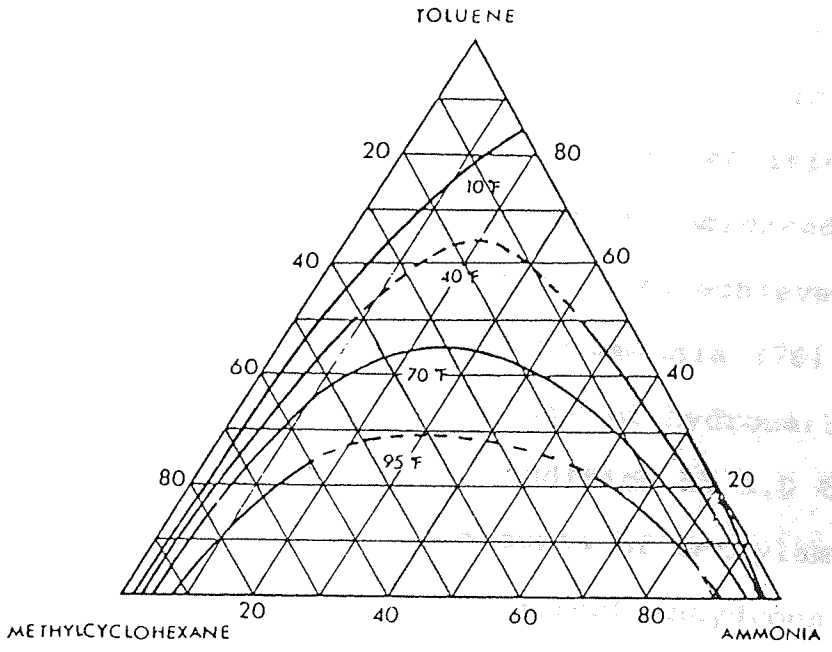

Figure 3.6 : Effect of Temperature Variations on Phase Equilibria.

instead of ths solubility being reduced by a temperature reduction it is reduced by water addition.

iii) Pro-solvents

High molecular weight hydrocarbons generally have low solubilities in liquid ammonia. In practical extractions this low solubility would necessitate use of high solvent to oil ratios resulting in high operating costs. The solubility could be increased by high temperature operation, but this is not practical since it would require high pressure equipment and hence increased capital investment. The addition of a pro-solvent is a better method of increasing the solubility. The pro-solvents which could be used with ammonia are high glycols, ethers and ether alcohols, methanol and other alcohols, amines, pyridine, the methylamines, other low molecular weight aliphatic amines, phenol and toluene. Among these mono-methylamine is most useful because of the ease of recovering it from the extract and raffinate streams together with ammonia in distillation column (75). The addition of 20 weight % mono-methylamine to ammonia increased the hydrocarbon solubility equivalent to that achieved by 17 to 23^{o}C temperature rise for pure ammonia (76) which is equivalent to doubling the solubility of hydrocarbons this effect may be neutralised by the addition of 5.0 to 5.5 weight % water (75). Moderate amounts of methylamine and water in anhydrous ammonia do not affect anhydrous ammonia.

3.6.2 Diluent

Solvents may sometimes be mixed with low-viscosity inert diluents to improve viscosity as in the dilution of tributyl phosphate with kerosene or even less viscous hydrocarbons for uranium extraction.

3.6.3 Practice and limitations

Although it is possible to alter the solvent power by addition of other liquids, the effectiveness of these modifying agents depends mainly on the properties and the characteristics of the primary solvent to which they are added. For most solvents, there are only a few modifying agents, due to the creation of unsuitable density factors, emulsion formation and mutual solubility, chemical interactions and corrosion problems. Some of these combinations cause some unexpected difficulties. For example, the addition of benzol to sulphur dioxide, which increases the solvent power considerably, reduces the selectivity. Addition of water to phenol reduces its solvent power but phenol-water mixtures are more corrosive than either phenol or water alone. Solubility of hydrocarbons in furfural and chlorex cannot be controlled by the addition of modifying solvents because both are chemically reactive. Although liquid sulphur dioxide is a good solvent for aromatics separation, very few liquids are soluble in liquid sulphur dioxide without chemical reaction or causing corrosion problems in the equipment. Furthermore,no modifying agents have been found to change the dissolving power of sulphur dioxide without reducing its selectivity.

In general, use of modifying agents for changing solvent power is restricted in application because of the disadvantages e.g. loss of selectivity, increase in corrosiveness, the production of emulsions, difficulty in separating the modifying solvent and the primary solvent from the hydrocarbon mixture and the incompatibility of the modifying solvent with the primary solvent over a wide range of concentration or hydrocarbon solubility. Extraction at a different temperature, or with modified solvents would certainly involve revision of the operation of the existing solvent recovery unit.

CHAPTER four 4

LIQUID-LIQUID EQUILIBRIA (LLE)

4.1 Introduction

In spite of its practical importance, LLE has not received as much attention in the literature as vapour-liquid equilibria (VLE). There are several reasons for this (77):

i) experimental determination of the LLE compositions can often be carried out on an ad hoc basis which reduces the incentive for correlation and publication,

ii) the correlation LLE can be, from a numerical point of view, much more difficult than the correlation of VLE,

iii) temperature effects are more pronounced for LLE than VLE, and

iv) economically, in the past, distillation plays a bigger role in industry than does extraction.

Traditionally, two different categories of models have been used in correlating LLE data:

i) Models which empirically describe component distribution ratios as functions of composition. Methods devised by Brancker, Hunter and Nash (79), Sherwood (49), Hand (78) and others are examples

of this type. Because of their empirical nature, models of this type can only be used for storage, interpolation and extrapolation purposes.

ii) Models which are founded in the thermodynamics of fluid-base equilibria. These models may, at least in principle, be used for both interpolation and extrapolation purposes.

4.2 EXPERIMENTAL DETERMINATION

When liquid extraction is considered as a possible means of separation, the solubility and distribution data must be known for the chosen solvent, since if the solvent selectivity is unfavourable, the separation by liquid extraction is not feasible and another solvent, or perhaps another operating temperature, must be employed. Whereas many technical and economic factors must be considered, solubility and solute distribution are the most important ones. If the requisite information is not available in the literature, or is incomplete, then it must be predicted or determined experimentally. Prediction by thermodynamic method is laborious, but it may serve as a guide in selecting solvents. Approximate qualitative methods of prediction are available and are subsequently reviewed, although it is frequently not possible to choose the most selective from a range of solvents, or to predict the extent of the mutual solubility promoted by the solute, these methods usually give sufficiently reliable information upon which to base a preliminary selection. Although potential solvents may be selected by approximate methods, solubility and tie line

data used in design are invariably determined experimentally and subjected to tests for thermodynamic consistency.

The experimental determination of solubility has recently been reviewed by Vold and Vold (80) and Zimmerman (81). Alders (64) and Gladel and Durandet (82) have reviewed the determination of solubility and solute distribution in some detail. It is clear that for a given apparatus, the five factors of particular importance in the determination of liquid-liquid equilibria are:

i) the purity of the materials used,

ii) temperature regulation,

iii) attainment of true equilibrium,

iv) method of sampling, and

v) analysis or detection of equilibrium.

It is considered that the following references give adequate details both of the apparatus required and of sufficiently accurate experimental techniques to permit a satisfactory determination of solubility and tie-line data (14 - 19).

4.2.1 Determination of Two-phase Areas

Of the existing methods of determining the shape of ternary two-phase areas the following are most frequently applied:

a) the analysis method, and

b) the titration method.

a) The analysis method

The principle of this method is that any heterogeneous system is separated into the coexisting phases, after which these phases are analysed separately. The analysis reveals the composition of the phases and hence their location in the ternary diagram.

Quantities of solvent and the pure components are weighed off or measured out (depending on whether the diagram is to be made on a basis of weight or volume) into a funnel/flask in such proportions as to make the resultant ternary system heterogenous. The separating funnel is placed in a thermostat that can be maintained at the required experimental temperature within ± 0.1°C. When the contents of the funnel have attained this temperature (which takes some 15 to 20 minutes in the case of not too viscous systems) the contents are vigorously stirred for a sufficient time for equilibrium between the phases to be reached. The funnel is kept in the thermostat bath until the coexisting phases have completely settled and separated, i.e. are possibly transparent.

If a high operating pressure is required, studies are normally carried out in a equilibrium bomb (75) which is jacketed and cooling water at a constant temperature from a thermocirculator, circulating through the jacket at sufficient rate to maintain the temperature of the contents constant. In view of the interesting solubility characteristics, an apparatus facilitating visual observation is preferred .

Vigorous agitation of an extraction system consisting of feedstock and solvent is usually necessary in order to establish equilibrium (or, more correctly, to approach it sufficiently closely) in a reasonably short time. The exchange of materials between the two phases takes place only by diffusion through the interfacial area and (if there is no stirring) by diffusion through the subsequent layers of the liquid phases. Thus, if the feedstock and the solvent were merely placed in a separating funnel, the exchange would take a very long time and would correspond to a very slow change in composition of the feed into the raffinate phase. Stirring greatly accelerates this process by two effects:

1) the interfacial area is enlarged, and

2) the material that has diffused across the interphase is distributed mechanically (and not only by diffusion) into the liquid phases.

The time required for exchange and the degree of stirring necessary depend, however, on several factors, amongst others on the viscosity of the phases and the interfacial tension. Typical estimation of the time involved for approach to equilibrium is as in Appendix IV.

By contacting two immiscible liquid phases in order to establish phase equilibrium, one of the phases is invariably dispersed into the other. The mixture formed thus consists of small droplets of one phase, (the dispersed phase) enclosed by the other (the continuous phase). Which of these two will be the dispersed phase is highly dependent on the phase ratio. Generally, the continuous phase is the one which constitutes the major quantity of the system.

The above mentioned phase settling involves three separate phenomena:

a) the coalescence of small droplets to larger ones,

b) the actual settling of the droplets, and

c) the formation of a second continuous phase from the settled droplets of the dispersed phase.

Which of these phenomena is the limiting factor in the total phase settling depends on many factors, e.g. temperature, phase ratio, interfacial tension, viscosity and density of the phases and on the way in which equilibrium has been established. In practice, this means that for extreme phase ratios and for coexisting phases near the plait point of a system phase settling may become extremely difficult.

The composition of this mixture is obtained by measuring its refractive index, specific gravity or another physical property, making use of the known (or previously determined) relationship between the physical property and the composition of the mixtures. Often, chemical analysis is resorted to. There are many modern analytical chemistry techniques for determining the compositions of ternary mixtures, e.g. ultra-violet and infra-red analyses, mass spectrometry, gas-liquid chromatography, etc.

b) The titration method

This method essentially consists of determining several points of the binodal curve by 'titration', calculating the composition of these 'saturated' mixtures and finally determining an appropriate physical property (e.g. density or

refractive index) of these mixtures. The physical property of the homogeneous (ternary) mixtures is plotted against the concentrations of their components. This graph is subsequently used for determining the composition of the two phases formed by the separation of ternary mixtures in the heterogeneous area, and thus finding the position of the tie-lines.

The reliability of the titration method is largely dependent on the accuracy with which the transition from a turbid to a clear system can be observed. The transition from a turbid to a clear solution is highly affected by very small changes in temperature.

The accuracy of the measurement by titration method can be checked by:

a) the position of initial heterogeneous mixture with respect to the tie-line,

b) the phase ratio, and

c) the material balance.

4.3 THERMODYNAMIC BASIS OF LIQUID-LIQUID EQUILIBRIA

In ternary systems, all three substances are present in both phases for phases in equilibrium. The activity 'a' of each substance must be the same in both phases, provided that the reference state chosen is the same throughout. This is assured by choosing as reference state, the pure components at the temperature and pressure of the system. Then, if the phases are A-rich and B-rich respectively,

$$a_{AA} = a_{AB},\ a_{CA} = a_{CB},\ a_{BA} = a_{BB} \qquad (4.3)$$

where a_{AB} = activity of A in B-rich phase, etc. If the activities can be expressed as functions of the concentration correctly, through consideration of data other than the liquid equilibria, then the equilibria can be predicted. Whilst the predicted equilibria are seldom sufficiently accurate for purposes of extractor design, it is possible to make useful predictions of the general trend of the equilibria, for purposes of choosing possible solvents in the absence of the data.

Provided the concentrations of C are taken as very small and the mutual solubility of pure A and B may be neglected, the initial distribution of C may often be estimated quickly. Introducing the definition of activity coefficient for C, $\gamma_C = a_C/x_C$ (4.4)

Equation(4.3)for C provides the distribution coefficient for C:

$$K_c = \frac{x_{CB}}{x_{CA}} = \frac{\gamma_{CA}}{\gamma_{CB}} \qquad (4.5)$$

where γ_{CB} = activity coefficient of C in the C-B binary.

γ_{CA} = activity coefficient of C in the C-A binary. Here, log $\gamma_{CA} = A_{CA}$ and log $\gamma_{CB} = A_{CB}$ where the A's are the Margules or van Laar constants for the binaries, or more generally, the logarithm of the activity coefficient of C in infinitely dilute solution in A or B, respectively. Thus,

$$\log K_{c,\ x_{c=0}} = A_{CA} - A_{CB} \qquad (4.6)$$

values of A's may be obtained from vapour-liquid data, generally. They may be estimated in the absence of data through such correlations as that of Pierotti, Deal and Derr (83) or, when applicable, through the regular solution theory of Hildebrand and Scott (44 , 84).

When the mutual solubility of components A and B is to be taken into account so as to calculate a complete binodal curve on a triangular phase diagram, Equation (4.3) must be satisfied for each of the three components for each tie-line to be estimated. Success will depend upon the applicability of the ternary activity - coefficient equations chosen to represent the ternary system. The problem is made difficult because these can rarely be made explicit in concentration.

Occasionally, the ternary solubility curve has been measured without equilibrium tie-lines. Then the computation to estimate equilibrium is much simpler: one need only compute one activity, a_c, for example, along the solubility curve, and tie-lines are located by joining places of equal values of this activity.

In general, much greater success in making estimates of this sort will be achieved if activity-coefficient equations containing at least one ternary constant can be used, but these require knowledge of some ternary equilibriums (either a liquid-liquid tie line, or vapour-liquid equilibrium measurement - even a ternary azeotrope) for evaluating the ternary constant. Treybal (24) shows the

excellent results obtained using the ternary Redlich-Kister equations (85). Renon and Prausnitz (86), have shown that ternary liquid equilibriums can be predicted quite well from binary data alone, using the "non-random, two liquid" (N.R.T.L.) activity coefficient equations.

4.3.1 Thermodynamic models for liquid-liquid equilibria

Three different types of models have been used:

i) models for activity coefficients or the excess Gibbs function,

ii) the equations of state, and

iii) group-contribution methods.

4.3.1.1 Models for activity coefficients

The different models used for correlating liquid-liquid equilibria are shown and briefly commented on in Table 4.1. The excess Gibbs energy G^E and the activity coefficients γ_i are interrelated by the following relationships:

$$G^E = RT \sum_i x_i \ln \gamma_i \qquad (4.7)$$

and

$$RT \ln \gamma_i = \left(\frac{\delta n_T G^E}{\delta n_i}\right)_{T,P,n_j} \qquad (4.8)$$

$$i = 1,2 \ldots N$$

where n_i is the number of moles of component i and n_T is the total number of moles. The differentiation is at constant temperature, pressure and number of moles of each component j except i.

TABLE 4.1: ACTIVITY COEFFICIENT MODELS FOR CORRELATING LIQUID-LIQUID EQUILIBRIA

Name and original reference	Equation for excess Gibbs function	Comments
Margules two-suffix (Margules, 1895)	$\frac{G^E}{RT} = \sum_i \sum_j A_{ij} x_i x_j$: $A_{ij} = A_{ji}$ $i,j = 1,2.....,N$	These equations can be used for correlating binary and ternary LLE but often the results are poor. They should not be used to predict ternary LLE from binary information or in extrapolation to concentrations outside the range of the data. The Margules and Van Laar equations contain only binary parameters. The Van Laar and Redlich-Kister equations are written for ternary mixtures: they can be extended to the general, multicomponent case.
Van Laar (Van Laar 1910)	$\frac{G^E}{RT} = \frac{A_{21}x_1x_2 + A_{31}x_1x_3 + A_{23}\frac{A_{31}}{A_{13}}x_2x_3}{x_1 + \frac{A_{21}}{A_{12}}x_2 + \frac{A_{31}}{A_{13}}x_3}$ (ternary: for binary $x_3 = 0$)	
Redlich-Kister (Redlich and Kister 1948)	$(\frac{G^E}{RT})_{12} = x_1x_2(B_{12} + C_{12}(x_1-x_2) + D_{12}(x_1-x_2)^2 + ..)$ (binary) $(\frac{G^E}{RT})_{123} = (\frac{G^E}{RT})_{12} + (\frac{G^E}{RT})_{13} + (\frac{G^E}{RT})_{23} +$ $+ x_1x_2x_3(C + D_1(x_2-x_3) + D_2(x_3-x_1) + ...)$ (ternary)	

Table 4.1 (Contd.. (1))

Name and original reference	Equation for excess Gibbs function	Comments
Kretschmer - Wiebe (Kretschmer and Wiebe, 1954)	It is assumed that one of the components linearly self-associating. The association equilibrium constant is correlated as a function of temperature. Binary equations are given by Kretschmer and Wiebe (1954): useful extensions to ternary systems are given by Sugi et al (1976) and Nagata et al (1978).	Mainly used for mixtures containing an alcohol. The correlation of binary and ternary systems is reasonably good, although difficulties are encountered when the two phase region is large. The prediction of ternary LLE from binary data appears questionable.
Black (Black,1959)	$\frac{G^E}{RT}$ = (Van Laar) + $C_{12}(x_1 - x_2)^2 x_1 x_2$ + $C_{23}(x_2 - x_3)^2 x_2 x_3$ + $C_{31}(x_3 - x_1)^2 x_3 x_1$ (ternary: for binary $x_3 = 0$)	Three parameters are needed per binary. Correlation of binary and ternary data reasonably successful. Should not be used to predict ternary VLE from binary data or to extrapolate beyond the range of the data.
Modifications of Wilson's equation (Wilson, 1964)	$\frac{G^E}{RT} = -C_{12}(x_1 \ln(x_1 + \Lambda_{12} x_2) + x_2 \ln(x_2 + \Lambda_{21} x_1))$ $C_{12} > 1$ (binary) $\Lambda_{ij} = (V_j/V_i) \exp(-(\lambda_{ij} - \lambda_{ii})/RT)$ $\lambda_{ji} = \lambda_{ij}$; $\Lambda_{ij} \neq \Lambda_{ji}$	Three parameters per binary. Cannot be generalized to multicomponent systems without additional assumptions. Not widely used for LLE.
	$\frac{G^E}{RT} = -\sum_{i}^{} x_i(\ln \sum_{j}^{} x_j \Lambda_{ij} + \ln \sum_{j}^{} x_j \rho_{ij})$ $\rho_{ij} = V_i/V_j$; $i,j = 1,2,.....,N$	Two parameters per binary. Correlate binary and ternary data well. Predictions of ternary LLE from binary data qualitatively satisfactory. May

Table 4.1 (Contd...(2))

Name and original reference	Equation for Excess Gibbs Function	Comments
	$\frac{G^E}{RT} = \sum_{i}^{} x_i \ln \frac{\xi_i}{x_i} + \frac{1}{2} \sum_{j}^{} \sum_{k}^{} (\beta_{jk}/RT)\, \xi_j \xi_k$ $\xi_i = \frac{x_i v_i \exp(-\lambda_{ii}/RT)}{\sum_{j} x_j v_j \exp(-\lambda_{ij}/RT)}$ $\beta_{jj} = \beta_{kk} = 0, \qquad \beta_{jk} = \beta_{kj}$ $i,j,k = 1,2, \ldots\ldots,N$	Three parameters per binary. Correlations and predictions appear to be of same quality as NRTL (see below). Not thoroughly tested.
	$\frac{G^E}{RT} = - \sum_{i}^{} C_i x_i \ln(\sum_{j}^{} x_j \Lambda_{ij})$ $C_i = (V_i/V^0)^{1/m}; \qquad i,j = 1,2, \ldots\ldots,N$ m = constant, often 3	Same remarks as for the modification of Nagata et al (1975)
Modifications of Wilson's equation (Wilson, 1964)	$\frac{G^E}{RT} = - \sum_{i}^{} x_i \ln(\sum_{j}^{} \varphi_j \Lambda_{ij}); \qquad i,j = 1,2,\ldots,N$ Λ_{ij} now takes into account interactions from both nearest and next nearest neighbours. An expression for Λ_{ij} is given. It has the form: $\Lambda_{ij} = f(\beta_{ij}, \Lambda^0_{ij}, \Lambda_{ij}, x_i \; x_j)$ β_{ij} is a constant, ~ 0.85	Same remarks as for the modification of Nagata et al. Requires additional computation, since the model cannot be written in an explicit form.

Table 4.1 (Contd....(3))

Name and original reference	Equations for Excess Gibbs function	Comments
NRTL (Renon, 1966) and modifications	$\frac{G^E}{RT} = \sum_{i}^{} x_i \frac{\sum_{j}^{} \tau_{ji} G_{ji} x_j}{\sum_{1}^{} G_{1i} x_1}$; i,j,1 = 1,2,...N $\tau_{ji} = (g_{ji} - g_{ii})/RT$; $G_{ji} = \exp(-\alpha_{ji}\tau_{ji})$ $g_{ji} = g_{ij}$; $\tau_{ji} \neq \tau_{ij}$; $G_{ji} \neq G_{ij}$ $\alpha_{ji} = \alpha_{ij}$	The most used model for LLE to date. There are three parameters per binary: τ_{ij}, τ_{ji}, and α_{ij}. The term α_{ij} may be fixed according to Renon and Prausnitz (1968). Correlation of binary and ternary LLF is often quantitatively correct. Prediction of ternary LLE from binary data is often qualitatively correct. Can be used in extrapolation with respect to composition.
LEMF	Similar to NRTL As NRTL with $\alpha_{ij} = -1$, all i and j	Two parameters per binary. Not thoroughly tested.
NRTL (Renon, 1966) and modifications	$\frac{G^E}{RT} = \text{NRTL} - \sum_{i}^{} x_i \ln\left(\sum_{j}^{} G_{ji} x_j\right)$	Only two parameters per binary. Approximately same quality of results as NRTL with α_{ij} fixed accordingly to Renon and Prausnitz (1968).
(Heil and Prausnitz, 1966)	$G_{ji} = (V_j/V_i) \exp(-\tau_{ji})$ i,j = 1,2,.....,N	Only two parameters per binary (G_{ij} does not contain α_{ij}). Not as good as NRTL for ternary LLE. Cannot be used for large miscibility gaps.

Name and original reference	Equations for Excess Gibbs function	Comments
UNIQUAC (Abrams and Prausnitz, 1975) and modifications	$G^E = G^E_{comb.} + G^E_{res.}$ $G^E_{comb.}/RT = \sum^{i} x_i \ln \frac{\varphi_i}{x_i} + \frac{z}{2} \sum^{i} q_i x_i \ln \frac{\theta_i}{\varphi_i}$ $G^E_{res.}/RT = - \sum^{i} q_i x_i \ln(\sum^{j} \theta_j \tau_{ji})$ $\theta_i = x_i q_i / \sum^{j} x_j q_j$ (surface area fraction) $\varphi_i = x_i r_i / \sum^{j} x_j r_j$ (volume fraction) $\tau_{ji} = \exp(-(u_{ji} - u_{ii})/RT)$ $\tau_{ji} \neq \tau_{ij}$; $z = 10$ $i,j = 1,2,\ldots,N$	Only two parameters per binary (τ_{ij} and τ_{ji}). Correlation of binary and ternary LLE is often quantitatively correct. Prediction of ternary LLE from binary data often qualitatively correct. Can be used in extrapolation with respect to composition. In this work we conclude that UNIQUAC is as good or better than NRTL for correlating LLE.
	"LSG" Similar to UNIQUAC "LCG"	Two parameters per binary. Not thoroughly tested. May yield similar results as UNIQUAC.

* Full references are given on page 350

The Margules, Van Laar, Redlich-Kister and Black equations have in common that they in the past have been useful for correlating liquid-liquid equilibrium data, often with quite good results. However, extrapolation to concentrations beyond the range of the data or the prediction of ternary phase diagrams from only binary information should not be carried out with these models - the results are often not even qualitatively correct.

Local composition models (modifications of Wilson's equation NRTL and UNIQUAC) have proven superior to the older models, both for correlating binary and ternary liquid-liquid equilibria and for predicting ternary phase diagrams from binary data. The correlation can often be done with an accuracy sufficient for design purposes, and the predictions are frequently qualitatively correct. Modifications of Wilson's equation and NRTL have received much attention in the literature on liquid-liquid equilibria in recent years - NRTL because it has proven relatively successful for correlating liquid-liquid equilibria, and Wilson's equation because it has only two adjustable parameters per binary, whereas NRTL has three. Among the many proposed modifications of Wilson's equation, that due to Hiranuma (87) is relatively well documented (88). Hiranuma's modification is difficult to use, since it is not explicit in concentration. All-in-all, in liquid-liquid equilibrium calculations NRTL is preferable over the various modifications of Wilson's equations.

The UNIQUAC model has only two adjustable parameters per binary. For a few systems, Abrams and Prausnitz (89)

show that UNIQUAC predicts very well ternary diagrams from binary information when binary vapour-liquid and liquid-liquid equilibrium data are correlated simultaneously with only a few ternary tie-lines.

4.3.1.2 Equations of state

The activity coefficient of component i in a mixture is related to the mixture P-V-T properties by the relationship:

$$\gamma_i = \frac{P}{P_i^\circ} \exp\left\{\frac{1}{RT}\int_0^P \left[\left(\frac{\delta nV}{\delta n_i}\right)_{T,P,n_j} - \frac{RT}{P}\right] dP\right\} \qquad (4.8)$$

where P_i° is the pure component vapour pressure and n_i is the number of moles of components i. An expression for γ_i can thus be derived from any equation of state which relates P, V and T. It is therefore, in principle, possible to predict liquid-liquid equilibria from equations of state.

The computation of liquid-liquid equilibria using equations of state has to date received only limited attention.

4.3.1.3 Group contribution models

The number of different mixtures in chemical technology is very large. The desired experimental information cannot always be found. It is, therefore, necessary to rely on some generalized method for prediction of the required information.

The basic assumption of group-contribution methods for predicting activity coefficients is that the liquid solution

can be treated as a solution of the groups which make up the components of the mixture. The "groups" are convenient structural units such as $-CH_3$, $-CH_2O-$, $-CH_2NO_2$ and H_2O. The size and shape of the group and the interactions between the groups determine the properties of the liquid mixture. Notable in this development are the pioneering work by Pierotti, Deal and Derr (83), Wilson and Deal (90) and subsequent contributions by Scheller (91), Ratcliff and Chao (92), Derr and Deal (93) and Fredenslund, Jones and Prausnitz (94). Lee, Greenkorn and Chao (95) extended the group contribution concept by expressing it in terms of a particular function description of a molecular model.

4.3.2.1 UNIFAC group contribution

The UNIFAC group contribution developed by Fredenslund et al (94) provides the chemical engineer with a straight forward, reliable method for predicting activity coefficients in non-electrolyte solutions when little or no experimental equilibrium data exists. The UNIFAC method has been applied to vapour-liquid, liquid-liquid and solid-liquid equilibria calculations with good results. Lo and Paulitis (96) combined UNIFAC with transition state theory to predict thermodynamic solvent effects on chemical reaction rates in solution.

For liquid-phase reactions, a number of different approaches can be used to obtain the activity coefficients from excess Gibbs energy expressions for mixtures (97). These approaches have two primary limitations:

i) Application of any solution theory to evaluate activity coefficients requires some knowledge of the transition state structure and properties, and these data are usually scarce.

ii) Predictive solution theories that have been used previously are not adequate for highly non-ideal solutions (e.g. polar or associating systems) where the solvent effects on reaction rates are greatest.

One advantage of utilizing UNIFAC to predict activity coefficient is that only the number and types of groups in the transition state are required, physical properties are not necessary. The UNIFAC method is also applicable to a wide range of solution non-idealities, including polar and associating systems, and is limited only by the number of accurate group interaction parameters that are currently available.

4.4 REPRESENTATION OF LLE DATA

Ternary LLE data may be conveniently represented on triangular graphs as shown in Section 2.2.

Another method of representation is by a distribution curve obtained by plotting the equilibrium composition of the solute in the solvent-rich phase against the equilibrium composition of the solute in the diluent-rich phase as shown in Figure 4.1. The slope of the equilibrium distribution curve thus obtained gives the value of the distribution coefficient, m, at any location of the curve. If the distributions favours the solvent-rich phase, then the curve is located above the 45^{o} line indicating that the distribution ratio is more than unity. The curve tends to be straight

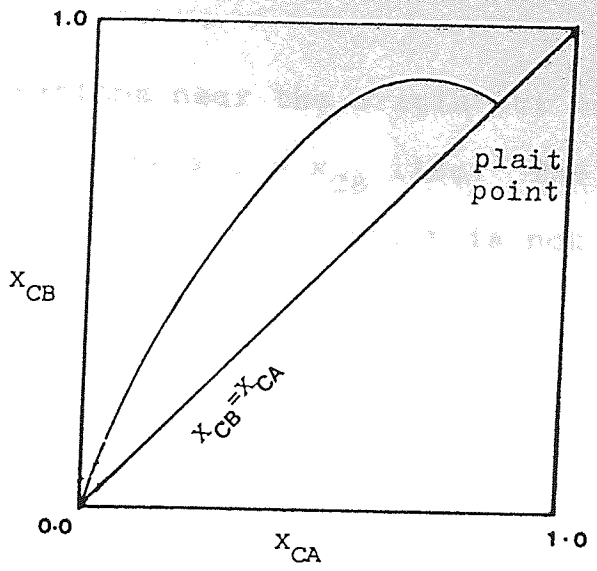

Figure 4.1 : EQUILIBRIUM DISTRIBUTION DIAGRAM.

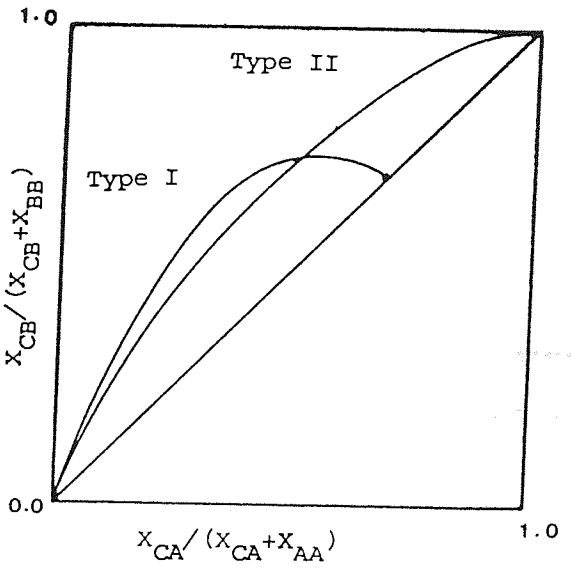

Figure 4.2 : SELECTIVITY DIAGRAM.

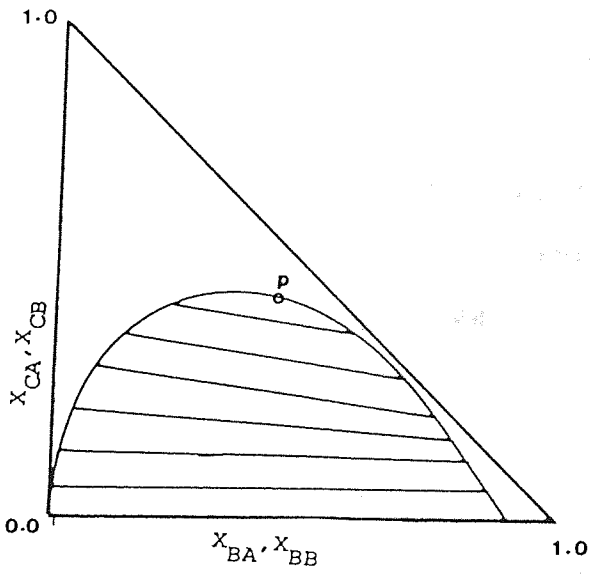

Figure 4.3 : RIGHT - TRIANGULAR DIAGRAM.

at low concentrations near the origin but terminates at the plait point on the $x_{CA} = x_{CB}$ line. The curve passes through a maximum if the plait point is not exactly at the peak of the binodal curve.

The equilibrium distribution data may also be represented on solvent-free basis in order that the true selectivity of the solvent may be obtained. Figure 4.2 is especially useful to assess the selective power of the solvent for extraction of the scale in question.

The points denoting various compositions of the liquid phases are liable to be crowded in certain regions of the equilateral triangular diagram. For the sake of convenience and clarity of these regions, right-triangular method as shown in Figure 4.3, is resorted to. The concentration of solute is represented as ordinate and that of either solvent or diluent concentration as abscissa. The concentration of the third component is obtained by difference. Figure 4.4 indicates the Janecke coordinates, where the concentrations of solvent in both phases are plotted against the concentration of solute in both phases, on solvent-free basis. For systems in which the solvent and diluent are completely immiscible, the method as shown in Figure 4.5, whereby the concentration of solute in the conjugate phases at equilibrium are plotted on solute-free parameters, is often used.

4.4.1 Tie-line correlation methods

Correlation methods of tie-lines in ternary phase systems are being increasingly used on account of availability of only a limited number of actual experimental tie-line data

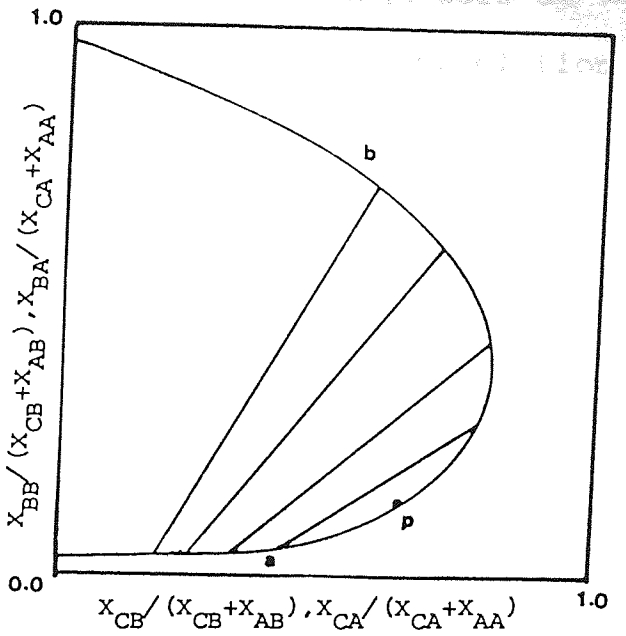

a - diluent rich
b - solvent rich

Figure 4.4 : JANECKE DIAGRAM ON SOLVENT-FREE COORDINATE.

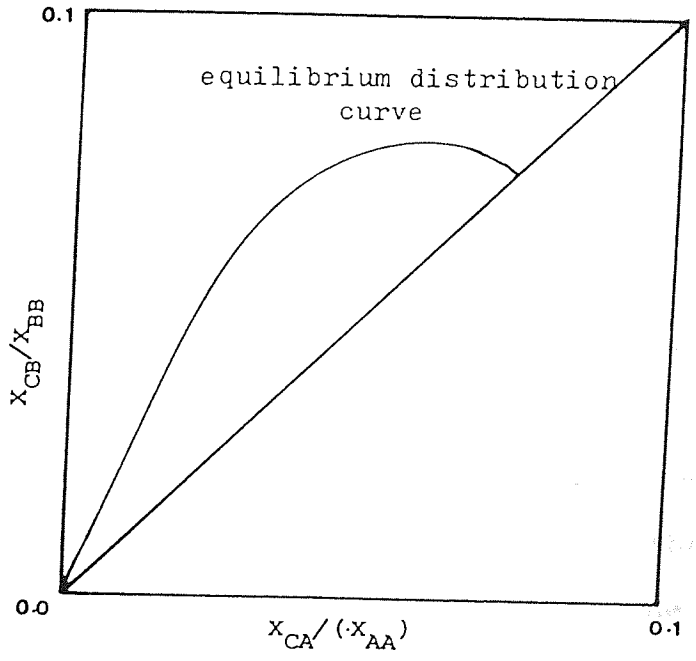

Figure 4.5 : DISTRIBUTION CURVE ON SOLUTE-FREE BASIS.

for most of the liquid systems. Equilibrium information is needed for actual design work at any point in the heterogenous region and hence interpolation methods have been proposed.

4.4.1.1 Graphical methods

Two types of construction of conjugate or auxillary curves, viz external and internal construction, are possible with the help of which interpolation of tie line at any location may be obtained.

In Figure 4.6, if DE is a tie-line DG may be drawn parallel to CB, and EF parallel to AC, the two constructed lines intersecting at H. A tie-line correlation curve or conjugation curve PHJ is then drawn through several such intersections obtained from corresponding known tie-lines. From any point on the tie-line correlation curve, two constructed lines parallel, respectively, to AC and BC will intersect the solubility curve at concentrations corresponding to conjugate solutions. The curves PHJ is not straight although the curvature is ordinarily small, and it necessarily passes through the plait point. The method is excellent for interpolation in cases where at least three or four tie-lines are known but is not very precise for extrapolating any considerable distance because of the curvature of the correlation curve. The position of the plait point can be found by extrapolation only when tie-lines very close to the plait point are known. The method is extensively used in the 'International Critical Tables'.

The modification shown in Figure 4.7, devised by

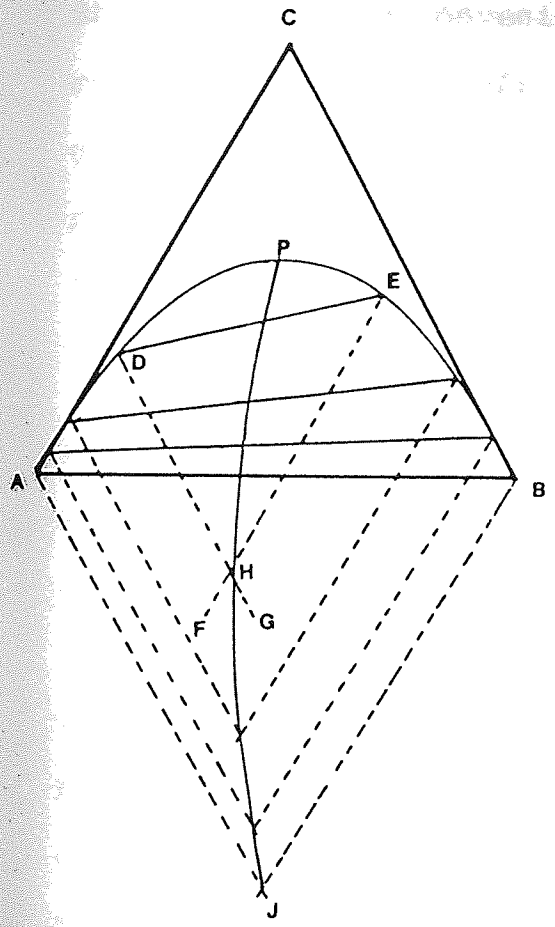

Figure 4.6 : EXTERNAL CONSTRUCTION FOR TIE LINE INTERPOLATION.

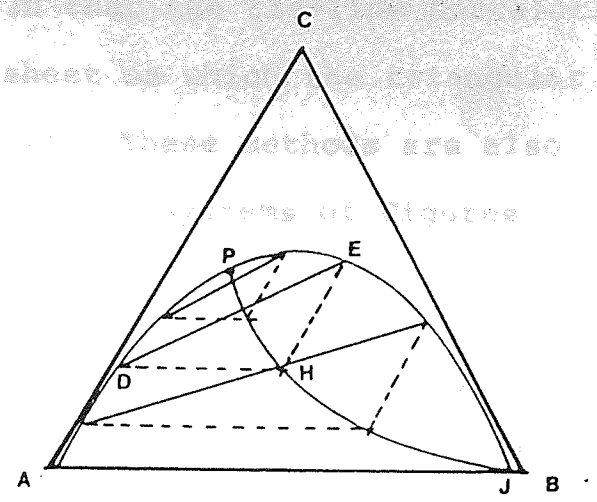

Figure 4.7 : INTERNAL CONSTRUCTION FOR TIE LINE INTERPOLATION.

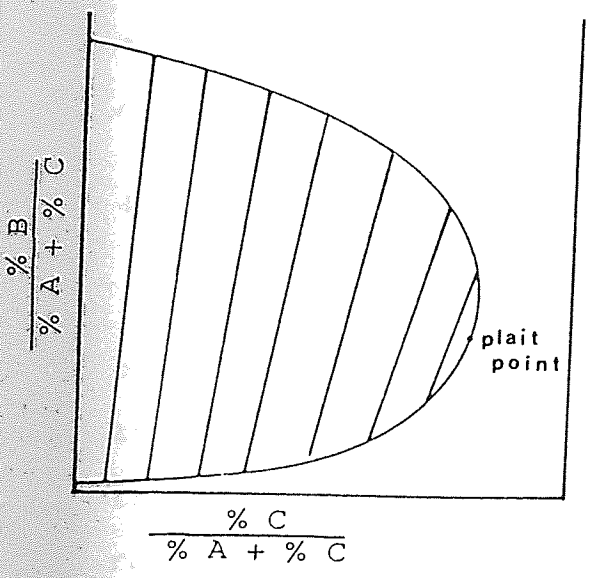

a) Type I

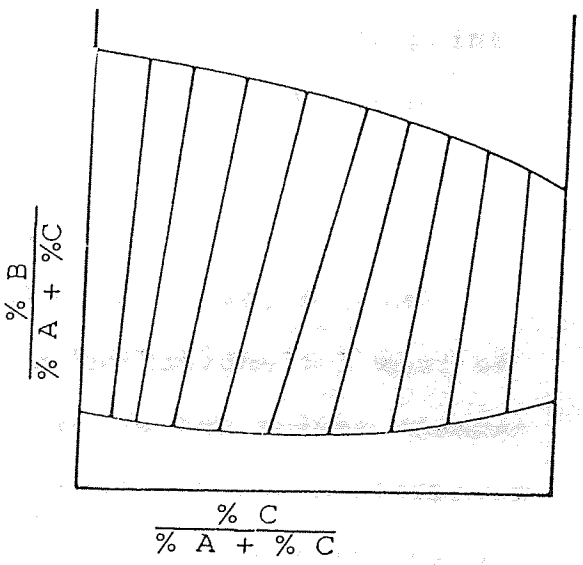

b) Type II

Figure 4.8 : TIE-LINE CORRELATION ON RECTANGULAR DIAGRAM.

Sherwood (49) is convenient in that the tie-line correlation curve does not fall off the sheet on which the triangular graphs are ordinarily available. These methods are also readily extended to the rectangular systems of Figures 4.8(a) and 4.8(b).

Hand ([78]) presented an interesting method of plotting the ternary data in such a manner as to make the tie-lines of type 1 systems all parallel to the base of the triangle, at least for some systems. The method is unfortunately not generally applicable, and not many systems yield to the treatment. In some cases, the tie-lines, when extended beyond the binodal curve, all intersect at a single point on the extended base of the triangle ([98]). It can be shown mathematically ([99]) that this can only occur if the system follows Hand's rule, and such behaviour is therefore not general. Nevertheless, if two tie-line intersect at a point on the extended base, it is very likely that the others do also, which provides a convenient means of interpolating and extrapolating equilibrium data. In such situation, the plait point can be located by a line from the point of intersection that is tangent to the binodal curve.

4.4.1.2 Empirical methods

The variation of the distribution ratio, m, has been found to be linear at low concentrations for most of the systems, and hence any variation in the solute concentrations due to extraction does not affect the equilibrium ratio appreciably. However, at higher concentrations of the solute, the extraction equilibria are very much affected as indicated by the wide variation of the

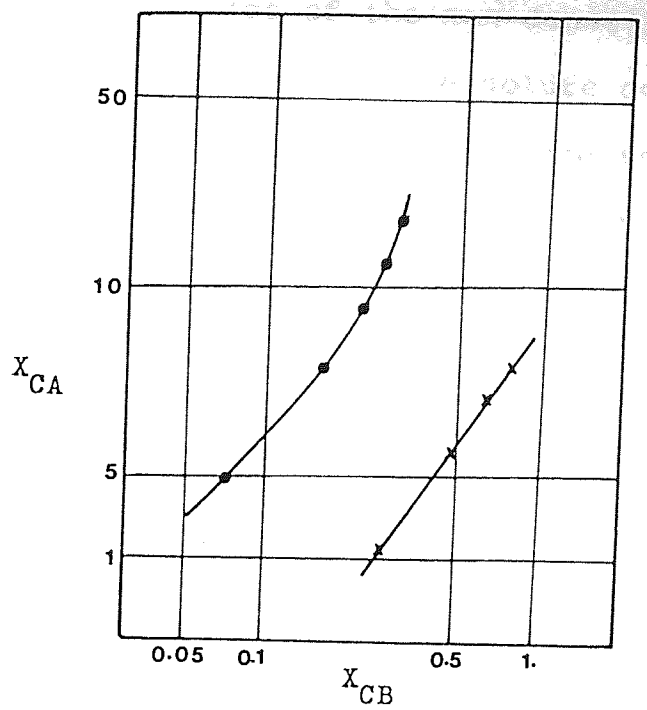

Figure 4.9 : CAMPBELL'S CORRELATION.

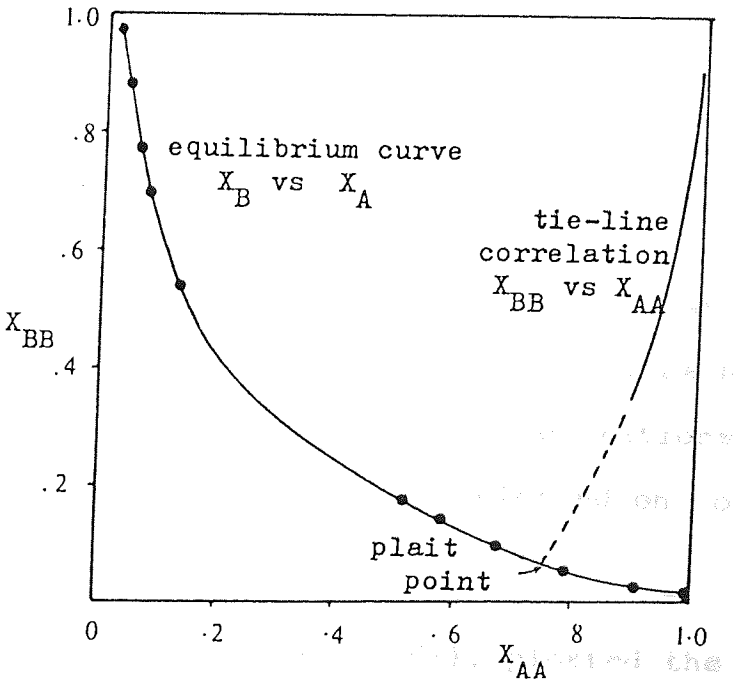

Figure 4.10 : BRANCKER'S CORRELATION.

distribution ratio values on account of the variations in the mutual solubilities of the non-consolute pair with increase in concentration of the solute component. Hence many investigators have suggested correlation methods for interpolation of tie-line data taking into account the equilibrium distribution of the diluent and solvent components instead of the distribution composition of the solute.

Campbell (100) suggested that the general equation for the distribution may be expressed in the form:

$$m = \frac{\left[\gamma_{CA} \, X_{CA} \, (1-k_A) \right]^{n'}}{\left[\gamma_{CB} \, X_{CB} \, (1-k_B) \right]^{n''}} \qquad (4.9)$$

where k is the degree of dissociation, n' and n" are the number of molecules of solute C at equilibrium in the diluent and solvent respectively. It has been observed however, that a simple equation of the form

$$m = X_{CA}^{n} / X_{CB} \qquad (4.10)$$

should correlate the data for a majority of distributed systems. Straight lines with a slight curvature near the plait point are obtained, when the concentrations of the solute in the conjugate phases are plotted on logarithmic papers, as shown in Figure 4.9.

Brancker, Hunter and Nash (101), plotted the concentration of the diluent in the diluent phase, X_{AA}, versus the concentration of the solvent in the solvent phase on the Cartesian coordinates which resulted in correlation lines sometimes with pronounced curvature . The plait point

for the system could be obtained by extrapolating this curve to meet the solubility curve plotted in the same graph, the point of intersection indicated the composition of the plait point, as shown in Figure 4.10.

For a study of the results of Brancker et al (101) Bachman (102) observed that straight line correlations could be directly obtained if proper functions of the concentrations are chosen as dependent and independent variables. He suggested:

$$X_{BB} = (r+b)\left[X_{BB}/X_{AA}\right] \qquad (4.11)$$

where 'r' and 'b' are constants.

Later, Othmer and Tobias (103) showed that the equations above is limited in application since it is based on ternary systems composed of practically immiscible non-consulate components. They modified Bachman's equation so that a plot of the conjugate values of $(\frac{1-X_{AA}}{X_{AA}})$ versus $(\frac{1-X_{BB}}{X_{BB}})$ on logarithmic coordinate produce straight lines. However, the Othmer and Tobias method also suffers from the fact that this formulation does not include the concentration of the distributed component. Hence, it would appear that the most useful formula is that of Hand (78) which correlates the concentration of the solute in the two conjugate solutions. Hand's equation is represented by:

$$\frac{x_{CA}}{x_{AA}} = K\left(\frac{x_{CB}}{x_{BB}}\right)^{r} \qquad (4.12)$$

The logarithmic plot of $\frac{x_{CA}}{x_{AA}}$ against $\frac{x_{CB}}{x_{BB}}$ is rectilinear.

With cartesian coordinates such as the above, the attempt to obtain empirical rectilinear plots of the tie-line data, thereby facilitating accurate interpolation, have been successful but it is less accurate if solutropy occurs.

Ishida (104) dealt with many solutropic systems as well as other ternary systems by plotting the data by an equation of the form:

$$\left(\frac{X_{CB}\ X_{BA}}{X_{CA}\ X_{BB}}\right) = K \left(\frac{X_{AB}\ A_{BA}}{X_{AA}\ X_{BB}}\right)^{n} \qquad (4.13)$$

When the solvent and diluent are practically insoluble, the values of $(X_{AB}X_{BA}/X_{AA}X_{BB})$ and $(X_{CB}X_{BA}/X_{CA}X_{BB})$ become more inaccurate at the lower concentration of solute, since the solute concentrations are too small for any accurate estimation by routine analytical methods. Hence, by using this method for such highly immiscible diluent-solvent binaries, better distribution data at near-zero concentrations of solute can be estimated when fairly accurate experimental tie-line data are available at higher solute concentrations.

4.4.2 Estimation of plait point

Plait points in the ternary systems indicate the maximum concentrations of the solute in the raffinate phase that can possibly be handled in any extraction system. Various methods are available and the three commonly used methods are:

i) The conjugate curve method,

ii) Brancker's method (101) and

iii) Treybal's method (24).

The first two methods have been discussed in Sections 4.4.1.1 and 4.4.1.2. The third method is more accurate prediction of the plait point. An illustration of this method is given in Figure 4.11. Treybal suggested plotting solubility data on the same diagram in which the tie-line data were plotted according to Hand's method. The point of intersection of the two curves should indicate the plait points, since at the plait point the distinction between the diluent-rich layer and solvent-rich layer vanishes.

4.4.3 Graphical stagewise analysis

The following graphical methods are adopted for evaluating the countercurrent multistage extraction process variables:

1) Difference point method (58),

2) Distribution coordinate method (17), and

3) Solvent-free coordinate method (59).

1) Difference point method.

Suppose that the feed F, final extract E, fresh solvent S (= stream E_{n+1}) and final raffinate R_n are to be fixed, then taking material balances:

a) Over 1st stage:

$$F + E_2 = R_1 + E_1 \qquad (4.14)$$

$$F - E_1 = R_1 - E_2 = D \text{ ; the difference stream} \qquad (4.15)$$

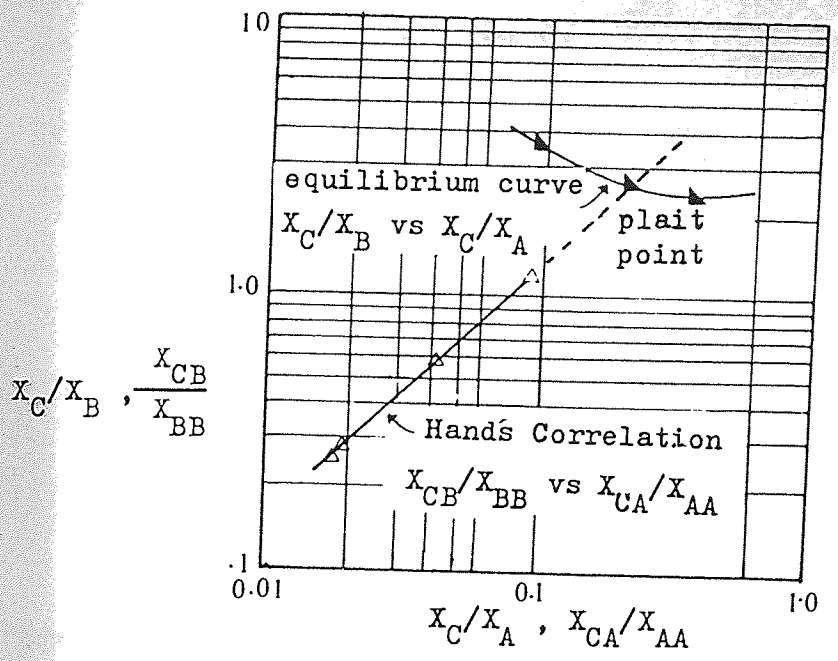

Figure 4.11 : TREYBAL'S METHOD OF PLAIT POINT ESTIMATION.

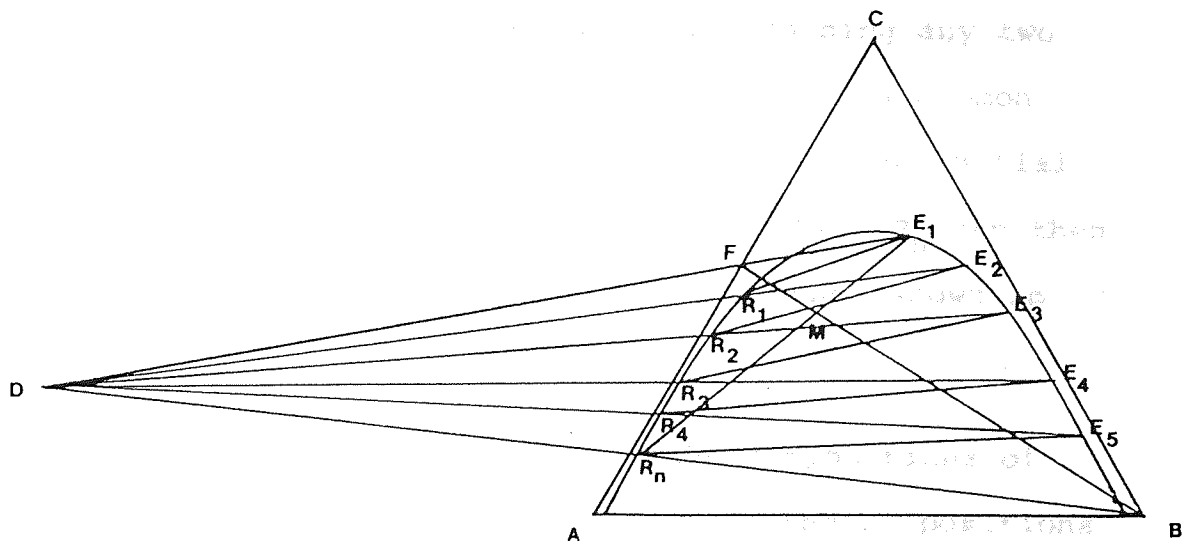

Figure 4.12 : DIFFERENCE POINT METHOD OF STAGEWISE ANALYSIS.

b) Over stages 1 to n:

$$F + E_{n+1} = R_n + E_1 = M_1, \tag{4.16}$$

$$F - E_1 = R_n - E_{n+1} = D \tag{4.17}$$

c) Over n^{th} unit:

$$R_{n-1} + E_{n+1} = E_n + R_n \tag{4.18}$$

$$R_{n-1} - E_n = R_n - E_{n+1} = D \tag{4.19}$$

Thus the difference in quantity between the raffinate leaving a stage R_n, and the extract entering the next stage E_{n+1}, is constant. Similarly it can be shown that the difference between the amounts of each composition in the raffinate and the extract streams will be constant. This means that, with the notation of a triangular diagram, lines joining any two points representing R_n and E_{n+1} will pass through a common pole. The number of stages required to pass from an initial concentration F to a final raffinate concentration R_n can then be found using a triangular diagram, by the method shown in Figure 4.12.

If the points F and S representing the compositions of the feed and fresh solvent S are joined, then the compositions of a mixture of F and S is shown by point M where

$$\frac{MS}{MF} = \frac{\text{mass of F}}{\text{mass of S}} \tag{4.20}$$

Draw a line from R_n through M to give E, on the binodal curve. Draw E, F and SR_n to meet at the pole D. It should be noted that D represents an imaginary mixture.

Then, in an ideal stage, the extract E_1 leaves in equilibrium with the raffinate R_1, so that the point R_1 is at the end of the tie-line through E_1. To find the extract E_2, draw PR_1 to cut the binodal curve at E_2. Then the points R_2, E_3, R_3, E_4, etc., can be found in the same way. If the final tie-line (say E_4R_4) does not pass through R_n, then the amount of solvent added is incorrect for the desired change in composition. This does not generally invalidate the method, since it will give the required number of ideal stages sufficiently accurately.

The main objection to the graphical methods of stagewise analysis is that the difference point will be found to be a considerable distance from the equilibrium curve, and for constant distribution ratio, the distance would be measured in metres. The result is that on occasions, the design engineer must tolerate small inaccurate diagrams where the constructional lines are terribly congested; or make use of the arithmetical stage-to-stage material balance calculations. The latter method is laboriously time consuming and therefore numerous suggestions have been made whereby this difficulty is overcome. One such method involves a small approximation but is very convenient:

For a counter current extraction process locate the feed composition on the triangular design and carry out the material balance construction to establish x_n and y_1. In Figure 4.13, draw the lines $\overline{y_1F}$ and $\overline{Ex_n}$ which if produced would intersect at the difference point D. However, on this occasion it is assumed that the difference point would be a considerable distance from the triangular diagram and cannot be determined.

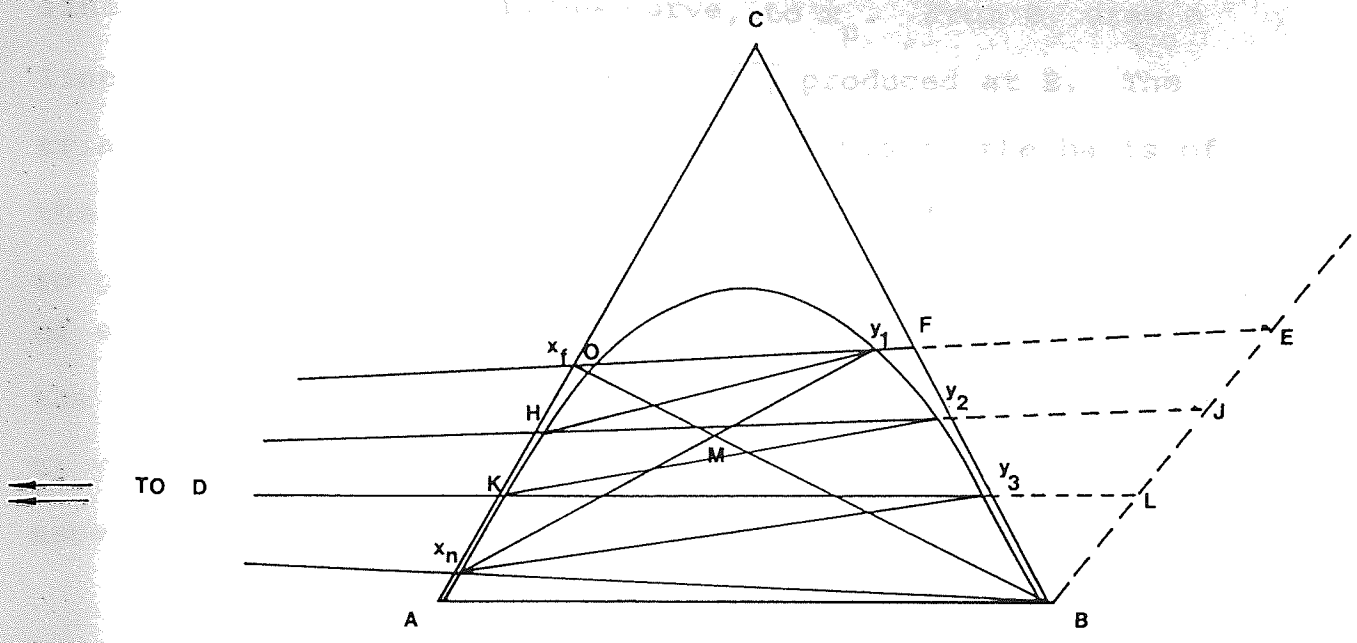

Figure 4.13 : APPROXIMATION METHOD FOR STAGEWISE ANALYSIS.

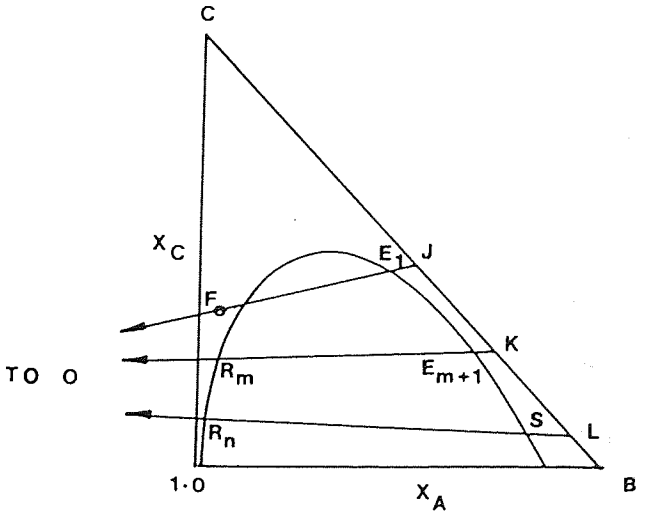

Figure 4.14 : ANALYTIC - GRAPHIC METHOD FOR STAGEWISE ANALYSIS.

Hence, draw a straight line from O, the intersection of the line $\overline{y_1 F}$ and the equilibrium curve, to x_n. From B, draw a line parallel to Ox_n to intersect $\overline{Fy_1}$ produced at E. The triangles DOx_n and DBE are similar and this is the basis of the stagewise analysis. Therefore, from y_1 draw the tie-line to give x_1,. This tie-line cuts $\overline{Ox_n}$ at H and by the property of similar triangles $\overline{OH}/\overline{Ox_n}$ is equal to $\overline{EJ}/\overline{EB}$ which establishes the point J. Join HJ which intersects the equilibrium curve at y_2 and by continuing in this way the number of stages necessary for the separation is estimated.

The accuracy of the above stagewise analysis depends on the extent of the curvature of the equilibrium line between O and x_n compared with the straight line $\overline{Ox_n}$ but in most cases encountered in practice, the equilibrium curve between O and x_n will approximate to a straight line coinciding with the line $\overline{Ox_n}$. In cases where the equilibrium curve is a straight line, the construction is rigorous.

Another alternative for cases when the difference point D falls at an inconveniently large distance from the phase diagram is by analytic-graphic computation as illustrated in Figure 4.14.

After locating points F, R_n, S and through the material balance point E, extend line FE, to the BC side of the triangle at J and line $R_n S$ to L. The equation of line FI is

$$X_C = \left(\frac{X_{CF} - X_{CS}}{X_{AF}}\right) X_A + X_{CS} \qquad (4.21)$$

and of line $R_n L$:-

$$X_C = \left(\frac{X_{CR_n} - X_{CL}}{X_{AR_n}}\right) X_A + X_{CL} \qquad (4.22)$$

Equating Equations (4.21) and (4.22) gives the coordinates of point O:

$$X_{AO} = \frac{X_{CJ} - X_{CL}}{(X_{CJ} - X_{CF})/X_{AF} - (X_{CL} - X_{CR_n})/X_{AR_n}} \qquad (4.23)$$

X_{CO} may be found by substituting X_{AO} so computed in Equation (4.23). The position of point K, representing the extension of line $OR_m E_{m+1}$ may be found from:

$$X_{CK} = \left(\frac{X_{CO} + X_{CR_n}}{(X_{AR_m} - X_{AO})}\right) X_{AO} + X_{CO} \qquad (4.24)$$

Therefore, locate R_1 at the end of the tie-line through E_1, compute X_{CK}, and plot K. Draw R_1 K to locate E_2 at the binodal curve, etc. The equations and calculations apply also to the equiliateral triangle and to cases where point D is on the solvent side of the diagram. They may also be extended to the Janecke coordinate system.

2) Distribution Coordinate Method

When the number of stages is large, it may be more convenient to use a distribution diagram as shown in Figure 4.15. The equilibrium line on the distribution diagram is located from the tie-line data. To fix the operating line on the equilibrium distribution diagram Figure 4.16 is used, in which a few lines are drawn at random to intersect the binodal curve to locate y_p and x_{p-1}, corresponding to any stage p within the region of the lines DFE_1 and DR_nS. These values of y_p and x_{p-1} are then transferred to the distribution diagram to get the operating line. The theoretical stages are then stopped off in a manner similar to McCabe-Thiele construction used in distillation.

3) Solvent-free Coordinate Method

This method is similar to Ponchon-Savarit method of stage calculations in distillation . Figure 4.17 shows the construction for solvent-free coordinates.

Material balance for the entire process on solvent-free basis is:

$$F' + B' = E_1 + R_n' = M \tag{4.25}$$

Ordinarily if the feed is solvent-free, F' will be equal to F and if the solvent used is pure, B' will be equal to zero. A material balance on the solute gives:

$$F'x_F' + B'y_B' = E_1'y_1' + R_n'x_n' = M'x_M' \tag{4.26}$$

and the solvent balance is:

$$F'N_F + B'N_B = E_1'N_E' + R_n'N_{Rn} = M'N_M \tag{4.27}$$

The points B, R_n, F, E_1 can be easily located if the respective concentrations for any specific extraction job are known. The point M lies on the intersection of the lines E_1, R_n and B_F. Equations 4.25 and 4.27, give the following relationships for estimation of N_M and x_M':

$$N_M = \frac{F'\ N_F + B'\ N_B}{F' + B'} \tag{4.28}$$

$$x_M' = \frac{F'\ x'_F + B'\ y'_B}{F' + B'} \tag{4.29}$$

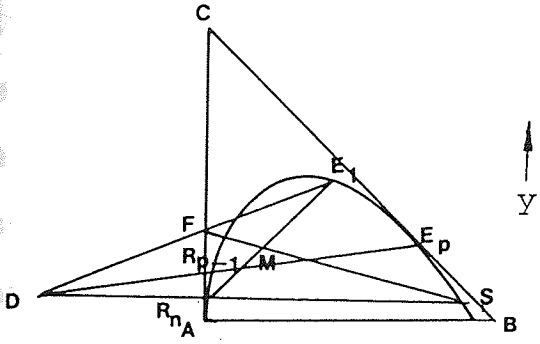

Figure 4.15 : Right Triangular Diagram

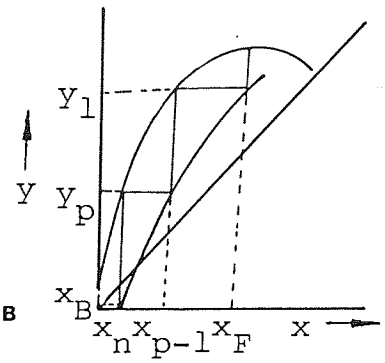

Figure 4.16 : Equilibrium Diagram

DISTRIBUTION COORDINATE METHOD.

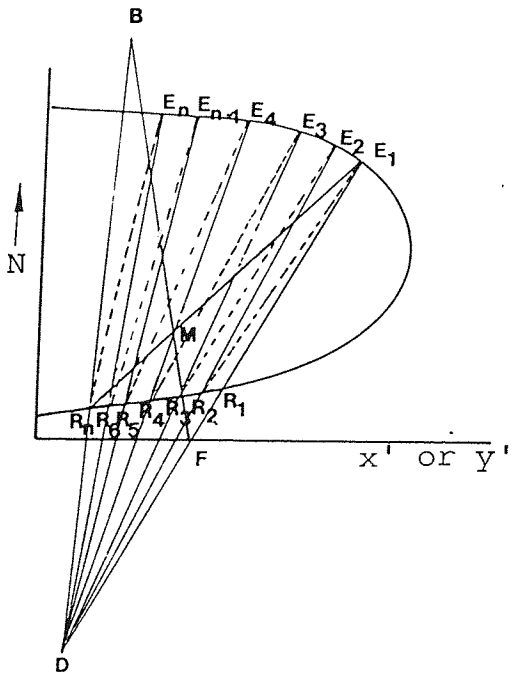

Figure 4.17 : SOLVENT - FREE COORDINATE METHOD.

As in the case of triangular coordinates the difference point D may be indicated by writing Equation (4.25) as:

$$E_1' - F' = B' - R_n' = D \qquad (4.30)$$

Thus the difference point D can be located graphically by extending the lines E_1F and BR_n. The point of intersection of these lines locates the difference point D. The number of countercurrent stages required for a given extraction job may be determined in the following manner. After locating the points F_1, E_1, B, R_n and D, the point E_n may be located on the binodal curve as this lies across the tie-line from R_n. A line from D to E_{n-1}, and E_{n-1} may then be located by a tie line from R_{n-1}. This procedure is repeated until the point E_1 is reached to determine the number of theoretical stages. When the number of stages required is large, the coordinates from the diagram may be transferred on solvent-free distribution diagram (selectivity diagram) using a procedure similar to the method described earlier.

When any operating line from the difference point D coincides with a tie-line, it indicates a condition for an infinite number of stages corresponding to minimum solvent-to-feed ratio as in the case of the triangular diagram. Usually a tie-line which on being extended passes through the feed composition will locate the difference point for minimum solvent-to-feed ratio condition.

CHAPTER five 5

MASS TRANSFER IN LIQUID-LIQUID EXTRACTION

5.1 INTRODUCTION

Mass transfer between phases occurs by diffusion through the interface. The rate of diffusion of a component is dependent among other things, on the ratio of the concentrations of this component in the two phases. The more this ratio differs from the value of the distribution coefficient (k) the greater will be the rate of diffusion.

The drop size of the dispersed phase is of primary importance. If the diameter of the drops is large it may happen that the concentration of the component near the surface of the drop is such as to make the concentration ratio at the surface and in the surrounding continuous phase almost equal to the value of k, but diffusion inside the drop may be so slow that the difference in concentration between the surface and the middle of the drop is still large. Mass transfer has then become very slow, though equilibrium has not yet been achieved. Hence it follows that the establishment of equilibrium is promoted by converting the dispersed phase into small drops.

The overall mass transfer coefficient in terms of the dispersed phase can be expressed, according to Whitman's two-film theory (105) as the combination of individual

resistant to mass transfer of the continuous (k_c^{-1}) and the dispersed (k_d^{-1}) phases as follows:

$$\frac{1}{K} = \frac{1}{k_d} + \frac{m}{k_c} \qquad (5.1)$$

The validity of this simple additivity concept rest upon the assumption that there is no resistance to transport at the actual interface.

Several different mechanisms have been proposed to describe conditions near the interface between two phases. A brief account of some of the most commonly used models is given below:

i) The film model was originally proposed by Nernst (106) and is the basis of the Whitman's two film theory (105). It assumes that turbulence dies near the interface and the resistances to mass transfer are confined largely to a region quite close to the phase boundary of thickness, y_o, in which transport occurs by molecular diffusion. Using the equations for molecular diffusion, the mass transfer coefficient is given by:

$$k = \frac{D}{y_o} \qquad (5.2)$$

This concept is a gross over-simplication of the real hydrodynamic conditions near an interface and specially at liquid-liquid interface. Its major pitfall is that it fails to predict the power dependence of the mass flux on the molecular diffusivity, D. The actual dependence is known to be between the zero and unit power while the model predict unity. Nevertheless, this theory has

been quite useful in several applications.

ii) The penetration model of Higbie (107), contrary to the stationary nature of the transport proposed by the film model, considers that mass transfer occurs during the repeated brief contacts of the two-phases. It proposed that small fluid elements of uniform solute concentrations are continually being brought into contact with a phase boundary, remain there for a short and constant penetration time, t_c, and undergo unsteady-state transfer of solute by molecular diffusion, before being swept away to be replaced by other fluid elements. Application of the Fick's second law:

$$\frac{\partial C_A}{\partial t} = D_{AB} \frac{\partial^2 C_A}{\partial Z^2} \qquad (5.3)$$

and a subsequent integration along the contact time, t_c, gives the following average flux over t_c:

$$N_A = 2\sqrt{\frac{D_A}{\pi t_c}} (C_A - C_o) \qquad (5.4)$$

Since k is defined by the mass flux per unit concentration difference, the time-average mass-transfer coefficient is given by:

$$k = 2\sqrt{\frac{D_A}{\pi t_c}} \qquad (5.5)$$

A procedure to estimate t_c is not provided by the theory. It was originally applied to a gas-liquid solute transfer. Higbie assumed that as a gas bubble rises through a liquid, the liquid surface renewal occurs in a time, t_c, approximately equal to that required for the bubble to

rise one bubble diameter. Substitution of the expression of t_c in the equation (5.5) gives the well known Higbie relation:

$$Sh = 1.13\ (Re)^{0.5}\ (Sc)^{0.5} \qquad (5.6)$$

This theory has been widely used and in each application the estimation of t_c was done according to the problem and/or the availability of measured variables which after algebraic combinations, produce a characteristic time scale.

iii) The surface renewal model of Danckwerts (108) is an extension of the penetration theory. Danckwerts assumed that the times of exposure of fresh elements of liquid were not identical as assumed by Higbie, but that the probability of replacement of any given liquid element was independent of the time for which it had already resided at the interface. Then the variables contact time may be anything from zero to infinity. The fractional rate of renewal, S, of the area exposed to penetration, in other words, the rate of replacement of the fluid elements in the surface, is assumed to be constant. Application of these concept to the transient diffusion equation render the following relations:

$$N_A = (C_A - C_o)\ \sqrt{D} \int_o^\infty \frac{Se^{-st}}{\sqrt{\pi t}}\, dt = \Delta C\ \sqrt{Ds} \qquad (5.7)$$

iv) The eddy cell model of Lamont and Scott (109) considers the surface renewal be due to turbulent eddies. According to this model the very small scale of turbulence in the equilibrium range are considered to be controlling

the mass transfer process. Lamont's calculation based on the eddy cell model gives the following relationship for the mass transfer coefficient at a free interface.

$$k \alpha (Sc)^{-\frac{1}{2}} (\varepsilon\nu)^{\frac{1}{4}} \qquad (5.8)$$

More details on these and other models are reviewed by Sherwood et al (110), Skelland (111), Treybal (24) and Scriven (112).

5.2 MASS TRANSFER TO AND FROM DROPS

Mass transfer to and from drops has been studied extensively and the efficiencies of mass transfer estimated for different stages of the drop life, i.e. during formation, during release, during travel through the continuous phase and during coalescence.

5.2.1 Mass Transfer During Drop Formation

During drop formation the surface area is estimated from the volume of the drop as a function of the time of formation. The relationship between the volume of the drop and the time of formation has been studied for four different regions. Correlations have been developed for each region giving volume as a function of the physical properties of the system (60, 113-117). The surface area-volume relationship was predicted experimentally for several systems and a linear relationship was obtained.

The theory of diffusion was applied to calculate the mass transfer efficiency using the equation:

$$E_f = F\left(\frac{D_t f}{\pi}\right)^{\frac{1}{2}} \tag{5.9}$$

Four models were recommended for the estimation of mass transfer efficiency. All these models were based on the above equation. The assumptions were:

i) The interfacial concentration is that at saturation.

ii) Mass transfer by diffusion is perpendicular to the interface.

iii) The process of diffusion is slow as compared with the process of drop growth.

iv) Variations in the diffusion coefficient in the direction of flow are neglected.

However, it was found that these models were inaccurate as they did not consider the internal circulation and interfacial turbulence, or the influence of rest time of a drop between formation and disturbances associated with the drop detachment (118).

The following empirical correlation was suggested (119) which included other parameters like density, viscosity and interfacial tension:

$$\frac{k_d f t_f}{d} = 0.0432\left(\frac{V_N}{d_g}\right)^{2.089}\left(\frac{d^2}{t_f D_d}\right)^{-0.334}\left(\frac{\mu_d}{\sqrt{\rho_D \sigma_D}}\right)^{-0.601} \tag{5.10}$$

The average absolute deviation from data was 26%. This correlation represented the overall mass transfer during drop growth, during the detachment and the influence of the rest drop.

5.2.2 Mass Transfer During Droplet Release

During droplet release changes occuring at the interface and an oscillation of the drop caused by release, result in a different magnitude of mass transfer efficiency to that during drop formation. Several workers (120-125) have described different mass transfer mechanisms so that the exact mode is uncertain.

5.2.3 Mass Transfer in the Dispersed Phase

Mass transfer efficiency within a drop depends upon the Reynolds number within it. The interfacial tension between the continuous and the dispersed phase (126) and the nature of the original interface (127) also have a significant effect on the efficiency of mass transfer. Therefore, efficiencies differ with different system properties.

Mass transfer within the drops is characterised for three different types of drops, namely: rigid, circulating and oscillating drops. Drops of very small diameter, usually below 1 mm, or larger in the presence of surface active agents, behave as rigid drops and the solute concentration varies according to the expression (128):

$$E = 1.0 - \frac{6}{\pi} \sum_{2n=1}^{\infty} \frac{1}{n^2} \exp(-n^2 \pi^2 \frac{D_d t}{a^2}) \qquad (5.11)$$

Internal circulation causes the liquid in the drop to mix and therefore a higher mass transfer coefficient is obtained. The circulation is laminar if the Reynolds number is less than 1.0. A Reynolds number above 6.0 produces turbulent circulation. The analysis of mass

transfer inside a circulating drop is explained by molecular diffusion. One correlation proposed is (129):

$$E = 1 - \frac{3}{8} \sum_{n=1}^{\infty} A\, n^2 \exp\left(-\frac{\lambda n\, 16\, D_d t}{a^2}\right) \qquad (5.12)$$

This equation is in general applied to regimes with Re < 1. For the case of turbulent circulation, another expression was proposed based on a turbulent flow; due to random radial motion, superimposed upon a circulatory pattern (130)

$$E = 1 - 2 \sum_{n=1}^{\infty} A\, n^2 \exp\left(-\frac{\lambda_n\, V t}{128\left(1 + \frac{\mu_d}{\mu_c}\right) d}\right) \qquad (5.13)$$

In general, at low continuous phase velocities, when the Reynolds number is above 200, the drops are oscillating. Low interfacial tension and a low dispersed phase viscosity also favour oscillation. The expression developed (131) for vigorously oscillating single drops takes into account the amplitude and frequency of the oscillations.

$$E = 1 - \exp\left(-\frac{2\pi D E}{V}\right) \int_{t_o}^{t_f} \frac{1}{f_1(t)} \left\{\left(\frac{3V}{4\pi(a_o + a_p |\mathrm{Sin}\ wt|)^2}\right)\right.$$

$$\left.\frac{1}{2} \ln\left(\frac{1+\alpha}{1-\alpha}\right) + (a_o + a_p |\mathrm{Sin}\ wt|)^2\right\} dt) \qquad (5.14)$$

where the symbols are as in the Nomenclature.

5.2.4 Mass Transfer in the Continuous Phase

Mass transfer in the continuous phase has also been studied separately for the cases of rigid and non-rigid drops. For a rigid drop, the mass transfer coefficient was correlated to Reynolds number and Schmidt number by:

$$Sh = A + C\ Re^{m} + Sc^{n} \qquad (5.15)$$

Similar correlations were obtained for non-rigid drops:

$$Sh = K(Re)^{\frac{1}{2}}\ (Sc)^{\frac{1}{2}} \qquad (5.16)$$

The proportionality constant, K, was found to be 1.13 (132). Later, however, the contribution of drop wake to the mass transfer was considered and the constant was modified to 0.6 (133). For oscillating drops (134-136) equation (5.16) was further modified by Treybal (24) for a swarm of drops as:

$$Sh = 0.725\ (Re)^{0.57}\ (Sc)^{-0.15}\ (1-\psi_d) \qquad (5.17)$$

where ψ_d is the fractional hold-up of dispersed phase. In another work the mass transfer coefficient in the continuous phase has been related to densities and viscosities and the mean diameter of drops. Interaction between drops in swarms and the effect of particle size distribution were also taken into account (137):

$$k_c = 0.371\{\frac{D(\rho_c - \rho_d)g}{2\mu_c + 3\mu_d}\ (\frac{d32}{2})\}^{\frac{1}{2}} \qquad (5.18)$$

5.2.5 Mass Transfer during Coalescence

The contribution made to mass transfer during the coalescence of a drop into an interface has been studied. An identical correlation to that for formation was developed (121,137,124)

$$k_{dc} = (\frac{D_d}{\pi t_f})^{\frac{1}{2}} \qquad (5.19)$$

where t_f is the time of formation.

However, this was later criticised because the driving force for mass transfer was much less than that during formation. Another expression was therefore derived (118)

$$\frac{K_{dc}t_f}{d} = 0.1727\left(\frac{\mu_d}{\rho_d D_d}\right)^{-1.115}\left(\frac{\Delta\rho g d}{\sigma}\right)^{1.302}\left(\frac{V_t^2 f_t}{D_d}\right)^{0.146} \qquad (5.20)$$

Generally, in pure systems the coalescence takes place rapidly without allowing enough time for a significant degree of mass transfer. Nevertheless, because of oscillations occuring as a drop approaches the interface, the mass transfer increases temporarily and this may be taken into account.

5.3 THE OVERALL MASS TRANSFER COEFFICIENT

The overall resistance to mass transfer is calculated as the sum of the resistances of the individual phases. The controlling coefficient can be predicted from the drop size. If the drop size is larger than 2 mm, the drops will oscillate and the continuous phase coefficient will be controlling. If the time taken for the concentration of the drops to change by 95% is short, of the order of 30 seconds, the extraction will be controlled by the continuous phase. This is the most common case.

5.4 APPLICATION OF DROPLET MODELS TO PRACTICAL EXTRACTION

In general, application of single drop mass transfer models to industrial contactors is very difficult. This arises because of the complexity of the mass transfer and droplet coalescence - redispersion processes, both of which may change with location and solute concentration within the contactor. The contributions made to mass transfer during each of the four stages of a drop's life have been discussed and a different correlation described for each stage. In practice, however, it is impossible to allocate a time for each stage. Also, once discrete drops form at the distributor, they do not necessarily travel throughout a column until they coalesce. Break-up or inter-drop coalescence may take place.

Furthermore, the mechanism of mass transfer to or from the formed drops is not the same along the column. Following mass transfer during travel, the physical properties such as interfacial tension, density difference or viscosity, change as does the driving force, i.e. the concentration difference and indeed the drop size. Hence, the mass transfer rate to an individual drop does not remain the same.

The presence of impurities is another important factor influencing mass transfer. Most mass transfer correlations presented previously apply to pure systems, with a minimum of impurities under ideal conditions. These seldom exist in practice. Because of impurities, interfacial tension differs and coalescence may be hindered.

In practice, calculation of mass transfer to or from formed drops involves estimation of a mean drop size which remains the same throughout the effective column height.

5.5 DROPLET PHENOMENA

The sizes and the size distribution of droplets in a solvent extractor depend upon the method of formation, the amount and nature of the droplet interactions with the internals of the vessel, the physical properties of the chemical system, the mode of operation and the geometric arrangements of the vessel. The drop sizes of various systems have been estimated by different experimental techniques including (139):

i) light transmittance (140-142),
ii) light scattering (143),
iii) photography (144),
iv) electronic particle counting (145),
v) sedimentometry, and
vi) liquid-liquid extraction by fast pseudo-first order reaction.

The dependence of the drop size on the method of formation, on whether the dispersed phase is discharged through some form of orifice or nozzle, or dispersed by mechanical agitation. The former is applicable to spray columns and sieve plate columns and can be further subdivided according to the nozzle velocity in:

i) drop formation at subjetting nozzle velocities, and

ii) drop formation under jetting conditions.

However, in the most common types of extraction equipment the dispersion is normally formed by the high shear stress created by some form of mechanical agitator.

In practice, drop break-up and coalescence occur simultaneously and the extreme complexity of this situation makes it very difficult to obtain a theoretical model from which drop sizes can be predicted. All the available drop size correlations in agitated systems are of a semi-empirical nature, combining the most important parameters of each of the isolated coalescence and break-up models.

As mentioned earlier in any real dispersion there exists a wide range of drop diameters. In calculating an average drop diameter which characterize the dispersions, attention must be given to the ultimate use of this average. Since the final objective is to calculate the total interfacial area, more weight should be given to the small drops. This follows from the fact that the specific surface (i.e. the surface per unit weight) increases as the particle size decreases. The following method has been suggested by Dallavalle (146) to correct for this phenomenon.

Consider the particles to be spheres then,

$$\text{Specific surface} = S_w = \frac{\text{area}}{\text{weight}} = \frac{6}{\rho d} \tag{5.21}$$

$$\text{Area of a sphere} = \pi d^2 \tag{5.23}$$

$$\text{Weight of a sphere} = \frac{\rho \pi d^3}{6} \tag{5.23}$$

where ρ is the density of the particle. Let y_i = weight fraction of particles with diameter d_i, and specific surface S_{wi}. Then,

$$y_i = \frac{n_i d_i^3}{\sum_i n_i d_i^3} \tag{5.24}$$

The average specific surface $\bar{S}_w$ is given by a weighted arithmetic mean,

$$\bar{S}_w = \frac{\text{Total Area}}{\text{Total Weight}} = \sum_i y_i S_{wi} = \frac{\sum_i n_i d_i^3 \cdot S_{wi}}{\sum_i n_i d_i^3} \tag{5.25}$$

Let d_{vs} be the diameter of a fictitious sphere having a specific surface equal to $\bar{S}_w$. Then,

$$d_{vs} = \frac{6}{\rho \bar{S}_w} = \frac{6}{\rho \sum_i y_i S_{wi}} = \frac{6}{\rho} \left\{ \frac{1}{\frac{\sum_i n_i d_i^3 S_{wi}}{\sum_i n_i d_i^3}} \right\} \tag{5.26}$$

Therefore,

$$d_{vs} = \frac{6}{\rho} \frac{\sum_i n_i d_i^3}{\sum_i n_i d_i^3 \cdot \frac{6}{\rho d_i}} = \frac{\sum_i n_i d_i^3}{\sum_i n_i d_i^2} \tag{5.28}$$

Thus, to estimate the total surface area of a particulate material the average volume-surface diameter, d_{vs}, should be used. This diameter is widely known as the Sauter mean diameter (d_{32} or d_{sm}).

Research workers (119,147) who have made drop size measurements in R.D.C.'s have used 300 drop samples as the basis for representing the dispersions. All of these workers with the exception of Misek (148,149) have presumed that d_{32} is the appropriate mean drop diameter to represent dispersion behaviour. Misek considered that a higher order of mean size

$$d_{43} = \Sigma nd_i^4/\Sigma nd_i^3 \qquad (5.29)$$

represented the hydrodynamic and mass transfer processes better.

Various workers (119,148,149,150) have concluded that it is not sufficient to evaluate a mean size, but the distribution of drop sizes must be considered in predicting column performance.

Chartres and Korchinsky (151), measured drop size distribution in a 23 cm diameter, 135 cm high R.D.C. column. Inlet drop sizes were found to have a strong influence on measured column drop sizes. With a large inlet droplet size, the column drop size was influenced by the break-up rate of drops which was dependent on the presence of solute and on the direction of mass transfer.

By analogy with droplet break-up mechanisms in packings, Misek (152) considered the vertical velocity of the drops leading to successive impacts on the stators and discs. From limited experimental work, Misek identified three regions of break-up in an R.D.C.;

turbulent, transitional and laminar. For the turbulent region, Re > 5.74 x 10^4 the hydraulic mean drop diameter is given by:

$$\frac{d_{12}N^2D_R^2\rho_c}{\sigma \exp(0.0887\ \Delta R)} = 16.3\left(\frac{H}{D_c}\right)^{0.46} \qquad (5.30)$$

where σ = interfacial tension

$$\Delta R = (D_c - D_R)/2 \qquad (5.31)$$

For the transitional region, Re < 5.74 x 10^4, and

$$\frac{d_{12}N^2D^2\rho_c}{\sigma \exp(0.0887\ \Delta R)} = 1.345 \times 10^{-6}\left(\frac{D^2N}{\mu_c}\right)^{1.42} \qquad (5.32)$$

In the laminar region, Re < 10^4

$$d_{12} = 0.38\left(\frac{\sigma}{\Delta\rho g}\right)^{0.5} \qquad (5.33)$$

Mumford (153) found that in the region of Re ≃ 10^4, the mean drop sizes were independent of hold-up and in agreement with the correlation proposed by Misek in equation(5.33). At increased speeds, the overall tendency was for drop sizes to increase, over the whole spectum, with hold-up.

Jeffreys and Mumford (154) have shown, the droplet break-up by impact on stators or discs was not the predominant mechanism, influencing drop sizes. However, drops may rupture by impact on the edge of the stators or discs as shown by Thornton (155).

Mumford and Al-Hemeri (147) derived an empirical formula for the Sauter-mean diameter in terms of system properties and the column height. d_{32}, decreased with column height and the results were correlated by:

$$d_{32}/R = 4.7 \times 10^{17} \left(\frac{NR^2\rho_c}{\mu_c}\right)^{-3.33} \left(\frac{\mu_d}{\mu_c}\right)^{0.23} \left(\frac{NR\mu_c}{\sigma}\right)^{2} (X)^{0.225} (\exp 0.4(\frac{N}{Z}) \quad (5.34)$$

Very recently Blazej et al (156) have proposed correlations for drop size under mass transfer conditions for water-acetone-toluene system in a 65 mm diameter column:

$$\frac{d_{32}}{D} = 1.43\left\{\frac{V_D(1-X)}{V_c}\right\}^{0.45}\left\{\frac{D.N(1-X)}{V_c}\right\}^{-0.56}\left\{\frac{\rho_c.H_T.V_c}{\mu_c(1-X)}\right\}^{-0.12} \quad (5.35)$$

Al-Aswad (157) extended the equation above to include column dimensions and obtained:

$$\frac{d_{32}}{D_r} = 1.48\left\{\frac{V_D.H.\rho_c}{\mu_c.X}\right\}^{-0.23}\left\{\frac{N^2D_R^3\rho_c}{\sigma}\right\}^{-0.004}\left\{\frac{V_D}{\rho_c D_c X^2}\right\}^{0.44}\left\{\frac{\Delta\rho}{\rho_c}\right\}^{-0.57}$$

$$\left\{\frac{H}{D_c-D_s}\right\}^{-0.24}\left\{\frac{n}{N_c}\right\}^{-0.07} \quad (5.36)$$

The average percentage error between his experimental drop size, obtained from a 450 mm diameter R.D.C. and those predicted from equation (5.36) was 17%.

In all the above studies there has been considerable disagreement over the shape of the drop size distribution curve. Some investigators reported a normal distribution (158-161) while others found the distribution to be log-normal (119,151,162,163,164). However, Chartres

and Korchinsky (151) have confirmed Olney's (119) conclusion that the drop size distribution in an R.D.C. obeys the upper limit distribution proposed by Mugele and Evans (165).

$$\frac{dv}{dr} = \frac{\delta}{\sqrt{\pi}} \exp(-\delta^2 r^2) \qquad (5.37)$$

$$\text{where } r = \ln\{\frac{a'd}{d_m - d}\} \qquad (5.38)$$

The upper limit distribution is a modified log-normal distribution which may be compared with the standard form of the log-normal distribution

$$\frac{dv}{dr} = \frac{\delta}{\sqrt{\pi}} \exp\{-\delta^2 r^2\} \qquad (5.39)$$

$$\text{where } r = \ln \frac{d}{d_{vg}} \qquad (5.40)$$

These investigators (119,151,164) emphasised the importance of applying drop size distribution in the mass transfer calculation instead of using Sauter mean diameter.

5.5.1 Effect of Impurities or Surface Active Agents

The presence of impurities or of surface active agents has a marked effect on droplet characteristics and hence on contactor efficiency and capacity. This has been overlooked in some otherwise impeccable researches. For example, Vermijs and Kramers (166) used natural rubber connectors and neoprene rubber packings with the system water-acetic acid - M.I.K. and commented only that both needed renewal at frequent intervals.

Lee and Lewis (167) also risked leaching of impurities from neoprene gaskets. Logsdail et al used flexible connections of rubber or P.V.C. (168). Similarly, Piper experienced leaching of plasticiser from P.V.C. tubing with kerosine (169). Contamination of this sort has recently been shown to significantly alter coalescence phenomena and lead to unreproducible results (170,171).

Care must be taken to select a solvent not subject to degradation. Otherwise in addition to extraneous impurities, the accumulation of products of solvent degradation at the interface can also affect interfacial tension.

Presence of a surfactant directly influences the interface as well as drop size and movement. The lowered interfacial tension results in smaller droplets and retardation of coalescence has a similar effect (172). In a spray column, hold-up has been found to increase by a factor of 2 to 2.5 for a coalescing system and 1.4 to 1.6 for a non-coalescing system (173). Surfactants retard circulation in droplets, the agent being collected like a cap at the rear of the drop. In practice some increase in mass transfer generally accompanies the addition of surfactants (172).

Davies et al (174) have studied the effect of a surface active agent on extraction efficiency in an R.D.C. Teepol was used to obtain an 18% reduction in interfacial tension with the system kerosene-water-phenol. The equivalent number of stages in the R.D.C. were then

compared at different rotor speeds with the number in the absence of Teepol. Smaller droplets, giving a large interfacial area and a considerable increase in extraction efficiency, were observed when Teepol was present. Column capacity was reduced due to the small drop sizes. Recent work has indicated that any sample of industrial chemicals prepared in bulk contains some materials which affect the properties of the interface when the sample is dispersed in an aqueous medium (175). Thus process development is preferably carried out with actual plant feed streams. The use of impure commercial materials for research (152,176) is inadvisable however because of these contaminants and the potential variation in specification.

On a commercial scale,surface active contaminants have led to the formation of a suitable dispersion in an R.D.C. at zero rotor speed (177). Reman (178) has reported that when extracting heavy distillates with furfural, emulsification caused by pitch contamination may reduce R.D.C. capacity by a factor of 2.5. The absence of droplet coalescence in R.D.C.'s during the extraction of phenols from a continuous aqueous phase with Fenosolvan or benzene has been attributed to the presence of surface active contaminants (179).

5.5.2 Effect of Mass Transfer

The effects of mass transfer on the ease of coalescence and droplet characteristics may vary considerably depending

on the direction of transfer.

To eliminate mass transfer from hydrodynamic studies it is necessary that the phases be mutually saturated before entering the contactor. This can be achieved by pre-contacting the phases for a sufficient period to attain equilibrium and then allowing time for separation to occur. Some systems are notoriously slow to coalesce, produce a secondary haze or fog on settling and several hours may be necessary before clear phases are obtained. Thus, the procedure sometimes adopted (178) of circulating the phases through the column or in a closed circuit prior to use may be open to criticism.

CHAPTER six 6

ROTATING DISC CONTACTOR

6.1 INTRODUCTION

A Rotating Disc Contactor was chosen because of its versatility, and since numerous studies had confirmed its hydrodynamic performance and mass transfer characteristics. Mumford and Al-Hemeri (147), Komosova and Ingham (180) and Kung and Beckmann (181) have discussed the correlations of dispersed phase hold-up, while the effects of drop size and size distribution on mass transfer rates have been studied by Chartres and Korchinsky (182) and the different correlations have been compared by Laddha (183).

The Rotating Disc Contactor was proposed by Reman in 1951 (178,184). It was originally used for the extraction of lubricating oils from crude oils using furfural as solvent. It has now found extensive use in various petroleum extraction processes (185) as well as in the food, metal separation, extraction of caprolactam (186), propane deasphalting (187,188,189), phenol recovery (190), purification of synthetic detergents and many other organic chemical industries.

The design of industrial scale R.D.C. has been subject to many studies (152,168,114,191) and its

advantages over other extraction devices were discussed (184,186,187,192,193) and may be summarised as:

i) High efficiency, measured as low H.T.U. or H.E.T.S. values.

ii) The ability to maintain this efficiency over a large volumetric capacity range. This is achievable by variation of rotor speed, so that the flow conditions in the contactor can be maintained at the optimum for any particular feed conditions.

iii) It is cheap and simple to build and operate (193). The low hold-up facilitates a rapid change from one product to another and hence the plant is more flexible. The power consumption of an RDC is low and the bearing wear less in comparison with the pumps of an equivalent mixer settler, because lower motor speeds are required.

iv) The power transmitted to the fluids need not be great and is controllable; therefore it is well suited for use with systems of low interfacial tension and low density difference.

v) Laboratory scale results have been successfully scaled up to commercial operation. Any discrepancies can in any event be overcome by the provision of a variable speed drive.

vi) Its use overcome difficulties due to the formation of a gel-like emulsion which created problems in

extraction in mixer-settlers and packed columns (166).

6.2 CONSTRUCTION

The rotating disc contactor consists of a vertical cylindrical shell divided into a number of compartments by a series of stator rings. A rotating disc, supported on a central shaft, is located in each compartment. The vortices generated by the discs are constrained between the stators. Adjacent to the top and bottom compartments are feed inlets which are arranged tangentially in the direction of rotation. The dense phase is introduced into the top of the column and the light phase into the bottom; counter-current flow is thus established by gravity. An open mesh grid may be fitted into the shell to separate the feed inlet zone from the settling compartment. This design has proved to be effective in minimising disturbance in the settling compartments. The method of construction permits the use of corrosion resistant materials.

The important column parameters that affect the performance of a rotating disc contactor for a given extraction system are the column diameter (D_C), the rotor disc diameter (D_R), the stator ring opening (D_S), the compartment height (H) and the speed of rotation of the central disc (N). These parameters and the flow rates of the liquid phases affect the hold-up of the dispersed phase, flooding rates of the two phases, residence times of the liquids, drop size and distribution, and mass transfer rates (191). The initial estimation

of column diameter may be made by a consideration of limiting flow rates. Based on the correlation plots proposed by Misek (152), the dimensions of the column internals may be approximately calculated by the following relationships in terms of column diameter, D_C expressed in centimeters:

Compartment height H, cm

$$H = 0.142(D_C)^{0.68} \tag{6.1}$$

Rotor disc diameter D_R, cm

$$D_R = 0.5\ D_C \tag{6.2}$$

Stator ring opening D_S, cm

$$D_S = 0.67\ D_C \tag{6.3}$$

In general, the diameter of the rotor disc is slightly less than that of the stationary annular ring opening of the stator to facilitate easy withdrawl of rotor assembly for any eventual repair and cleaning. For optimum design the geometry is based on dimensional ratios in the range (114,152,166,168,193):

$$\frac{D_S}{D_C} = 0.66 \text{ to } 0.75,\ \frac{D_R}{D_C} = 0.5 \text{ to } 0.66,\ \frac{H}{D_C} = 0.33 \text{ to } 0.5$$

However, these ratios pertaining to the choice of column geometry may be varied slightly to provide flexibility in design. Such variations may be by taking into account the effect of altering the column geometrical features and column flow capacity and mass transfer efficiency. For example, increasing the rotor diameter decreases the column throughput but increases the

efficiency. But, the increase in stator ring opening or compartment height will increase the throughput capacity but decreases the efficiency of the contactor.

6.3 MODE OF OPERATION

The lighter liquid enters the contactor at the bottom and flows upwards countercurrently to the descending heavier liquid, which enters at the top. One of the liquids will be dispersed by the action of the rotating discs, which are flat to create uniform shearing conditions and hence obtain as small a spread in droplet sizes as possible. It is thought that the dispersed phase droplets spin at fairly high speeds and that this factor accounts for the high efficiencies attainable with R.D.C.s. Variation in the rotor speed provides a simple and effective method of obtaining optimum extraction conditions in each case.

The principle of contacting the liquid phases as embodied in the rotating disc contactor stands in sharp contrast to that applied in most conventional types of commercial apparatus. In the latter apparatus an attempt is made to secure a large interfacial area and rapid initial transfer by repeating a number of times the process of dispersion under highly turbulent conditions followed by coalescence. However, the uniformity of the dispersion cannot be adequately controlled and interstage coalescence limits capacity. In the rotating-disc contactor no interstage settling and redispersion is employed. As

already mentioned, the size of the droplets formed is controlled and maintained in each compartment with the use of the appropriate rotor speed. Flat rotor discs and stator rings without any protrusions create uniform shearing conditions and aid in obtaining a small spread in droplet size. It has been found that protrusions in general give rise to high local shearing stresses and thus to the formation of a considerable amount of fine droplets which under certain circumstances reduce the capacity appreciably. The flow pattern of the liquid in the compartments is such that the desired countercurrent flow of the dispersed and continuous phase occurs. This flow of liquid consists of a rotation of the whole liquid mass on which there is superimposed a slower movement of the liquid from the shaft towards the wall of the contactor in the vicinity of the rotor discs, and from the wall back towards the shaft in the vicinity of the stator rings. Thus the resulting flow of the liquid is toroidal. In each compartment two vortices of opposite senses geared together occur and form a complete vortex.

The energy transferred from the rotor discs to the liquid creates further a rather uniform turbulence in the liquid phase and this appears to be beneficial for obtaining high mass transfer rate, that is high efficiencies.

6.4 MODIFIED R.D.C.

In an attempt to improve the R.D.C.'s efficiency, or possibly to circumvent the Shell patent (184), many

modified R.D.C. have been proposed. The Asymmetric Rotating Disc (A.R.D.) extractor is the most important modification of the R.D.C. and was developed by Misek et al (148,194). Its essential difference from the R.D.C. is that the shaft, carrying the rotating-disc agitators, is off-centre in the column. A transfer zone is located at the side of the column, providing a path to the mixing chambers above and below the one being considered. It is claimed that this arrangement reduces axial mixing considerably. Seidlova and Misek (142) published a detailed study giving data on the pattern of liquid movement over the cross section for the A.R.D.

Another modified R.D.C. is a multi-rotor extractor designed by Reman (195). This has two or more rotors in the column shell. This is claimed to minimise instability of the vortex flow pattern in large diameter columns. Other designs incorporate perforated disc rotors (196, 197), and an R.D.C. in which the stator rings were omitted with the discs of two sizes, and the larger discs perforated (198) have also been considered.

Various other extractors are not simple modifications of one of the more common designs but a combination of more than one type. Perhaps the most important extractor of this kind is the Kuhni column (199,200) which incorporates the principles of the Oldshue-Rushton, the sieve-plate and the R.D.C. extractors. The Kuhni column employs shrouded turbine impellers to promote radial discharge characteristics within the compartments. The column is

divided into compartments by plates perforated only at the centre so that the flow from one compartment to the next is directed towards the agitator.

However, the 'standard' R.D.C. remains by far the most common and probably the most versatile extractor of its type.

6.5 HYDRODYNAMIC CHARACTERISTIC

6.5.1 Flooding

Flooding is a typical hydrodynamic phenomenon particularly associated with differential contactors. For each flowrate of one phase there is a maximum corresponding flowrate of the other phase. For a specific system in an R.D.C. this maximum is a function of rotor speed, since this determines the drop size distribution and hence their rise or fall velocities and also the continuous phase flow pattern. Any attempt to exceed the maximum results in either of the liquids being rejected, for example in the case of the dispersed phase a dense layer of droplets accumulates near the inlet. This is termed "flooding".

The dispersed phase hold up h_f at flooding can be estimated from (168):

$$h_f = \frac{(L^2 + 8L)^{0.5} - 3L}{4(1-L)} \qquad (6.4)$$

where $L = \frac{V_d}{V_c}$, the ratio of the superficial velocity

of the dispersed phase to the superficial velocity of the continuous phase under flooding conditions; whilst this expression is not strictly applicable when the mean drop size is not constant over the entire range of hold-up, e.g. when mass transfer results in the drop size increasing due to enhanced rates of drop coalescence, it is useful for correlation of experimental data. In non-mass transfer studies, however, Thornton (201) found good agreement between their experimental data and equation (6.4).

Reman (192,191,184,202) studied the effect of system variables on the limiting capacity. The capacity was found to decrease with increasing rotor speed, disc diameter and ratio of dispersed to continuous flow rate $(\frac{V_d}{V_c})$, but to increase with increasing stator opening and compartment height. The capacity data obtained were correlated by considering energy input/volume, $(N^3 D_R^5 / H D_c^2)$, as determining the drop size of the dispersed phase. A constriction factor, C_R, was introduced to allow for the effect of constrictions on settling of the drops. C_R was defined as the minimum of the three area ratios

$$(\frac{D_s}{D_c})^2 \text{ or } (1 - \frac{D_R}{D_c}) \text{ or } (\frac{D_s + D_R}{D_c}) \sqrt{(\frac{D_s - D_R}{D_c})^2 + (\frac{H}{D_c})^2}$$

This is bound to be inconclusive however, since it omits the physical properties of the system, notably the phase densities ρ_d, ρ_c, the continuous phase viscosity μ_c and the interfacial tension, σ (which is an important factor determining drop size and hence settling rates and the volumetric capacity of the contactor). One

rudimentary guide to operating range can be produced by plotting energy input per unit volume vs. system interfacial tension as in Figure 6.1 (191). The lower region, marked 'poor contacting' represents the range in which large droplets are produced so that mass transfer efficiency is reduced.

Under certain conditions when the dynamic equilibrium between droplet break-up and coalescence is shifted towards the later, phase inversion may occur. This is characterised by the continuous phase becoming dispersed and vice versa.

Kung and Beckmann (181) and Reman and Olney (192), have also observed that equation (6.4) is adequate for estimation of flooding rates. Logsdail et al (168) have reported that the presence of an undistributed solute in the dispersed phase enhanced the flooding velocity whereas its presence in the continuous phase decreased the flooding velocity.

Misek has proposed a nomogram for estimation of column capacity, characteristic velocity and drop size in the operation of R.D.C. (152).

6.5.2 Hold-Up

In a Rotating Disc Contactor column, the motion of drop swarms would be expected to depend on the tortuosity of the path offered by the stator compartments and the rotor in addition to the complex nature of the movement

of both phases due to the rotating action of the rotor discs and the further breakdown of the dispersed drops. These complex factors are difficult to evaluate, though their effect on the total drop population (hold up) in the column could be investigated. Thus, it was found desirable to experimentally determine the dispersed phase hold up and correlate the hold up data according to the equation proposed earlier for spray columns by Thornton (201), and used by Logsdail et al (168).

$$V_d + V_c\left(\frac{X}{1-X}\right) = V_N X(1-X) \qquad (6.5)$$

V_N is defined as the mean vertical velocity of the drops at substantially zero flow rates and at rotor speeds N. A correlation was subsequently developed to relate V_N to system and column properties:

$$\frac{V_N \mu_c}{\sigma} = 0.012\left(\frac{\Delta\rho}{\rho_c}\right)^{0.9}\left(\frac{g}{D_R N^2}\right)^{1.0}\left(\frac{D_s}{D_R}\right)^{2.3}\left(\frac{H}{D_R}\right)^{0.9}\left(\frac{D_R}{D_c}\right)^{2.7} \qquad (6.6)$$

Kung and Beckmann (181) observed that hold-up increased with decreasing stator opening and compartment height and increasing disc diameter and rotor speed. A modified form of equation (6.6) was proposed:

$$\frac{V_d}{X_d} + \frac{K_1 V_c}{1-X_d} = V_N(1 - X_d) \qquad (6.7)$$

where K_1 is a geometric factor and has a value,

$$K_1 = 1.0 \text{ at } \frac{D_s - D_R}{D_c} > 1/24$$

$$= 2.1 \text{ at } \frac{D_s - D_R}{D_c} < 1/24$$

At rotor speeds greater than 1.5 m/s, V_N was correlated by:

$$\frac{V_N \mu_c}{\sigma} = K_1 \left(\frac{\Delta\rho}{\rho_c}\right)^{0.9} \left(\frac{g}{D_R N^2}\right)^{1.0} \left(\frac{D_s}{D_c}\right)^{2.3} \left(\frac{H}{D_c}\right)^{0.9} \left(\frac{D_R}{D_c}\right)^{2.6} \quad (6.8)$$

where the value of K_1 = 0.012 to 0.0225.

Repeated droplet coalescence and break-up may occur in the R.D.C. dependent upon the energy input and system properties. The equations discussed above make no allowance for this effect. Misek (152) attempted to include the effect in the equation

$$\frac{V_d}{X_d} + \frac{V_c}{1-X_d} = V_N(1-X_d)\exp\{X_d(Z/M - 4.1)\} \quad (6.9)$$

where Z = a coalescence coefficient strongly influenced by hold-up and hence the number of collisions resulting in coalescence. However, equation (6.9) found limited use owing to the strong dependence of the factor Z on the system properties. In a subsequent study, Misek (203) proposed a modified expression:

$$\ln\left(\frac{d}{d_o}\right) = 1.59 \times 10^{-2} (Re^*)^{0.5} X_d = ZX_d \quad (6.10)$$

$$\text{where } Re^* = \left(\frac{D_R \mu_c}{\rho_c}\right)\left(\frac{\sigma}{\rho_c d_o}\right) \quad (6.11)$$

However, the rate of drop interaction is very much influenced by the liquid-liquid system properties, column geometry and the level of energy transmission. At low hold-up, coalescence effects are significant even in the discharge region of the impeller (204). It appears therefore that the use of this Z factor is rather over-simplified and the applicability of equations (6.4) and

(6.5) remains to be proven.

A typical plot on toluene dispersed in water by Laddha et al (183) give the values of characteristic velocity, V_N, by using Equation (6.5). Earlier, Kung and Beckmann (159) showed the tendency for V_N to approach near constancy below a critical rotor speed, and for toluene-water system a value of 1.52 m/s was obtained for the critical rotor peripheral velocity.

Some workers have reported the variation of hold-up along the radial and axial directions. Strand and co-workers (114) determined radial and axial point values of hold-up in 15 cm and 110 cm column diameter R.D.C.'s. Results for the smaller columns were erratic presumably due to small dimensions. However, in the larger diameter column, the radial hold-up was found to remain substantially constant except in the vicinity of the rotor shaft. In the axial direction, the hold-up was found to increase up the column. Towards the end of the column, the hold-up decreased. Other workers (147,158) have reported similar results for axial hold-up profiles. These, generally, show a maximum value at a point about midway up the column.

Mumford and Al-Hemeri (147) proposed an empirical correlation for point hold-up x', at a dimensionless height, h:

$$x' = \{0.0013\ N + 0.38\{(V_d-1)-1\}(h-h^2) + 0.076(1-\frac{1}{V_d})\} \quad (6.12)$$

An analysis of the work of Rod (205) and of Mumford (153) revealed that the above contention may only be true at low values of dispersed phase flow rate and rotor speeds.

Murakami and co-workers (206) derived a correlation, based on dimensional analysis, for the dispersed phase hold-up over the whole length of the column:

$$X = 3.3\left\{\frac{N.D_R}{V_c}\right\}^{0.55}\left\{\frac{V_d}{V_c}\right\}^{0.80}\left\{\frac{D_s^2 - D_R^2}{D_c^2}\right\}^{-0.3}\left\{\frac{H}{D_c}\right\}^{-0.66}$$

$$\left\{\frac{D_R}{D_c}\right\}^{0.40}\left\{\frac{\Delta\rho}{\rho_c}\right\}^{-0.13}\left\{\frac{\rho_c D_c V_c}{\sigma}\right\}^{0.18}\left\{\frac{V_c^2}{g_c D_c}\right\}^{0.60} \qquad (6.13)$$

The exponents of the dimensionless groups were estimated by plotting the various groups and then estimating the slope of the tie-line to obtain the exponent of the dimensionless terms. A more practical correlation, over a wide range of column diameters (5.0 cm to 45.0 cm) was proposed by Jeffreys et al (207), in which they used published data obtained in small columns for different liquid systems, as well as their own data which is obtained in 45 cm column:

$$X = 1.05 \times 10^{14}\left\{\frac{ND_R}{V_c}\right\}^{0.521}\left\{\frac{V_d}{V_c}\right\}^{0.775}\left\{\frac{D_s^2 - D_R^2}{D_c}\right\}^{-0.187}$$

$$\left\{\frac{H}{D_c}\right\}^{-0.873}\left\{\frac{D_R}{D_c}\right\}^{-0.201}\left\{\frac{\Delta\rho}{\rho}\right\}^{4.843}\left\{\frac{\rho_c D_c V_c}{\sigma}\right\}^{1.082}$$

$$\left\{\frac{V_c^2}{gD_c}\right\}^{0.892}\left\{\frac{\rho_c V_c D_c}{\mu_c}\right\}^{-2.367} \qquad (6.14)$$

6.5.3 Backmixing

Longitudinal or backmixing is an important parameter in the design of continuous differential contactors.

Backmixing in the R.D.C. occurs due to non-ideal flow in which a random movement of fluid is superimposed on the main flow. This phenomena destroys the true counter-current flow pattern and tends to decrease the concentration driving force.

Strand et al (114) observed that there are several phenomena that may affect the spread of residence times of a droplet phase in the presence of a counter flowing continuous phase. Among these are:

i) Coalescence and break-up of drops.

ii) Droplet velocity distribution across the column radius due to vessel geometry and rotor speed.

iii) Droplet velocity distribution due to different settling velocities of the various size fractions.

iv) Axial spreading of small drops due to turbulent velocity fluctuations in the continuous phase.

The extent of longitudinal mixing in an extractor can be evaluated by several methods. The most common is to measure the concentration of a tracer substance along the extraction column length during steady state mass transfer. Such a technique was followed by Westerterp and Landsman (208) in backmixing studies in two small R.D.C.'s of 4.1 and 5.0 cm diameter. Results were interpreted by means of a diffusion model. The axial diffusivity was considered as the sum of a flow contribution and a rotational contribution. Results were

correlated by:

$$Pe = \frac{2n}{1+13\times10^{-3}(NR/V)} \qquad (6.15)$$

Most of the studies on backmixing have concentrated on the continuous phase. Determinations of the dispersed phase axial mixing are much more difficult to make (209). Values of the dispersed phase axial diffusivities obtained by Stemerding et al (219) in 6.4 and 64 cm diameter columns were much higher than those of the continuous phase. The ratio of dispersed to continuous phase axial dispersion coefficient varied from about 100 to 1, with the ratio approaching to unity at decreasing velocities of the dispersed phase. Stainthorp and Sudall (210) determined backmixing in both phases using a 35 cm diameter R.D.C. under conditions of actual mass transfer, for the system water-O-cresol-kerosene. A dye impulse technique was used to arrive at an estimate for back-mixing of both phases. The extent of backmixing was expressed as the ratio of the back flow between stages to the feed rate. The measurement for the dispersed phase did not agree with the models proposed by previous workers. A back mixing factor for the dispersed phase about twice that, predicted theoretically, was recommended (210).

Recently, Murakami and Misonou (211) have derived correlation on the basis of dimensional analysis for the back mixing ratio, and operating conditons and geometry of the R.D.C. This was claimed to give good agreement with experimental results.

6.5.4 Drop Size

Mass transfer efficiency in any R.D.C. is dependent on the drop size which is controlled by the use of an appropriate rotor speed. The flat profiles of the discs and the stators create a uniform shearing stress which favours creation of a relatively narrow drop size distribution. Any imperfection on the surfaces could cause very small drops to form which could reduce the volumetric capacity and create phase separation problems.

The drops are influenced by four basic factors:

i) Rotation around the shaft induced by disc rotation;

ii) Centrifugal force applied by the disc rotation;

iii) Buoyancy force due to density difference causing the lighter liquid to rise, and;

iv) Swirl due to tangential inlet of either or both of the phases.

The flow pattern of drops in the R.D.C. depend upon the speed of rotation. Two general flow patterns were observed as illustrated in Figure 6.2. At rotor speeds below 1.5 m/s, the dispersed phase droplets were trapped under the stator rings. The amount of entrapment was a function of the column geometry, rotor speed and liquid flowrates. At rotor speeds above 1.5 m/s, and also at flowrates near to flooding, the flow pattern was as shown in Figure 6.2. In this case back mixing

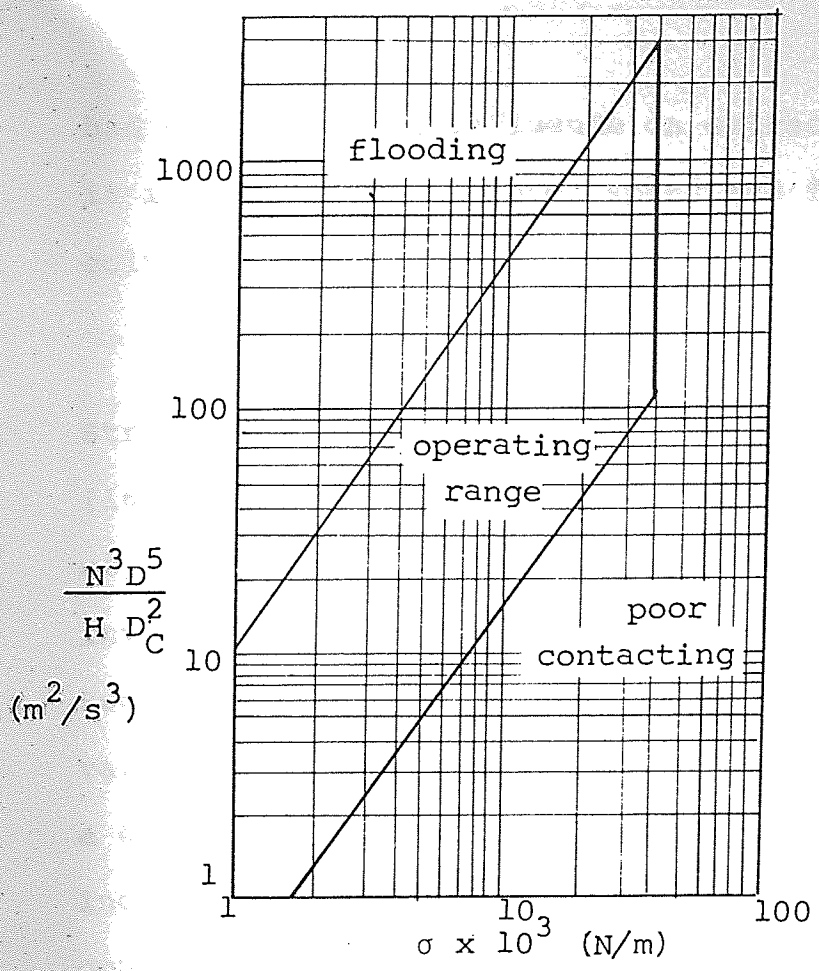

Figure 6.1 : R.D.C. Power Input Group Operating Range.

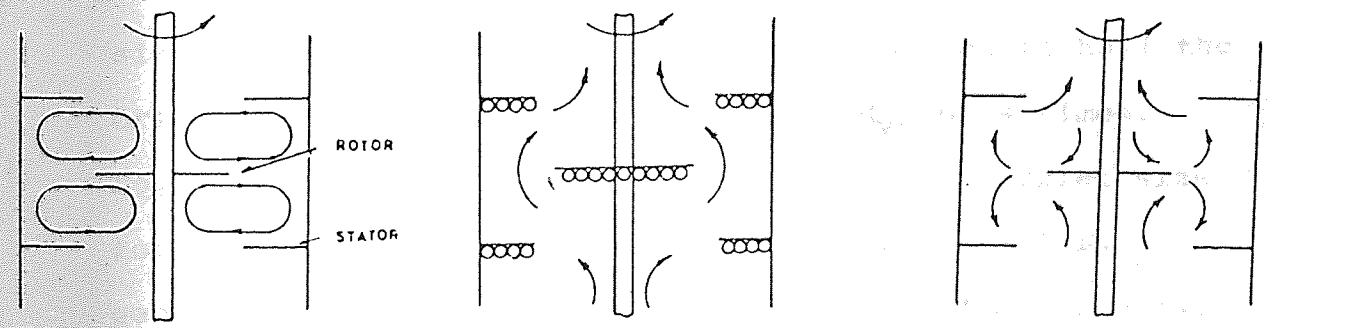

ealised flow pattern

Dispersed phase flow pattern ($Re < 7.5 \times 10^4$)

Dispersed phase flow pattern ($Re > 7.5 \times 10^4$)

Figure 6.2 : Typical Flow Patterns in a R.D.C.

had an increasing influence on extractor efficiency since it is a function of rotor speed and flowrates as well as column geometry.

Drop size has been studied in the R.D.C. by Strand et al (114), Kagan et al (186), Logsdail et al (168) and Misek (152). The droplet size as a function of radial distance from the axis and rotor speed was investigated by Kagan et al (186) by photographic technique. The increase in rotor speed up to an optimum value resulted in a decrease in mean droplet size and a corresponding increase in interfacial area. Further increase in rotor speed decreased the mean drop size considerably. Radial distribution of drop size indicated that the size of drops decreased by 1 to 3 times between the middle of the rotor disc and its tip depending upon the liquid dispersed. Doubling the rotor diameter showed further breakage of drops to about ⅓th of their initial size. However, decreasing the stator opening to half the original value increased the value of d_{VS} by 4 times. Logsdail et al (168) observed that the mean droplet size for a given system is a function only of the column geometry and the rotor speed and is independent of phase flow rates. They inferred from high speed flash photographs of the drop dispersions that the mean droplet size remained substantially constant for all flow rates up to flooding for any given column geometry and rotor speed. This behaviour was found to be generally true for various water-solvent systems provided undistributed solutes were absent. It has been observed that coalescence of

droplets is enhanced when mass transfer occurs from the drop to the continuous phase whereas drop coalescence is inhibited for the reverse direction of transfer. In a coalescing system the mean drop size would be expected to increase as the dispersion moves away from the rotor, to be again broken down in its next contact with the rotor.

It is obvious that the capacity of the R.D.C. is governed by the size of dispersed droplets. Hinze (212) suggested that the mechanism by which particles of the dispersed phase are broken up in a given hydrodynamic field may be understood from a consideration of energy dissipation. He showed that the maximum surviving particle size in a given situation, such as in a locally isotropic turbulent field, should correspond to a critical value of a suitably defined Weber number involving the energy dissipated per unit volume, leading to the following relationship for the maximum stable drop size:

$$d_{max} \alpha \frac{\sigma^{0.6}}{(p/v)^{0.4}\rho_c^{0.2}} \qquad (6.16)$$

where (p/v) is the energy dissipated per unit volume. Strand et al (114) recommended the following form for R.D.C.

$$d_{max} = C\left(\frac{g_c\sigma}{\rho_c}\right)^{0.6} (\Sigma)^{-0.4} \qquad (6.17)$$

where Σ is the power input per unit mass. The power input term, Σ, has been related to the power number, N_{po}, defined as $(Pn/\rho_c N^3 D_R)$ by

$$\Sigma = N_{po}\{\frac{4}{\pi} \cdot \frac{N^3 D_R^5}{ZD_C^2}\} \qquad (6.18)$$

In the above, the power number N_{po} incorporates P_n the power input per compartment. The value of the power number N_{po} has been observed (178) to be a function of disc Reynolds number. Oliver (213) has recommended that a mean value of 0.03 for N_{po} may be assumed in the usual range of R.D.C. operation above critical rotor speeds.

Strand et al (114) observed that when water was dispersed, the value of C in Equation (6.17), varied in the range 0.8 to 1.2, the ratio, d_{av}/d_{max}, remained almost a constant and therefore suggested that the mean drop size be taken as 0.7 times the mean diameter given by Equation (6.16).

Within the turbulent mixing region in an R.D.C., the following expression was derived to predict the drop size (155,203)

$$\frac{d_o N^2 D_R \rho_c}{\sigma e^{0.887\Delta D}} = 16.3(\frac{H}{D_R})^{0.46} \qquad (6.19)$$

where ΔD is the distance of impeller from wall. The followings were assumed:

a) Splitting of drops occurs under conditions when the magnitude of the dynamic pressure, acting upon the drop, surpasses the magnitude of the cohesive surface forces of the drop.

b) The highest dynamic pressure acts upon the liquid near the column wall and is proportional to the square of the continuous phase velocity at this location.

c) The velocity of the continuous phase in the vicinity of the impeller is proportional to its peripheral speed and diminishes exponentially towards the column wall.

d) The vertical velocities of both the dispersed and continuous phases have a negligible effect on the splitting of drops.

e) The influence of compartment height may be expressed by a simple exponential function of $(\frac{H}{D_R})$.

However, the above equations do not consider the equilibrium drop size arising from the competing effects of coalescence and the break-up of the drops. These factors would greatly change the interfacial area calculated from this drop size.

6.5.5 Drop Size Distribution

In most studies, there has been considerable disagreement over the shape of the drop size distribution curve in the agitated system. Some investigators reported a normal distribution (158-161) while others found that the distribution to be log-normal (119,162,163 , 165). Chartres and Korchinsky (151) have confirmed Olney's (119) conclusions that d_{32} may not be a proper mean drop size to represent the transfer rate for the total drop population and that the drop size distribution in an R.D.C. obeys the upper limit distribution proposed by Mugele and Evans (165):

$$\frac{dv}{dy} = \frac{\delta}{\sqrt{\pi}} \exp(-\delta^2 y^2) \qquad (6.20)$$

$$\text{where } y = \ln\{\frac{\bar{a}d}{d_m - d}\} \qquad (6.21)$$

The upper limit distribution is a modified log-normal distribution which may be compared with the standard form of the log-normal distribution:

$$\frac{dv}{dy} = \frac{\delta}{\sqrt{\pi}} \exp(-\delta^2 y^2) \qquad (6.22)$$

$$\text{where } y = \ln \frac{d}{d_{gm}} \qquad (6.23)$$

Korchinsky and Azimzadeh-Khateylo (164) found that the upper limit distribution accurately represented the drop size data in an Oldshue-Rushton column. They emphasised the importance of applying drop size distribution in the mass transfer calculation instead of using the Sauter mean diameter (d_{32}). Chartres and Korchinsky (151) stated that the size of sample of drops used to represent a dispersion is also extremely important. They also pointed out the marked effect of inlet drop size on column drop size and measured extraction efficiency.

6.6 MASS TRANSFER IN R.D.C.

The prediction of mass transfer performance of a differential column usually involves the evaluation of the height of a transfer unit and the number of transfer units. There are three definitions of a transfer unit (214):

i) The true number of transfer units

$$(N.T.U.)_t = \int_{x_o}^{x_1} \frac{k.a.dx}{G_c} \qquad (6.24)$$

ii) The apparent number of transfer units

$$(N.T.U.)_a = \int_{x_o}^{x_1} \frac{dx}{x-x^*} \qquad (6.25)$$

where $y = mx^*$

iii) The measured number of transfer units

$$(N.T.U.)_m = \int_{x_o}^{x_1} \frac{dx}{x-x^*} \qquad (6.26)$$

The height of a transfer unit is given by the expression

$$(H.T.U.) = \frac{G}{K_L.a.S} \qquad (6.27)$$

The theoretical stage concept uses the fact that the amount of mass transfer taking place in a contactor may be regarded as a number of discrete equilibrium contacts. The height required for one contact is then analogous to height equivalent to a theoretical plate utilized in distillation column analysis. An efficiency may be used to express equipment performance, defined as the H.E.T.S., divided by the height of a practical stage. Although used in practice, this approach is of course fundamentally unsound when applied to a differential mass transfer operation.

In any event any attempt to calculate the equipment performance, expressed in terms of the terminal concentrations, will include any deviations from ideal behaviour. Thus, the $(N.T.U.)_a$ and $(N.T.U.)_m$ are only

valid for the conditions prevailing at the time of measurement, and in the specific equipment used. The prediction of the interfacial area and the extend of both radial and longitudinal mixing involve many empiricisms which results in the estimation of contactor performance being only approximate.

Mass transfer studies in the R.D.C. have been carried out by various workers and the effect of different parameters on the overall efficiency assessed. Reman and Olney (192) observed that efficiency increased with increasing specific load, peripheral speed and the ratio of dispersed to continuous phase flowrate but decreased with decreasing stator opening and compartment height. They also found that enhanced back-mixing reduced the efficiency at high rotor speeds and specific loadings. Data may be interpreted by plotting efficiency against power input (N^3R^5/HD^2). This is of doubtful validity, however, since system properties and the effect of axial mixing were not considered.

In subsequent work Logsdail et al (168) employed the systems toluene-acetone-water and butylacetate-acetone-water and produced a correlation of the form:

$$\left(\frac{(H.T.U.)_{oc}}{V_c}\right)\left(\frac{g^2\rho_c}{\mu_c}\right)^{1/3}(X_d) = \left(\frac{Xd}{K_{oc}\hat{a}}\right)\left(\frac{g^2\rho_c}{\mu_c}\right)^{1/3} = K\left(\frac{\mu_c g}{V_N^3(1-X_d)^3\rho_c}\right)^{2m/3}\left(\frac{\Delta\rho}{\rho_c}\right)^{\frac{2(m-1)}{3}} \qquad (6.28)$$

The constant K, exponent m and velocity V_N were determined by experiment. An accuracy to within 20% was obtained. Unfortunately, this correlation is of little practical significance since it is specific to the equipment and experimental conditions used in the investigation.

In a recent study, Al-Hemeri (215) interpreted mass transfer data by comparing observed mass transfer coefficients with values calculated assuming the stagnant drop, circulating drop, oscillating drop and fresh surface models (216). Generally, best agreement was obtained with the last two models. It was suggested that the total mass transfer comprised the net effect of a large number of oscillations and complete cycles of formation and coalescence. On this basis, he developed the expression:

$$\sum_{n=1}^{n}\left\{\sum_{i=1}^{i}\int\left\{\frac{dx}{x-x^*}\right\}_i\right\}_n = \sum_{n=1}^{n}\left\{\sum_{i=1}^{i} A_i/V_i \int K_i dt\right\}_n \qquad (6.29)$$

where i refers to any particular phenomenon, i.e. drop formation, drop oscillation, etc., and n is the compartment number. The above mass transfer model relies on the single drop correlations for transfer coefficients and therefore its application to an agitated interfacing multidrop system is of doubtful validity.

The importance of allowing for backmixing in all mass transfer calculations involving the R.D.C. has been realised for some time. Backmixing is either expressed by a dispersion coefficient or by a backmix ratio (217).

Olney (119) introduced the concept of axial dispersion in the R.D.C. and the following mass transfer models were proposed:

i) For the continuous phase,

$$E_c \frac{d^2y}{dZ^2} + \frac{V_c}{1-h} \frac{dy}{dZ} = \frac{-6h}{1-h} \int_{d_o}^{d_m} \frac{K_D(d)}{d} f(d)\{x(d)-my\}\delta(d) \qquad (6.30)$$

ii) For the dispersed phase,

$$E_d \frac{d^2}{dZ} \int_{d_o}^{d_m} x(d) f(d) \delta(d) - \int_{d_o}^{d_m} \frac{K_D(d)}{d} f(d)\{x(d)-my\}\delta(d) \qquad (6.31)$$

where f(d) is a function representing the drop size distribution in the column.

No analytical solution is available for the solution of Equations (6.30) and (6.31) so that a numerical solution is necessary. The other limitations are the dependence on empiricisms for values of the dispersion coefficient and the drop size distribution, both of which are not accurately predictable.

More recently Bruin et al (218) calculated "true" H.T.U. values for cobalt extraction in a 0.06 m diameter unit by modifying the values for plug flow using the Peclet number equations of Stemerding and Zuiderweg (219) viz

$$\frac{1}{Pe_1} = \frac{\varepsilon}{Pe_d} + \frac{1}{Pe_c} \qquad (6.32)$$

$$\frac{1}{Pe_2} = \frac{1}{Pe_d} + \frac{\varepsilon}{Pe_c} \qquad (6.33)$$

$$Pe_o = \{\frac{(Pe_1)0.1H}{(H.T.U.)_{true}} + 1\}/\{\frac{0.1H}{(H.T.U.)_{true}} + \frac{Pe_1}{Pe_2}\} \quad (6.34)$$

$$H.D.U. = \frac{1}{\frac{Pe_o}{H} + \frac{0.8}{H_T}\frac{\ln \varepsilon}{\varepsilon - 1}} \quad (6.35)$$

and $$(H.T.U.)_{true} = \frac{H_T}{N_{ov}} - H.D.U. \quad (6.36)$$

where H_T = Height of dispersion

H.D.U. = Height of a dispersion unit

The Peclet numbers are defined in the normal way by

$$Pe_c = \frac{V_c H_T}{(1-x_d)E_c}, \qquad Pe_d = \frac{V_d H_T}{x_d E_d} \quad (6.37)$$

Borrel et al (220) measured values of Pe_c and Pe_d in a 0.05 m diameter R.D.C. by a trace injection technique. They found that as the rotor speed increased the Peclet number for the continuous phase increased, as expected, and that in two phase systems backmixing in the continuous phase was accentuated by the droplets present. The actual value of Pe_c varied between 40 and 20, depending upon rotor speed and flowrates.

CHAPTER seven 7

EXPERIMENTAL INVESTIGATION

7.1 EXPERIMENTAL APPROACH

Lists of many possibilities of ternary systems were considered from various compilations (13, 36, 43) and a selection was based on:

i) The compounds should be available in a reasonable pure form and be relatively inexpensive, non-toxic and free from other hazards. Indicator of hazards given by Sax (221) and Muir (222) were taken as guide for handling the chemicals.

ii) The physical properties be conducive to good phase separation. (Density and viscosity values of a wide range of organic chemicals are published (223)).

iii) All the components should be amenable to simple chemical analysis independently.

iv) Two phase area of the system is significantly large for a wide range of compositions to be studied.

v) Availability of solubility and tie-line data of the system in reliable texts.

vi) Care was taken to select solvents not subject to degradation. Otherwise, in addition to extraneous impurities, the accumulation of products of solvent degradation at the

interface can also affect interfacial tension.

In view of the above criteria for system selection, the following ternary Type 1 systems were chosen:

1) Acetone (C) - Water (B) - Toluene (A)

2) Isopropanol (C) - Water - (B) - Cyclohexane (A)

3) Methanol (C) - Water (B) - Xylene (A)

The additives, sulphuric acid and acetic acid were added to the aqueous phase of less than 5% by weight to ensure that it is not in the mixed solvent regime. All measurements were made at a constant temperature i.e. 20 ± 0.5°C.

7.2 DETERMINATION OF PHASE EQUILIBRIA

There are a number of methods of determining the mutual solubility and tie-line data of an immiscible liquid system, (10, 11, 12) but the most convenient and reliable method is to utilize the Smith-Bonner (224) cell, as illustrated in Figure 7.1. This cell can be used:

a) to determine the mutual saturation curve by cloud point titration and

b) to equilibrate a two phase mixture to obtain tie-line data.

The apparatus consisted of a glass vessel of 100 ml capacity surrounded by a glass jacket welded to the cell through which was circulated water to maintain the contents of the cell at any desired temperature. The cell was provided with an agitator whose speed could be controlled,

Figure 7.1 : SMITH-BONNER CELL.

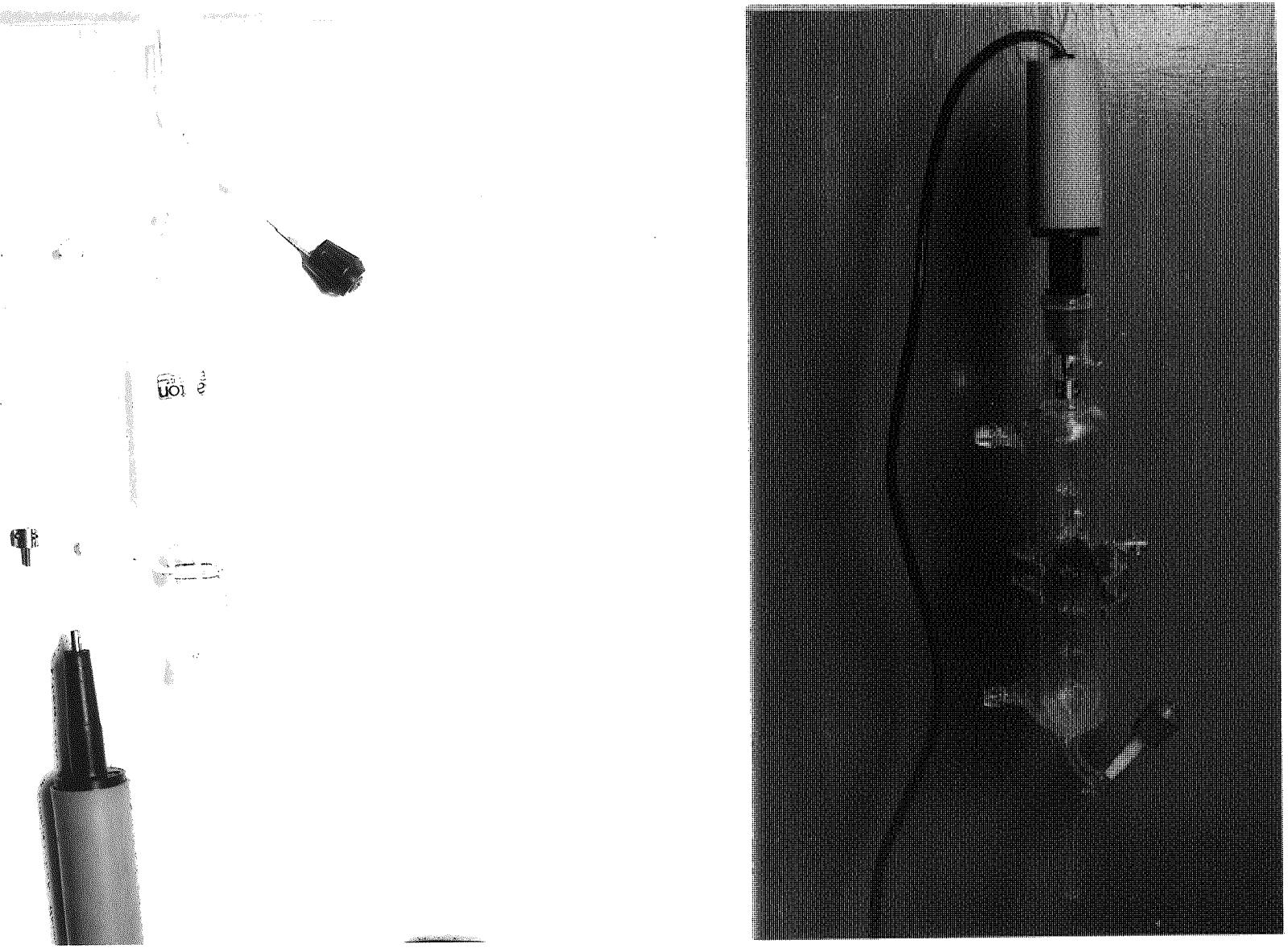

and a side arm near the top as shown in Figure 7.1 and Figure 7.2, for charging the liquid components. The cell contained a discharge tube with p.t.f.e. valve for emptying the contents on completion of an experiment; or, for discharging the heavy phase for sampling following an equilibration experiment. The water jacket was connected to a Tecam C-400 circulator thermostatic bath containing a circulating pump and temperature controller capable of maintaining the temperature at any desired level up to 50°C. Because of the time required to attain phase equilibria and sufficient tie-line data it was more convenient to operate three cells simultaneously as in Figure 7.3.

7.2.1 Determination of Mutual Solubility Curve

Mutual solubility curves were determined by cloud point titration using the cell and method recommended by Bonner and Smith (224) In the first series of experiments, homogeneous mixtures of known volumes of solvent A and solute C were placed in the cell, which was maintained at 20°C and agitated with the speed control adjusted to the mid-point of the range. This is equivalent to approximately 500 rpm. The contents of the cell were allowed to reach the set temperature.

Component B was slowly titrated into the mixture in the cell, so that the temperature remained constant at 20°C and the titration continued until 'cloudiness' appeared. A source of light was placed behind the cell to assist the observation. On approaching cloud point, the light appeared like a car's headlamp in misty weather. At this point, the exact quantity of component B that had been added was recorded. This was the

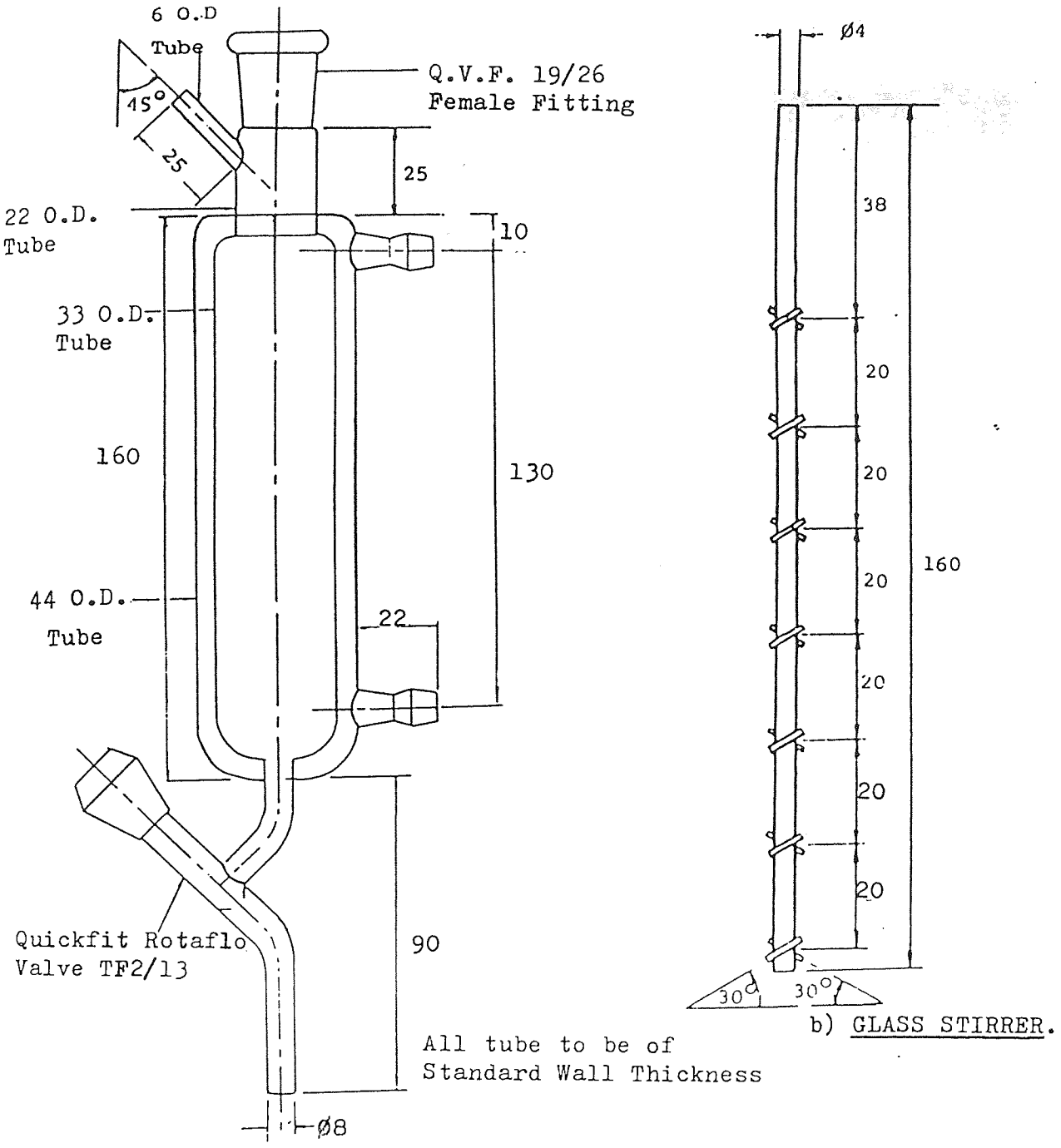

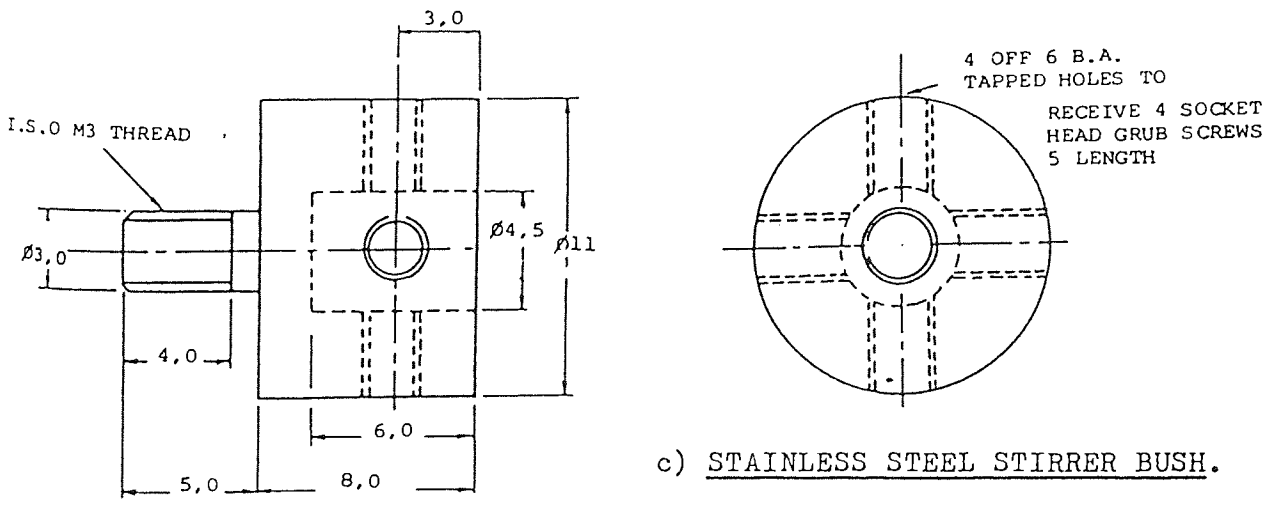

Figure 7.2 : THE SMITH - BONNER CELL AND ITS ANCILLARY PARTS.

Figure 7.3 : ARRANGEMENT OF THE CELLS AND THE TEMPERATURE CONTROLLING UNIT.

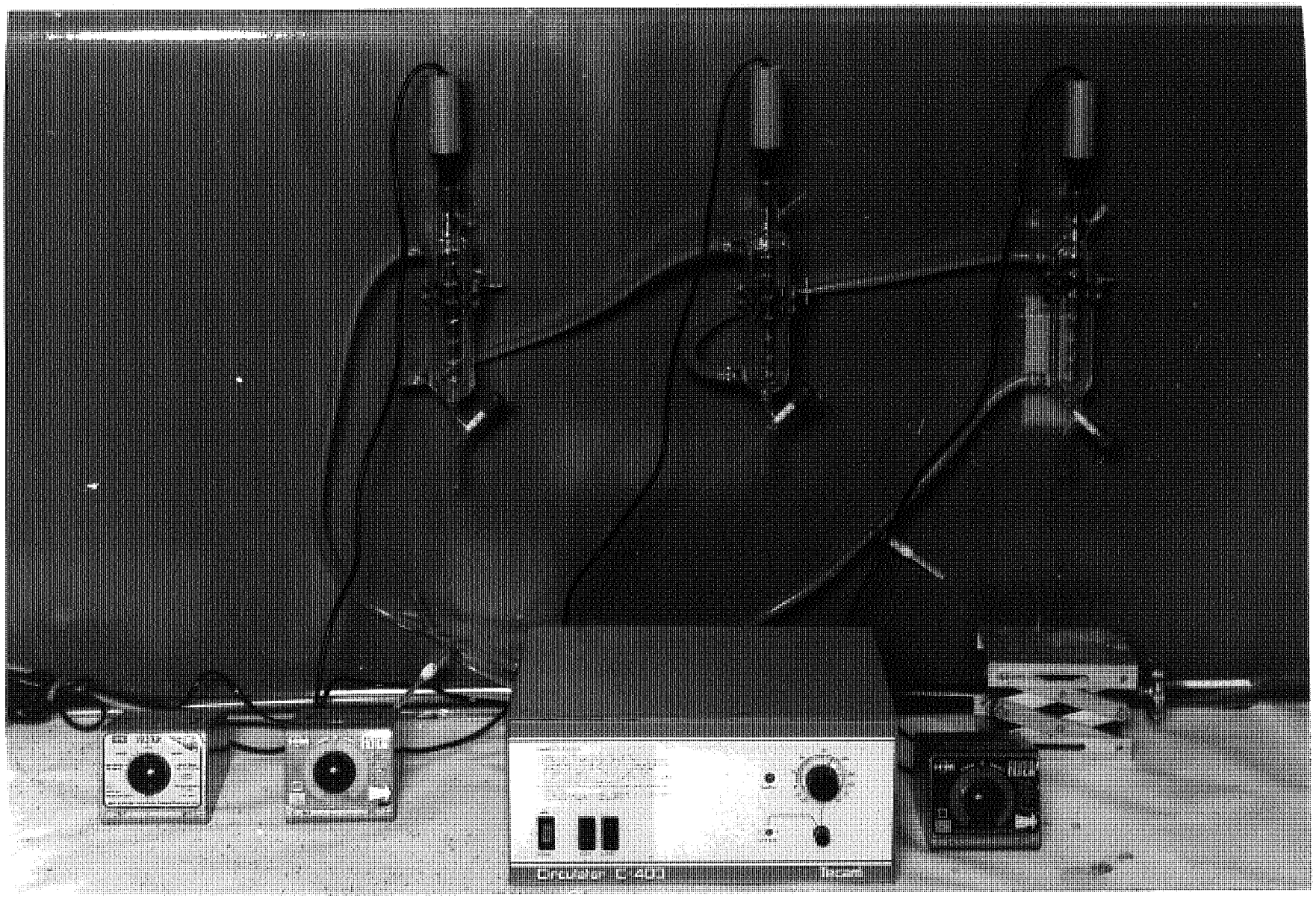

cloud point at which the component B added, saturated the mixture so that the amounts of solvent A and solute C were in equilibrium. It represents one point on the ternary solubility curve.

In the second series of experiments, homogeneous solutions of B and C were placed in the cell and the cloud point determined by titrating with A.

In each determination, the titration was performed very slowly so that the mixture in the cell was always maintained at the constant cell temperature of 20°C. Furthermore, the agitation was continued for about 15 minutes after the cloud point had been detected to ensure the feint turbidity was permanent. Not less than six well spaced points were required to construct one side of the mutual solubility curve. Samples were taken at each point of turbidity and analysed for refractive indices. Solute compositions versus refractive indices were tabulated and plotted.

The same procedure was repeated when additives were added to the solvent. Independent calibration charts were then plotted.

All results were tabulated in Appendix II.

7.2.2 Determination of Tie-lines

In these series of experiments, heterogeneous mixtures of A, B and C were placed in the Smith-Bonner cells and agitated for at least two hours at 20°C. This time was found to be adequate to achieve almost complete equilibrium in accordance to the sample calculation in Appendix IV.

Following this the agitation was stopped, the stirrers removed and the cells stoppered, but the constant temperature water was left circulating. The mixture was left for about one hour to settle into two distinct clear layers with a sharp interface. Each phase was transferred into a sample bottle with screw caps and sealed with p.t.f.e. tapes and later analysed for their refractive indices. The precise amount of solute present in each phase could then be determined from the calibration curves already plotted; and since the compositions of these solutions would be on the saturated mutual solubility curve this could be located on the ternary diagrams. A test of the accuracy of the experimental work could be made since the tie-line of the compositions of the extract and raffinate in equilibrium with one another must pass through the total mixture point based on the amounts added to the Smith - Bonner cell.

The above procedure was repeated with total mixtures containing different compositions of components, to obtain a number of tie-lines.

Similar procedure was adopted when acetic or sulphuric acid was added to the aqueous phase.

Due to its exothermic nature, precautions must be taken in preparing the aqueous solution, by ensuring only gradual addition of the sulphuric acid to the water and water should never be poured onto acid. After addition, a few minutes should be allowed to bring the temperature of the solution to near ambient temperature.

All results were tabulated in Appendix II.

7.2.3 Analytical Techniques

Solute concentrations were determined by measurements of refractive indices. Calibration charts of refractive indices versus solute concentrations were prepared by measuring the refractive indices of saturated solutions obtained during the determination of mutual solubility curves. The Abbe 60 Refractometer was used and only small quantities of the liquid were required for the test. The refractometer was maintained at a constant temperature of 20 ± 0.2^{o}C by means of a Townson and Mercer temperature controlling unit.

Considerations were given to the use of other methods e.g. titration, chromatography and conductivity measurements but these were found not applicable to every system. In the titration method, a third component is added to make the solution titratable. The conductivity method only applies to systems with measureable conductivity changes. Chromatography is tedious and time-consuming due to the requirement of correct choice of stationary and moving phases, operating temperatures etc. for each phase analysed.

7.2.4 Confirmatory chemical tests

Various confirmatory chemical tests, some examples are given in Appendix III, were carried out on some of the equilibrated phases to detect any possible by-products from side reactions upon the addition of the acids to the systems. The components in the phases were also separated by chromatography.

7.3 EXPERIMENTAL INVESTIGATIONS ON A PILOT SCALE ROTATING DISC CONTACTOR

The design, hydrodynamics and mass transfer efficiency characteristics of R.D.C. were described in Chapter 6.

In general, in the design of an R.D.C. for a particular extraction duty, the column diameter and the rotor speed are the main variables to be determined. The diameter of the column is related to limiting hold-up, and flooding flow-rates which are dependent upon the physical properties of the system.

The equipment used in this work is as shown in Figure 7.4, and illustrated in the flow diagram in Figure 7.5. The height of the R.D.C was 125 cm and it comprised two column sections each of 25 compartments. The shaft was a stainless steel rod 7.9 mm in diameter and was divided into two equal parts screwed together in the middle. It was supported by a p.t.f.e. bush inserted into a spider situated between the two column sections. This arrangement is shown in Figure 7.6. The bottom of the shaft rested in a p.t.f.e. bush centrally positioned in the bottom flange as shown in Figure 7.7.

Dimensions and other details of the column are summarised in Table 7.1. Stators and discs were made of 1.6 mm thick 18/8 stainless steel sheet. Discs were welded to the shaft and then machined to obtain a smooth, flat surface.

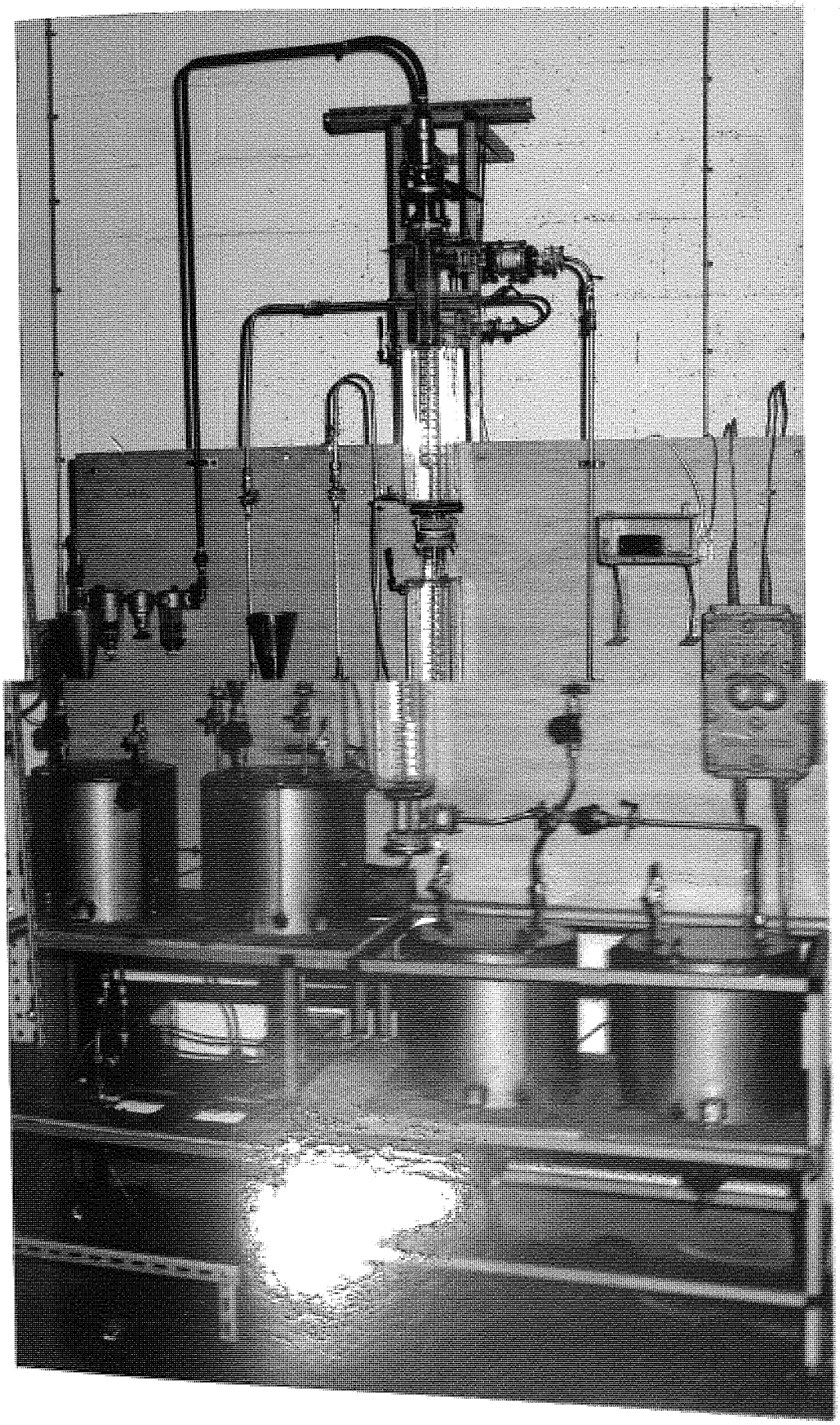

Table 7.1 : R.D.C. DIMENSIONS

Variables or Parts	Dimensions	
Column inside diameter (D)	5.0 cm.	Q.V.F. Glass
Column height	125.0 cm.	
Column wall thickness	0.5 cm.	
Stator and disc thickness	1.6 cm.	
Rotor shaft diameter	0.79 cm.	Stainless Steel
Disc diameter (R)	2.9 cm.	
Stator opening (S)	3.7 cm.	
Compartment height (H)	2.1 cm.	
Number of compartments	50	
S/D	0.74	
R/D	0.58	
H/D	0.42	
Maximum volumetric total capacity	60 l/hr.	

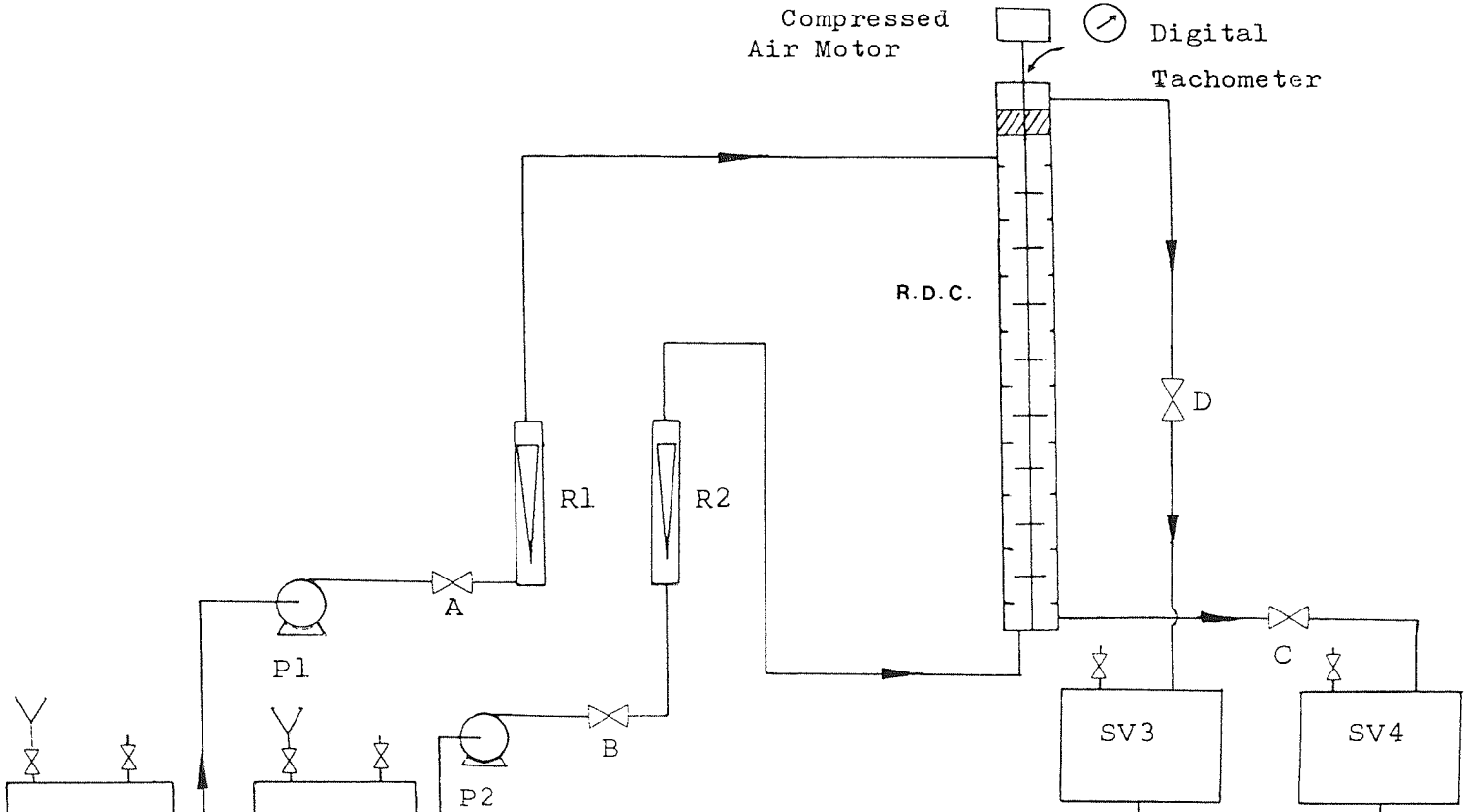

Figure 7.5 : Schematic Flow Diagram of the Pilot Scale Rotating Disc Contactor.

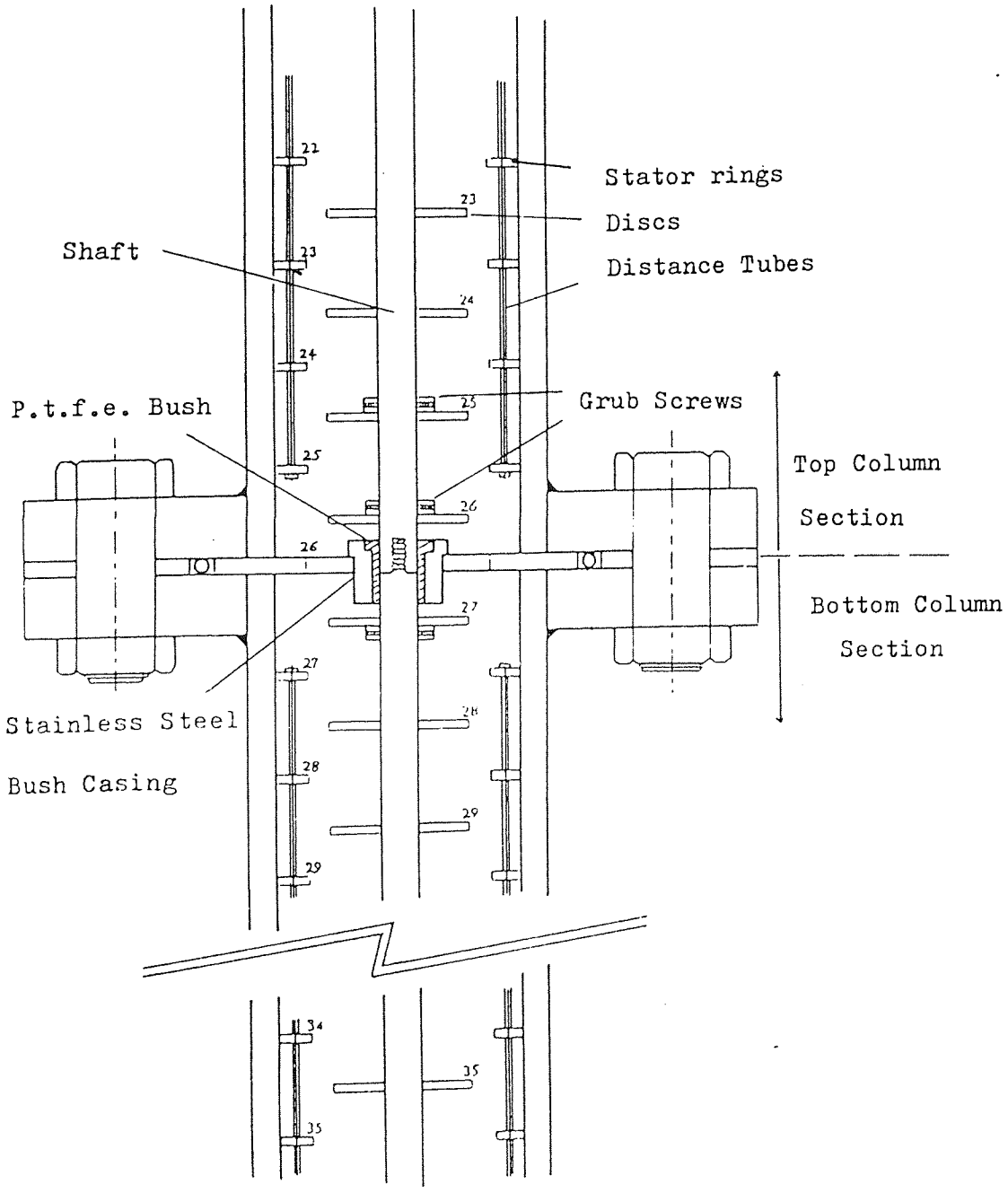

Figure 7.6 : CONSTRUCTIONAL DETAILS OF MIDDLE OF COLUMN.

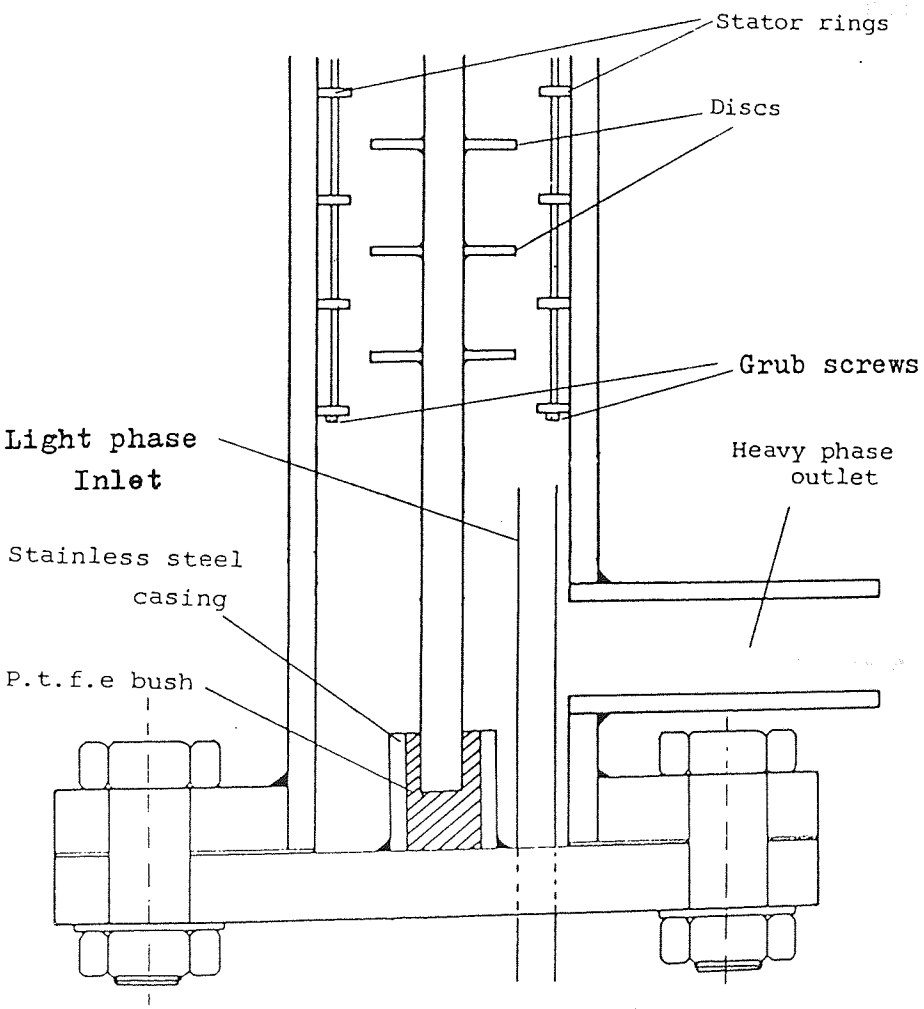

Figure 7.7 : CONSTRUCTIONAL DETAILS OF BOTTOM OF COLUMN.

Three discs near the middle of the shaft were fixed by grub screws so that they could be moved up or down for ease of assembly. The stator rings were supported by three equi-spaced distance of 0.8 mm stainless steel wires which were fastened to the top stator ring by grub screws. This was found to be rigid enough to support the stators without introducing extraneous baffling effects. The rings were machined to a close fit with the column wall to avoid short-circuiting of liquids. In any event, the neighbourhood of the collar is effectively a dead zone and any disturbance caused by protruding screws would be very small (153). To isolate the phase inlets and outlets from the turbulence in the column and to assist phase separation, knitted mesh-type - 0.3 mm thick Teflon (p.t.f.e.) sections with 75% free volume were fixed slightly above the heavy phase inlet. To cope with the column operating pressure a type 109B crane single seal was assembled at the top of the rotor shaft.

The top of the column is illustrated in Figure 7.8. The seal was fixed to the shaft with grub screws and the shaft was machined to fit the inside diameter of the seal and the seal seat. A p.t.f.e. gasket was used to seal between the seal seat and top flange of the R.D.C. The seal and the seal seat were held together inside the top flange by socket head bolts. An aluminium bearing casing was bolted to this part of the construction. Here the shaft was supported by a radial bearing and a thrust bearing was used against axial thrust. A smaller diameter collar was fixed to the shaft by grub screws and an oil reservoir was provided together with a water reservoir for the aluminium bearing casing. The oil reservoir contained Type Tellus F3 Shell oil for lubrication of the

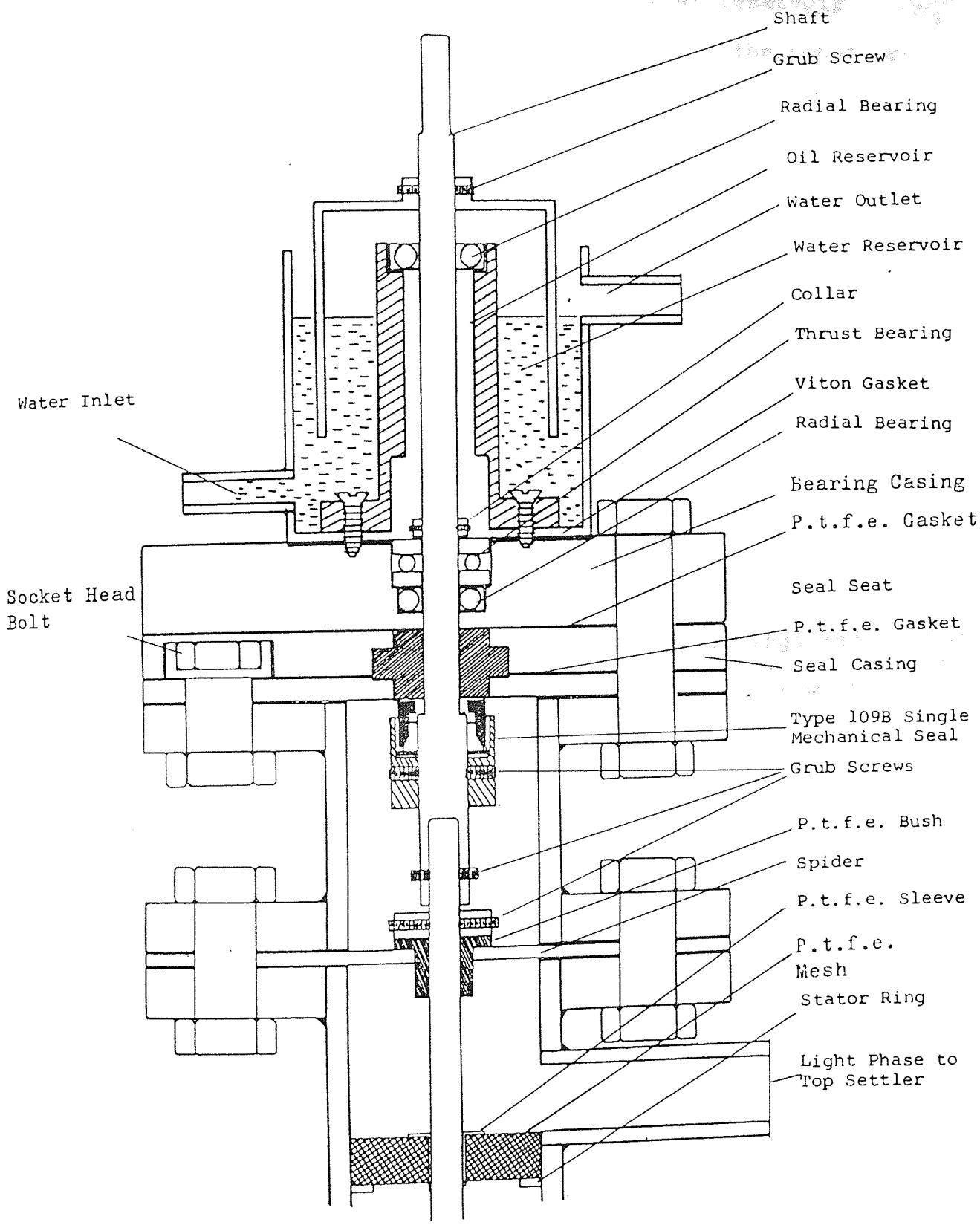

Figure 7.8 : CONSTRUCTIONAL DETAILS OF TOP OF COLUMN.

bearings. The shaft was also supported by a thrust bearing mounted on top of the oil reservoir. A water reservoir was provided above the seal. Full details of the construction of the top column section are given in Figure 7.8.

The rotor shaft was driven by a compressed air motor; the speed is variable up to 900 r.p.m. (the maximum obtainable) and was measured by a high precision Compact electronic tachometer, model DOT/M48 with visible light sensor Type VLS 1.

The feed, solvent, raffinate and extract storage vessels are each of 30 litres capacity. The feed and solvent are pumped counter-currently through the column using a stainless steel 'Stuart Turner' centrifugal pump, type no. 10 and 12, capable of handling 0.45 - 1.25 l/s against a hydrostatic head level of 2.0 to 10.0 in stainless steel casings and impellers were incorporated in these pumps together with graphite and 'Viton A' seals.

Rotameters R1 and R2 were installed in the solvent and feed lines for flowrate measurements. The end seals were provided by nitrile 'O' rings. The floats were of stainless steel and of size 7S. They were capable of measuring volumetric flowrates in the range of 0.1 to 0.4 litres per minute.

Preliminary observations and reference to the photographic work of Honekamp and Burkhart (225) suggested that the errors due to magnification and distortion of droplets caused by viewing through small diameter glass columns would be negligible with an aqueous continuous phase. Therefore, the working part of the column was set in a vessel of perspex which has the form of right parallel pipe. This vessel was

filled with water in order to compensate the wall curvature of the column during photographing. The water temperature was maintained at the mean temperature of both phases, i.e. approximately 20°C.

Pipe work was mainly of 1.3 cm stainless steel with p.t.f.e. tubing in certain sections. Four sampling points at convenient locations just before the inlet and after the outlets for both continuous and dispersed phases; comprised of a 10 mm diameter hole with a stainless steel quick-acting toggle valve. Drain-points were incorported under each storage vessel to allow complete draining of the system. Vent valves were also fitted on each storage vessel. Facility for liquid level indication was provided by glass tubes at one side of each storage vessel.

No provision was made for temperature control of the equipment environment but temperature was always within 18°C - 20°C. The equipment was located in an isolated pilot plant room, provided with flameproof switch gear and lighting and an efficient low level air extraction system.

7.3.1 Chemical System

High energy levels are created in the Rotating Disc Contactor compartments due to the high degree of turbulence by the rotors. Since it is well established that in a turbulent environment, the size of the drops is roughly proportional to $(\frac{\sigma}{\rho_c})^{0.6}$, a high interfacial tension system is to be preferred for study. The resulting drop sizes then tend to be larger and thus easier to record and measure.

The system Acetone-Toluene-Water was chosen for the

investigation with the water as the denser continuous phase in all experiments. The advantages of this system were:

i) The physical property data was available (226, 227 , 228) and the fire and safety properties of the system was also known (229). These were tabulated as in Appendix I.

ii) Advantages from the point of availability, cost , stability and low toxicity have been described (153).

iii) The system has been adopted as a standard in liquid extraction column research by the European Federation of Chemical Engineering Working Party on Distillation, Absorption and Extraction (229). This facilitates comparison of results.

iv) The solvent could be easily recovered and purified.

v) Analytical techniques are available for the determination of acetone content in the aqueous and organic phases.

vi) The equilibrium relationship is approximately linear, in the immiscibility region. This facilitates the theoretical analysis of the experimental data. The equilibrium data are also not greatly affected by small variations in temperature (153).

Materials of the highest grade available were used and no further purification was made. The material grades and specifications are listed in Appendix I. Constant monitoring of the purity of the chemicals by measuring the interfacial

tension , was done during the whole experimental work and if there were serious discrepancies, the liquids were replaced.

The physical properties of the systems, although some were known, were measured as follows:

a) Specific gravity

The standard pycnometer technique was employed for all solutions. Measurements were made at 20 ± 0.1°C.

b) Viscosity

The method of timing the passage of the fluid through a capillary immersed in a constant temperature bath (20 ± 0.1°C) was used. The types of viscometer used were Cannon-Fenske BS/IP/CF No. 25 and No. 50.

c) Interfacial Tension

The standard Du Nuoy ring method was used on a "Cambridge" torsion balance at 20 ± 0.1°C. The measurement was done with mutually saturated liquid phases.

7.3.2 Cleaning procedure

A 1-2% v/v aqueous solution of Decon-90 decontaminant was used to clean the column vessels and the process lines. The whole system was filled with the cleaning solution for at least five hours and this was then circulated throughout the system with the agitator on for about an hour. The solution was drained and the system was then flushed through with tap water and finally rinsed with distilled water. Care

was taken to ensure that all sample points and drainage points were well flushed and free of traces of detergent. Checks were made by measuring the surface tension of the distilled water.

7.3.3 Preparation of Fluid System

Toluene was employed as the dispersed phase; the specification is given in Appendix I. It was used without further purification and its purity was carefully monitored. If a significant discrepancy in the value of the surface tension was obtained, it was then replaced. The continuous phase was once-distilled water throughout, produced from an all-glass still. The measured average physical properties are given in Appendix I. Before use, the phases were mutually saturated by recycling them through the column for at least two hours and left to separate and settle overnight.

Toluene and distilled water were filled in the storage vessels, SV_1 and SV_2 respectively.

Similar procedure and precautions, as described in Section 7.2.2 in preparing the solution of the aqueous phase with acid additives, were exercised.

7.3.4 Hydrodynamic Studies

Hydrodynamic studies are conventionally performed in the absence of solute, and under non-mass transfer conditions, to avoid extraneous droplet break-up and coalescence effects which are dependent upon the rate, and direction of solute transfer.

The non-mass transfer investigations were performed in support of the main study to provide a good understanding of the pilot scale R.D.C. hydrodynamics via dispersed hold-up, drop size and drop size distribution; this was in addition of knowing the limiting capacity of the equipment via flooding phenomena.

7.3.4.1 Flooding

The operating procedure to determine the onset of flooding was as follows:

The column was filled with water by operating valve A and switching pump P1 after priming the pump by opening valve G. Valve C was then partly opened and valve A adjusted to give a continuous phase flowrate through the column and into the extract storage vessel corresponding to approximately 4.0 on the rotameter. The water level in the column was maintained by adjusting valve C.

Air was admitted to the agitator motor and the agitator speed adjusted to 500 r.p.m. as indicated on the digital tachometer. Valve H was then opened to prime pump P2; the pump switched on and valve B adjusted to give a reading of approximately 1.0 on the dispersed phase rotameter. Valve D was opened fully to allow toluene, which accumulates at the top of the column, as coalesced dispersed phase at the inter-phase near the knitted mesh pad to overflow unhindered into the raffinate storage vessel (N.B.: The vent valves on all four vessels must be fully opened to atmosphere throughout experimentation). After about two minutes operation, the

interface position was checked and valves A, B and/or C adjusted slightly as necessary to achieve a normal, steady-state column operation.

Valve A was opened a little further to give a 0.5 full increment in flow on the rotameter and the behaviour of the droplets in the column observed, if there was no accumulation of droplets in the middle of the column after two minutes, the continuous phase flowrate was again increased by 0.5 increment. Once droplet accumulation was apparent in the middle of the column, five minutes were allowed before marginally increasing the continuous phase flowrate. Flooding would be indicated by the accumulation of dispersed phase as droplets near the bottom of the column to such an extent that they were rejected via the continuous phase outlet. The readings on both rotameters corresponding to the onset of flooding were then recorded. The continuous phase flowrate was then reduced to 3.0 on the rotameter and the column allowed to return to normal operation.

The above procedure was repeated at five other continuous phase flowrates, up to a reading of approximately 7.0 on the rotameter and both flowrates were recorded corresponding to flooding in each case. The experiment was repeated at a higher rotor speed, i.e. 700 r.p.m.

The rotameter readings were converted to flowrates in litres/minute using the calibration curves and then these velocities converted into superficial velocities V_c, V_d in cm/s. V_c was plotted against V_d with rotor speed as parameter.

7.3.4.2 Dispersed phase hold-up

The most convenient method for determining the average dispersed phase hold-up under steady-state conditions below flooding is to measure the increase in dispersed phase level above a pre-set interface after the phase flows are shut-off instantaneously and the rotor stopped to allow complete settling. The procedure was as follows:

Steady-state operating conditions was established as described in Section 7.3.4.1. (For purposes of comparison, a fixed continuous phase rotameter setting of 4.0 would allow a full range of dispersed phase flowrates and hold-ups to be studied).

The interface position at the top of the column was observed and the setting of valve C was adjusted, if necessary, to bring it well below the dispersed phase outlet. When the interface level had remained steady for three to five minutes, its position h_i on the graduated scale was noted. Valves A, B and C were closed rapidly and all the pumps switched off and the rotor stopped. Three or four minutes were allowed for all the dispersed phase droplets to settle and coalesce at the interface. The new position of the interface h_f was noted and hence the difference $\Delta h = (h_f - h_i)$ was calculated. The above procedure was repeated at three or four higher dispersed phase flowrates, keeping the continuous phase flowrates constant and ensuring that the flooding conditions was not reached. The measurements were converted to give % dispersed phase hold-up:

$$h = \frac{\Delta h}{H_E} \times 100$$

where H_E was the effective height for the column, i.e. the distance between the dispersed phase distributor and the initial interface level.

The experiment was repeated at higher rotor speeds. h was plotted against V_D with rotor speed as parameter (at a constant value of V_C).

7.3.4.3 Photography and Associated Techniques

A Pentax Spotmatic 35 mm was employed for this work. The flameproof tube lights in the rig, although essential for visual observation, provided insufficient illumination for photography; therefore another tube light was placed at the back of and parallel to the column. Ilford 400 ASA films were used in most cases. Aperture openings, shutter speeds and focal lengths were adjusted accordingly . In most cases a shutter speed of 1/1000 second was found to give the best results especially at high rotor speeds. Two photographs, from the top and bottom sections were taken for each event, after hydrodynamic equilibrium was attained. The criterion for equilibrium was taken as a steady interface level and its attainment normally required about 7 to 10 minutes.

Drop size measurements were taken from prints with approximately 2 to 4 times magnification. A Carl-Zeiss T4.I.3 particle size analyser was used to analyse the photographs. Ellipsoids were recorded as spheres of equivalent diameter. A total of more than 200 drops were counted in a random manner from each photograph.

7.3.5 Mass Transfer Studies

The operating procedure was similar to that described above for the hydrodynamic studies. However, since acetone was used as a solute, particular care was required because of its higher volatility and hence flammability (i.e. the flash point of acetone is $-19^{o}C$ (22l)). The presence of small amounts of acetone in toluene will significantly reduce the flashpoint of the entire mixture.

The distribution curve for the system acetone-toluene-water was established using the procedure described in Section 7.2.

7.3.5.1 Operating Procedure

25 litre feed solution comprising toluene containing between 5% to 15% by weight of acetone was prepared and transferred into the feed reservoir, SV2 with valve H closed. Solvent reservoir SVl was filled with distilled water. The cetrifugal pumps Pl and P2 were switched on, and the continuous phase flow established through the column at the desired rate. The rotor speed was set and a flow of dispersed phase was established (N.B. Any combination of phase flowrates and agitator speed, but the conditions should not exceed 70% of 'flooding' values and best results involve $V_D/V_C \cong 0.5$ to 2.0).

Valve C was adjusted to maintain a constant interface level in the column and the extract and raffinate phases

collected at their respective storage reservoirs. Minor adjustments to valves A and B were made, as necessary, to maintain the required flowrates.

Initial runs were carried out to determine the time taken for the column to reach steady state conditions and this was done by taking samples from the quick-acting toggle valve outlet streams sample points S3 and S4 at 3 minute intervals, until identical acetone concentrations were obtained for consecutive time intervals. This was found to be about 15 minutes. After steady state conditions had been reached, 20 mls samples were taken from the sample points S1, S2, S3 and S4, using clean glass bottles with screw caps and sealed with p.t.f.e. tapes.

The dispersed phase hold-up was determined in the manner described in Section 7.2.4.3.. Analysis of the samples for acetone concentration was according to method described in Section 7.2.3. Following analysis, the raffinate concentration was adjusted by acetone addition to provide feed for the next set of experiments.

CHAPTER eight

8

DISCUSSION OF RESULTS

8.1 LIQUID-LIQUID EQUILIBRIA STUDIES

Three systems namely i) Acetone-Toluene-Water
ii) Propan-2-ol-Cyclohexane-Water
and iii) Methanol-Xylene-Water
have been studied at 20°C. The additions of acids were at two weight percentages i.e. 2% and 5%.

The ternary solubility curves were plotted on triangular graph paper using the weight percentages obtained from the experimental results, tabulated in Appendix II. For each tie-line equilibria determination, the concentration of solute in each phase was plotted on the curve. Each pair of points was joined by straight lines. Each straight line should pass through the point within the unstable two phase region beneath the binodal solubility curve, corresponding to the composition of the heterogeneous mixture charged into the cell. For clarity reasons, individual points for the solubility determination and those representing the initial mixture and the two points on both phases were not marked on the triangular diagram.

Individual calibration curve and experimental equilibrium diagram are given in Appendix II.

The reliability of the equilibrium data were tested by applying the Othmer-Tobias and Hand's correlations. Othmer-Tobias correlations indicates that there is a linear relation between the values of

$$\log \frac{1-X_{AA}}{X_{AA}} \text{ vs } \log \frac{1-X_{BB}}{X_{BB}}$$

Hand correlates the concentrations of the solute in the two conjugate solutions and the plot

$$\log \frac{x_{CA}}{x_{AA}} \text{ vs } \log \frac{x_{CB}}{x_{BB}}$$

is rectilinear.

i) Acetone-Toluene-Water.

The solubility and tie-line data obtained was compared to that of Walton and Jenkins (231) and of the three authors presented in the European Federation of Chemical Engineers' "Recommended Systems for Liquid Extraction Studies" (229). Excellent agreement was achieved. Upon the addition of 2% and 5% sulphuric acid, there was a significant change in the tie-lines. Favourable results were also achieved with the 2% addition of acetic acid to the water phase. The solutropic phenomena of the system was eliminated in the presence of the acid, as shown in the distribution diagram in Figure (8.4).

The activity of each component in each respective phase was also evaluated by means of the double suffix Van Laar equation (24), using suitable 'end value constants' obtained from those calculations using available corresponding data (24). These calculations were corrected to that at 20°C by the method suggested by Dauphin (230) for small temperature differences. These values were checked for agreement to those obtained using a different method for activity evaluation or different source of binary data. The agreement of predicted to the experimental solubility and equilibrium data are reasons to believe that the data obtained were reliable. A sample of the calculation is given in Appendix V.

ii) Propan-2-ol-Cyclohexane-Water

Data obtained from phase equilibrium studies for the system were compared to those of Verhoeye (232) and Washburn et al (234). The agreement was excellent. Significant changes in the tie-lines in the presence of the acids were again observed.

iii) Methanol-Xylene-Water

The system is isopycnic. Hartley (235) published the equilibrium data at 20°, 30° and 50°C. The experimental data agreed satisfactorily with his results for 20°C. Besides altering the slope of tie-lines, it was observed that under uniform conditions, the presence of acids accelerates dispersion. Only 2% addition was carried out due to difficulty in differentiating the very close convergence of tie-lines. Isopycnic was apparent at an earlier or lesser concentration of solutes.

Figures (8.1) and (8.5) illustrate the interpolated triangular diagram, passing through common points under the binodal curve, to emphasize the direction of tilt of the tie-lines. The graphical method of interpolation discussed in Section 4.4.1.1, although adequate, was more accurate if the mirror images of the parallel construction lines were drawn especially in the region of the plait point. Table 8.1 shows the obtained interpolated data.

Regression analysis of the Othmer-Tobias' and Hand's correlations were done using the statistical package 'NLR 1' on the University of Manchester Regional Computer Centre. The results in Tables 8.2 and 8.3, confirm the changes in slopes and intercepts in Figures (8.2), (8.3), (8.6) and (8.7). For Hand's correlation, such changes are inconsistent due to the fact that the line is supposed to be rectilinear especially for solutropic systems.

The distribution diagrams illustrated in Figures 8.4 and 8.8 confirms the deviations obtained in the presence of acids. Solutropic characteristic of the systems: Acetone-Toluene-Water was eliminated.

Only the double suffix Van Laar equation (24) was used to assess the consistency of the experimental results thermodynamically. The NRTL and UNIQUAC methods have been extensively applied by various researchers on all the three systems studied and the evaluated parameters have been compiled elsewhere (236).

Generally, all thermodynamic correlations for ternary and multicomponent systems would require at least binary

interactions data to evaluate the various essential parameters. Unfortunately, such data for sulphuric acid is almost non-existent especially when the acid is present in such a small quantity. However, experimental determination of such data is beyond the scope of the present study. Nevertheless, the above consistency tests are considered adequate to confirm the reliability of the experimental method and analysis. Similarly, Al-Saadi's (1) method of determining the salting effect from quaternary systems could not be applied due to absence of ternary interactions data, involving sulphuric acid.

Chemical confirmatory tests and chromatography ascertained that the added acid remained in the water phase throughout equilibrium determination and no chemical reaction took place in the presence of the added amounts of sulphuric acid.

Table: 8.1

INTER POLATED DATA.

i) Systems : Acetone - Toluene - Water at $20^{o}C$.

AQUEOUS LAYER			HYDROCARBON LAYER		
ACETONE Wt. %	TOLUENE Wt. %	WATER Wt. %	ACETONE Wt. %	TOLUENE Wt. %	WATER Wt. %
PURE					
20.4	0.0	78.6	19.4	80.6	0.0
28.6	0.4	71.0	31.0	68.4	0.6
37.4	0.9	61.7	42.0	56.5	1.5
45.0	1.7	53.3	53.7	43.0	3.3
53.8	3.4	42.8	63.3	29.9	7.8
2% H_2SO_4					
17.6	0.0	82.4	19.6	80.4	0.0
27.4	0.4	72.2	32.1	67.4	0.5
34.9	0.7	64.4	44.1	54.3	1.6
39.4	1.1	59.5	55.1	41.3	3.6
49.6	2.3	49.1	64.3	28.4	7.3
5% H_2SO_4					
15.3	0.0	84.7	24.4	75.6	0.0
25.0	0.0	75.0	34.6	74.6	0.8
33.9	0.6	65.5	44.8	53.4	1.8
43.3	1.4	55.3	54.9	41.4	3.7
52.9	3.4	43.7	63.2	27.2	9.6

Table 8.1: (Contd.)

ii) System : PROPAN-2-01 - CYCLOHEXANE - WATER at 20°C

AQUEOUS LAYER			HYDROCARBON LAYER		
Propan-2-ol Wt.%	Cyclo-Hexane Wt.%	Water Wt.%	Propan-2-ol Wt.%	Cyclo-Hexane Wt.%	Water Wt.%
PURE					
13.4	0.0	86.6	6.7	92.6	0.7
28.3	0.3	71.4	10.4	88.3	1.3
.40.3	1.2	58.5	16.0	82.3	1.7
50.7	4.5	44.8	19.7	78.3	2.0
56.7	10.4	32.9	32.0	63.6	4.4
2% H_2SO_4					
13.1	0.0	86.9	6.8	92.5	0.7
27.4	0.3	72.3	11.8	86.9	1.3
39.5	1.0	59.5	17.9	79.6	2.5
49.7	5.4	34.9	22.9	73.8	3.3
55.7	13.2	31.1	28.9	66.6	4.5
5% H_2SO_4					
13.3	0.0	86.7	9.5	89.7	0.8
25.0	0.2	74.8	14.7	83.5	1.8
38.1	1.7	60.3	19.5	78.0	2.5
49.1	5.8	55.1	23.9	72.8	3.3
55.8	13.4	30.8	28.5	77.1	4.4

Table 8.2

OTHMER-TOBIAS' CORRELATIONS

1) ACETONE-TOLUENE-WATER.
(C) (A) (B)

Pure Water : $\left(\frac{1-X_{BB}}{X_{BB}}\right) = 0.5432 \left(\frac{1-X_{AA}}{X_{AA}}\right)^{0.4183}$

Water + 2% H_2SO_4 : $\left(\frac{1-X_{BB}}{X_{BB}}\right) = 0.5891 \left(\frac{1-X_{AA}}{X_{BB}}\right)^{0.7453}$

Water + 5% H_2SO_4 : $\left(\frac{1-X_{BB}}{X_{BB}}\right) = 0.5969 \left(\frac{1-X_{BB}}{X_{BB}}\right)^{0.7693}$

Water + 2% AcOH : $\left(\frac{1-X_{BB}}{X_{BB}}\right) = 1.4525 \left(\frac{1-X_{AA}}{X_{AA}}\right)^{1.3647}$

2) PROPANOL-CYCLOHEXANE-WATER.
(C) (A) (B)

Pure Water : $\left(\frac{1-X_{BB}}{X_{BB}}\right) = 3.7326 \left(\frac{1-X_{AA}}{X_{AA}}\right)^{1.048}$

Water + 2% H_2SO_4 : $\left(\frac{1-X_{BB}}{X_{BB}}\right) = 4.0668 \left(\frac{1-X_{AA}}{X_{AA}}\right)^{1.0629}$

Water + 5% H_2SO_4 : $\left(\frac{1-X_{BB}}{X_{BB}}\right) = 8.411 \left(\frac{1-X_{AA}}{X_{AA}}\right)^{2.098}$

3) METHANOL-XYLENE-WATER.
(C) (A) (B)

Pure Water : $\left(\frac{1-X_{BB}}{X_{BB}}\right) = 5543.1 \left(\frac{1-X_{AA}}{X_{AA}}\right)^{2.027}$

Water + 2% H_2SO_4 : $\left(\frac{1-X_{BB}}{X_{BB}}\right) = 3.8929 \left(\frac{1-X_{AA}}{X_{AA}}\right)^{0.1472}$

Table 8.3

HAND'S CORRELATION

1) ACETONE-TOLUENE-WATER.
(C) (A) (B)

Pure Water : $\frac{x_{CA}}{x_{AA}} = 0.147 \left(\frac{x_{CB}}{x_{BB}}\right)^{0.548}$

Water + 2% Acetic : $\frac{x_{CA}}{x_{AA}} = 0.166 \left(\frac{x_{CB}}{x_{BB}}\right)^{0.814}$

Water + 2% H_2SO_4 : $\frac{x_{CA}}{x_{AA}} = 0.163 \left(\frac{x_{CB}}{x_{BB}}\right)^{0.702}$

Water + 5% H_2SO_4 : $\frac{x_{CA}}{x_{AA}} = 0.1795 \left(\frac{x_{CB}}{x_{BB}}\right)^{0.727}$

2) PROPANOL-CYCLOHEXANE-WATER.
(C) (A) (B)

Pure Water : $\frac{x_{CA}}{x_{AA}} = 0.766 \left(\frac{x_{CB}}{x_{BB}}\right)^{0.976}$

Water + 2% H_2SO_4 : $\frac{x_{CA}}{x_{AA}} = 0.498 \left(\frac{x_{CB}}{x_{BB}}\right)^{1.468}$

Water + 5% H_2SO_4 : $\frac{x_{CA}}{x_{AA}} = 1.882 \left(\frac{x_{CB}}{x_{BB}}\right)^{1.9693}$

3) METHANOL-XYLENE-WATER.
(C) (A) (B)

Pure Water: $\frac{x_{CA}}{x_{AA}} = 174.64 \left(\frac{x_{CB}}{x_{BB}}\right)^{1.88}$

Water + 2% H_2SO_4: $\frac{x_{CA}}{x_{AA}} = 1.821 \left(\frac{x_{CB}}{x_{BB}}\right)^{0.134}$

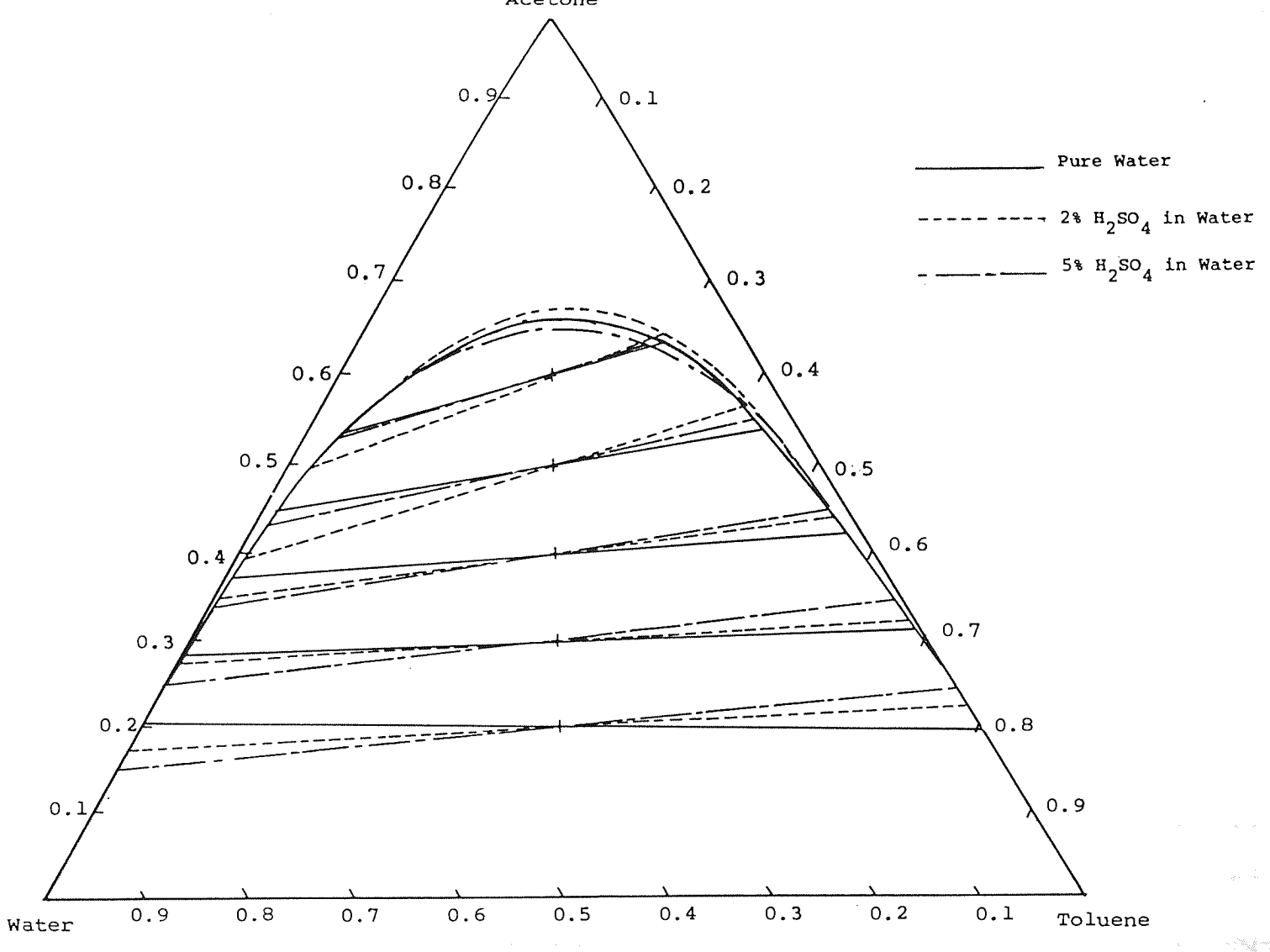

Figure 8.1: Interpolated Equilibrium Diagram for System :Acetone-Toluene-Water at 20°C.

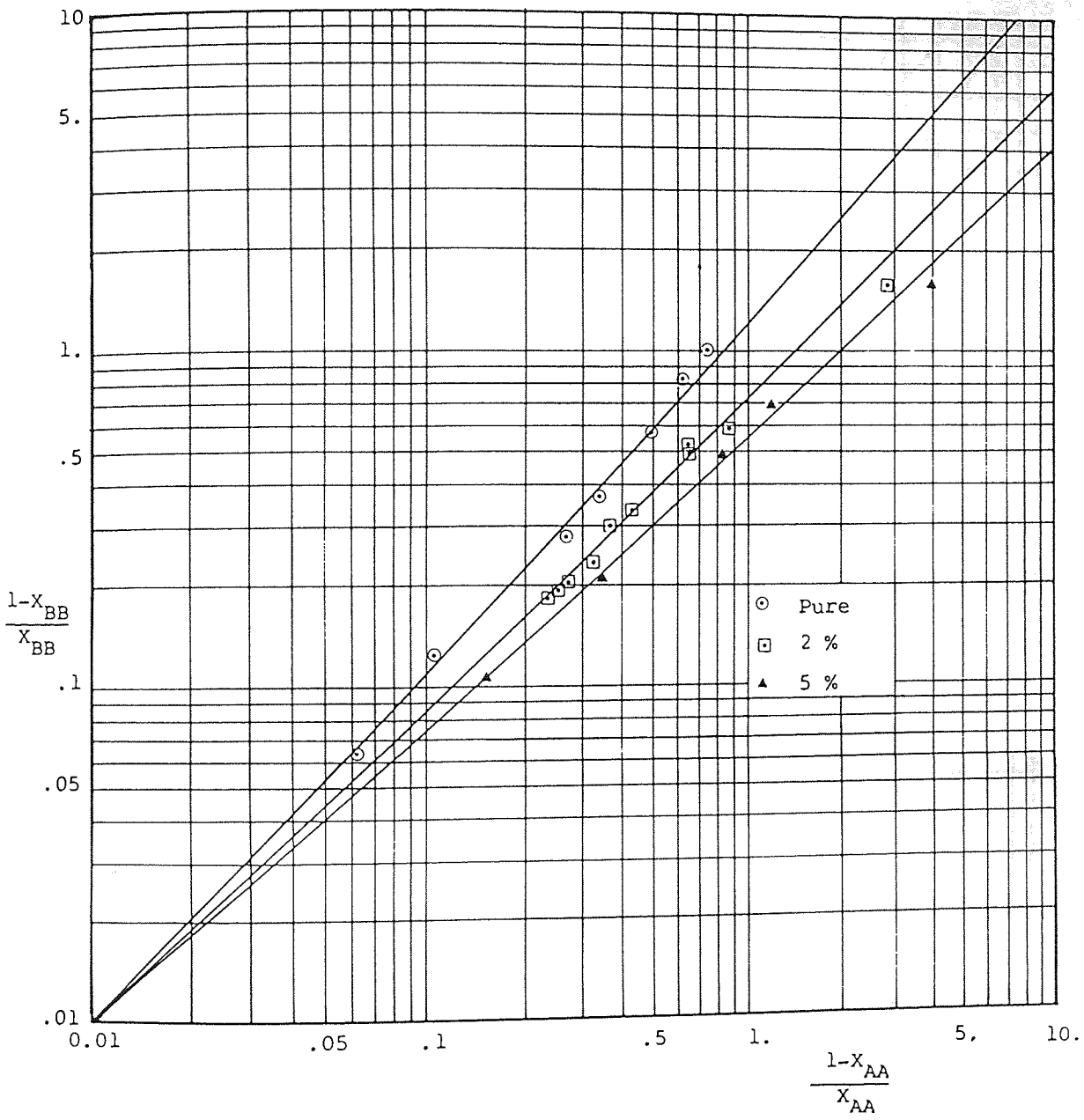

Figure 8.2 : Othmer - Tobias Correlation

System : Acetone (C) - Toluene (A) - Water (B) at 20°C.

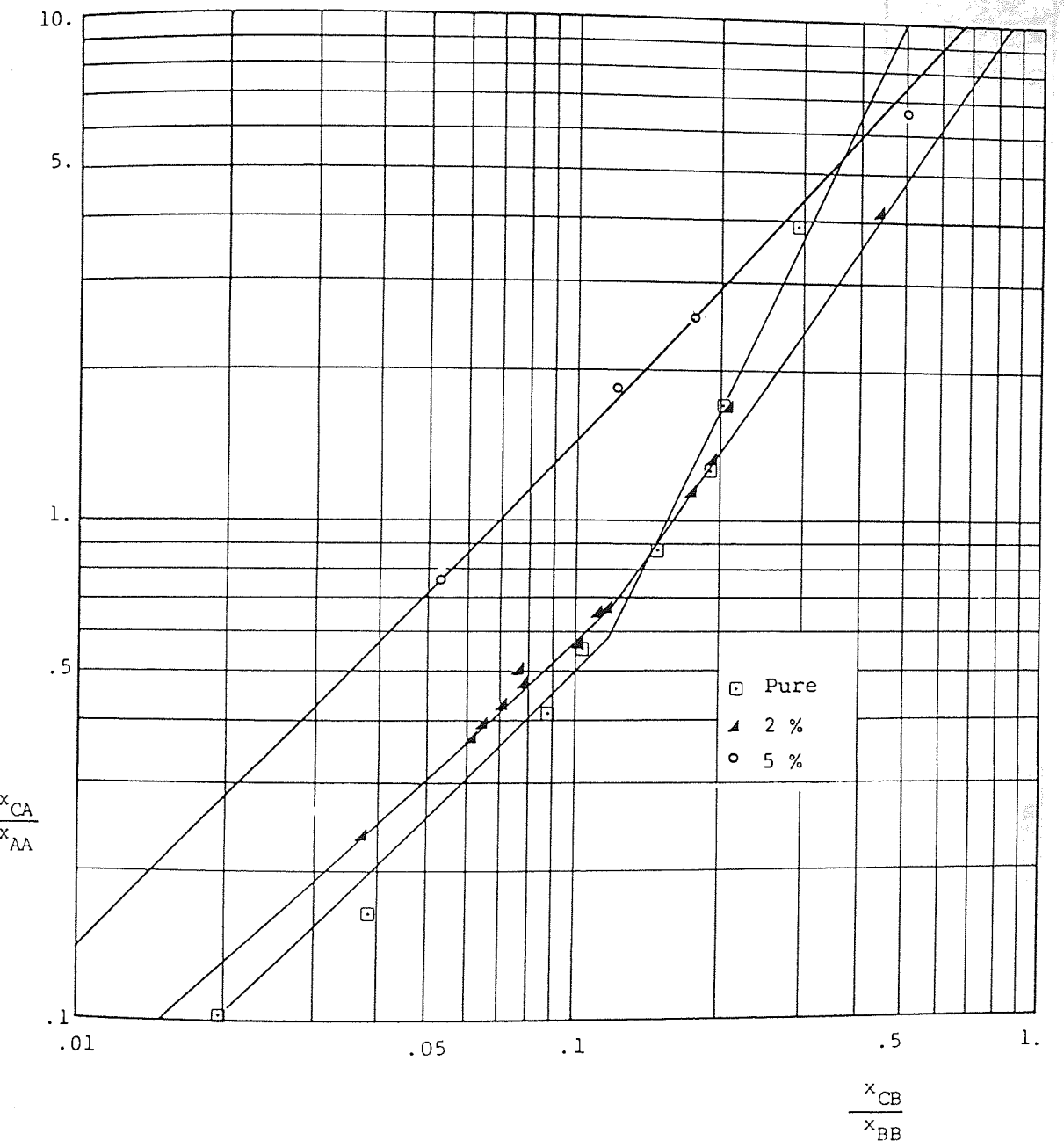

Figure 8.3 : Hand's Correlation -

System : Acetone (C)-Toluene(A)-Water(B) at 20°C.

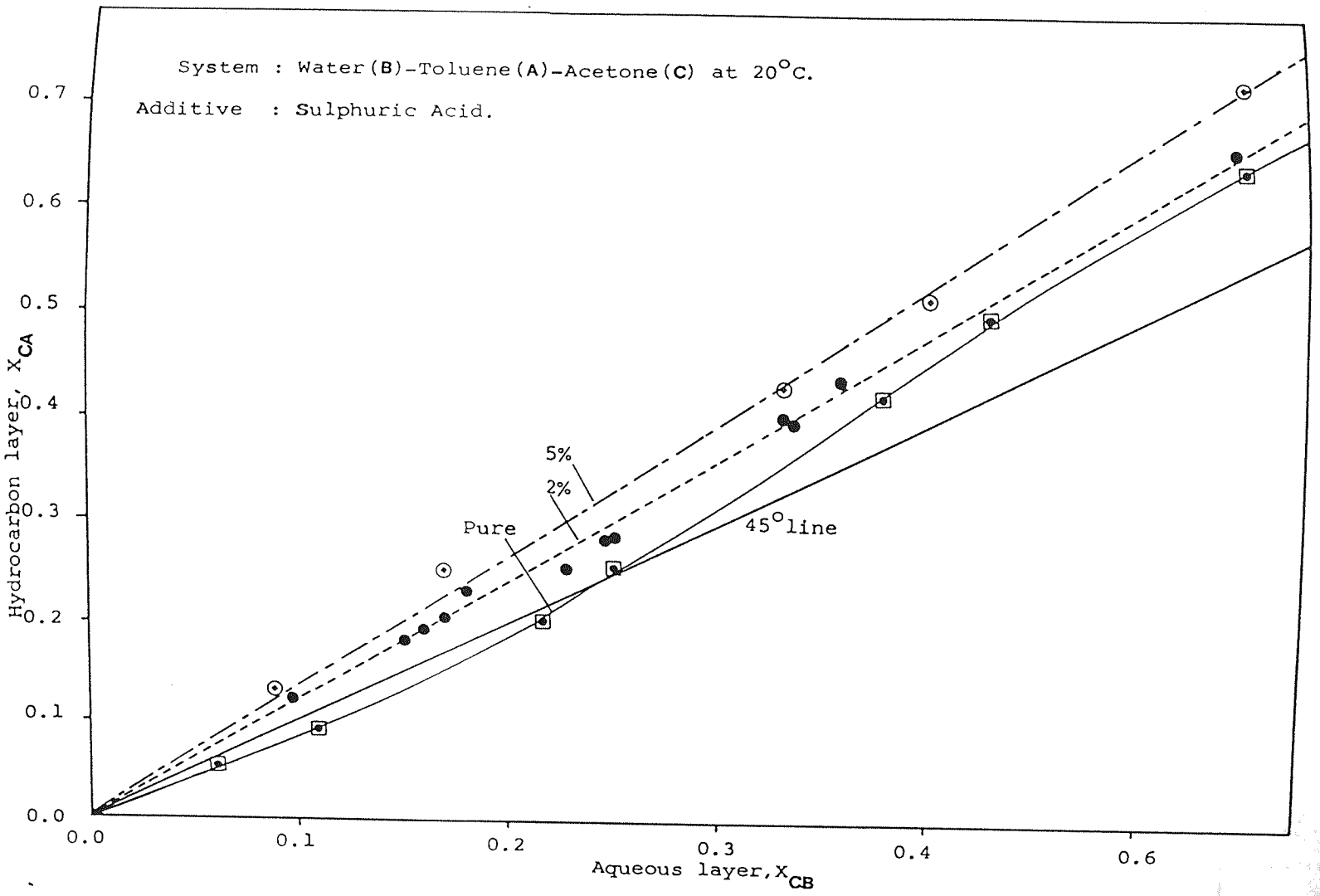

Figure 8.4 : Distribution Diagram - System : Acetone(C)-Toluene(A)-Water(B) at 20°C.

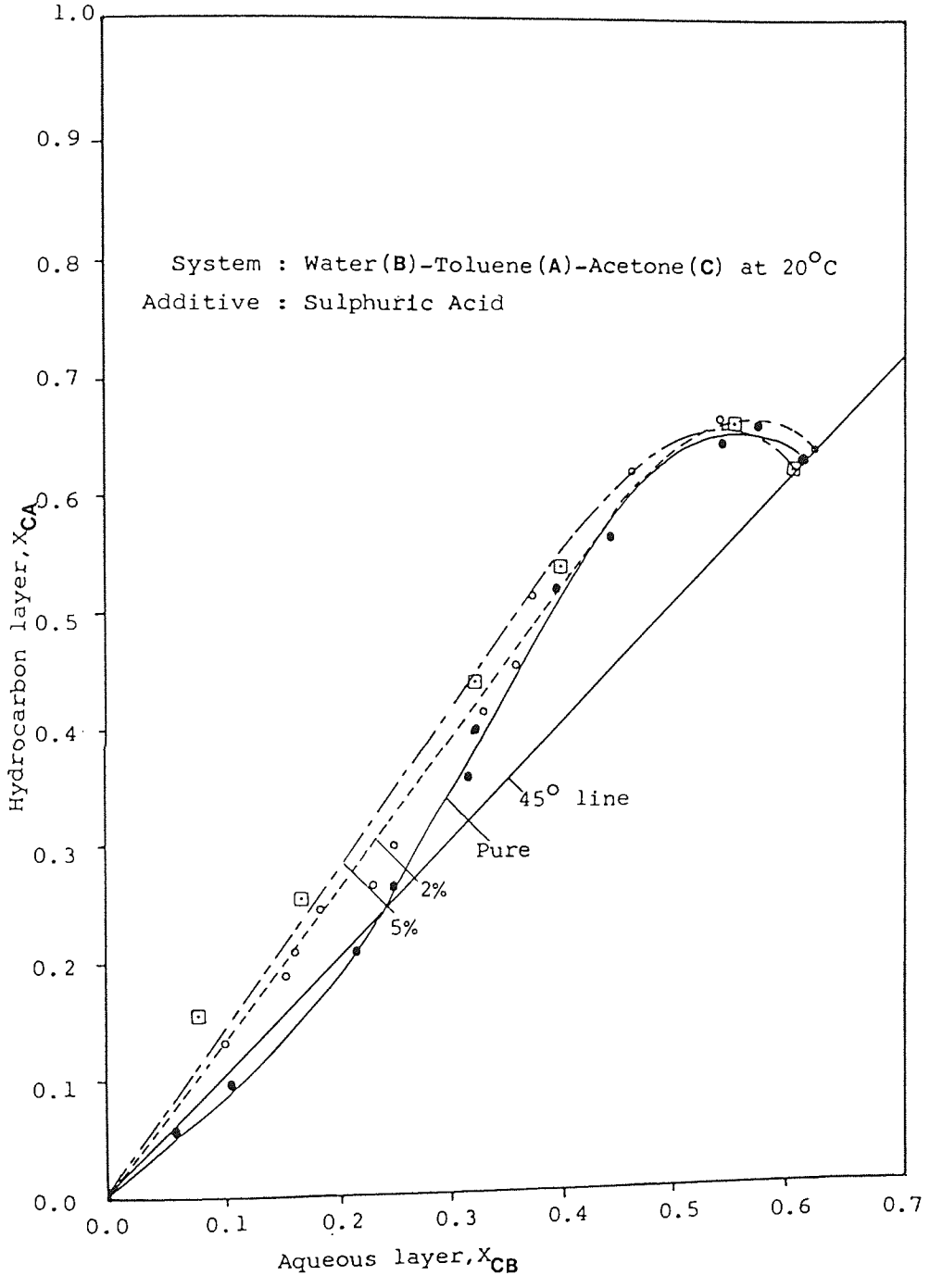

Figure 8.4 (b): Extrapolated Distribution Diagram-

System : Acetone(C)-Toluene(A)-Water(B) at 20°C.

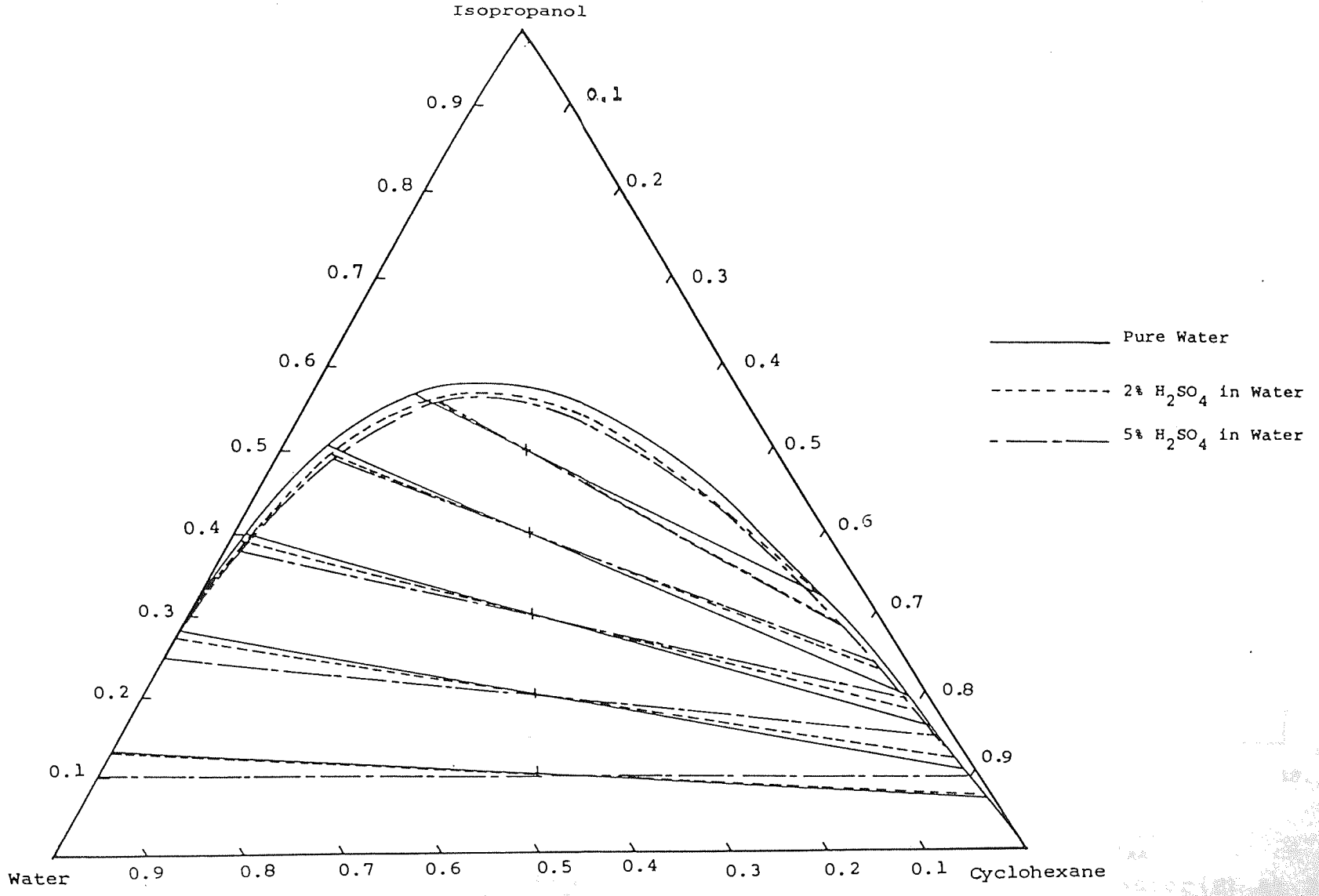

Figure 8.5: Interpolated Equilibrium Diagram for System:Propan-2-ol-Cyclohexane-Water at 20oC.

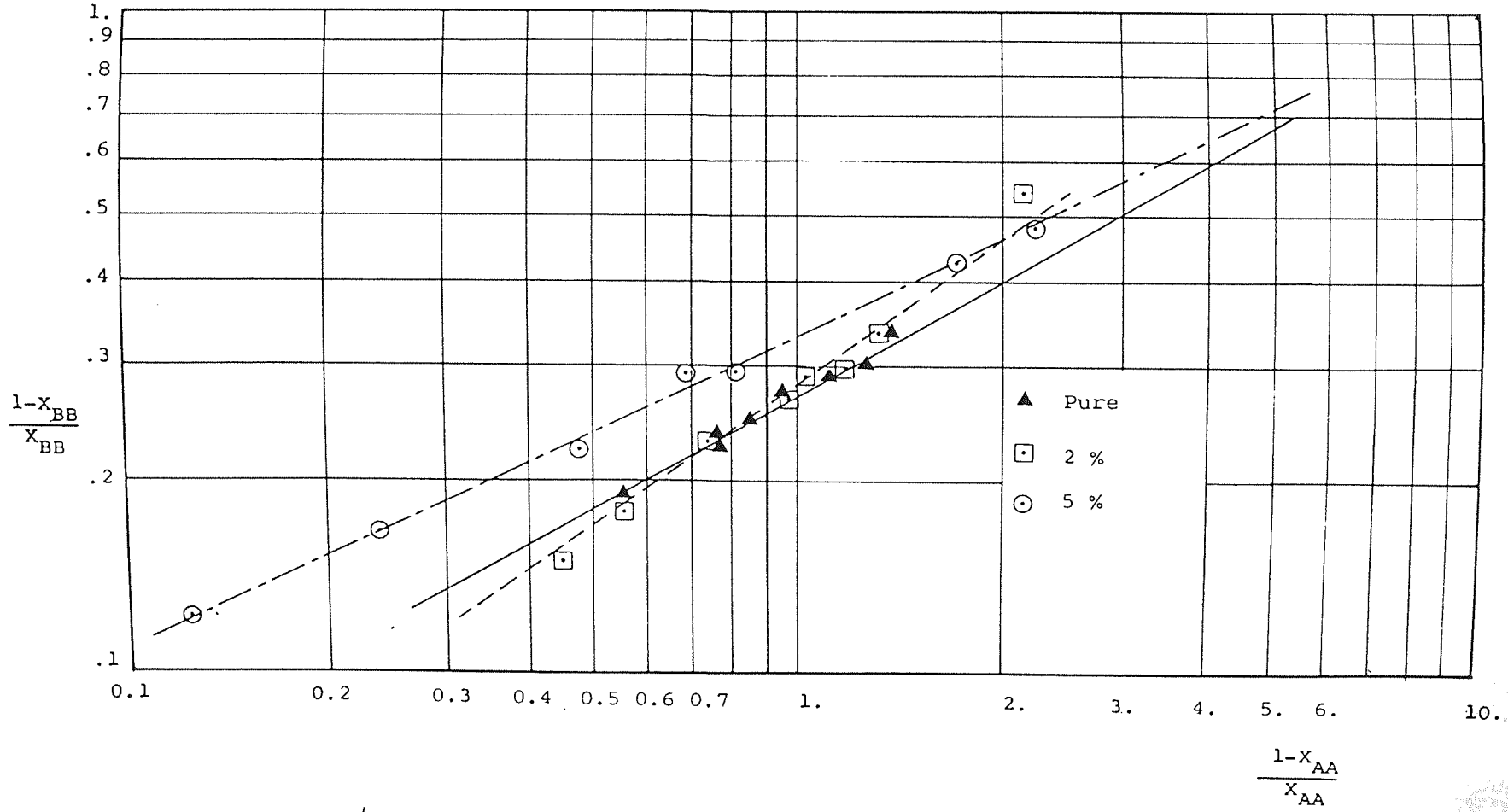

Figure 8.6: Othmer-Tobias' Correlation for System: Propan-2-ol (**C**) - Cyclohexane (**A**) - Water (**B**) at 20°C.

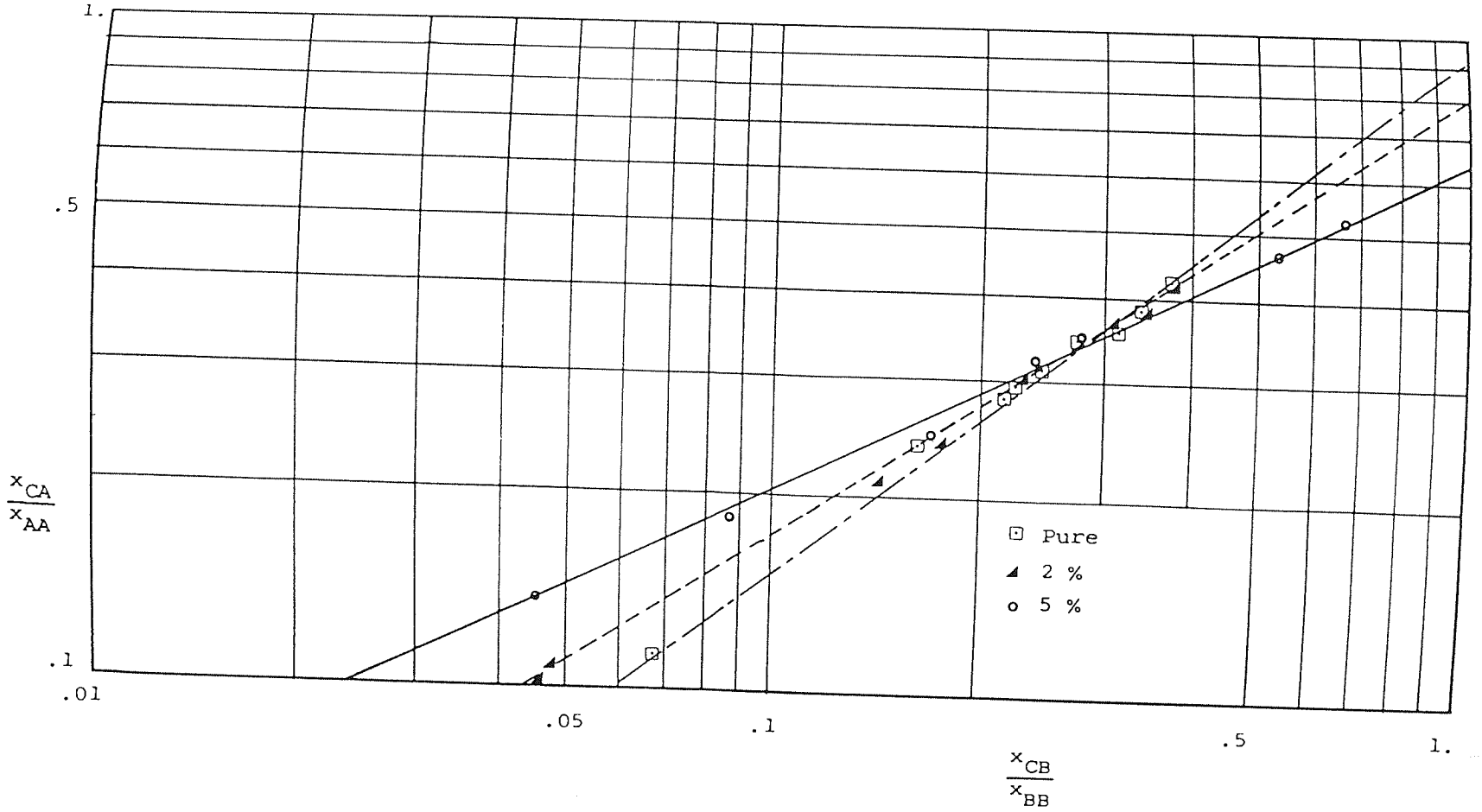

Figure 8.7: Hand's Correlation for System: Propan-2-ol (C) - Cyclohexane (A) - Water (B) at 20 °C.

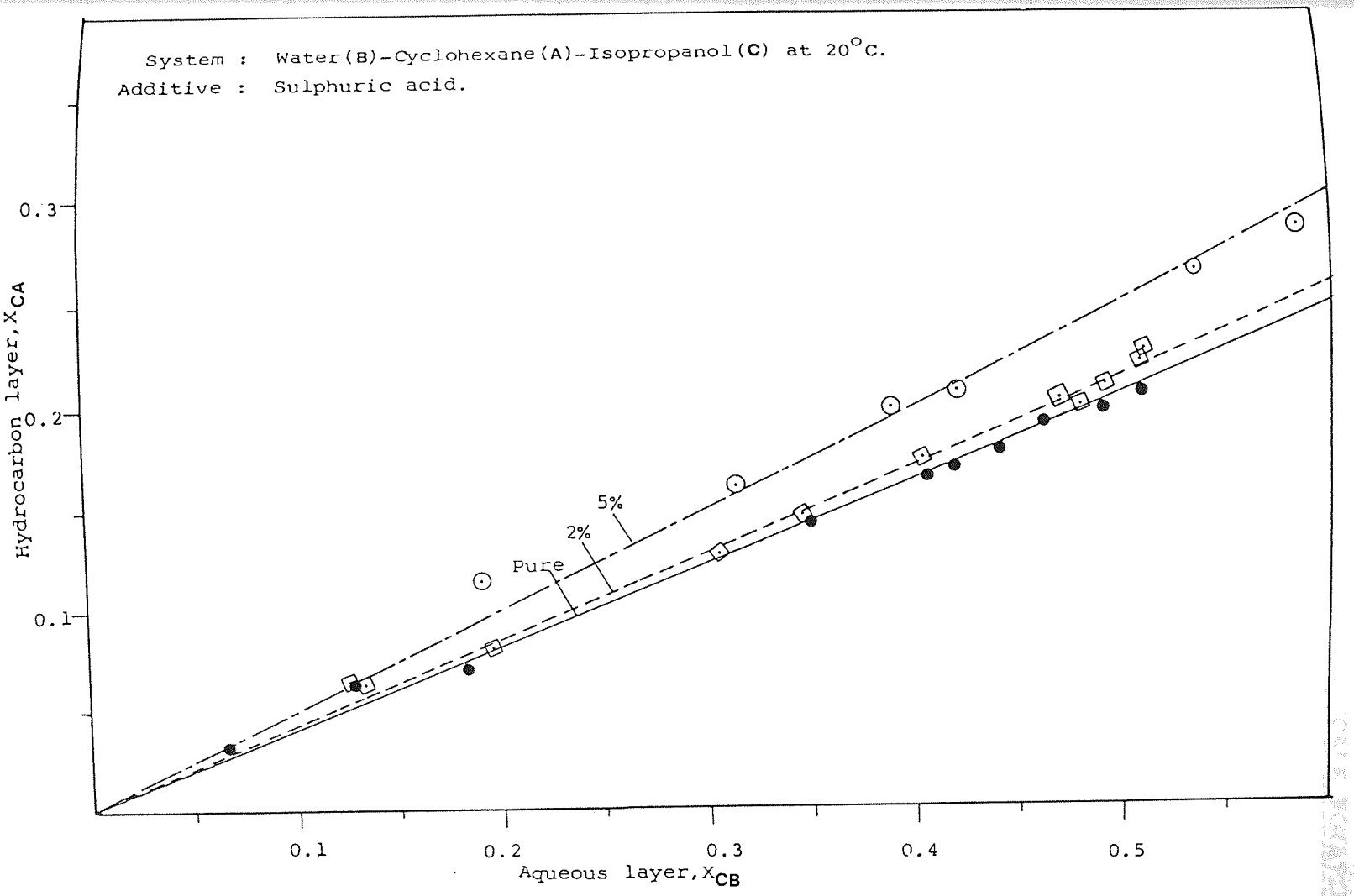

Figure 8.8: Experimental Distribution Diagram for System : Propan-2-ol(C)-Cyclohexane(A)-Water(B) at 20°C.

8.2 EXTRACTION STUDIES OF THE PILOT-SCALE ROTATING DISC CONTACTOR

8.2.1 Non-mass transfer studies

The non-mass transfer investigations were performed in support of the main study to provide a good understanding of the pilot-scale R.D.C. hydrodynamics via dispersed phase hold-up, drop size and drop size distribution, this in addition of knowing the limiting capacity of the equipment via flood phenomena.

Some repetitions of earlier studies in the same equipment (2) was necessary due to the use of different liquid-liquid systems and due to the minor modifications in the equipment e.g. the use of a smaller rotameter, the installation of sample points in the pipe lines and the renewal of the knitted mesh-pad.

8.2.1.1 Flooding Phenomena

Flooding rates represent the maximum volumetric capacity of a contactor under a given set of conditions. Flooding was characterised by the complete rejection of the dispersed phase, a dense layer of droplets at the heavy phase outlet at the bottom of the column, which is the conventional flooding phenomena (51, 114, 215).

Recalling Equation (6.5) and introducing the condition that at flooding with respect to h and setting $(\frac{dV_C}{dh})$ and $(\frac{dV_D}{dh})$ equal to zero,

$$\frac{V_D}{h} + \frac{K_1 V_c}{1-h} = V_s\ (1-h) \qquad (8.1)$$

$$V_{D.f} = 2\ V_s\ h_f^{\ 2}\ (1-f) \qquad (8.2)$$

$$V_{c.f} = V_s (1-h_f)^2\ (1-2h_f) \qquad (8.3)$$

which relates the phase flowrates at flooding to the corresponding hold-up, h_f. Elimination of V_s between Equations (8.2) and (8.3) yields (8.4).

$$h_f = \frac{(L^2+8L)^{0.5} - 3L}{4(1-L)} \qquad (8.4)$$

A plot of $V_{D.f}$ against $h_f^{\ 2}(1-h_f)$ should yield straight lines through the origin. Equation (8.4) and this method of correlation are strictly applicable only if the drop size distribution and hence V_s are independent of hold-up. Although in industrial scale columns, in the absence of any enhancement due to solute transfer, inter-drop coalescence does not occur to any great extent and is not a common feature of R.D.C. operation, it may occur in small columns at high hold-ups. Thus, coalescence leading to larger drops and greater hold-up is one possible explanation for the deviations observed. Characteristic velocity, V_s, may be obtained from the approximate slope of the curves in Figure (8.10).

The experimental flooding data obtained is as in Table 8.4.

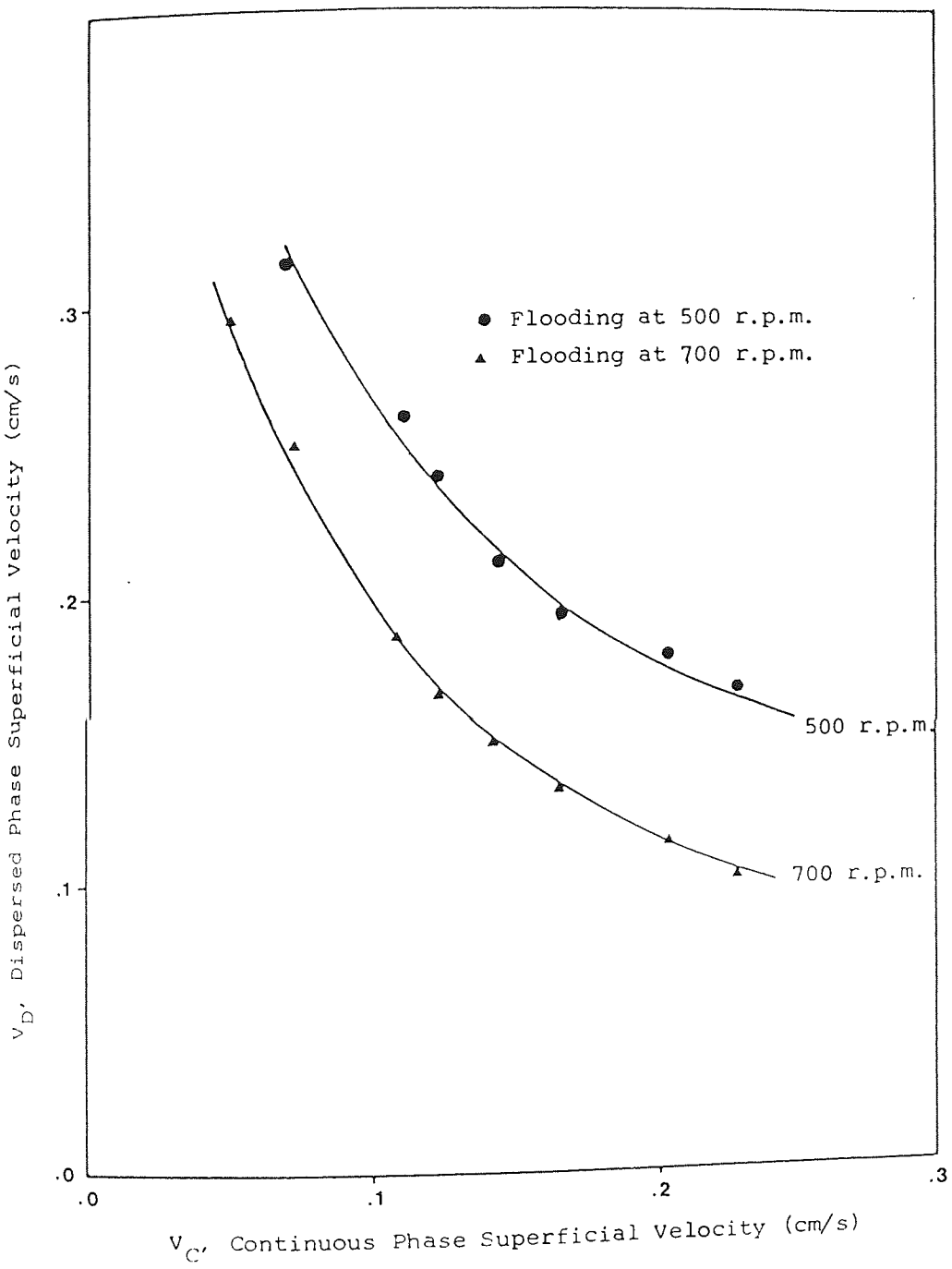

Figure 8.9 : Experimental Flooding Curves.

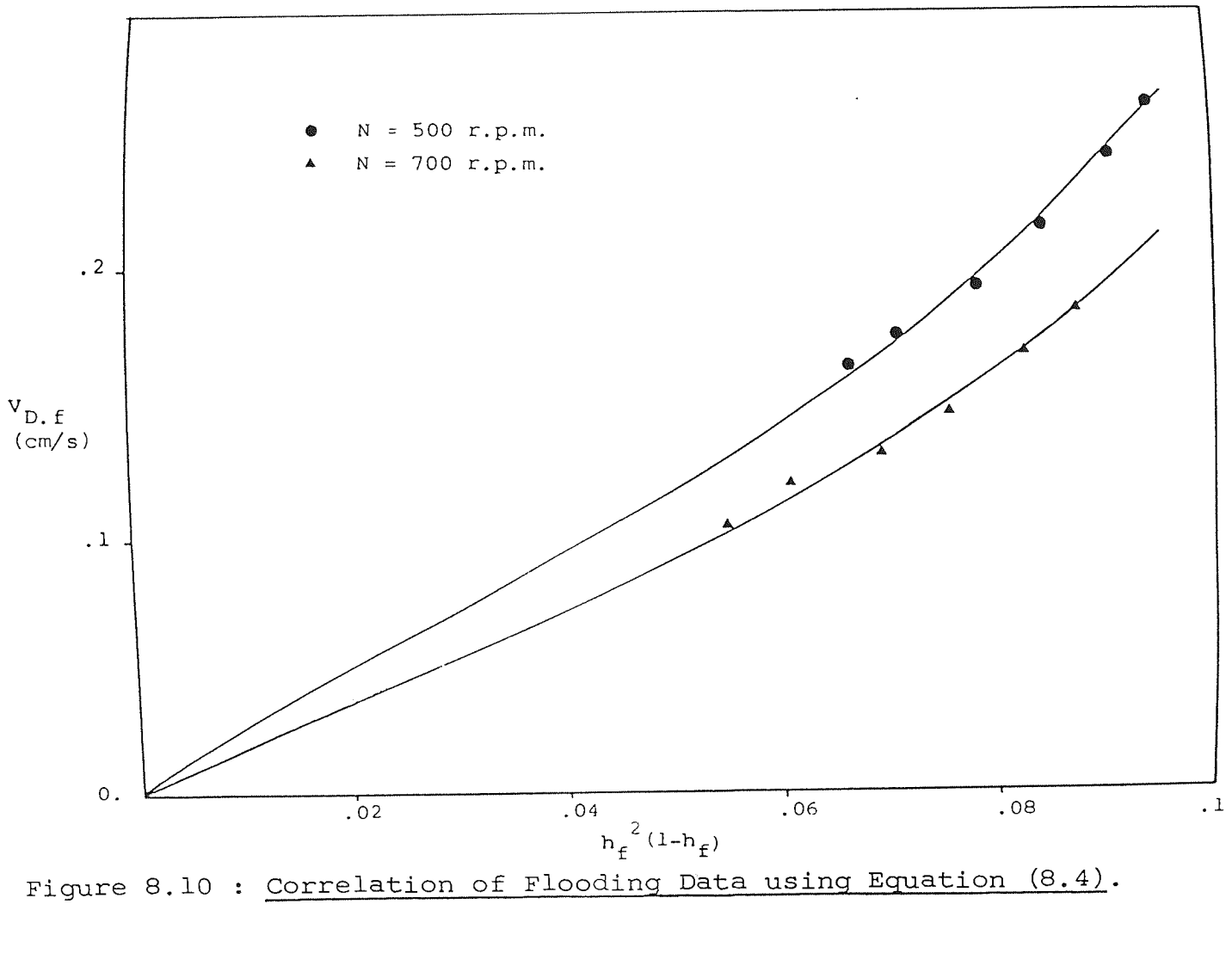

Figure 8.10 : Correlation of Flooding Data using Equation (8.4).

Continuous phase	Dispersed phase			
	N=500 rpm		N=700 rpm	
$V_{c.f}$ (cm/s)	$V_{d.f}$ (cm/s)	$h_f^2(1-f)$	$V_{d.f}$ (cm/s)	$h_f^2(1-f)$
.068	.314	.1053	.252	.1019
.106	.260	.0943	.184	.0871
.120	.240	.0902	.166	.0819
.140	.214	.0842	.148	.0754
.162	.192	.0782	.132	.0690
.200	.174	.0706	.112	.0595
.224	.165	.0664	.104	.0550

Table 8.4 Flooding data

8.2.1.2 Dispersed phase hold-up

Only the average values of the dispersed phase hold-up have been determined in this work. The simultaneous shut-off method (166, 168, 211, 233) was applied by operating the column under the desired conditions, and when the steady state had been attained and measured by steady interface level, all the inlet and outlet valves were closed rapidly and the rotor stopped to allow the dispersion to settle under gravity and displace the interface. The average hold-up was then determined by dividing the shift in the position of the interface by the effective height of the column, i.e. the height from the bottom distributor to the previous position of interface. This method was found satisfactory, and was in agreement with some workers (51, 215).

The experimental data was checked against the correlation of Kasatkin et al(233) for operation of a 5.4 cm column:

$$X = 1.58\left(\frac{N.D_R}{V_C}\right)\left(\frac{V_D}{V_C}\right)^{0.96}\left(\frac{D_S^2-D_R^2}{D_C^2}\right)^{-0.7}\left(\frac{H}{H_T}\right)^{-0.43}\left(\frac{\Delta\rho}{\rho_C}\right)^{-1.31}$$

$$\left(\frac{\rho_C V_C D_C}{\mu_C}\right)^{-0.13}\left(\frac{\rho_C V_C^2 D_C}{\sigma}\right)^{0.245}\left(\frac{V_c^2}{g.D_C}\right)^{0.96} \qquad (8.5)$$

Since the column dimensions are constant, insertions of the appropriate physical properties into Equation (8.5) when the continuous phase velocity, V_c = 0.1783 cm/s, yields results in Table(8.5). Those correlated values are much too high.

Al-Aswad (157) correlated the dispersed hold-up as a function of the physical properties of the system, the column geometry and the power input in the rotor. By a regression computer programme and by using the data of his work on a 450 cm R.D.C. he obtained:

$$X = 1.05\times10^{4}\left[\frac{N\ D_r}{V_C}\right]^{0.521}\left[\frac{V_d}{V_c}\right]^{0.775}\left[\frac{D_S^2-D_R^2}{D_C^2}\right]^{-0.187}$$

$$\left[\frac{H}{D_C}\right]^{-0.873}\left[\frac{D_R}{D_C}\right]^{0.201}\left[\frac{\Delta_\rho}{\rho_c}\right]^{4.843}\left[\frac{\rho_C D_C V_C^2}{\sigma}\right]^{1.082}$$

$$\left[\frac{V_c^2}{g\ D_c}\right]^{0.892}\left[\frac{\rho_c V_c D_c}{\mu c}\right]^{-2.367} \qquad (8.6)$$

The calculated values though slightly higher than those obtained experimentally, the straight lines in Figure 8.11 demonstrate similar order of magnitude and thus Al-Aswad (157) correlation was found to be more realistic than that of Kasatkin (233).

Dispersed Phase V_D cm/s	N = 500 r.p.m.			N = 700 r.p.m.		
	X%			X%		
	Exp.	Kas.	A-A	Exp.	Kas.	A-A
.110	2.60	10.53	3.62	3.65	14.71	4.314
.132	2.73	12.35	4.16	3.83	17.46	4.960
.153	3.35	14.40	4.66	4.74	20.12	5.560
.178	3.82	16.65	5.24	5.22	23.22	6.250
.200	4.05	18.62	5.74	6.02	24.42	6.840
.225	4.80	20.85	6.29	6.75	29.13	7.490
.246	5.41	22.70	6.74	7.15	31.74	8.030

Constant continuous phase, V_C = 0.1783 cm/s

Exp. = Experimental

Kas. = Kasatkin correlation (233)

A-A = Al-Aswad correlation (157)

Table 8.5 Dispersed phase hold-up

Possible explanations for the above could be the fact that the R.D.C. used, although very much smaller, has been built under similar optimum internal design as Al-Aswad's column (157) and similar method and criteria of measurements have been undertaken.

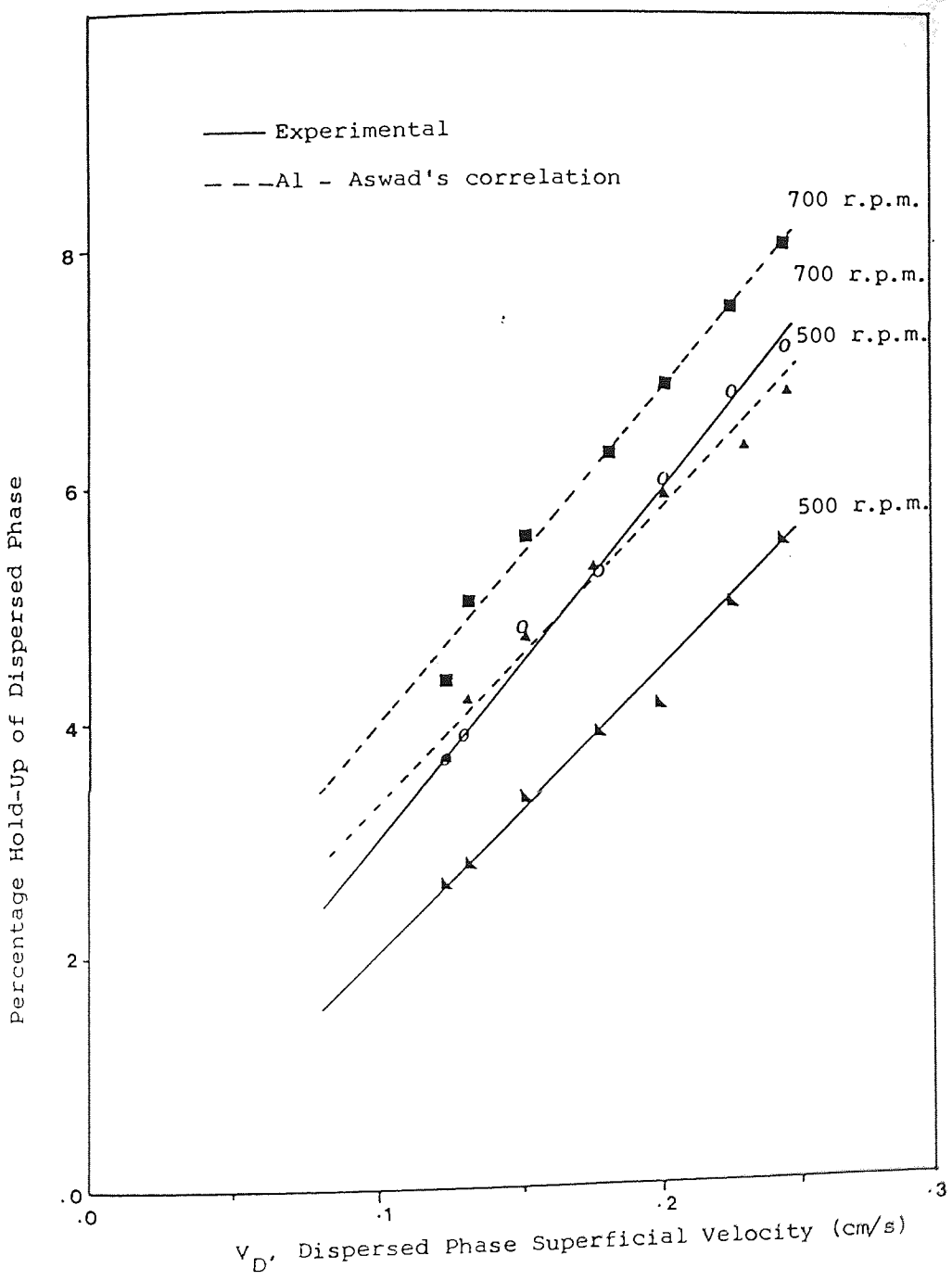

Figure 8.11 : Experimental Dispersed Phase Hold-Up and Al-Aswad's(157) Correlation.

8.2.1.3 Drop size

The observed Sauter mean diameter drop size, d_{32}, values were compared with the predicted values by most of the published correlations (114, 147,152, 156). Blazej et al (156) have proposed correlations to estimate a drop size distribution and the drop size in 6.5 cm diameter R.D.C. under mass transfer conditions for water-acetone-toluene system. The drop size correlation is:

$$\frac{d_{32}}{D_r} = 1.43\left[\frac{V_d(1-X)}{V_c.X}\right]^{0.45}\left[\frac{D_r.N(1-X)}{V_C}\right]^{-0.565}\left[\frac{\rho_C HV_C}{\mu_C(1-X)}\right]^{-0.117} \qquad (8.7)$$

Large differences have been observed. However, it is considered the best available correlation to use due to the size of the columns involved and the fact that measurements are made on a section of the column rather than a specific compartment, as illustrated in Figure (8.11).

Another model (157) which has been considered as a function of the following dimensionless groups.

$$\frac{d_{32}}{D_r} \alpha \left[\frac{V_d Ho_c}{\mu_C X}\right]^a \left[\frac{N^2 D_r^3 \rho_c}{\sigma}\right]^{-b} \left[\frac{V_d^2}{g D_r}\right]^{-c} \left[\frac{X}{1-X}\right]^{d} \left[\frac{\mu_d}{\mu_c}\right]^{e} \left[\frac{\rho_d}{\rho_c}\right]^{f} \qquad (8.8)$$

on a 450 mm diameter R.D.C. column,

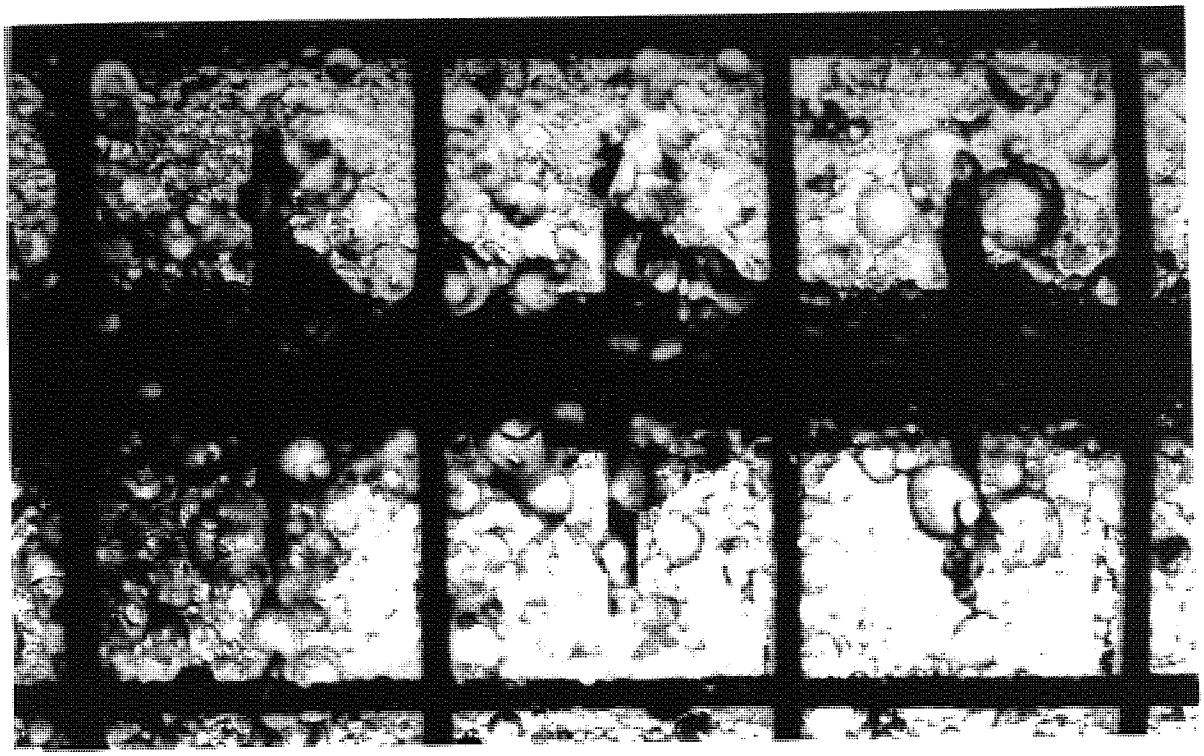

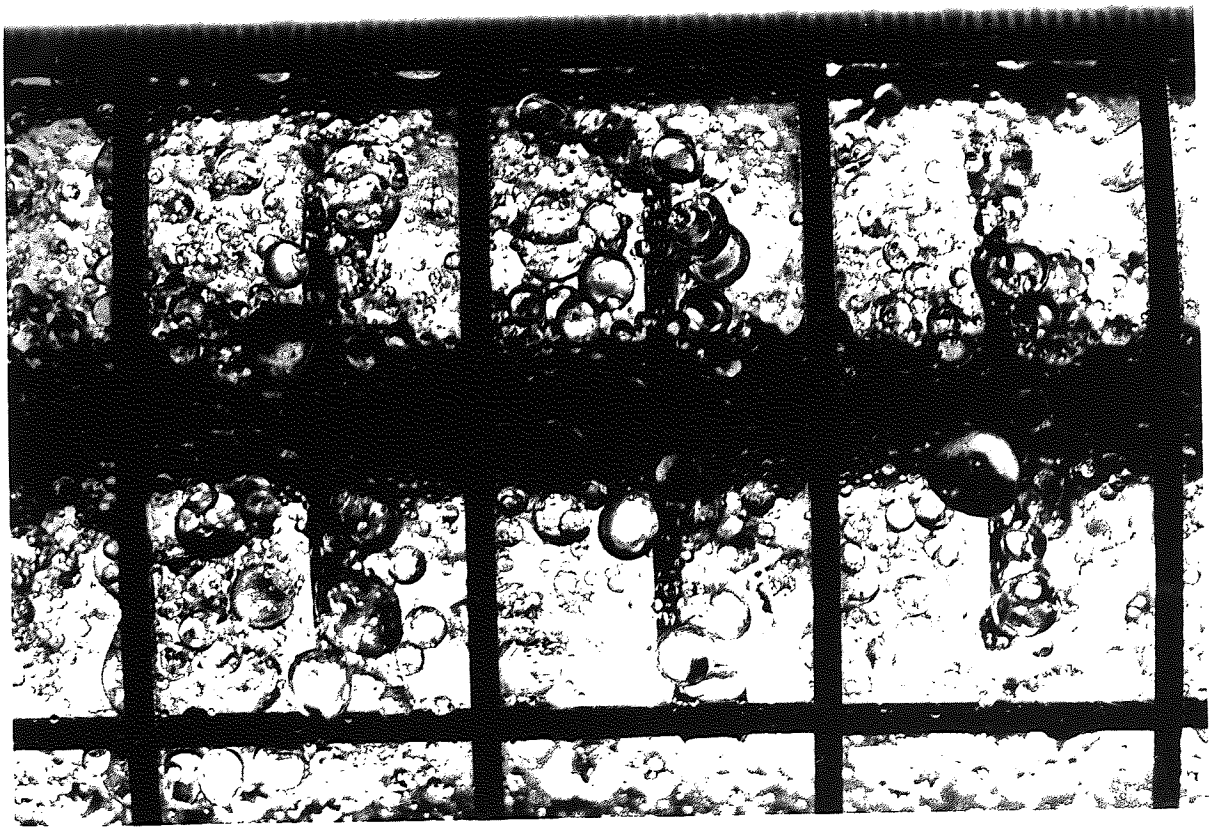

$$\frac{d_{32}}{D_r} = 1.48\left[\frac{V_d H \rho_c}{\mu_c X}\right]^{-0.23}\left[\frac{N^2 D_r^{\,3} \rho_c}{\sigma}\right]^{-0.004}\left[\frac{V_d^{\,2}}{g_c D_c X^2}\right]^{0.44}$$

$$\left[\frac{\Delta\rho}{\rho_c}\right]^{-.057}\left[\frac{H}{D_c - D_s}\right]^{-0.24}\left[\frac{n}{N_c}\right]^{-0.07} \qquad (8.9)$$

As mentioned earlier, the above correlation is not suitable for small columns when drops are measured over a section of the column and not a specific compartment and there is no facility to measure density difference from one compartment to another.

Better results were obtained from the Mugele-Evans (165) method i.e. using parameters obtained from drop size distribution, as described in the following section.

8.2.1.4 Drop size distribution

Figure (8.13) shows the drop size distribution as drop cumulative volume against drop diameter for rotor speed 500 r.p.m. The cumulative volume of the drop size sample is calculated as:

$$v = \Sigma n_i \left(\frac{\pi}{6} d_i^{\,3}\right) \qquad (8.10)$$

For a distribution of drop diameter, taking $d_o = 0$ and $d_m = \infty$ as end points of the curve, assuming there actually are 'smallest' and 'largest' droplets in the group, $\frac{dv}{dd}$ may be taken as infinitesimal or zero beyond actual d_o and d_m. Assuming that the 'classes'

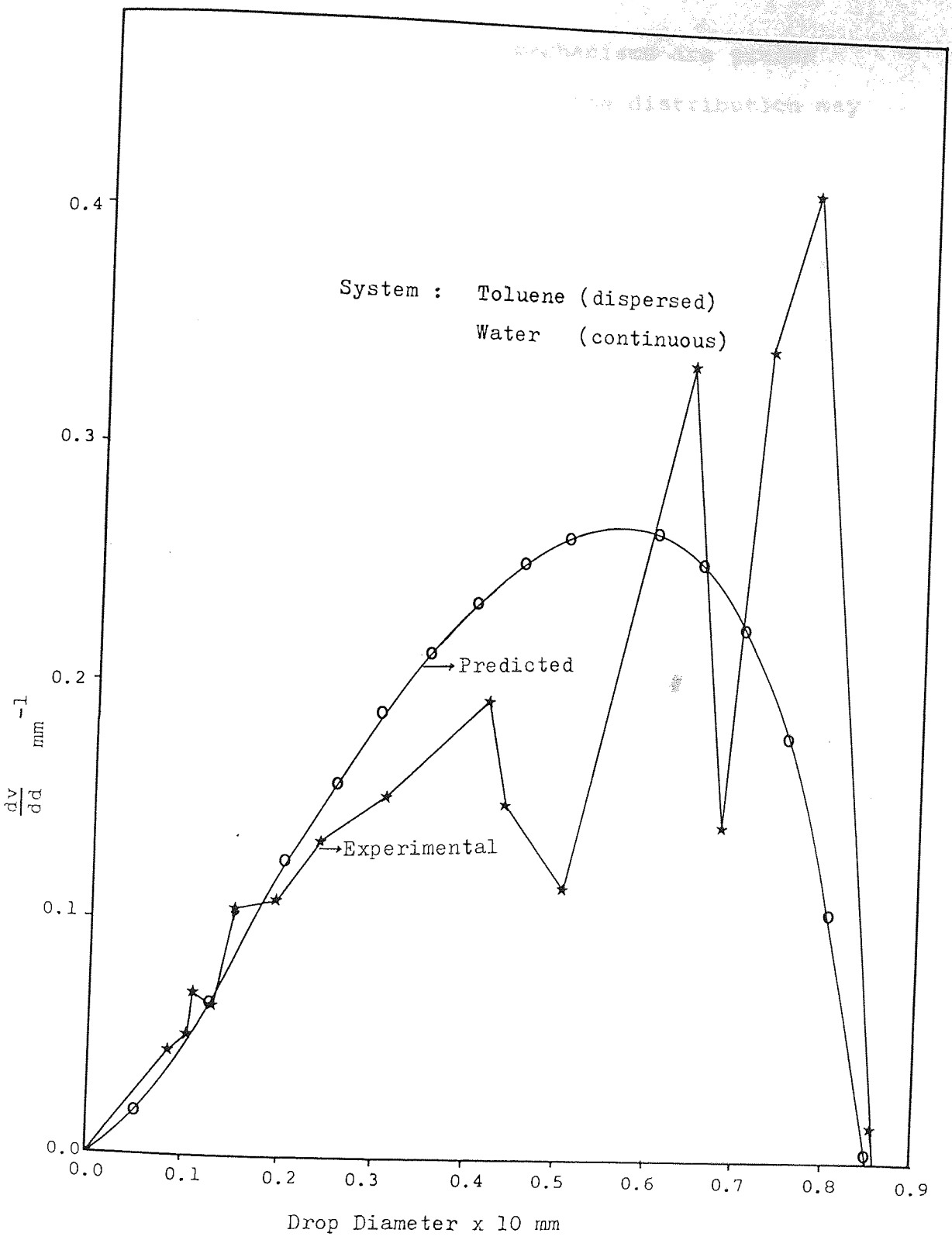

Figure 8.13: Comparison of Experimental and Predicted Upper-Limit Drop Size Distribution at 500 r.p.m.

established by the fundamental mechanisms are graded exponentially rather than linearly, the distribution may be represented by:

$$\frac{dv}{dy} = \emptyset\ (y) \tag{8.11}$$

where $y = \ln d/\bar{d}$ (8.12)

When the drops data are plotted up on this basis, they ordinarily give a somewhat symmetrical distribution about some value of y which is close to a single maximum in the curve. Some sets of measurements however, do not include sufficiently small diameters to make the maximum apparent: the nature of $\emptyset$ (y) can be assumed simply as the 'normal distribution ' function:

$$\emptyset\ (y) = \frac{\delta e^{-\delta^2 y^2}}{\sqrt{\pi}} \tag{8.13}$$

From these considerations, the volume distribution equation is taken as:

$$\frac{dv}{dy} = \frac{\delta}{\sqrt{\pi}}\ e^{-\delta^2 y} \tag{8.14}$$

where $y = \ln \left[\frac{\bar{a}d}{d_m - d}\right]$ (8.15)

and d_m may be calculated from the formula:

$$\frac{d_m}{d_{50}} = \frac{d_{50}(d_{90}+d_{10}) - 2d_{90}d_{10}}{d_{50}^2 - d_{90}d_{10}} \tag{8.16}$$

d_{10}, d_{50} and d_{90} are read from the 10th, 50th and 90th percentiles on the d against 100v plot. The parameter $\bar{a}$ is determined from the line representing the distribution. Since y = 0 at the 50th percentile (where $d = d_{50}$, the volume median),

$$0 = \ln\left[\frac{\bar{a}\, d_{50}}{d_m - d_{50}}\right] \tag{8.17}$$

or

$$\bar{a} = \frac{d_m - d_{50}}{d_{50}} \tag{8.18}$$

The parameter δ is determined by the slope of the line, hence by any point on it. If the coordinate on the log scale is designated by u:

$$u = \frac{d}{d_m - d} \tag{8.19}$$

If values of u_{90} and u_{50} at the 90th and 50th percentile are read, we find:

$$\delta = \frac{0.394}{\log(u_{90}/u_{50})} \tag{8.20}$$

and

$$d_{32} = d_m/(1+\bar{a}e^{\frac{1}{4\delta^2}}) \tag{8.21}$$

Appendix VI shows a sample calculation of the drop size distribution. Log-probability graph paper was used to plot the drop size cumulative volume against the drop diameter. From this graph, d_{10}, and d_{50} and d_{90} were determined and the upper limit distribution parameters d_m, $\bar{a}$ and δ were calculated and applied in the Mugele-Evans equation.

8.2.2 Mass Transfer Studies

The column extraction efficiency, as well as its hydrodynamics under mass transfer conditions, were carried out at different acetone concentrations in the feed stream. Hydrodynamics did not include the flooding test since it is impractical to carry out separate experiments to measure flooding rates because this would have consumed large quantities of solvents and solute. There were no continuous distillation facilities to recover the solute quantities either. However, all the mass runs were carried out below 70% of the flooding flowrates obtained during the non-mass transfer experiments as recommended by Treybal (24).

Experiments involving the transfer of acetone were performed at acetone concentrations in the feed stream of less than 15% to avoid the formation of emulsions that might happen at higher acetone concentrations. The feed concentrations were kept at 10% and 15% by weight and the flowrates were kept in the common ratio to enable comparisons to be carried out with and without acid additions in the aqueous phase.

8.2.2.1 Experimental Mass Transfer Coefficient

The overall experimental dispersed phase mass transfer coefficient under each set of operating conditions was calculated using Equation (8.22)

$$N = KA\ \Delta C_m \tag{8.22}$$

where N is the rate of mass transfer which is calculated from the mass balance across the column.

A is the interfacial area which is estimated by using Equation (8.23) which is:

$$a = \frac{6X}{d_{32}} \tag{8.23}$$

where 'a' is the specific area as cm^2 per cm^3 of the column volume. Hence

$$A = a.V \tag{8.24}$$

where V is the total column volume.

Simpson's rule was applied to determine the actual mean driving force (ΔC_m) by using the acetone concentration profile. The driving force can be determined as Δy_1, Δy_2. Δy_3, Δy_4 etc. respectively, where

$$\Delta y_n = y_n^* - y_n \tag{8.25}$$

and y is the acetone concentration in the aqueous phase.

Simpson's rule is:

$$\Delta y_m = \frac{1}{18}\left[\Delta y_1 + 4\Delta y_2 + 2\Delta y_3 + 4\Delta y_4 + 2\Delta y_5 + 4\Delta y_6 + \Delta y_7\right] \tag{8.26}$$

Δy_m was then converted to ΔC_m by dividing it by the extract phase density.

So, overall experimental mass transfer coefficient can be calculated as:

$$K_{exp} = \frac{N}{A\Delta C_m} \qquad (8.27)$$

8.2.2.2 Theoretical Mass Transfer Coefficient

A novel method of calculation (157) has been carried out to evaluate the overall theoretical dispersed phase mass transfer coefficient K_{cal}. These calculations involve the use of the drop distribution diagram to determine the volume percentage of the stagnant, circulating and oscillating drops in the drop sample population. Droplet Reynold's number has been used as a measure of the state of the drops as follows (125, 132, 146)

Stagnant drops	$Re < 10$
Circulating drops	$10 < Re < 200$
Oscillating drops	$Re > 200$

where droplet $Re = \frac{d\rho_c V_o}{\mu_c}$

where d is the drop diameter and V_o is the vertical relative velocity of drops in the R.D.C. determined by applying Misek's equation (152),

$$V_o = \left[\frac{V_d}{X} + \frac{V_c}{1-X}\right] \qquad (8.28)$$

To find the maximum diameter of the stagnant drops in the whole drop population, set Re = 10

$$\frac{d_s \rho_c V_o}{\mu_c} = 10 \qquad (8.29)$$

where d_s is the maximum diameter of the stagnant drops regime. To find the minimum diameter of oscillating drops regime, set Re = 200

$$\frac{d_o \rho_c V_o}{\mu_c} = 200 \qquad (8.30)$$

where d_o is the minimum diameter of the oscillating drops regime. The circulating drops regime is determined in between d_s and d_o. As it shows in Table VI.1, d_s is too small to be analysed by the technique used in this study (Section 8.2.1.4). So the drop population was considered to contain circulating and oscillating drops only with d_o the boundary between the two regimes.

i) Circulating drops regime

Volume percentages of the circulating drops was determined from the drop distribution diagrams. The individual mass transfer coefficients of the dispersed and continuous phase for the circulating drop were calculated as follows:

a) Dispersed phase mass transfer coefficient was estimated by the Kronig and Brink (129) equation:

$$k_{d.c} \cong \frac{17.9}{\bar{d}_c} D_d \qquad (8.31)$$

where $\bar{d}$ is the circulating drop mid-sector diameter and D_d is the molecular diffusion of acetone in the dispersed phase, estimated by the correlation in Appendix I.5.

b) Continuous phase mass transfer coefficient was estimated by Garner et al (133) correlations:

$$\frac{k_{c.c}\ \bar{d}_c}{D_c} = -126 + 1.8\ Re^{0.5}\ Sc^{0.42} \qquad (8.32)$$

where D_c is the molecular diffusion of acetone in the continuous phase estimated as in D_d.

The overall mass transfer coefficient at the circulating drops $K_{o.c}$ is calculated as

$$\frac{1}{K_{o.c}} = \frac{1}{k_{d.c}} + \frac{m}{k_{c.c}} \qquad (8.33)$$

ii) Oscillating drops regime

The rest of the drop population was considered as the oscillating drop regime. The individual mass transfer coefficients of the dispersed and continuous phases for this regime are as follows:

a) Dispersed phase mass transfer coefficient was first estimated by Rose and Kintner (131)

$$k_{d.o} = 0.45(D_d\ \omega)^{0.5} \tag{8.34}$$

and then by Angelo et al (115) equation

$$k_{d.o} = \frac{\sqrt{4D_d\omega(1 + \varepsilon + \frac{3}{8}\varepsilon^2)}}{\pi} \tag{8.35}$$

where ε is the eccentricity which is estimated by Al-Hassan's (242) correlation as:

$$\varepsilon = 0.434\left(\frac{\omega\ \bar{d}_o}{V_o}\right)^{-0.46}\left(\frac{\bar{d}_o V_o^2 \rho_c}{\sigma}\right)^{-0.53}\left(\frac{\mu V_o}{\sigma}\right)^{-0.11} \tag{8.36}$$

where $\bar{d}_o$ is the oscillating drop mid-sector diameter.

b) Continuous phase mass transfer coefficient was estimated by Garner (133) correlation, equation (8.37)

$$\frac{k_{c.o}\bar{d}_c}{D_c} = 50 + 0.0085\ Re\ Sc^{0.7} \tag{8.37}$$

The overall mass transfer coefficient of the oscillating drop $k_{o.o}$ was first estimated as follows:

$$\frac{1}{K_{o.o}} = \frac{1}{k_{d.o}} + \frac{m}{k_{c.o}} \tag{8.38}$$

where $k_{d.o}$ is the dispersed phase coefficient calculated by Rose and Kintner (131) equation. Secondly by Angelo et al (115) equation as:

$$K_{o.o} = k_{d.o}\left[\frac{1}{1+m\sqrt{\frac{D_d}{D_c}}}\right] \qquad (8.39)$$

The theoretical mass transfer coefficient for the whole drop population was then calculated as:

$$K_{cal} = K_{o.c}\ \nu + K_{o.o}\ (1-\nu) \qquad (8.40)$$

8.2.2.3 Discussion of Results

Tables (8.6) and (8.7) summarises the experimental results obtained at various phase ratios for the two chosen rotor speeds, i.e. 500 r.p.m. and 700 r.p.m.

Generally, the drop size decreases with the increase in solute concentrations, rotor speeds and acid additions. Dispersed phase hold-up percentages and the overall mass transfer coefficients are also increased with the increase in percentage addition of the acid and the increase in rotor speeds.

Only experimental values of the pure systems could be compared to those obtained theoretically because the calculations would involve physical properties e.g. diffusivity which would definitely differ from the available correlations when the additives were present. However, the agreements obtained in Table 8.8 are reasonable and the values obtained by Angelo et al (115) correlation achieve better agreement in most cases.

Table 8.6 Mass Transfer Results

Rotor Speed: 500 r.p.m.

Feed (weight fraction)	C/D	d_{32} (cm)			Percentage Dispersed Phase Hold-Up %			$K_{exp} \times 10^3$ (cm/s)		
		Pure	2%	5%	Pure	2%	5%	Pure	2%	5%
0.10	1/4	0.4828	0.3610	0.3223	5.636	4.545	5.455	0.9040	1.3950	1.3366
0.10	4/4	0.5243	0.4794	0.3857	3.820	3.909	5.909	0.7377	1.2105	1.5388
0.10	8/4	0.6535	0.5580	0.5122	1.820	2.273	5.273	0.5218	1.3556	1.5141
0.15	1/4	0.5253	0.4242	0.3857	3.727	4.110	4.218	0.7756	0.7810	0.8210
0.15	4/4	0.4855	0.5558	0.3498	3.518	4.213	4.352	0.6230	1.0159	1.0576
0.15	8/4	0.3660	0.3537	0.3884	8.910	7.412	8.080	1.2600	1.3721	1.5338

C/D: Rotameter reading of continuous phase to dispersed phase.

Table 8.7 Mass Transfer Results

Rotor Speed: 700 r.p.m.

Feed (weight fraction)	C/D	d_{32} (cm)			Percentage Dispersed Phase Hold-Up %			$K_{exp} \times 10^3$ (cm/s)		
		Pure	2%	5%	Pure	2%	5%	Pure	2%	5%
0.10	1/4	0.4914	0.3595	0.2693	1.636	3.636	7.4545	0.7313	0.7614	0.8962
0.10	4/4	0.4836	0.3167	0.3194	2.818	6.455	5.9090	0.8059	0.9974	1.2399
0.10	8/4	0.5730	0.3716	0.2742	1.545	7.000	12.8180	0.6853	1.0312	1.1891
0.10	1/2	0.4918	0.3595	0.2693	1.636	3.636	7.4540	0.7314	0.7614	0.8962
0.15	1/4	0.4076	0.3466	0.2540	3.318	3.273	6.0900	0.6519	0.7321	0.8842
0.15	4/4	0.4006	0.3443	0.3313	3.320	5.364	5.4500	0.9519	1.0690	1.8740
0.15	8/4	0.4954	0.4354	0.3645	2.636	5.000	6.8200	1.1277	1.3680	1.3690
0.15	1/2	0.4389	0.2972	0.2659	4.273	4.636	5.5400	0.4939	0.8091	0.8336
0.15	5/1	0.4827	0.4794	0.3399	2.540	2.910	5.8220	0.9693	1.5753	1.9527

C/D: Rotameter reading of continuous phase to dispersed phase.

Table 8.8

Experimental and Theoretical Overall Mass Transfer Coefficients

Feed	C/D	N = 500 r.p.m.			N = 700 r.p.m.		
		K_{exp}	$K_{cal}^{(1)}$	$K_{cal}^{(2)}$	K_{exp}	$K_{cal}^{(1)}$	$K_{cal}^{(2)}$
.10	1/4	0.904	1.245	1.032	0.731	0.867	0.785
.10	4/4	0.738	0.798	0.745	0.806	0.902	0.811
.10	8/4	0.522	0.634	0.533	0.685	0.921	0.888
.15	1/4	0.776	0.814	0.682	0.659	0.823	0.721
.15	4/4	0.630	0.943	0.855	0.952	0.892	0.804
.15	8/4	1.260	1.927	1.321	1.128	1.128	1.223

C/D: Rotameter reading of continuous phase to dispersed phase.

$K_{cal}(1)$: Overall mass transfer coefficient calculated using Rose and Kintner (131) and Garner (133) correlation for oscillating drops.

$K_{cal}(2)$: Overall mass transfer coefficient calculated using Angelo et al. (115) correlation for oscillating drops.

CHAPTER nine 9

CONCLUSION

Liquid-Liquid Equilibrium Studies

The three systems studied showed excellent agreement to other published data at the same temperature when pure water was used. Significant tilting in the tie-lines are apparent upon the addition of the acid. The distribution diagrams show the favourable change in the slopes. The change varies with the increase in acid addition. However, the tie-lines are consistent with Othmer-Tobias' and Hand's correlations when the acid and water are treated as one component in the ternary systems.

The Liquid-Liquid Equilibrium predictions via activity coefficient evaluation is a useful tool only if the necessary binary or ternary interactions data are available.

In the above study, sulphuric acid is probably too little to initiate any chemical reaction with any other components in the ternary system. Therefore, the changes observed are only due to physical influences of the acid.

Considerable economy may be achieved by introducing additives into solvents in extraction processes without impairing the original properties of the solvents or extensive review of the existing process.

Hydrodynamics of the R.D.C.

i) Drop Size and Drop Size Distribution.

Al-Aswad's (157) dropsize correlation was found not possible to be applied in the study of a small R.D.C. where drops are measured over a section and not just a specific compartment. The Kasatkin (233) correlation which includes the effects of rotor speed, dispersed phase flow-rates, column geometry, interfacial tension and density difference upon drop size was more practical to be used but it was less accurate than those values obtained using parameters from the Mugele-Evans upper limit distribution function in the study of drop size distribution. The distribution function represents the drops distribution adequately and the shape and size depends mainly on the rotor speed, the flowrates of both phases and the systems used.

ii) Dispersed Phase Hold-up.

Most empirical correlations for dispersed phase hold-up have been based on larger diameter columns, e.g. 100 mm and 450 mm. 'Wall effects' may be significant in small columns, because droplet break-up, coalescence and flow in an unrestricted phase differ from those in the vicinity of the wall. However, Al-Aswad's (157) correlation was at least of the same magnitude to the experimental data, indicating similar internal column geometry to be the possible criteria in choosing correlations to be applied rather than actual size of columns.

Mass Transfer Study

i) Both drop size and dispersed phase hold-up are different when mass transfer is occuring compared to non-mass transfer conditions. Therefore, data obtained under non-mass conditions must be applied with caution in column design.

ii) The use of the distribution diagram to calculate the mean driving force viz Simpson's Rule results in more precise experimental mass transfer coefficient.

iii) The use of the drop size distribution in the calculation of the theoretical overall mass transfer coefficient gives results that are comparable with experimental coefficients. The wide deviations between the calculated mass transfer coefficients based on a uniform drop size assumption, confirms that different mass transfer mechanisms occur simultaneously.

iv) The presence of additives, generally decreases the drop size and increases hold-up resulting in higher overall mass transfer coefficients.

v) It can be concluded, therefore, polar molecules chosen in this study has successfully affected the distribution equilibria, bringing a significant increase in extraction efficiency.

CHAPTER ten 10

RECOMMENDED FUTURE WORK

i) The Smith-Bonner cells and the circulating unit designed and operated in this study are clearly useful for the determination of liquid-liquid equilibrium data for any ternary system at any temperature (up to maximum temperature of water bath). However, the sampling technique and method of analysis of samples established was tedious and time consuming. Connection of a refractometer with a suitable designed, completely sealed cell (with provision of temperature regulation) to the circulating unit would allow samples to be withdrawn rapidly; instant analysis of samples would be possible.

ii) Generally, LLE predictions discussed in Chapter 4 require knowledge of the binary interaction which are not available for binaries involving water with added sulphuric acid. However, if polar molecules such as glycol had been used such parameters can be obtained and used in the determination of activity coefficients and the equilibria established without experimental work.

iii) Only up to 15% weight percentage of acetone was used in the mass transfer studies on the system: Acetone-Toluene-Water. The stagewise analysis for the operating curve was obtained in a small area and very close to the base line. Estimation procedure had to be applied. Another system would not have such limitation and thus full range could be studied and better accuracy acquired.

iv) Solute-solvent interaction tables similar to those given in Section 2.4.7, may be useful for screening potential additives. For a solute to be extracted, it would be desirable to reduce the activity coefficient of the solute, giving a high distribution coefficient into the solvent. The additives, therefore, should have similar influence on the solvent, giving better overall effect on admixture.

R.D.C. Improvements

i) A non-return valve could usefully be installed prior to the dispersed phase inlet to prevent backflow of the continuous phase. This can otherwise result in secondary haze formation.

ii) A needle-type valve would enable closer control of interface level to be achieved.

iii) The introduction of flexible p.t.f.e. connections would ease assembly and changing for cleaning.

iv) The introduction of the dispersed phase via a distributor plate or perforated tube rather than an open pipe would be prefered to produce a uniform initial distribution of drop size. However, attempts to design such a plate resulted in erratic column performance due to the practical size of the plate. Too small a plate caused difficulty in mounting and selection of size and number of punched holes; too large a plate hindered the flow of the continuous phase and resulted in premature flooding. A circular pipe with punched holes may be a possible design.

v) Larger volume storage tanks may save time and ensure the uniformity of solute concentrations in the feed. At present, frequent filling of the feed tanks and emptying of the product tanks is required after only a few runs. Separate vessels were therefore needed to provide a uniform feed and to store the solvents before adjustments were made.

vi) There is no circulating facility in the rig; thus necessitating manual transfers. Suitable rearrangements of the feed and product tanks and the provisions of pumps or cross-piping connections may achieve this.

APPENDIX I

i) Variation of Physical Properties with Solute Concentration for System : Acetone- Toluene - Water at 20°C.

ii) Specifications of Chemicals Used.

iii) Physical Properties of Pure Constituents of the system at 20°C.

iv) Fire and Safety Properties of the system.

v) Correlation for Interfacial Tension at 20°C (229).

vi) Correlation for Liquid Diffusivities at 20°C (229).

vii) Table of Liquid Diffusivities at various Solute Concentration for system : Acetone- Toluene- Water at 20°C.

viii) Physical Properties of Conjugate Phases at 20°C.

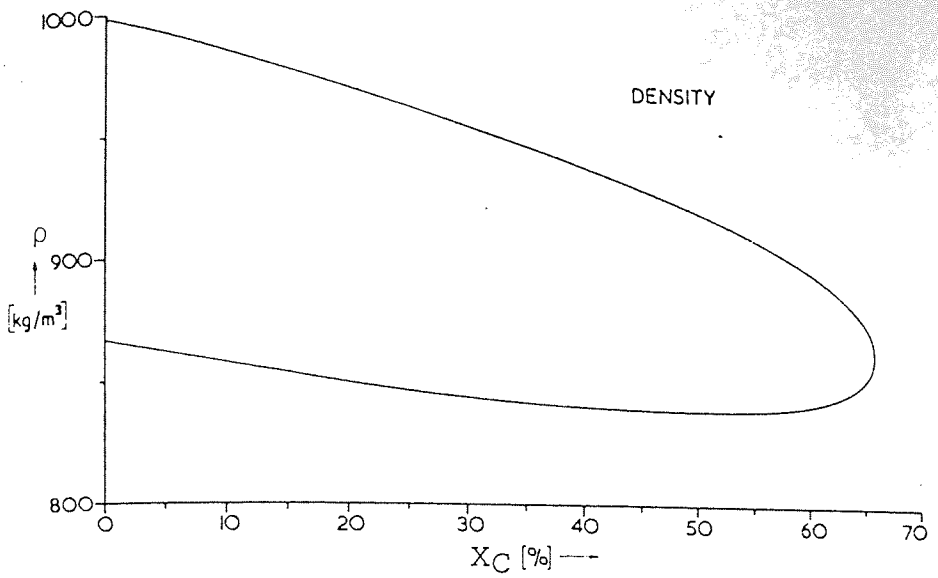

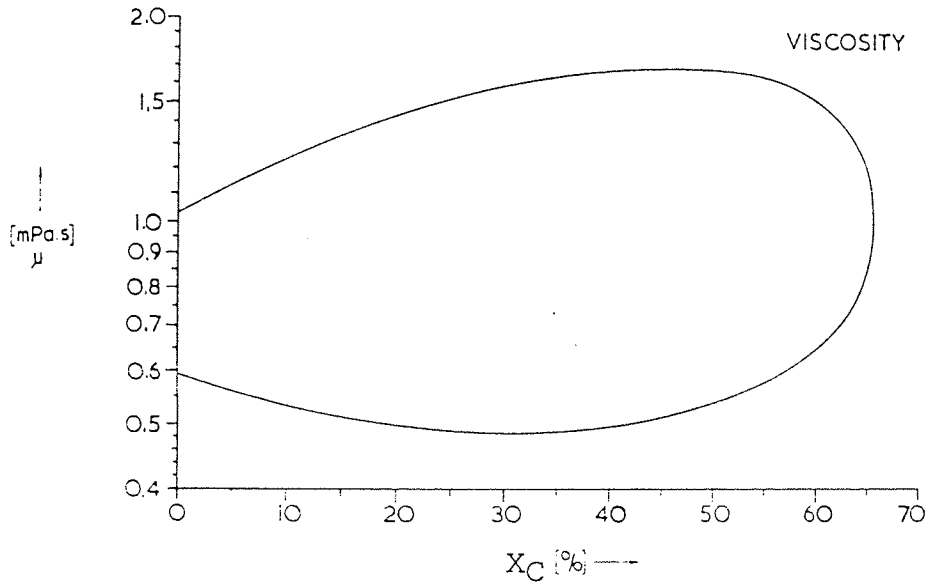

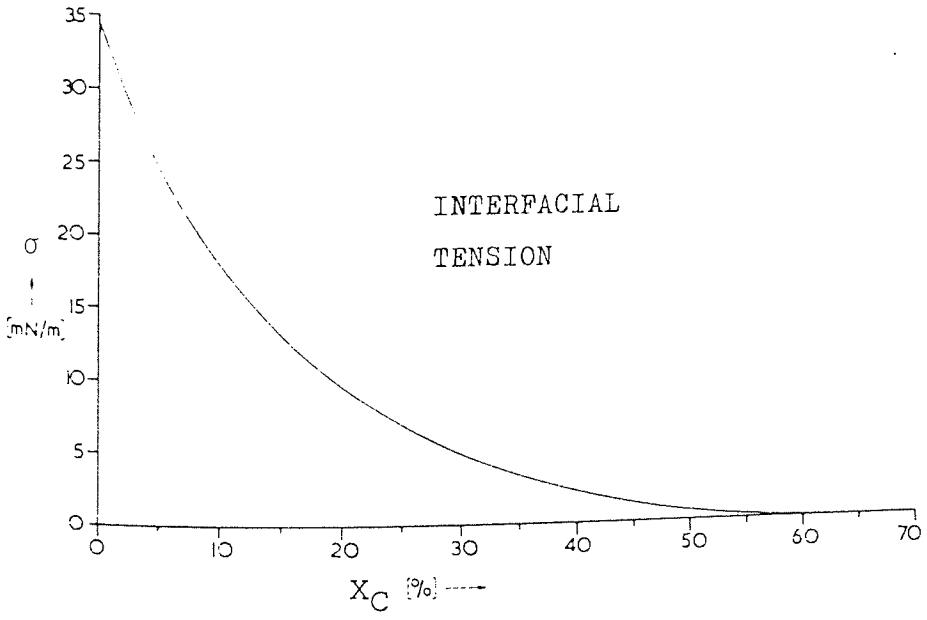

Figure I.1 : Variation of Physical Properties with Solute Concentration for System : Acetone-Toluene-Water at 20°C.(229)

Table: I.1

Specifications of Materials Used.

i) ACETONE - Analar

Wt. per ml. at 20°C	0.789 - 0.791 g
Boiling Range (95%)	56.0 - 56.5° C
Refractive Index	1.3580 - 1.3600

Maximum Limits of Impurities

Water	0.2
Acidity	0.02
Alkanity	0.03 ml N/1
Non-Volatile Matter	0.0005
Aldehyde (HCHO)	0.002
Methanol (CH_3OH)	0.5
Substances Reducing Permanganate	0.0002

ii) TOLUENE - Low in Sulphur GPR

Wt. per ml. at 20°C	0.860 - 0.866 g
Boiling Range (92%)	110 - 111° C
Refractive Index	1.493 - 1.497

Maximum Limits of Impurities

Water	0.04
Non-Volatile Matter	0.003
Sulphur Compounds (CS_2)	0.0005

iii) PROPAN-2-OL

Wt. per ml. at 20°C	0.786 g
Boiling Range (95% min)	81 - 83° C

Maximum Limits of Impurities

Non-Volatile Matter	0.01
Aldehydes and Ketones	0.1
Water	0.25

iv) CYCLOHEXANE

Wt. per ml. at 20°C	0.776 - 0.779 g
Refractive Index	1.424 - 1.427
Boiling Range (95%)	79.0 - 81.0° C
Freezing Point	not below 2° C

Maximum Limits of Impurities

Non-Volatile Matter	0.005

v) METHANOL - Analar

Wt. per ml. at 20°C	0.790 - 0.792 g
Boiling Range (95%)	64.5 - 65.5° C
Refractive Index	1.328 - 1.330

Maximum Limits of Impurities

Water	0.1
Acidity	0.02 ml N%

Alkalinity	0.01 ml N%
Non-Volatile Matter	0.001
Aldehydes and Ketones	0.005

vi) XYLENE - Analar

Description : consists of the three isometric xylenes and ethyl benzene.

Wt. per ml. at $20^{o}C$	0.863 - 0.866 g
Distillation range (92%)	138.0 - 142.0^{o} C

Maximum Limits of Impurities

Water	0.03
Acidity	0.012 ml N%
Alkalinity	0.012 ml N%
Non-Volatile Matter	0.002
Benzene	0.1
Toluene	1

vii) SULPHURIC ACID - (98%)

Wt. per ml at $20^{o}C$	1.835 - 1.840 g

Maximum Limits of Impurities

Non-Volatile Matter	10 ppm
Chloride	0.1 ppm
Nitrate	0.1 ppm
Phosphate	0.05 ppm
Silicate	0.1 ppm

Aluminium	0.05ppm
Ammonium	0.5 ppm
Oxygen Absorbed	0.2 ppm

vii) ACETIC ACID - glacial ANALAR

Wt. per ml. at 20°C	1.048 - 1.050 g
Freezing Point	Not below 16.2° C

Maximum Limits of Impurities

Water	0.2
Non-Volatile Matter	0.001
Acetic Anhydride	0.2
Chloride	0.001
Formate	0.01
Sulphate	0.001

Table I.2: PHYSICAL PROPERTIES OF PURE CONSTITUENTS OF THE SYSTEMS AT 20°C.

Constituents	Density kg/m^3	Viscosity mPa.s	Surface Tension mN/m	Refractive Index
Water	998.2	1.003	72.75	1.333
Toluene	866.7	0.586	28.4	1.4967
Acetone	790.5	0.322	23.4	1.359
Cyclohexane	779.3	1.02	25.5	1.4266
Propan-2-ol	786.5	2.256	21.7	1.3776
Xylene	864.2	1.4958	28.9	1.3515
Methanol	791.4	0.597	22.6	1.3288
Sulphuric Acid (98% conc.)	1841.0	-	55.1	-
Acetic Acid	1049.3	1.229	27.5	1.3715
2% H_2SO_4	1014.2	1.515	70.42	1.335
5% H_2SO_4	1031.8	2.278	71.88	1.337

Table I.3: FIRE AND SAFETY PROPERTIES OF THE SYSTEM .

Property \ Compound	Acetone	Toluene
Boiling Point ^{o}C	56.5	110.4
Melting Point ^{o}C	- 94.6	- 95.0
Flash Point ^{o}C (closed cup)	- 19	4.0
Explosive Limits in Air		
lower % vol.	2.6	1.2
upper % vol.	12.8	7.0
Ignition Temp. ^{o}C	538	508
Vapour Density (Air=1)	2	3.14
Vapour Pressure @ 20^{o}C mm Hg	185	22
Threshold Limit Value		
ppm in air	1000	200
mg/m^3 of air	2400	750
Evaporating Rate (Ether = 1)	2.1	6.1
Odour Threshold ppm	200-450	50

Table I.4: INTERFACIAL TENSION AT 20°C (229).

$$\sigma = \frac{1}{1 - C_4 x_c} \sum_{n=0}^{n=3} C_n (x_c - x_{cp})^n \quad mN/m$$

C_o	C_1	C_2	C_3	C_4	x_{cp}	Standard error (mN/m)
0	0	135.405	79.72012	-5	0.6367	0.658

System : Acetone - Toluene - Water.

Table I.5: LIQUID DIFFUSIVITIES AT 20°C (229).

$$D = A - B x_c \quad cm^2 / s$$

Solute	System	Phase	$Ax10^{-5}$	$Bx10^{-5}$	Standard Relative Error %
Acetone	Water-Toluene	Water	1.154	2.67	0.4
		Toluene	2.790	4.63	0.4

Table I.6: LIQUID DIFFUSIVITIES (229)

Diffusivity of Acetone in the Toluene (A) - Acetone (C) - Water (B) System at 20°C.

x - Water Phase		y - Organic Phase	
x_C % wt.	D x 10^{-5} cm^2/s	y_C % wt.	D x 10^{-5} cm^2/s
0.59	1.14	0.72	2.70
0.92	1.14	0.82	2.71
1.14	1.13	0.83	2.73
1.44	1.11	0.83	2.80
2.06	1.08	1.13	2.76
2.95	1.09	1.22	2.70
3.45	1.07	2.02	2.76
3.70	1.04	3.25	2.78
4.84	1.01	3.26	2.65
5.96	1.01	3.27	2.66
		4.32	2.60
		4.32	2.57
		4.36	2.59
		4.37	2.64

Table I.7: PHYSICAL PROPERTIES OF CONJUGATE PHASES (229).

Water (B) - Acetone (C) - Toluene (A) at 20°C

x_C % wt.	ρ_x kg/m^3	ρ_y kg/m^3	μ_x mPa.s	μ_y mPa.s	σ mN/m.
0	997.8	866.5	1.006	0.586	35.40
1.08	995.6	865.3	1.024	0.581	31.80
1.54	995.2	864.9	1.035	0.579	30.50
2.43	997.4	864.8	1.065	0.578	27.80
3.13	993.7	864.5	1.078	0.575	27.00
5.10	991.3	864.2	1.140	0.570	23.10
6.27	989.2	863.0	1.170	0.562	21.50
7.67	987.8	862.6	1.20	0.560	19.30
10.58	983.7	859.9	1.265	0.547	16.90
13.05	980.0	857.1	1.328	0.534	15.00
14.10	979.5	856.7	1.353	0.530	14.50
20.07	970.9	853.8	1.480	0.511	10.00
20.50	971.3	850.5	1.485	0.501	9.30
32.30	950.3	839.0	1.583	0.463	3.80
35.40	949.8	839.1	1.597	0.455	3.40
36.80	943.9	835.5	-	0.452	3.00
39.78	939.5	834.2	1.579	0.448	2.80
39.84	936.7	842.0	1.542	0.485	3.00
58.20	893.9	867.1	1.375	1.092	0.5
68.20	879.8	879.8	1.275	1.275	0.2

APPENDIX II

i) Tables for a) Solubility Data
b) Tie - Line Data & Othmer-Tobias and Hand's coordinate

ii) Triangular Plot of Equilibrium Data

iii) Solute Concentration vs Refractive Index Curves

Table II.1 Solubility data for Acetone-Water-Toluene at 20°C

RI: Refractive Index

HYDROCARBON LAYER			
Acetone wt % (C)	Water wt % (B)	Toluene wt % (A)	RI
.0100	.0006	.9894	1.48200
.0500	.0009	.9491	1.47640
.1000	.0020	.8980	1.47050
.1985	.0078	.7937	1.45670
.2957	.0146	.6897	1.44420
.4260	.0171	.5569	1.42815
.4650	.0273	.5077	1.42860
.4857	.0322	.4821	1.42574
.5488	.0365	.4147	1.41995
.5655	.0458	.3887	1.41210
.5770	.0525	.3705	1.40790
.5776	.0462	.3762	1.41110
.5974	.0593	.3433	1.40720
.6407	.0899	.2694	1.40000
.6590	.1347	.2063	1.39595
.5949	.0608	.3443	1.40750

AQUEOUS LAYER			
Acetone wt % (C)	Water wt % (B)	Toluene wt % (A)	RI
.0050	.9947	.0003	1.33705
.0500	.9495	.0005	1.33980
.1000	.8994	.0006	1.34245
.1997	.7987	.0016	1.34835
.2991	.6979	.0030	1.35405
.3325	.6599	.0076	1.35600
.3519	.6440	.0081	1.35540
.3857	.6059	.0084	1.35930
.3968	.5952	.0092	1.35990
.4271	.5618	.0112	1.36158
.4449	.5393	.0158	1.36300
.4782	.5009	.0209	1.36441
.5087	.4650	.0263	1.36590
.5919	.3427	.0654	1.37111
.6284	.2693	.1023	1.37315
.6423	.1955	.1622	1.37405

Table II.2 Tie-lines for system Acetone-Water-Toluene at 20°C

AQUEOUS LAYER				HYDROCARBON LAYER			
Acetone wt% (C)	Water wt % (B)	Toluene wt % (A)	$\frac{1-X_{BB}}{X_{BB}}$	Acetone wt % (C)	Water wt % (B)	Toluene wt % (A)	$\frac{1-X_{AA}}{X_{AA}}$
.060	.940	0.000	.0638	.058	.000	.942	0.0616
.110	.890	0.000	.1236	.095	.000	.905	0.1050
.217	.783	0.000	.2771	.208	.000	.792	0.2626
.250	.750	0.000	.3330	.260	.003	.737	0.3569
.324	.673	0.003	.4859	.354	.011	.635	0.5748
.376	.618	0.006	.6181	.432	.018	.550	0.8182
.392	.600	0.008	.6667	.515	.029	.486	1.0576
.546	.417	0.037	.7153	.641	.090	.269	2.7175

Table II.3

Hands Correlation for System Acetone-Water-Toluene at 20°C

AQUEOUS LAYER			
x_{CB}	x_{BB}	x_{AB}	x_{CB}/x_{BB}
.0194	.9806	.0000	.0198
.0369	.9631	.0000	.0383
.0792	.9208	.0000	.0860
.0937	.9063	.0000	.1034
.1299	.8693	.0008	.1494
.1586	.8398	.0016	.1889
.1682	.8296	.0022	.2027
.2231	.7674	.0095	.2907

HYDROCARBON LAYER			
x_{BA}	x_{CA}	x_{AA}	x_{CA}/x_{AA}
.0000	.0890	.9110	.0977
.0000	.1427	.8573	.1665
.0000	.2941	.7059	.4166
.0132	.3541	.6327	.5597
.0448	.4483	.5069	.8844
.0693	.5163	.4144	1.2459
.1020	.5630	.335	1.6806
.2635	.5824	.1541	3.7794

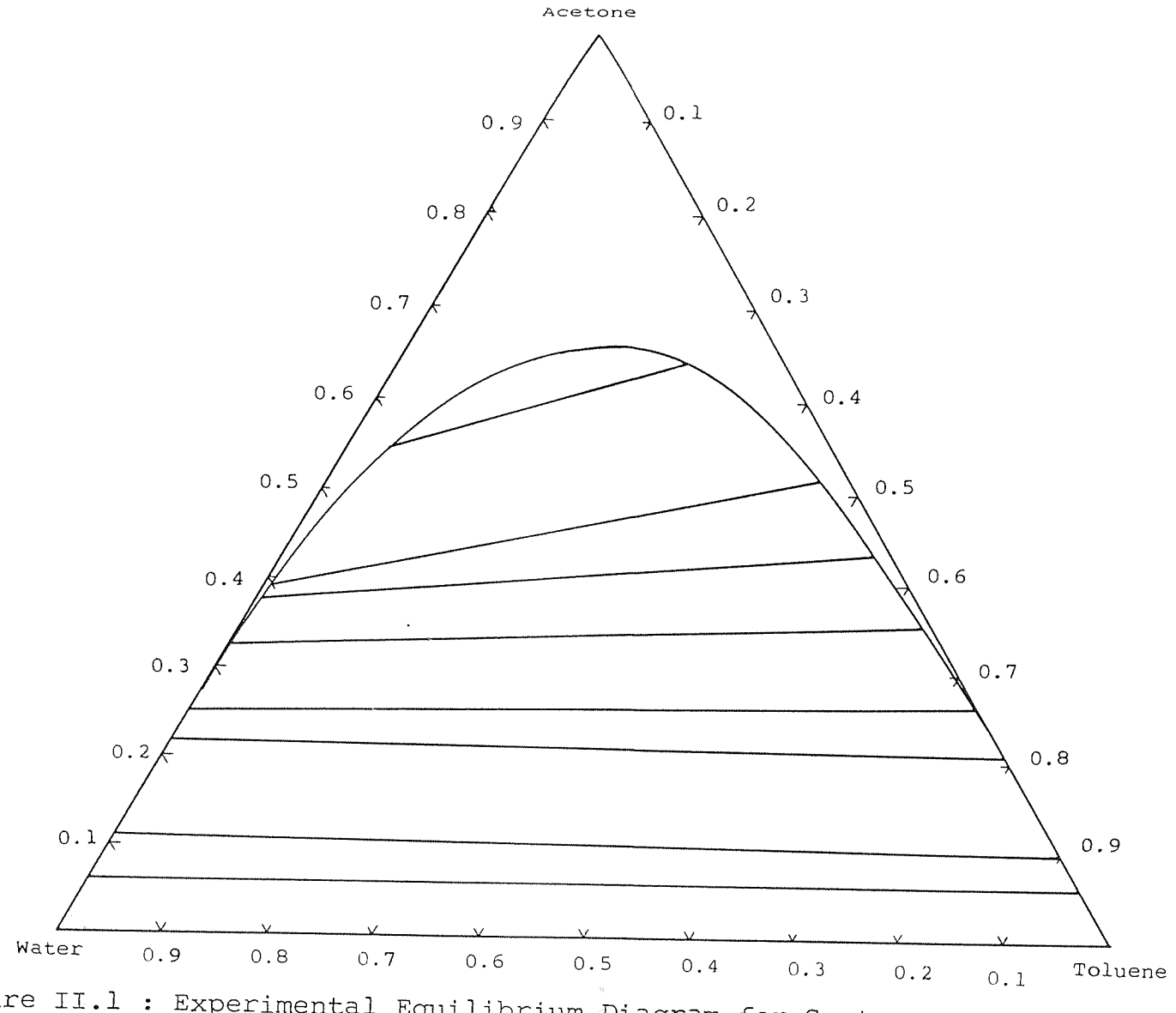

Figure II.1 : Experimental Equilibrium Diagram for System : Acetone-Toluene-Water at 20°C.

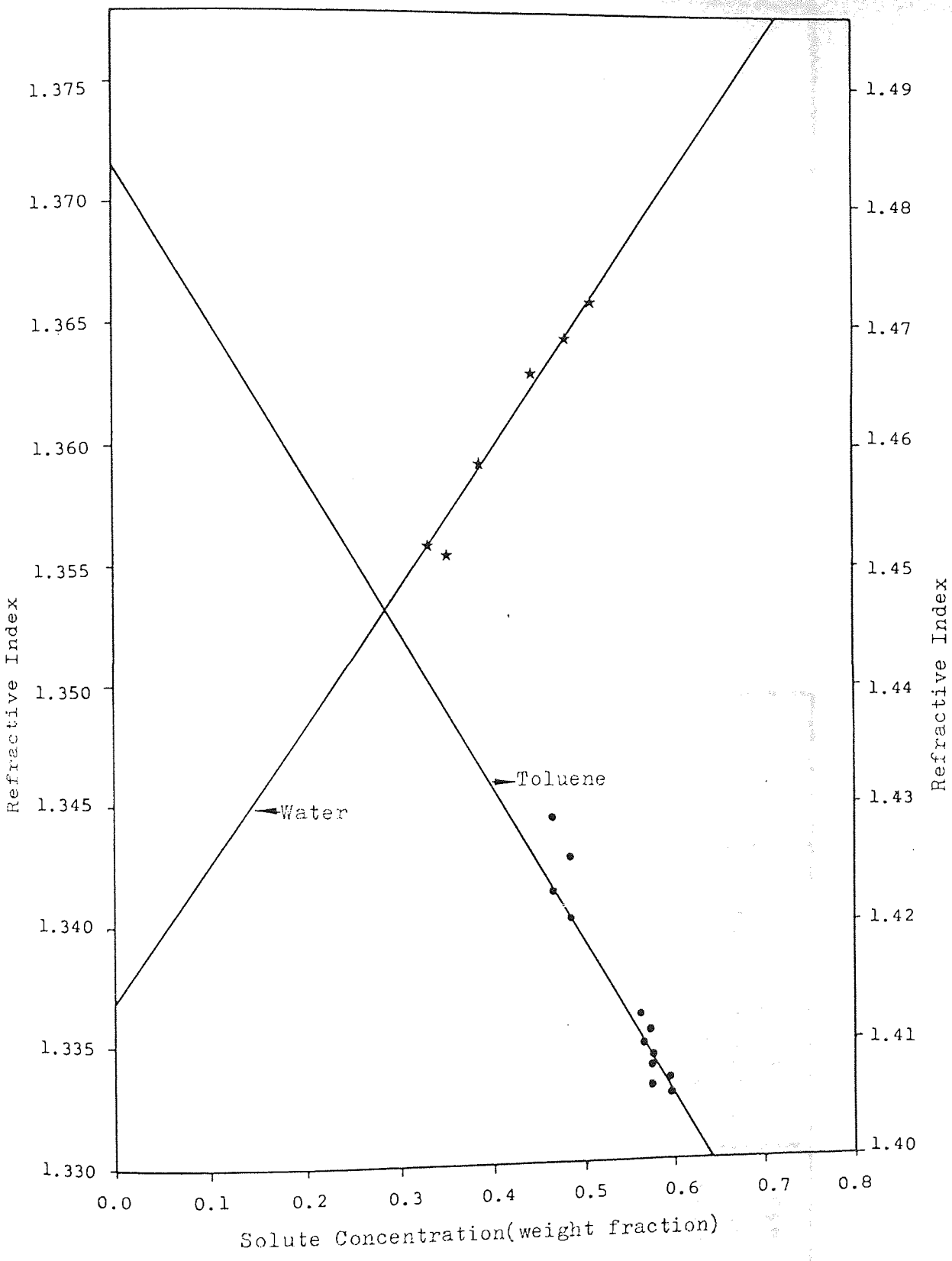

Figure II.2 : Solute Concentration vs Refractive Index for System:Acetone-Toluene-Water at $20^{o}C$.

Table II.4 Data for Solubility Curve

System: Acetone - 2% H_2SO_4 in Water-Toluene at 20°C

AQUEOUS LAYER			
Acetone wt% (C)	Water wt% (B)	Toluene wt% (A)	RI
0.3194	0.6750	0.0056	1.35615
0.4066	0.5834	0.0100	1.36074
0.4153	0.5728	0.0119	1.36165
0.4324	0.5538	0.0138	1.36280
0.4671	0.5185	0.0144	1.36288
0.4983	0.4781	0.0236	1.36611
0.5189	0.4431	0.0380	1.36668
0.5578	0.3969	0.0452	1.37075
0.6158	0.2342	0.1500	1.37191
0.6317	0.1993	0.1690	1.37403
0.6457	0.1473	0.2069	1.37321

HYDROCARBON LAYER			
Acetone wt% (C)	Water wt% (B)	Toluene wt% (A)	RI
0.3167	0.0152	0.6681	1.45078
0.3286	0.0303	0.5172	1.42347
0.4526	0.0088	0.6627	1.45308
0.4677	0.0192	0.5131	1.42773
0.6608	0.0855	0.2537	1.39589
0.6774	0.0641	0.2585	1.39641

Table II.5 Othmer-Tobias Correlation for Tie Lines

System: Acetone - 2% H_2SO_4 in Water-Toluene at 20°C.

AQUEOUS LAYER			
Acetone wt% (C)	Water wt% (B)	Toluene wt% (A)	$\frac{1-X_{BB}}{X_{BB}}$
.098	.902	.000	.1086
.153	.847	.000	.1806
.162	.838	.000	.1933
.172	.828	.000	.2077
.182	.818	.000	.2250
.230	.770	.000	.2987
.249	.751	.000	.3316
.253	.747	.000	.3387
.332	.665	.003	.5038
.336	.659	.005	.5175
.358	.635	.007	.5748
.370	.624	.006	.6026
.380	.612	.008	.6340
.544	.418	.038	1.3923

HYDROCARBON LAYER			
Acetone wt% (C)	Water wt% (B)	Toluene wt% (A)	$\frac{1-X_{AA}}{X_{AA}}$
.129	.000	.871	.1481
.188	.000	.812	.2315
.200	.000	.800	.2500
.213	.000	.787	.2706
.242	.002	.756	.3228
.262	.002	.736	.3587
.294	.005	.701	.4265
.294	.005	.701	.4265
.411	.013	.576	.7361
.411	.013	.576	.7361
.448	.015	.537	.8622
.512	.022	.466	1.1459
.549	.029	.422	1.3697
.663	.086	.251	2.9841

Table II.6 Tie Line Data for Hands Plot

System: 2% H_2SO_4 in Water-Acetone-Toluene at 20°C.

AQUEOUS LAYER			
x_{CB}	x_{BB}	x_{AB}	x_{CB}/x_{BB}
.0354	.9646	.0000	.0422
.0576	.9424	.0000	.0611
.0613	.9387	.0000	.0653
.0656	.9344	.0000	.0702
.0699	.9301	.0000	.0752
.0917	.9083	.0000	.1010
.1008	.8992	.0000	.1120
.1600	.8400	.0000	.1905
.1442	.8549	.0008	.1687
.1468	.8519	.0014	.1723
.1597	.8383	.0020	.1905
.1666	.8317	.0017	.2004
.2326	.7643	.0031	.3043
.3014	.6853	.0133	.4398

HYDROCARBON LAYER			
x_{CA}	x_{AA}	x_{BA}	x_{CA}/x_{AA}
.1902	.8098	.0000	0.2349
.2686	.7314	.0000	0.3672
.382	.9618	.0000	0.3970
.3003	.6997	.0000	0.4292
.3338	.6574	.0089	0.5078
.3577	.6335	.0088	0.5646
.3909	.5876	.0214	0.6652
.4532	.5219	.0249	0.8684
.5037	.4450	.0513	1.1318
.5037	.4450	.0513	1.1318
.5366	.4055	.0579	1.3233
.5841	.3351	.0808	1.7429
.5339	.3752	.0909	1.4230
.6036	.1441	.2523	4.1902

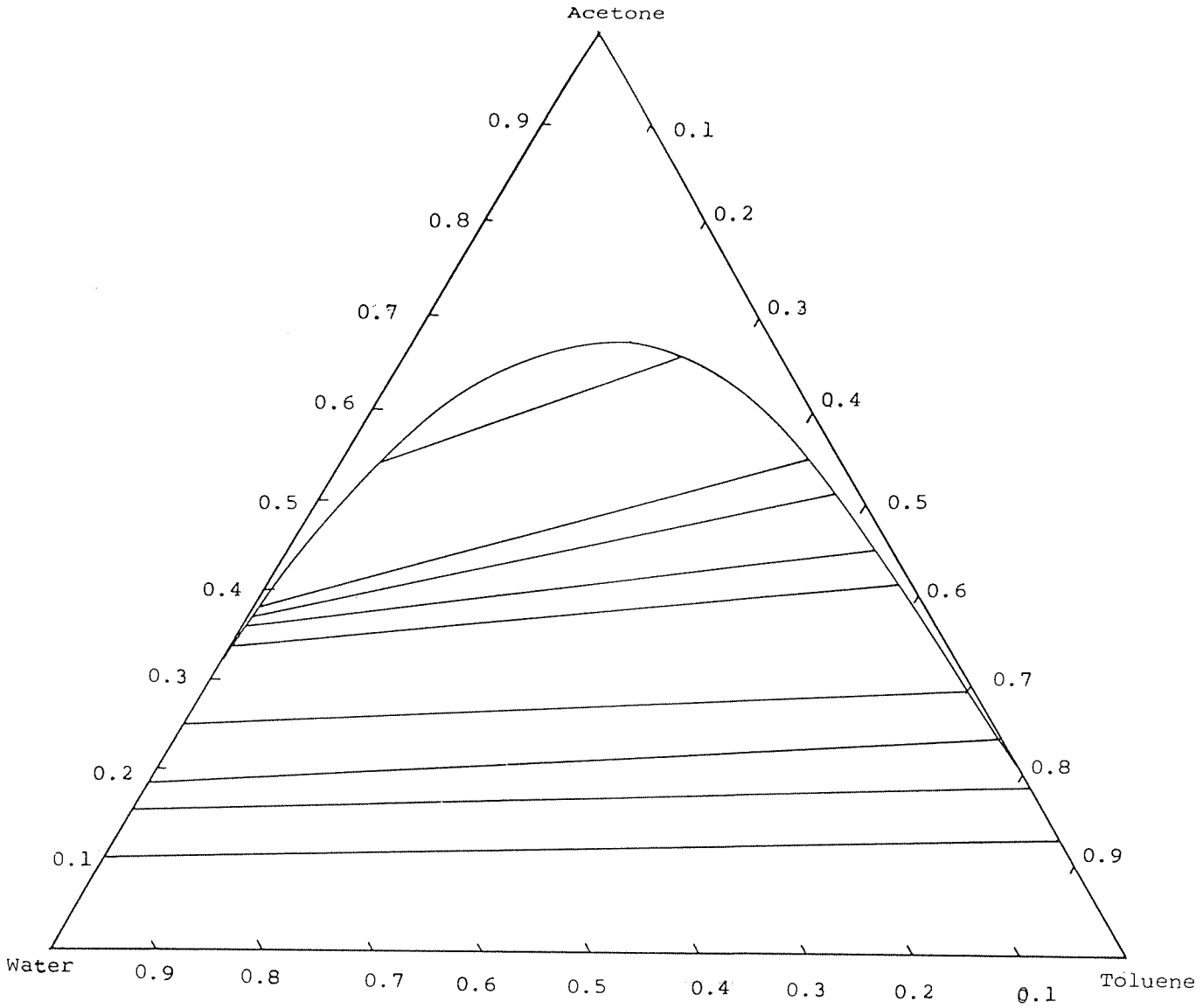

Figure II.3 : Experimental Equilibrium Diagram for System : Acetone-Toluene-2% Sulphuric Acid in Water at 20°C.

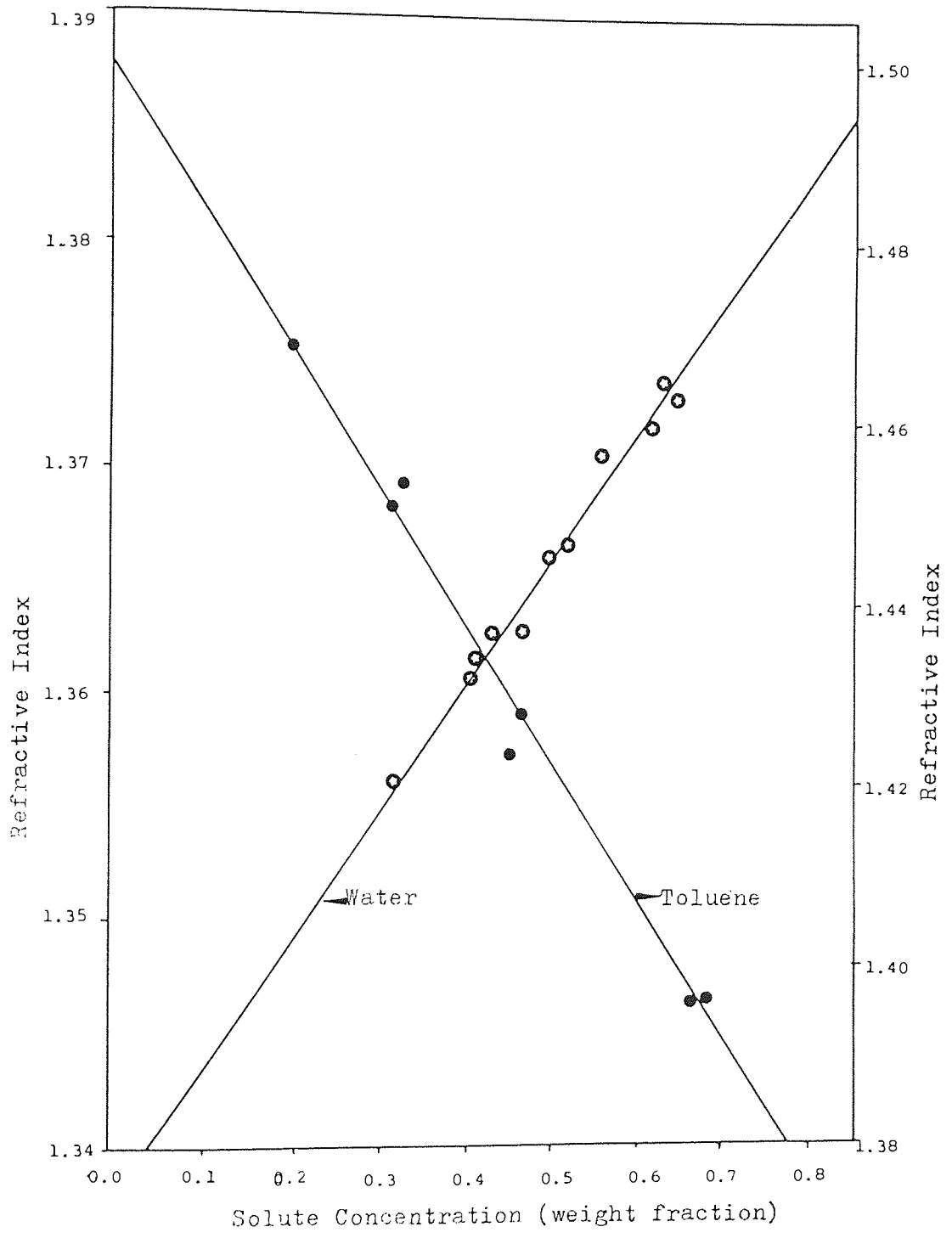

Figure II.4 : Solute Concentration vs Refractive Index for System : Acetone-Toluene-2% Sulphuric Acid in Water at $20^{\circ}C$.

Table II.7 Data for Solubility Curve

System: Acetone - 5% H_2SO_4 in Water-Toluene at 20°C

AQUEOUS LAYER			
Acetone (C)	Water (B)	Toluene (A)	RI
0.3517	0.6379	0.0103	1.3606
0.3977	0.5920	0.0103	1.3631
0.4417	0.5407	0.0176	1.3549
0.4107	0.5764	0.0128	1.3634
0.4265	0.5586	0.0149	1.3642
0.4883	0.4920	0.0197	1.3672
0.4957	0.4870	0.0173	1.3669

HYDROCARBON LAYER			
Acetone (C)	Water (B)	Toluene (A)	RI
0.3789	0.0128	0.6083	1.4409
0.5030	0.0195	0.4775	1.4237
0.5479	0.0249	0.4272	1.4172
0.5581	0.0266	0.4154	1.4161
0.5589	0.0750	0.3661	1.4130
0.5607	0.0258	0.4135	1.4153

Table II.8 Tie-Line Data

System: 5% H_2SO_4 in Water-Acetone-Toluene at 20°C. a) Othmer-Tobias and b) Hands Plots

AQUEOUS LAYER			
Acetone (C)	Water (B)	Toluene (A)	$\frac{1-X_{BB}}{X_{BB}}$
.072	.928	.000	0.0776
.170	.830	.000	0.2048
.328	.669	.003	0.4948
.400	.589	.011	0.6978
.559	.315	.046	1.5316

HYDROCARBON LAYER			
Acetone (C)	Water (B)	Toluene (A)	$\frac{1-X_{AA}}{X_{AA}}$
.167	.002	.831	0.2034
.253	.004	.743	0.3459
.434	.013	.553	0.8083
.516	.020	.464	1.1552
.644	.163	.203	3.9261

AQUEOUS LAYER			
x_{CB}	x_{BB}	x_{AB}	x_{CB}/x_{BB}
.0286	.9714	.000	.0294
.0721	.9279	.000	.0742
.1567	.8424	.0009	.1860
.2041	.7923	.0036	.2576
.3941	.5855	.0204	.6731

HYDROCARBON LAYER			
x_{CA}	x_{AA}	x_{BA}	x_{CA}/x_{AA}
.2399	.7526	.0076	0.3188
.3456	.6399	.0144	0.5401
.5313	.4268	.0420	1.2448
.5991	.3396	.0613	1.7641
.5359	.1065	.3576	5.0319

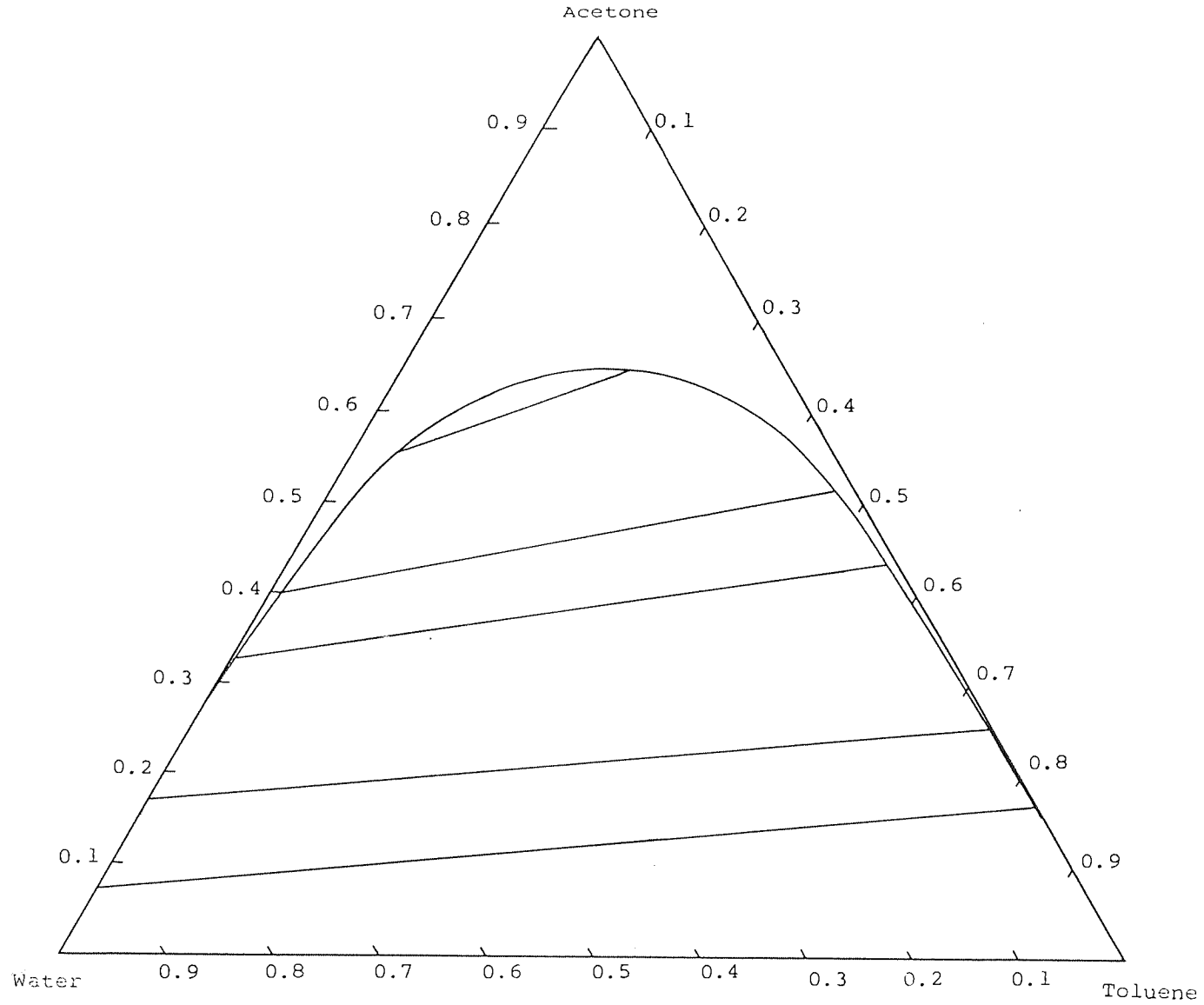

Figure II.5 : Experimental Equilibrium Diagram for System : Acetone-Toluene-5% H_2SO^4 in Water at 20°C.

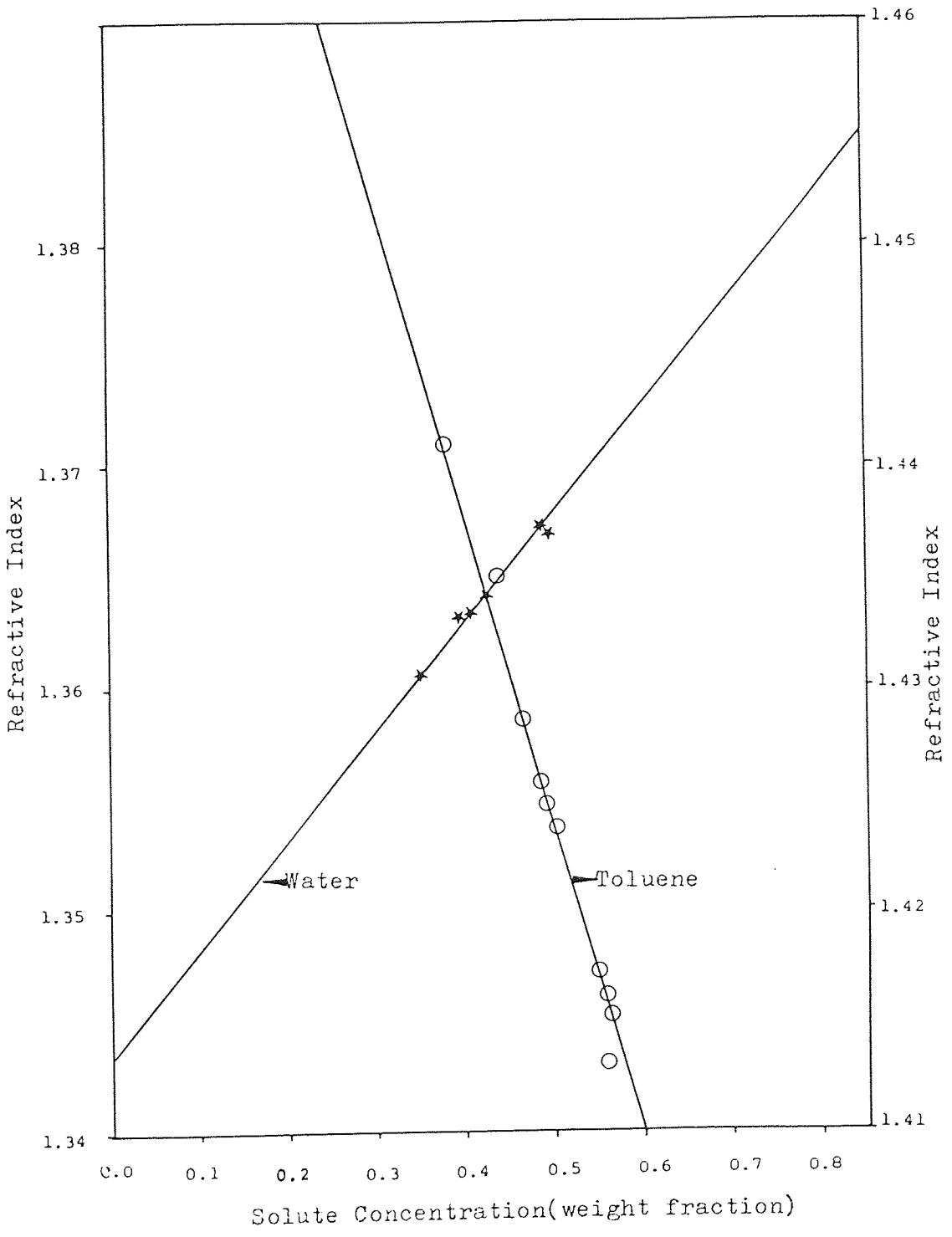

Figure II.6 : Solute Concentration vs Refractive Index for Acetone-Toluene-5% Sulphuric Acid in Water at 20°C.

Table II.9 Data for Solubility Curve

System: Acetone - 2% Acetic Acid in Water-Toluene at 20°C.

AQUEOUS LAYER			
Acetone (C)	Water (B)	Toluene (A)	RI
.3621	.6326	.0053	1.35735
.3736	.6182	.0082	1.35808
.4046	.5872	.0082	1.35922
.4367	.5493	.0140	1.36094
.5141	.4618	.0241	1.36444
.5417	.4258	.0325	1.36597
.5547	.4104	.0349	1.36698
.5687	.3880	.0432	1.41690

HYDROCARBON LAYER			
Acetone (C)	Water (B)	Toluene (A)	RI
.3928	.0224	.5847	1.43970
.4029	.0218	.5752	1.43765
.4414	.0231	.5354	1.43496
.4472	.0297	.5231	1.43115
.4658	.0258	.5084	1.42874
.4787	.0235	.4977	1.42650
.4901	.0342	.4756	1.42483
.6327	.0796	.2878	1.40005

Table: II.10 Tie Line Data for a) Othmer-Tobias

b) Hands

System: 2% Acetic Acid in Water-Acetone-Toluene at 20°C.

AQUEOUS LAYER			
Acetone (C)	Water (B)	Toluene (A)	$\frac{1-X_{BB}}{X_{BB}}$
.015	.985	.000	0.0870
.066	.934	.000	0.1481
.188	.812	.000	0.2853
.268	.732	.000	0.4006
.416	.573	.011	0.8727
.550	.417	.033	2.3223

(a)

HYDROCARBON LAYER			
Acetone (C)	Water (B)	Toluene (A)	$\frac{1-X_{AA}}{X_{AA}}$
.080	.000	.920	0.01523
.129	.000	.871	0.07070
.222	.000	.778	0.23150
.284	.002	.714	0.36610
.451	.015	.534	0.74520
.623	.076	.301	1.39810

AQUEOUS LAYER			
x_{CB}	x_{AB}	x_{BB}	x_{CB}/x_{BB}
.0049	.0000	.9951	.0049
.0224	.0000	.9776	.0230
.0699	.0000	.9301	.0752
.1063	.0000	.9837	.1189
.1902	.0120	.8066	.2358
.2966	.0359	.6922	.4284

(b)

HYDROCARBON LAYER			
x_{CA}	x_{AA}	x_{BA}	x_{CA}/x_{AA}
.0014	.9986	.0000	0.0014
.1902	.8098	.0000	0.2349
.3116	.6884	.0000	0.4526
.3837	.6080	.0083	0.6310
.5409	.4037	.0554	1.3398
.5952	.1813	.2235	3.2827

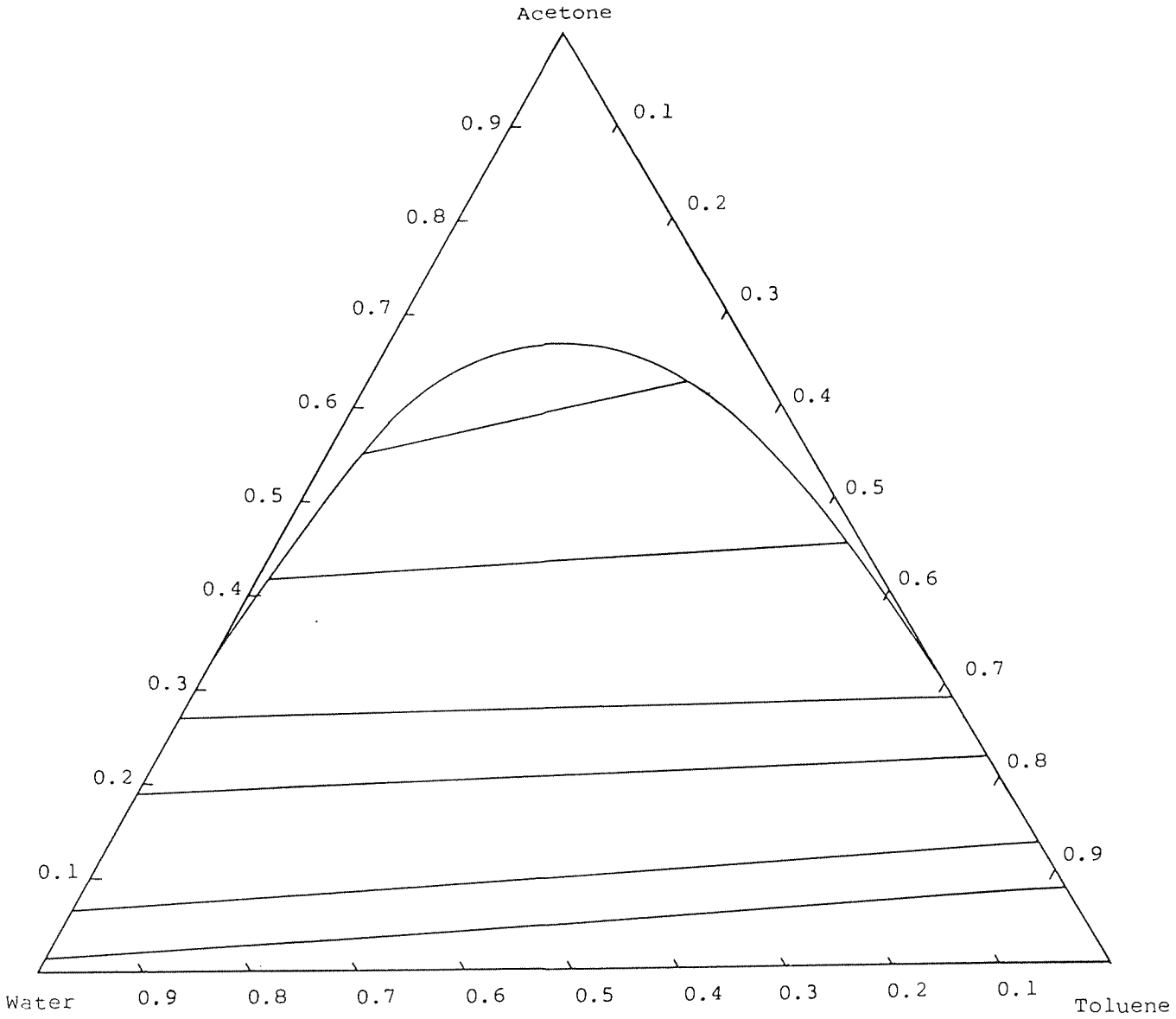

Figure II.7 : Experimental Equilibrium Diagram for System : Acetone-Toluene-2% Acetic Acid in Water at 20°C.

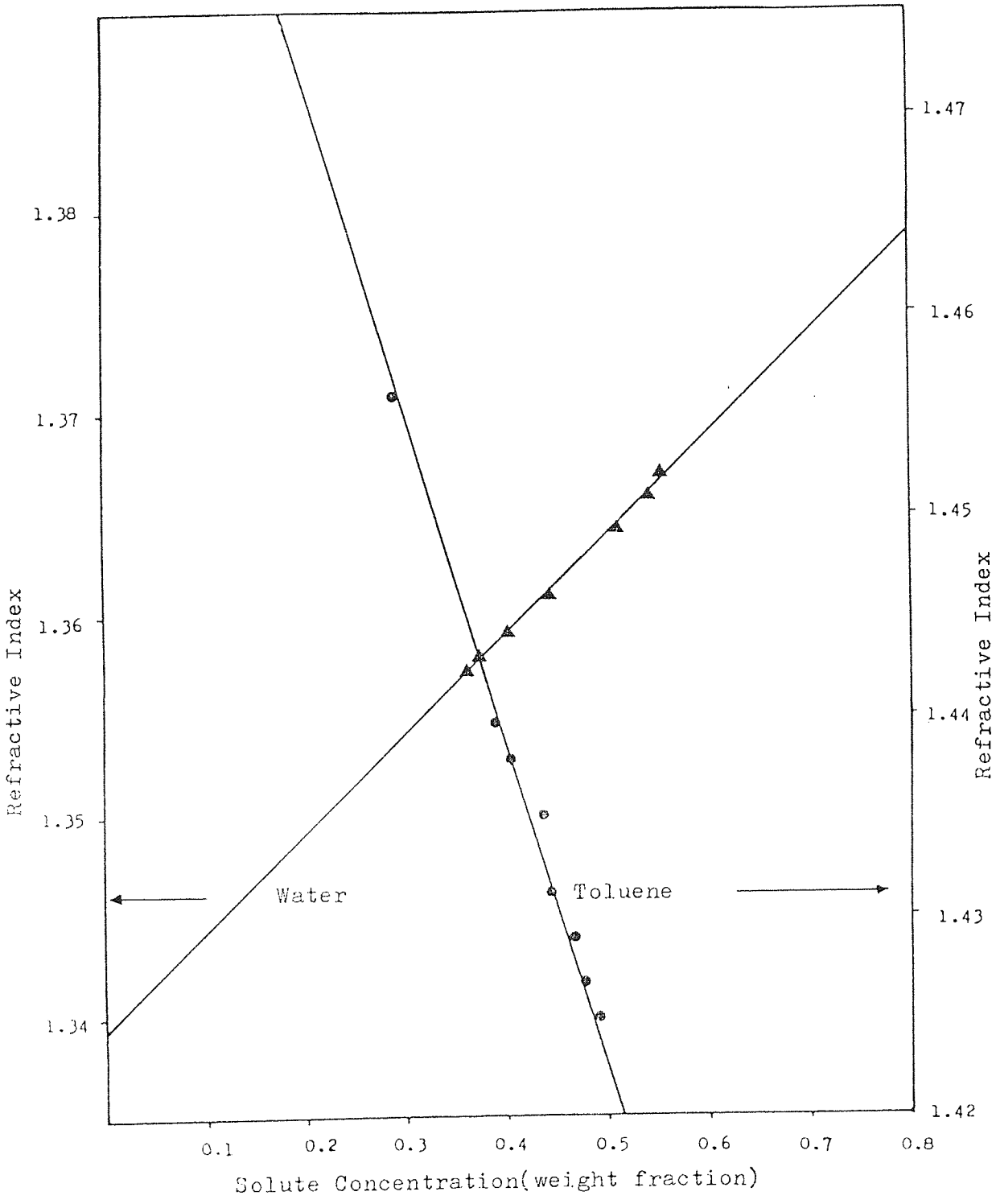

Figure II.8 : Solute Concentration vs Refractive Index for System : Acetone-Toluene-2% Acetic Acid in Water at $20^{o}C$.

Table II.11 Data for Solubility Curve

System: Isopropanol-Water-Cyclohexane at 20°C.

AQUEOUS LAYER			
Propan.	Cycloh.	Water	RI
0.2476	0.0042	0.7482	1.35710
0.3000	0.0078	0.6922	1.36030
0.3185	0.0076	0.6739	1.36125
0.3357	0.0087	0.6556	1.36260
0.3796	0.0182	0.6022	1.36490
0.4233	0.0394	0.5373	1.36856
0.4278	0.0293	0.5429	1.36825
0.4591	0.0554	0.4856	1.37078
0.4744	0.0294	0.4962	1.36780
0.4962	0.0839	0.4199	1.37371
0.4964	0.0836	0.4200	1.37250
0.5246	0.2363	0.2391	1.34200
0.5294	0.2099	0.2607	1.38220
0.5299	0.2100	0.2601	1.38253
0.5318	0.1307	0.3375	1.37798
0.5324	0.1973	0.2703	1.38176
0.5341	0.1948	0.2711	1.38179
0.5408	0.2144	0.2449	1.38295
0.5456	0.1774	0.2770	1.37543
0.5679	0.1044	0.3277	1.37685

HYDROCARBON LAYER			
Propan.	Cycloh.	Water	RI
0.1351	0.8518	0.0131	1.41775
0.1961	0.7775	0.0264	1.41453
0.2430	0.7224	0.0345	1.41102
0.3175	0.6293	0.0532	1.40688
0.3304	0.6140	0.0556	1.40564
0.3708	0.5250	0.1042	1.40160
0.4017	0.4976	0.1001	1.40587
0.4342	0.4303	0.1356	1.39372
0.4577	0.4239	0.1184	1.39235
0.4634	0.3827	0.1539	1.39098
0.4771	0.3636	0.1593	1.39033
0.4922	0.3251	0.1827	1.38855
0.5073	0.2957	0.1970	1.38678
0.5248	0.2600	0.2152	1.38524
0.5755	0.2568	0.1677	1.38733

Table II.11 Othmer-Tobias Correlations for Tie-lines

System: Isopropanol-Water-Cyclohexane at 20°C.

AQUEOUS PHASE			
Iso. (C)	Water (B)	Cyclo. (A)	$\frac{1-X_{BB}}{X_{BB}}$
0.271	0.727	0.002	0.3755
0.126	0.874	0.000	0.1442
0.182	0.818	0.000	0.2225
0.064	0.936	0.000	0.0684
0.350	0.644	0.006	0.5528
0.406	0.562	0.012	0.7794
0.418	0.568	0.014	0.7606
0.440	0.540	0.020	0.8519
0.463	0.511	0.026	0.9569
0.491	0.471	0.038	1.1231
0.509	0.442	0.049	1.2624
0.514	0.419	0.057	1.3866
0.566	0.330	0.104	2.0300

ORGANIC PHASE			
Iso. (C)	Water (B)	Cyclo. (A)	$\frac{1-X_{AA}}{X_{AA}}$
0.090	0.010	0.900	0.1111
0.067	0.009	0.924	0.0823
0.074	0.007	0.919	0.0881
0.037	0.005	0.958	0.0438
0.144	0.016	0.840	0.1905
0.167	0.018	0.815	0.2270
0.171	0.019	0.810	0.2346
0.179	0.020	0.801	0.2484
0.194	0.022	0.784	0.2755
0.198	0.023	0.779	0.2837
0.207	0.024	0.769	0.3004
0.226	0.027	0.747	0.3387
0.323	0.046	0.631	0.5848

Table II.12 Hand's coordinate for tie-lines.

System: Isopropanol-Water-Cyclohexane at 20°C.

AQUEOUS PHASE				HYDROCARBON PHASE			
x_{CB}	x_{BB}	x_{AB}	x_{CB}/x_{BB}	x_{CA}	x_{BA}	x_{AA}	x_{CA}/x_{AA}
.0201	.9799	.0000	.0205	.0502	.0226	.9272	.0541
.0414	.9585	.0000	.0433	.0885	.0396	.8718	.1015
.0626	.9374	.0000	.0668	.0982	.0310	.8709	.1128
.1005	.8989	.0005	.1118	.1175	.0435	.8390	.1400
.1399	.8584	.0017	.1630	.1806	.0669	.7525	.2400
.1775	.8188	.0038	.2168	.2066	.0742	.7192	.2872
.1801	.8156	.0043	.2208	.2103	.0779	.7117	.2955
.1952	.7985	.0063	.2444	.2189	.0815	.6996	.3129
.2119	.7796	.0085	.2719	.2345	.0886	.6769	.3464
.2351	.7519	.0130	.3127	.2382	.0923	.6695	.3558
.2523	.7303	.0173	.3454	.2475	.0956	.6568	.3768
.2671	.7121	.0208	.3752	.2660	.1059	.6280	.4236
.3252	.6321	.0427	.5145	.3484	.1654	.4862	.7166

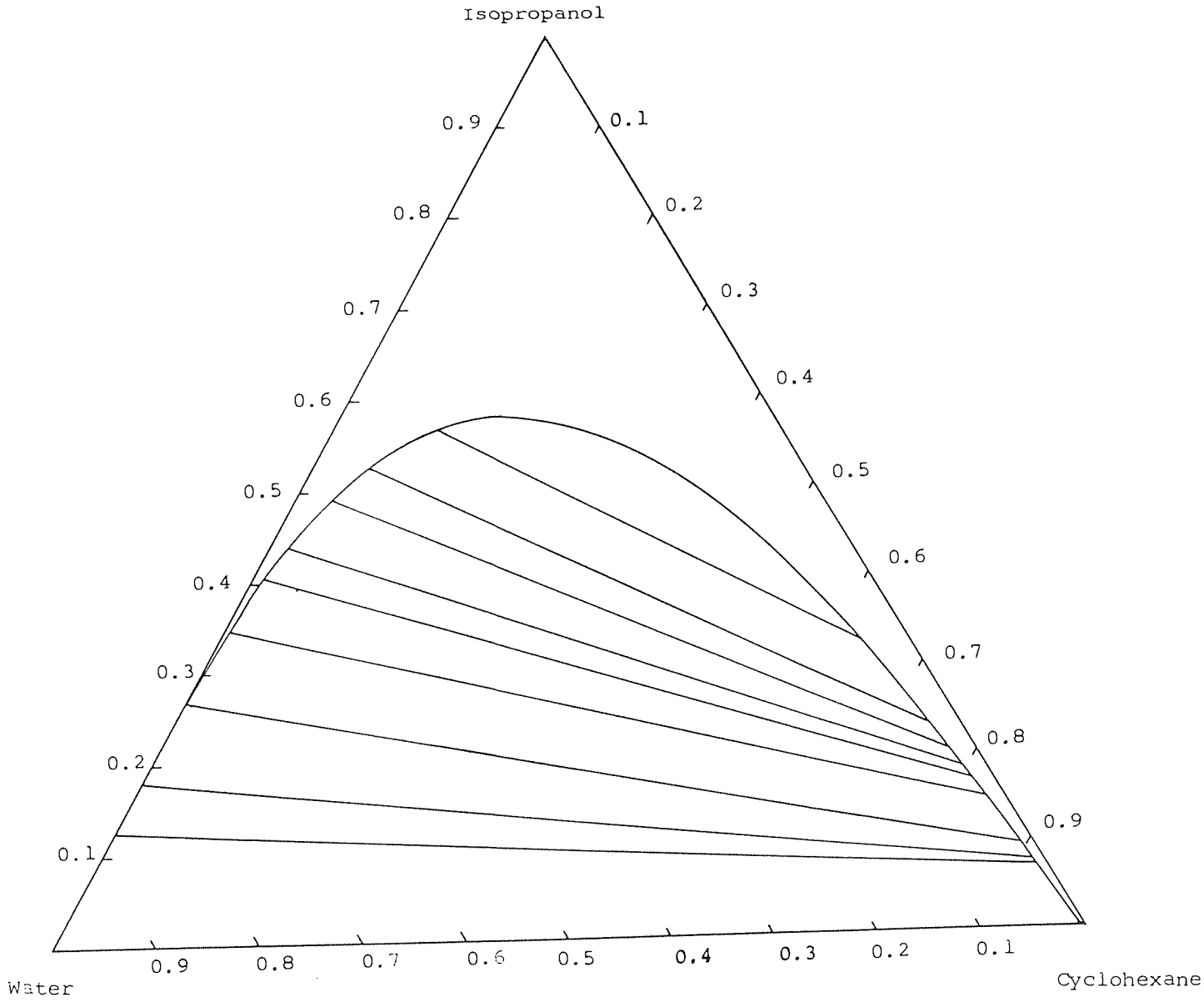

Figure II.9 : Experimental Equilibrium Diagram for System Isopropanol-Cyclohexane-Water at 20°C.

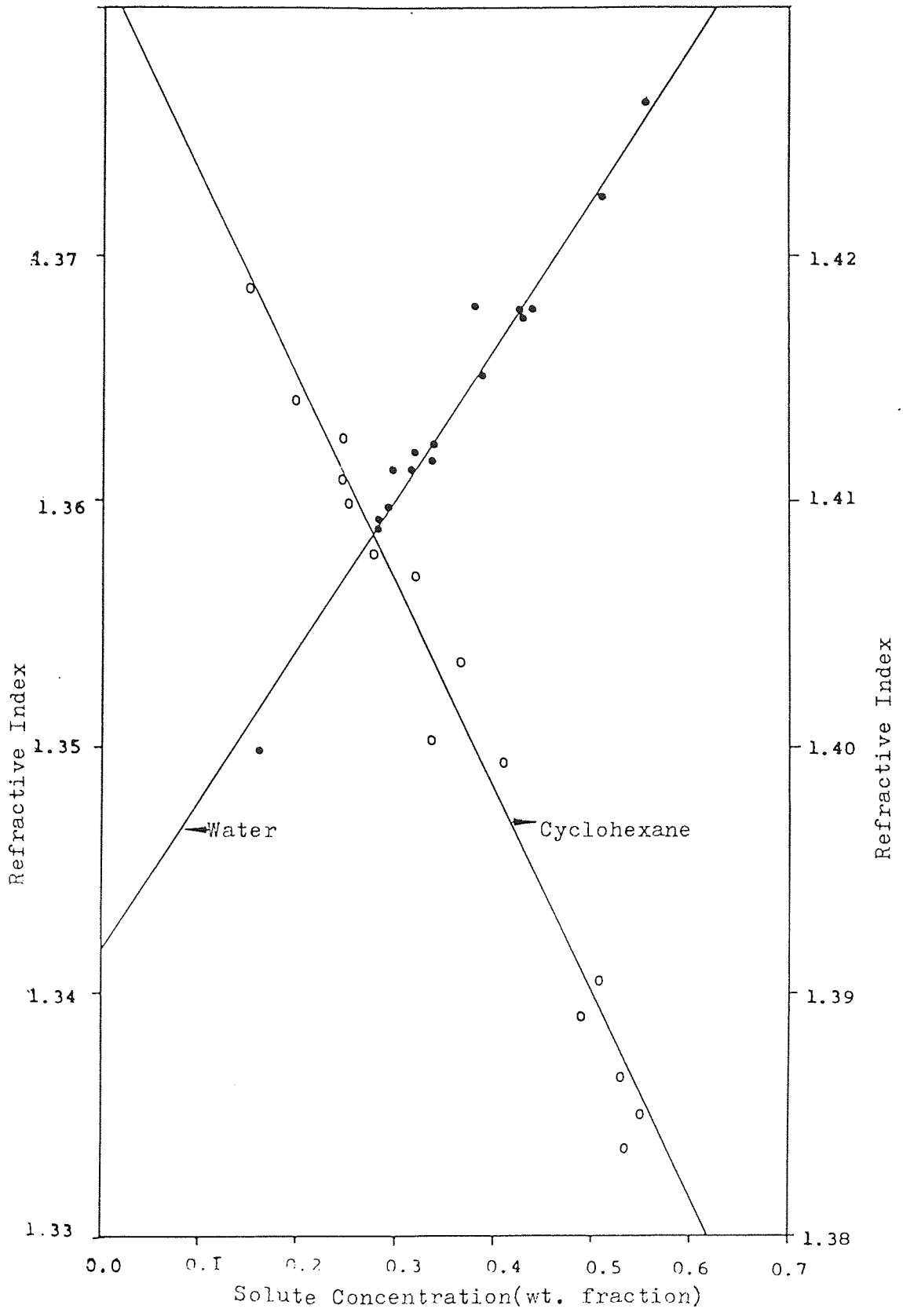

Figure II.10 : Solute Concentration vs Refractive Index for System : Isopropanol-Cyclohexane-Water at 20°C.

Table II.13 Data for Solubility Curve
System: Isopropanol - 2% H_2SO_4 in Water - Cyclohexane at 20°C.

AQUEOUS LAYER			
Propanol	Cycloh.	Water	RI
0.1614	0.0064	0.8321	1.34984
0.2765	0.0110	0.7125	1.35918
0.2783	0.0044	0.7173	1.35886
0.3149	0.0099	0.6761	1.36132
0.3372	0.0110	0.6518	1.36231
0.3376	0.0100	0.6524	1.36158
0.4245	0.0286	0.5469	1.36784
0.4254	0.0266	0.5481	1.36743
0.4370	0.0268	0.5362	1.36783

HYDROCARBON LAYER			
Propanol	Cycloh.	Water	RI
0.1969	0.7803	0.0228	1.41409
0.2449	0.7280	0.0271	1.41093
0.3152	0.6247	0.0601	1.40814
0.3180	0.6303	0.0516	1.40700
0.3729	0.5544	0.0727	1.40372
0.4447	0.4407	0.1146	1.40019
0.4499	0.4458	0.1043	1.39944
0.5072	0.3351	0.1577	1.39042
0.5289	0.2812	0.1899	1.38646
0.5354	0.2653	0.1993	1.38356

Table II.14 Othmer-Tobias plot for Tie-line Data
System: Cyclohexane - 2% H_2SO_4 in Water-Isopropanol at 20°C.

(A) (B) (C)

AQUEOUS LAYER			
(C)	(B)	(A)	$\frac{1-X_{BB}}{X_{BB}}$
.0803	.917	.000	0.0905
.1140	.884	.002	0.1312
.1820	.814	.004	0.2285
.3160	.676	.008	0.4793
.3480	.643	.009	0.5552
.3810	.606	.013	0.6502
.4030	.579	.018	0.7271
.4770	.469	.054	1.1322
.5080	.413	.079	1.4213
.5440	.307	.149	2.2573

HYDROCARBON LAYER			
(C)	(B)	(A)	$\frac{1-X_{AA}}{X_{AA}}$
.000	.000	1.000	.0000
.000	.000	1.000	.0000
.011	.000	1.000	.0000
.081	.006	0.913	.0953
.110	.012	0.878	.1390
.141	.017	0.842	.1877
.155	.020	0.825	.2121
.201	.026	0.700	.4286
.224	.031	0.745	.3423
.283	.044	0.673	.4859

Table II.15 Hand's Coordinate

System: Cyclohexane-2% H_2SO_4 in Water-Isopropanol at 20°C
(A) (B) (C)

AQUEOUS LAYER				HYDROCARBON LAYER			
x_{CB}	x_{BB}	x_{AB}	x_{CB}/x_{BB}	x_{CA}	x_{AA}	x_{BA}	x_{CA}/x_{AA}
.0278	.9722	.0000	.0286	.0000	1.0000	0.0000	0.0000
.0404	.9590	.0006	.0421	.0000	1.0000	0.0000	0.0000
.0680	.9308	.0012	.0730	.0134	0.9866	0.0000	0.0136
.1321	.8652	.0027	.1527	.0963	0.8800	0.0238	0.1094
.1498	.8471	.0032	.1768	.1276	0.8260	0.0464	0.1545
.1696	.8257	.0047	.2054	.1602	0.7755	0.0643	0.2066
.1840	.8093	.0067	.2274	.740	0.7511	0.7490	0.2317
.2438	.7338	.0224	.3322	.2350	0.6636	0.1013	0.3541
.2766	.6885	.0349	.4017	.2405	0.6486	0.1109	0.3708
.3390	.5857	.0753	.5788	.2902	0.5595	0.1504	1.4812

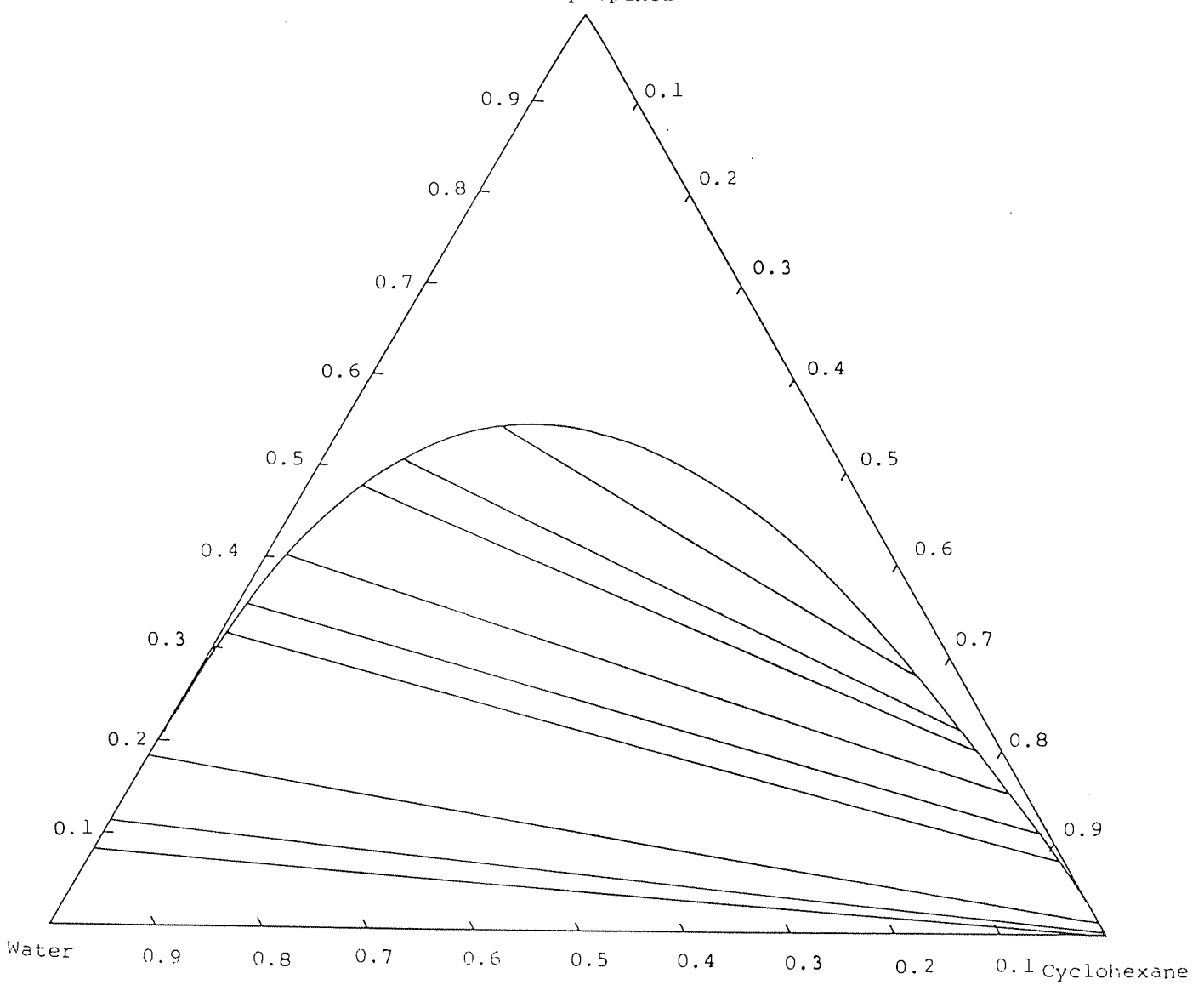

Figure II.11 : Experimental Equilibrium Diagram for System : Isopropanol-Cyclohexane-2% Sulphuric Acid in Water at 20 °C.

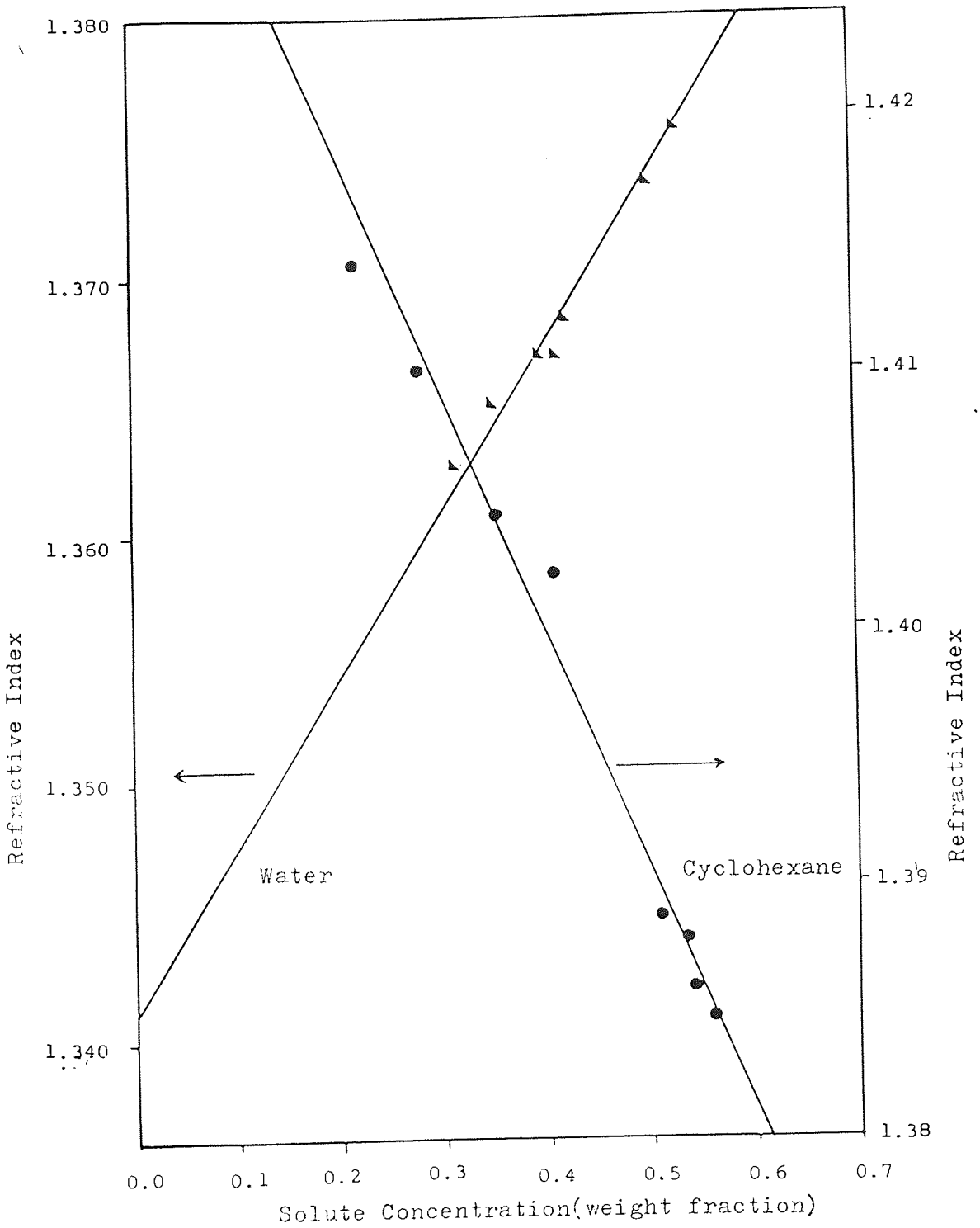

Figure II.12: Solute Concentration vs Refractive Index for System : Isopropanol-Cyclohexane-2% Sulphuric Acid in Water at 20°C.

Table II.16 Solubility Data and REfractive Indices for

System: Isopropanol - 5% H_2SO_4 in Water-Cyclohexane at 20°C.

(C) (B) (A)

Aqueous Layer			
Propanol	Cycloh.	Water	RI
0.3114	0.0078	0.6808	1.36262
0.3508	0.0100	0.6392	1.36496
0.3980	0.0219	0.5801	1.36979
0.4110	0.0214	0.5676	1.36790
0.4206	0.0275	0.5518	1.36829
0.5000	0.0628	0.4374	1.37362
0.5271	0.0888	0.3841	1.37572

Hydrocarbon Layer			
Propanol	Cycloh.	Water	RI
0.2766	0.6853	0.0381	1.40995
0.3546	0.5857	0.0597	1.40438
0.4103	0.5083	0.0814	1.40212
0.4656	0.4195	0.1149	1.40041
0.5089	0.3362	0.1549	1.38861
0.5315	0.2926	0.1759	1.38778
0.5418	0.2684	0.1898	1.38585
0.5554	0.2202	0.2244	1.38472

Table II.17 Othmer-Tobias Correlation for Tie-lines

System: Isopropanol (C) - 5% H_2SO_4 in Water (B) - Cyclohexane (A) at 20°C

Aqueous Layer			
C	B	A	$\frac{1-X_{BB}}{X_{BB}}$
.110	.890	.000	0.1236
.192	.808	.000	0.2376
.314	.678	.008	0.4749
.389	.592	.019	0.6892
.421	.552	.027	0.8116
.558	.307	.135	2.2573
.535	.368	.097	1.7174

Hydrocarbon Layer			
C	B	A	$\frac{1-X_{AA}}{X_{AA}}$
.098	.011	.891	.1223
.127	.015	.858	.1655
.163	.019	.818	.2225
.201	.024	.775	.2903
.210	.026	.773	.2937
.284	.041	.675	.4815
.264	.036	.700	.4286

Table II.18 Hands Coordinates for Tie-lines

System:: Isopropanol - 5% H_2SO_4 in Water - Cyclohexane at 20°C

(C)				(B)			(A)
Aqueous Layer				Hydrocarbon Layer			
x_{BB}	x_{CB}	x_{AB}	x_{CB}/x_{BB}	x_{CA}	x_{AA}	x_{BA}	x_{CA}/x_{AA}
.9567	.0433	.0000	.0453	.1271	.8254	.0475	.1540
.9199	.0801	.0000	.0871	.1608	.7759	.0633	.2072
.8526	.1448	.0026	.1698	.2011	.7207	.0782	.2790
.8004	.1928	.0067	.2409	.2409	.6633	.0958	.3632
.7737	.2164	.0099	.2797	.2474	.6505	.1021	.3803
.5613	.3741	.0646	.6665	.3145	.5341	.1514	.5888
.6242	.3327	.0431	.5330	.2986	.5626	.1357	.5279

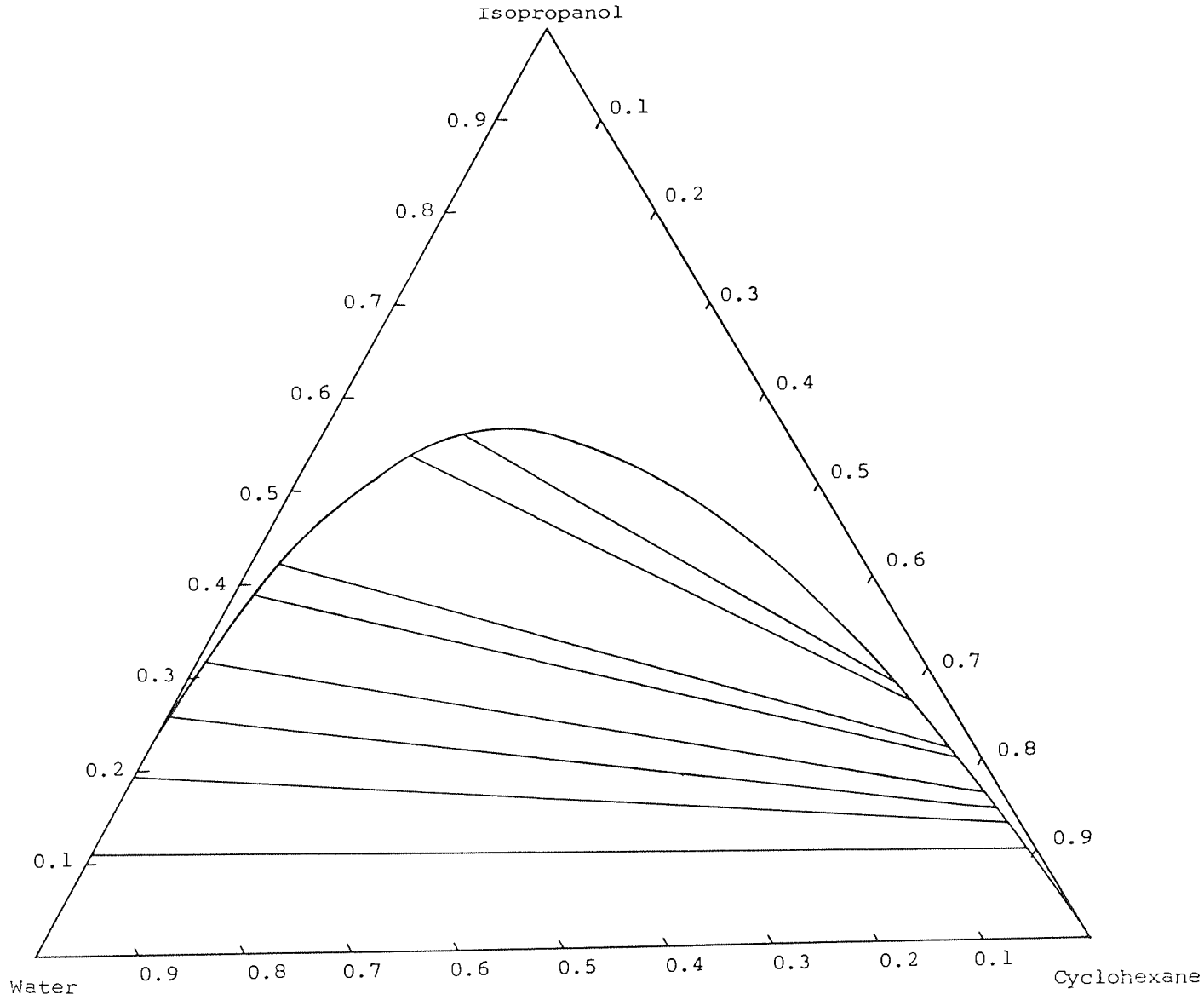

Figure II.13 : Experimental Equilibrium Diagram for System Isopropanol-Cyclohexane-5% Sulphuric Acid in Water at 20°C.

Table II.19 Solubility Data at 20°C

System: Water (B) - Methanol (C) - Xylene (A)

Aqueous Layer			
Methanol (C)	Water (B)	Xylene (A)	RI
.0044	.6361	.3595	1.34150
.0073	.5226	.4701	1.34285
.0082	.5045	.4873	1.34324
.0107	.4738	.5155	1.34328
.0182	.3992	.5826	1.34382
.3439	.6544	.0017	1.34111
.4364	.5622	.0015	1.34232
.4407	.5535	.0058	1.34266
.4982	.4932	.0086	1.34331
.5530	.4342	.0128	1.34332
.5651	.4175	.0174	1.34377
.6006	.3772	.0223	1.34404
.6222	.3552	.0226	1.34451
.6021	.3782	.0197	1.34404
.6205	.3444	.0251	1.34484
.6461	.3246	.0293	1.34484
.6540	.3127	.0333	1.34527
.6878	.2618	.0504	1.34600
.7298	.1797	.0905	1.35045

Hydrocarbon Layer			
Methanol (C)	Water (B)	Xylene (A)	RI
.0639	.0023	.9338	1.48564
.0699	.0027	.9274	1.48627
.0936	.0034	.9030	1.48109
.1105	.0039	.8856	1.47920
.1250	.0050	.8700	1.47645
.2313	.0122	.7565	1.41398
.2365	.0107	.7528	1.41088
.2653	.0114	.7233	1.44512
.3177	.0161	.6662	1.43458
.3802	.0151	.6547	1.43884
.3717	.0203	.6080	1.42726
.4606	.0307	.5023	1.40296
.4732	.0354	.4914	1.44481
.4820	.0358	.4822	1.40347
.5513	.0480	.4007	1.39313
.5631	.0531	.3838	1.38847
.6626	.0997	.2377	1.36821
.6710	.1000	.2290	1.36676
.6731	.0823	.2446	1.36888

Table II.20 Othmer-Tobias Correlation

System: Water-Methanol-Xylene at 20%

Aqueous Layer			
(C)	(A)	(B)	$\frac{1-X_{BB}}{X_{BB}}$
.727	.094	.179	4.5866
.722	.101	.177	4.6497
.714	.078	.208	3.8077
.667	.042	.291	2.4362
.605	.020	.375	1.6667
.600	.019	.381	1.6247
.595	.018	.577	0.7331
.593	.016	.391	1.5575
.534	.012	.454	1.2026
.533	.010	.457	1.1882
.470	.007	.523	0.9120
.468	.007	.525	0.9048
.397	.003	.600	0.6666
.223	.000	.777	0.2870

Hydrocarbon Layer			
(C)	(A)	(B)	$\frac{1-X_{AA}}{X_{AA}}$
.031	.969	.0	.0320
.024	.976	.0	.0246
.022	.978	.0	.0225
.023	.977	.0	.0235
.017	.983	.0	.0173
.022	.978	.0	.0225
.017	.983	.0	.0173
.018	.982	.0	.0183
.016	.984	.0	.0163
.016	.984	.0	.0163
.015	.985	.0	.0152
.014	.986	.0	.0142
.012	.988	.0	.0121
.011	.989	.0	.0111

Table II.21 Hand's Coordinate

System: Water-Xylene-Methanol at 20°C

(B) (A) (C)

AQUEOUS PHASE				HYDROCARBON PHASE			
x_{CB}	x_{AB}	x_{AB}	x_{CB}/x_{BB}	x_{CA}	x_{AA}	x_{BA}	x_{CA}/x_{AA}
.6772	.0264	.2964	2.2847	.0958	.9042	.0	.1060
.6766	.0286	.2949	2.2946	.0753	.9247	.0	.0814
.6448	.0213	.3339	1.9309	.0694	.9306	.0	.0746
.5632	.0107	.4368	1.2893	.0724	.9276	.0	.0780
.4735	.0047	.5218	0.9075	.0542	.9458	.0	.0573
.4676	.0045	.5279	0.8858	.0694	.9306	.0	.0746
.3659	.0033	.6308	0.5800	.0542	.9458	.0	.0573
.4586	.0037	.5376	0.8531	.0573	.9427	.0	.0608
.4224	.0026	.5750	0.6616	.0511	.9489	.0	.0539
.3638	.0014	.6347	0.6560	.0511	.9489	.0	.0539
.3353	.0015	.6632	0.5055	.0480	.9520	.0	.0505
.3335	.0015	.6650	0.5014	.0450	.9550	.0	.0471
.2711	.0006	.7283	0.3722	.0387	.9613	.0	.0402
.1390	.0000	.8610	0.1614	.0356	.9644	.0	.0369

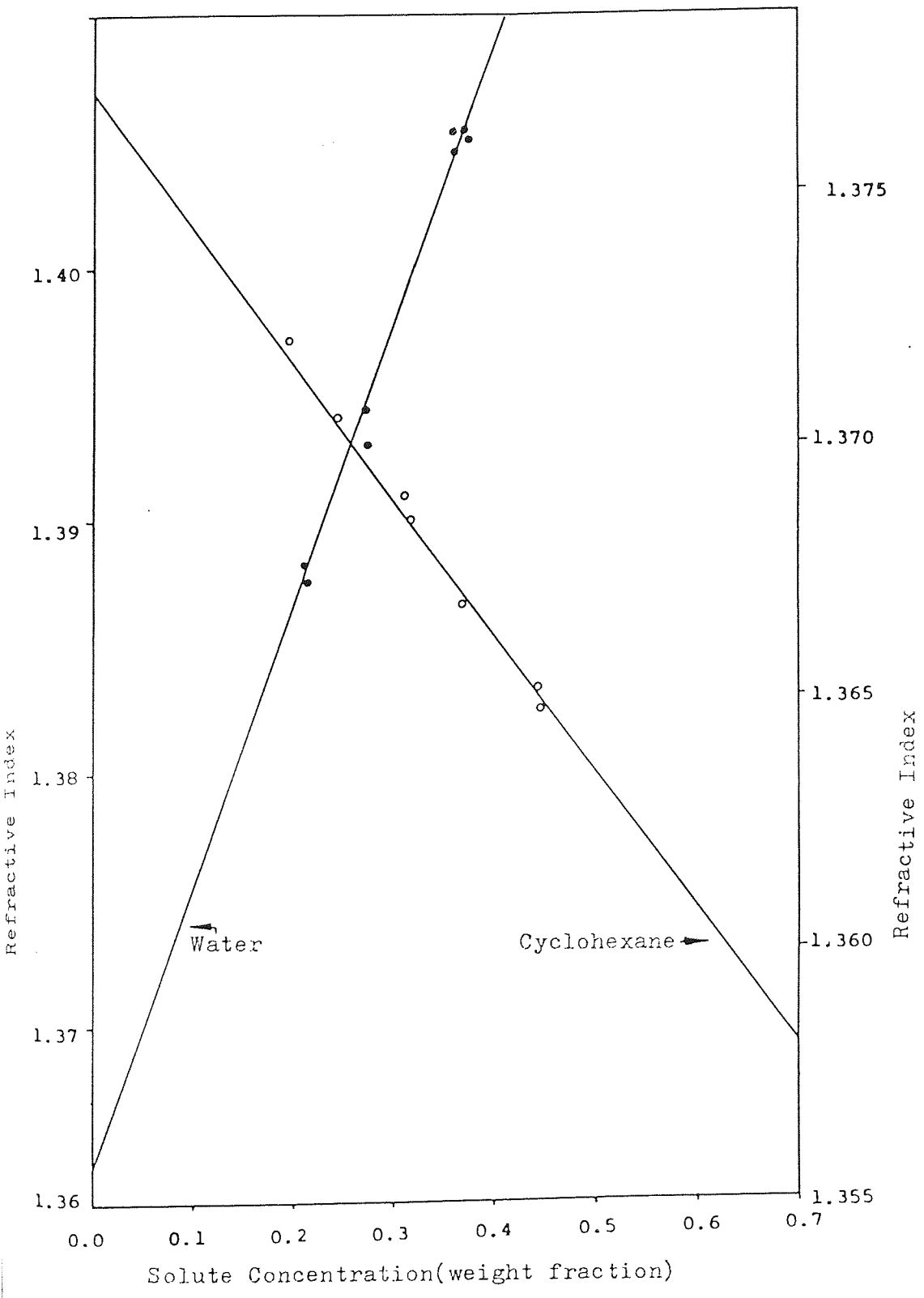

Figure II.14 : Solute Concentration vs Refractive Index for System : Isopropanol-Cyclohexane-5% Sulphuric Acid in Water at 20°C.

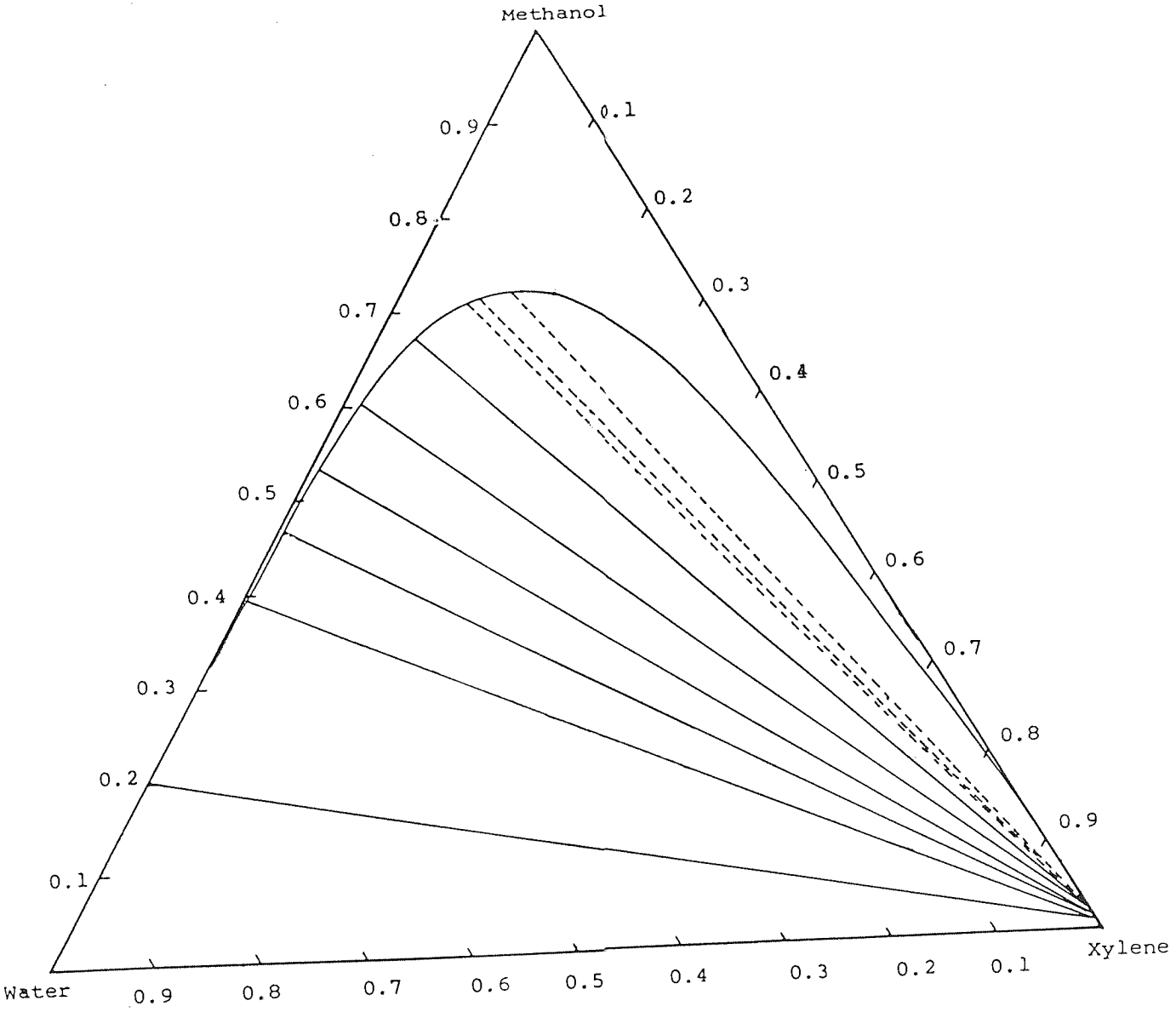

Figure II.15 : Experimental Equilibrium Diagram for System: Methanol-Xylene-Water at 20 °C.

Table: II.22 Solubility Data at 20°C

System: Methanol-Xylene-2% H_2SO_4 in Water.

Aqueous Layer			
Methanol (C)	Water (B)	Xylene (A)	RI
.4308	.5286	.0406	1.34393
.4582	.5363	.0055	1.34347
.5183	.4766	.0051	1.34405
.5503	.4389	.0109	1.34450
.5516	.4399	.0085	1.34371
.6118	.3669	.0213	1.34438
.6480	.3260	.0260	1.34492
.6639	.2921	.0439	1.34635
.7011	.2379	.0610	1.34789
.7024	.2241	.0735	1.34901

Hydrocarbon Layer			
Methanol (C)	Water (B)	Xylene (A)	RI
.0828	.0021	.9151	1.47964
.1610	.0550	.7839	1.48004
.1843	.0073	.8084	1.46632
.2648	.0107	.7244	1.41510
.2916	.0142	.6942	1.44175
.3830	.0205	.5966	1.42159
.4625	.0331	.5044	1.40792
.5108	.0437	.4456	1.39343
.6451	.0791	.2759	1.37336
.6767	.0828	.2405	1.36830
.6900	.0872	.2228	1.36507
.6997	.1114	.1889	1.36416
.7091	.1372	.1536	1.35872
.7156	.1383	.1461	1.35754
.7362	.1094	.1544	1.35853

Table: II.23 Othmer-Tobias Correlation for the Tie-lines

System: 2% H_2SO_4 in Water-Xylene-Methanol

Aqueous Layer			
(C)	(A)	(B)	$\frac{1-X_{BB}}{X_{BB}}$
.699	.070	.230	3.3478
.662	.037	.301	2.3223
.655	.033	.312	2.2051
.635	.025	.340	1.9412
.615	.018	.367	1.7248
.588	.011	.401	1.4938
.540	.000	.460	1.1739
.540	.000	.460	1.1739
.522	.000	.478	1.0921

Hydrocarbon Layer			
(C)	(A)	(B)	$\frac{1-X_{AA}}{X_{AA}}$
.014	.986	.0	.0142
.004	.996	.0	.0040
.013	.987	.0	.0132
.002	.998	.0	.0020
.014	.986	.0	.0142
.002	.998	.0	.0020
.002	.998	.0	.0020
.016	.984	.0	.0163
.004	.996	.0	.0040

System: Methanol-Xylene-2% H_2SO_4 in Water at 20°C.

AQUEOUS PHASE			
x_{CB}	x_{AB}	x_{BB}	x_{CB}/x_{BB}
.6378	.0196	.3426	1.8614
.5684	.0096	.4220	1.3471
.5578	.0085	.4338	1.2859
.5302	.0063	.4635	1.1439
.5043	.0045	.4913	1.0264
.4719	.0027	.5254	0.8981
.4183	.0000	.5817	0.7190
.4183	.0000	.5817	0.7190
.4008	.0000	.5992	0.6689

HYDROCARBON PHASE			
x_{CA}	x_{AA}	x_{BA}	x_{CB}/x_{AA}
.0450	.9550	.0	.0471
.0136	.9864	.0	.0138
.0418	.9582	.0	.0436
.0066	.9934	.0	.0067
.0450	.9550	.0	.0471
.0066	.9934	.0	.0067
.0511	.9489	.0	.0539
.0063	.9415	.0	.0067
.0131	.9869	.0	.0133

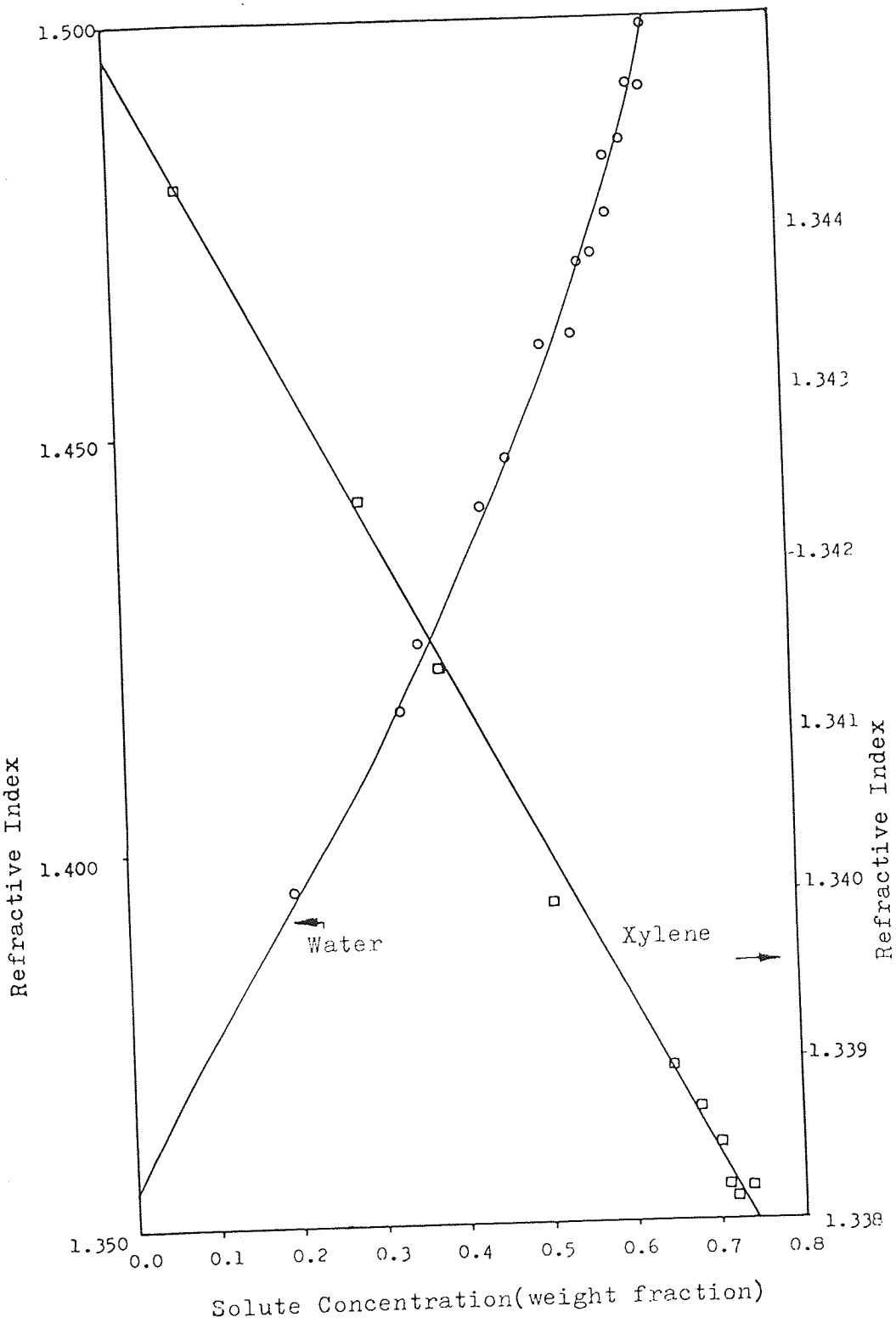

Figure II.16 :Solute Concentration vs Refractive Index for System : Methanol-Xylene-Water at 20°C.

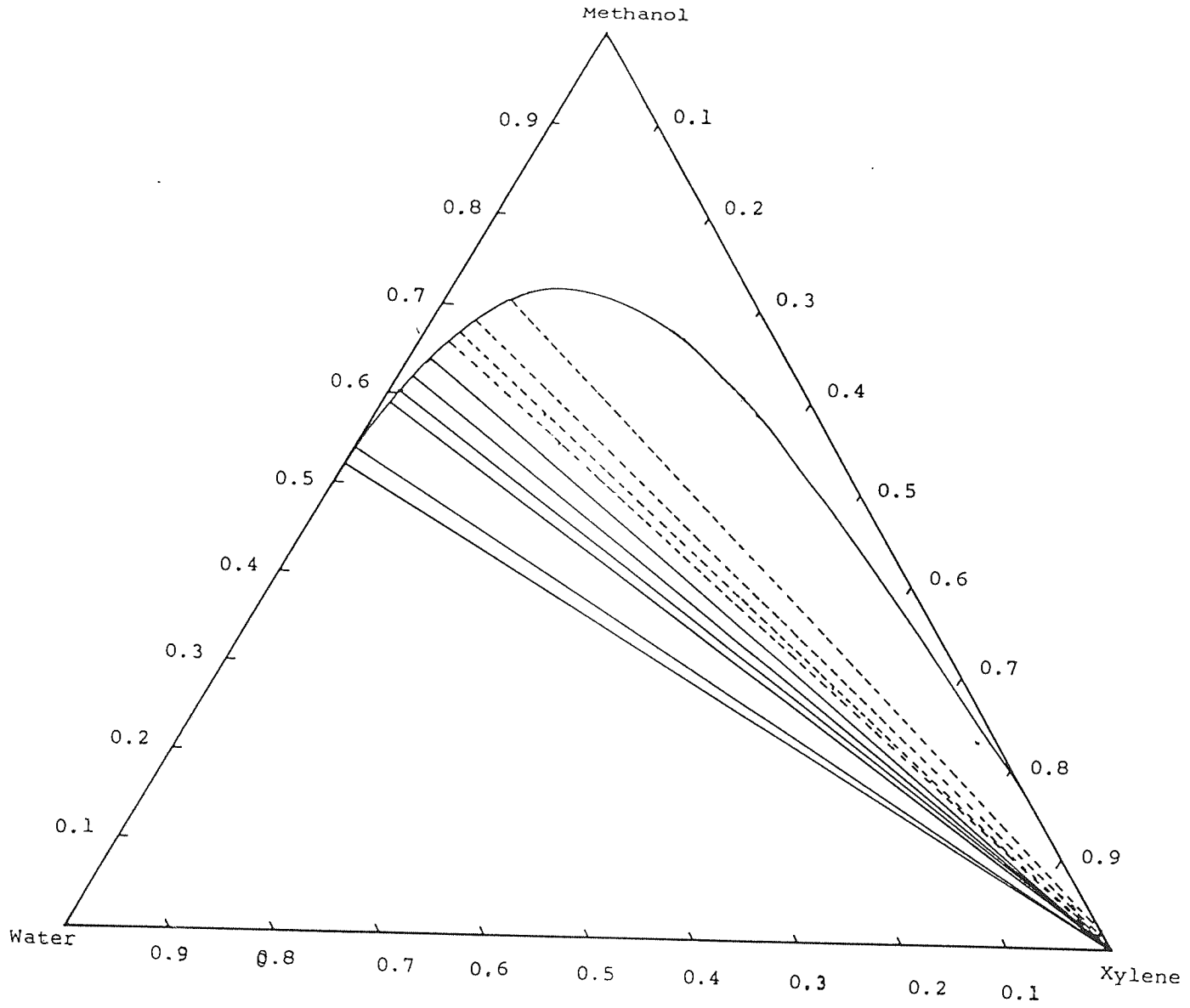

Figure II.17 : Experimental Equilibrium Diagram for System : Methanol-Xylene-2% Sulphuric Acid in Water at 20°C.

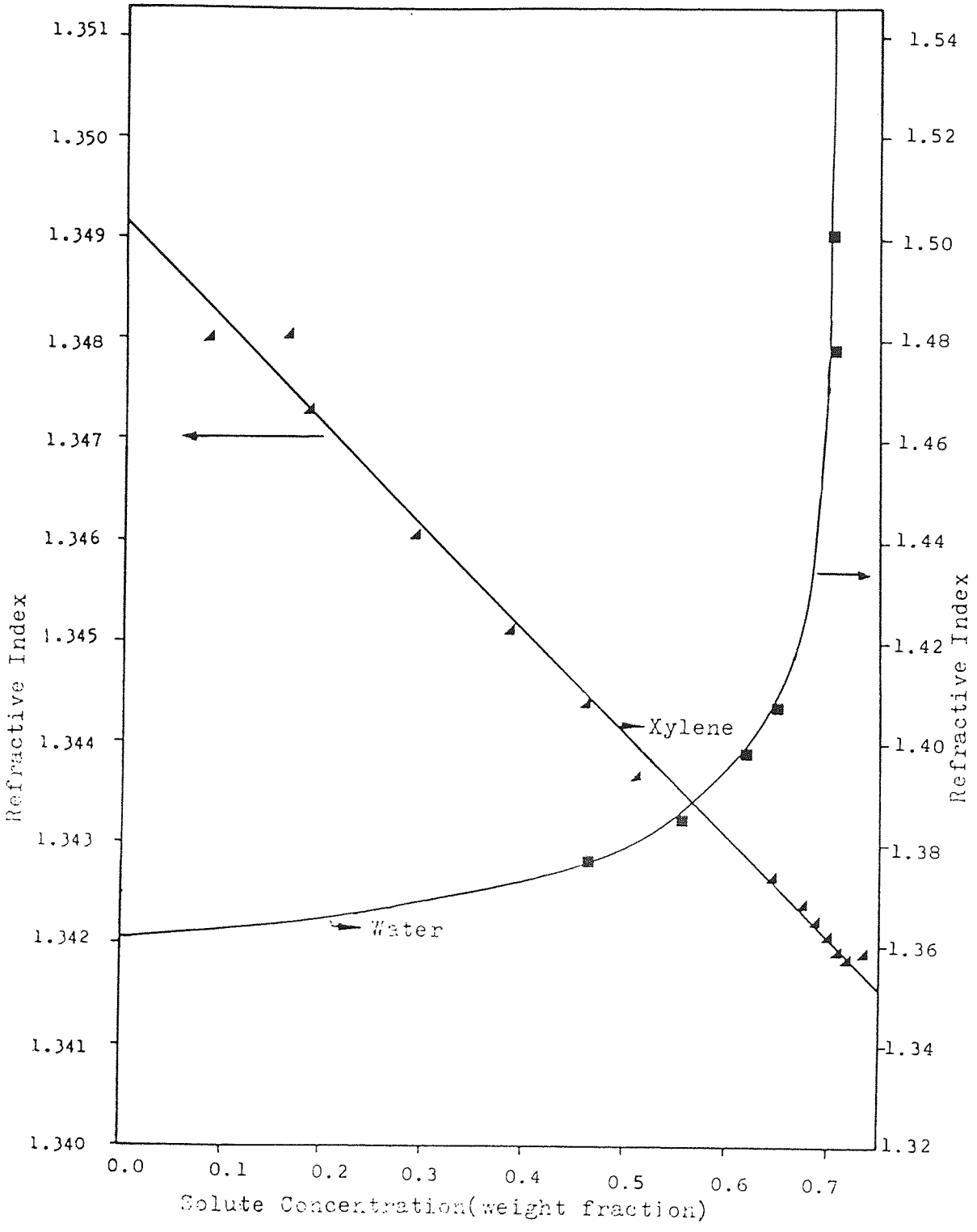

Figure II.18 : Solute Concentration vs Refractive Index for System : Methanol-Xylene-2% Sulphuric Acid in Water at 20°C.

APPENDIX III

Chemical Confirmatory Tests.

APPENDIX III

CHEMICAL CONFIRMATORY TESTS.

1) a) Test for Aldehydes and Ketones.

In a test tube 0.2g 2, 4 DNPH was added to 3 ml methanol followed cautiously by 0.5 ml concentrated sulphuric acid. The test tube was shaken and warmed until the reagents dissolved, after which the sample (0.2 g) was added and the test tube warmed gently. If there was no precipitate, the tube was cooled under tap water. If no precipitate was formed, 3 or 4 drops of water was added to the test tube and then the tube was left standing in cold water for approximately 5 minutes. A yellow, orange or red precipitate formed would indicate either aldehyde or ketone.

b) Differentiation of Aldehydes or Ketones.

Schiff's Test : The sample was dissolved in ethanol. Then, the mixture was shaken with 1 ml Schiff's reagent. Aliphatic aldehyde would restore the magenta colour within a few minutes.

Tollen's Test : One drop of sodium hydroxide was added to 1 ml aqueous silver nitrate and then enough dilute ammonia solution was added to dissolve the precipitate of silver oxide thus formed. The sample was added, and the tube left standing with occasional shaking in a beaker of boiling water. The formation of silver mirror on the tube walls would indicate the presence of an aldehyde.

Fehling's Solution : The unknown was added to a mixed Fehling's solution, and boiled gently. The presence of aldehydes and other easily oxidized groups would reduce the blue copper (II) solution to green copper (I) solutions to a precipitate of red copper (I) oxide.

2) Test for Alcohols (especially Propan-2-ol)

A positive Iodoform reaction would indicate the group CH_3 - CHOH (which is easily oxidized to CH_3CO).

The unknown (0.2 g) was dissolved in about 3 ml potassium iodide solution in a test tube. 0.5 ml dilute sodium hydroxide was then added, after which 2 ml of strong sodium hypochlorite solution was added. The mixture was shaken and if necessary warmed for a few minutes. Iodoform (CHI_3) would precipitate as yellow crystals or a yellow turbidity if CH_3CO was present.

3) Test for Alkene and Alkyne Groups.

a) Test for Unsaturation or Easy Substitution. The unknown was dissolved in 1 ml water or chloroform, or carbon tetrachloride. A solution of bronine in the same solvent was slowly added from a dropper. A blank test was run simultaneously with solvent alone.

Decolourization of the bromine (compared with the blank) woul indicate addition of bromine to a double or triple bond, or substitution in an activated aromatic nucleus.

b) Test for Unsaturation or Easy Oxidation. The unknown was dissolved in water, ethanol or acetone. 1-2 drops of dilute potassium permanganate was added from a dropper. A simultaneous blank test was run with solvent alone.

If the colour of MnO_4^- was discharged, unsaturated compounds and other easily oxidized groups were indicated.

4) Acids Detection (especially for hydrocarbon phase)

Addition of a bicarbonate would evolve carbon dioxide in the presence of any acid.

APPENDIX IV

i) Sample Calculation for Approach to Equilibrium.

ii) Sample Calculation for Rotor Speed Requirement.

APPENDIX IV

1. SAMPLE CALCULATION FOR APPROACH TO EQUILIBRIUM.

The time required for approach to equilibrium has been estimated by Newman (128)

$$E = \frac{Q_t}{Q_o} = 1 - \frac{6}{\pi^2} \sum_{n=1} \frac{e^{\frac{-D\pi^2 n^2 t}{r^2}}}{n^2} \qquad \text{(IV.1)}$$

Vermuellen (176) showed that this result could be accurately represented by the empirical equation:-

$$E = 1 - e^{\left(\frac{-D\pi^2 t}{r^2}\right)^{\frac{1}{2}}} \qquad \text{(IV.2)}$$

Kronig and Brink (129) included the effects of internal circulation on diffusion and for Re > 1 and at zero interfacial tension, derived:-

$$E = 1 - \frac{3}{8} \sum_{n=1} A_n 2\, e^{\frac{-\mu_n\, 16\, D\, t}{r^2}} \qquad \text{(IV.3)}$$

where A_n and U_n are eigen values. Dankwerts (237), however, has pointed out that Equation (IV.3) may not be as strictly limited as the above restrictions suggest. Under conditions of constant continuous phase temperature and negligible continuous phase resistance was found to be well represented by the empirical equation (238)

$$E = 1 - e^{\left(-2.25\, \frac{D\pi^2 t}{r^2}\right)^{\frac{1}{2}}} \qquad \text{(IV.4)}$$

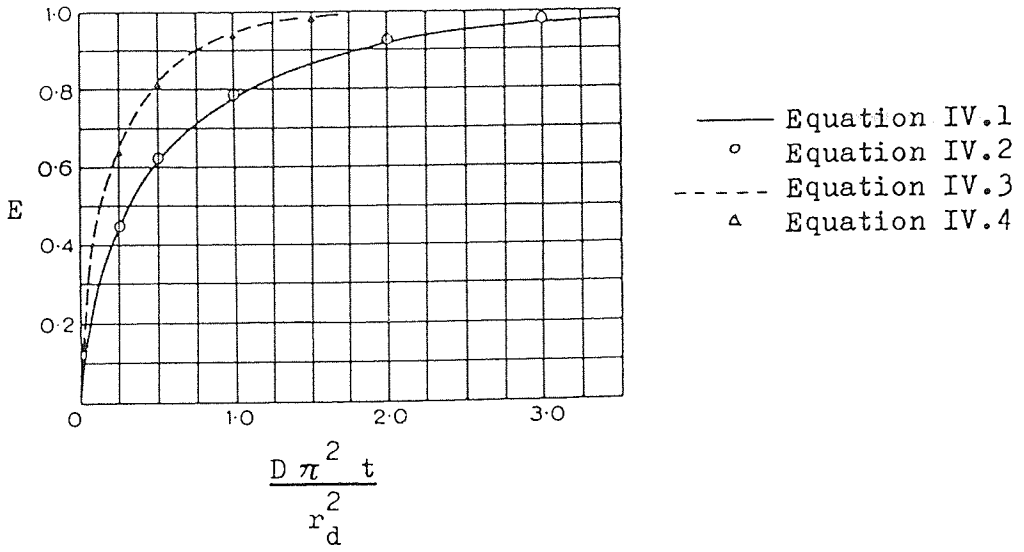

Figure IV.1 Equations for Diffusion into Stagnant and Circulating Drops.

From the plot of E vs $(\frac{D\pi^2 t}{r_d^2})$ as in Figure IV.1, E approaches unity when $(\frac{D\pi^2 t}{r_d^2})$ is above 3.0. If a value of 5.0 is taken, E = 0.9999 according to Equation (IV.2) and E = 0.9959 according to Equation (IV.4), which should be taken as sufficient approach to equilibrium.

From Appendix I for physical properties for the systems,

Diffusivity ranges : (1.0 to 6.0) X 10^{-5} cm/S

Drop Diameter ranges : up to 0.4 cm.

Taking the extreme cases for maximum time i.e. minimum in the viscosity range and maximum for the drop diameter:-

$$t_{max} = \frac{5.0 \times r_d^2}{D \times \pi^2}$$

$$= \frac{5.0 \times (.2)^2}{1.01 \times 10^{-5} \times \pi^2}$$

$$= 2006.4 \text{ S}$$

$$= 33.4 \text{ min.}$$

Therefore, between one to two hours should be considered as sufficient for the attainment of set temperature as well as adequate approach to equilibrium for the three systems studied.

2. SAMPLE CALCULATION FOR ROTOR SPEED REQUIREMENT.

Rotor tip speed = $\pi \times D_r \times N$

Kung and Beckman (181) stated that the rotor tip speed should exceed 91.5 metres/minute for toluene-water system to prevent the accumulation of drops beneath the disc.

Taylor vortices will be formed if the Taylor number exceeds 42.0, that is if :-

$$T = \left(\frac{VD_c \rho_c}{\mu_c}\right) \left(\frac{D_c - D_r}{0.5D_r}\right)^{0.5} \qquad \text{(IV.5)}$$

where V is the linear velocity of the continuous phase.

$$V = \frac{Q}{\pi/4 \times (D_c)^2 \times 3600}$$

where Q is the feed volumetric flow rate, m^3/h.

i) Rotor tip speed = $\pi \times D_r \times N$

When the rotor speed is 500 r.p.m. :-

Rotor tip speed = $\pi \times 0.029 \times 500$

= 45.55 metres/minute.

ii) For the lowest volumetric flow rate of 3.0 m^3/s.

$$V = \frac{3.0}{\pi/4 \times (D_c)^2}$$

$$= 15.28 \quad m/s$$

$$T = \frac{VD_c \rho_c}{\mu_c} \quad \frac{D_c - D_r}{0.5D_r}^{0.5}$$

$$= \frac{15.28 \times 0.5 \times 0.98}{1.08} \quad \frac{0.5 - 0.029}{0.5\ (0.029)}^{0.5}$$

$$= 42.7$$

Therefore, the chosen rotor speeds of 500 and 700 r.p.m. and the volumetric flow rates between **3.o** to 6.0 m^3/s were sufficient to overcome agglomeration of drops beneath the discs and to create Taylor vortices for effective function of the R.D.C.

APPENDIX V

Sample Calculation for Thermodynamic Consistency Tests.

APPENDIX V.

SAMPLE CALCULATION FOR THERMODYNAMIC CONSISTENCY TEST.

The consistency of the experimental results were assessed by determining the activity of the solute in each phase by means of the double suffix Van Laar equation (24). For this purpose the "end value constants" of the binary acetone-toluene were evaluated from vapour-liquid equilibrium data of this system published by ORYE et al (239) which yields at 45°C.

$$A_{CA} = 0.2867 \qquad A_{AC} = 0.2068$$

These were correlated for temperature to 20°C to give the end values reported in Table V.1. For this purpose the equation:-

$$T \ln \gamma = T.A = \text{constant}$$

was employed because the temperature range is very small.

The end value constants for the binary acetone-water were evaluated from BEARE et al (240) and HALA (241) at 25°C and they compare favourably and are listed in Table V.1. Finally as toluene and water are almost immiscible in one another, their effect on the activity in each phase was taken to be zero in accordance with the recommendation of Treybal (24). The double suffix Van Laar:

$$\log \gamma_C = \frac{x_A^2 A_{CA}\left(\frac{A_{AC}}{A_{CA}}\right)^2 + x_B^2 A_{CB}\left(\frac{A_{BC}}{A_{CB}}\right)^2 + x_A x_C\left(\frac{A_{AC}}{A_{CA}}\right)\left(\frac{A_{BC}}{A_{CB}}\right) A_{CA}+A_{CB}-A_{BA}\left(\frac{A_{CB}}{A_{BC}}\right)}{x_C + x_A\left(\frac{A_{AC}}{A_{CA}}\right) + x_B\left(\frac{A_{BC}}{A_{CB}}\right)^2}$$

becomes :-

$$\log \gamma_C = \frac{0.4536\, x_A^2 + 0.1618\, x_B^2 + 0.6078\, x_A\, x_C}{x_C + 0.7407\, x_A + 0.7211\, x_B^2}$$

This equation was used to calculate the activity coefficients and thus the activities of acetone in each phase, and the results are summarised in Table V.3.

The distribution curve was predicted from the results in Table V.4, and this is plotted in Figure V.3. It can be seen that the agreement between the experimental distribution and the predicted distribution is good.

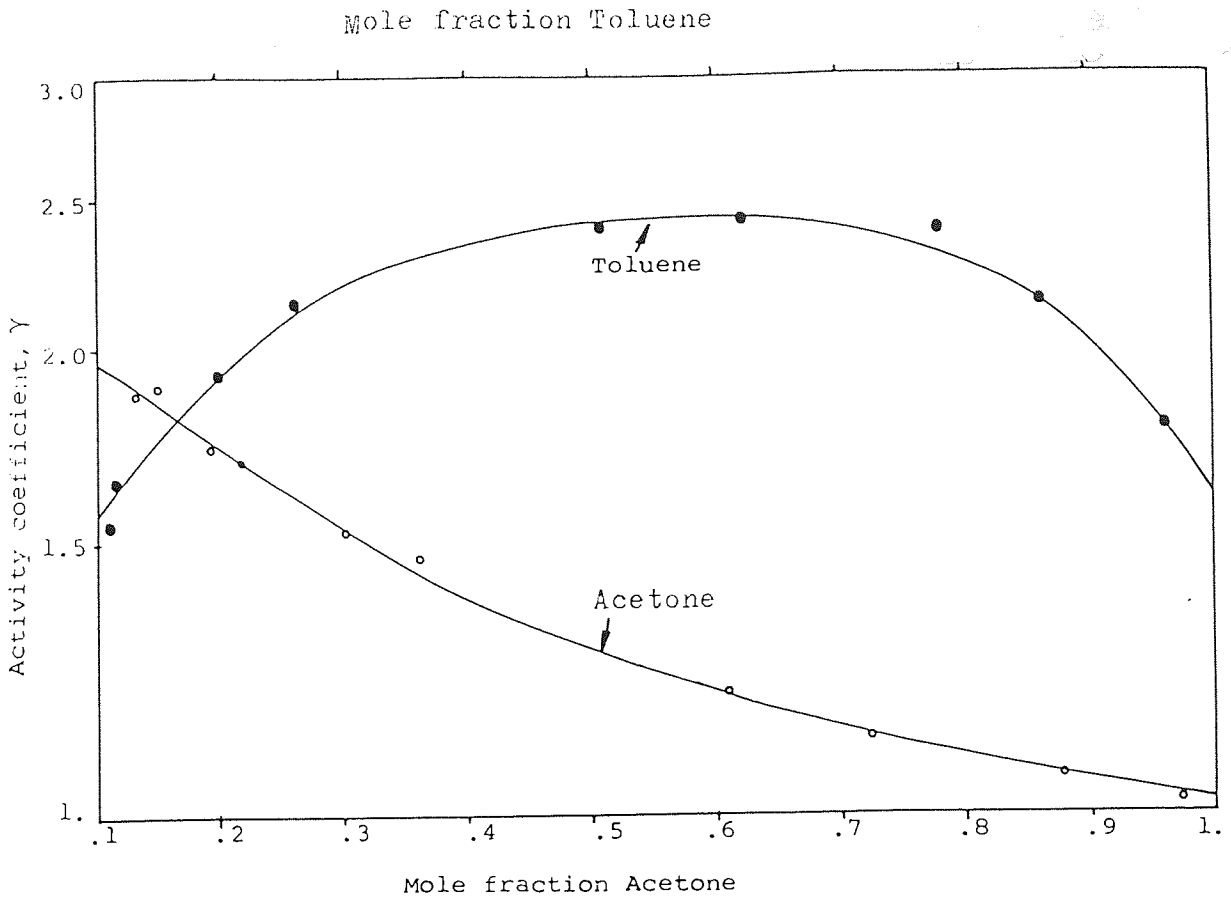

Figure V.1 : Activity Coefficient vs Solute Concentration.

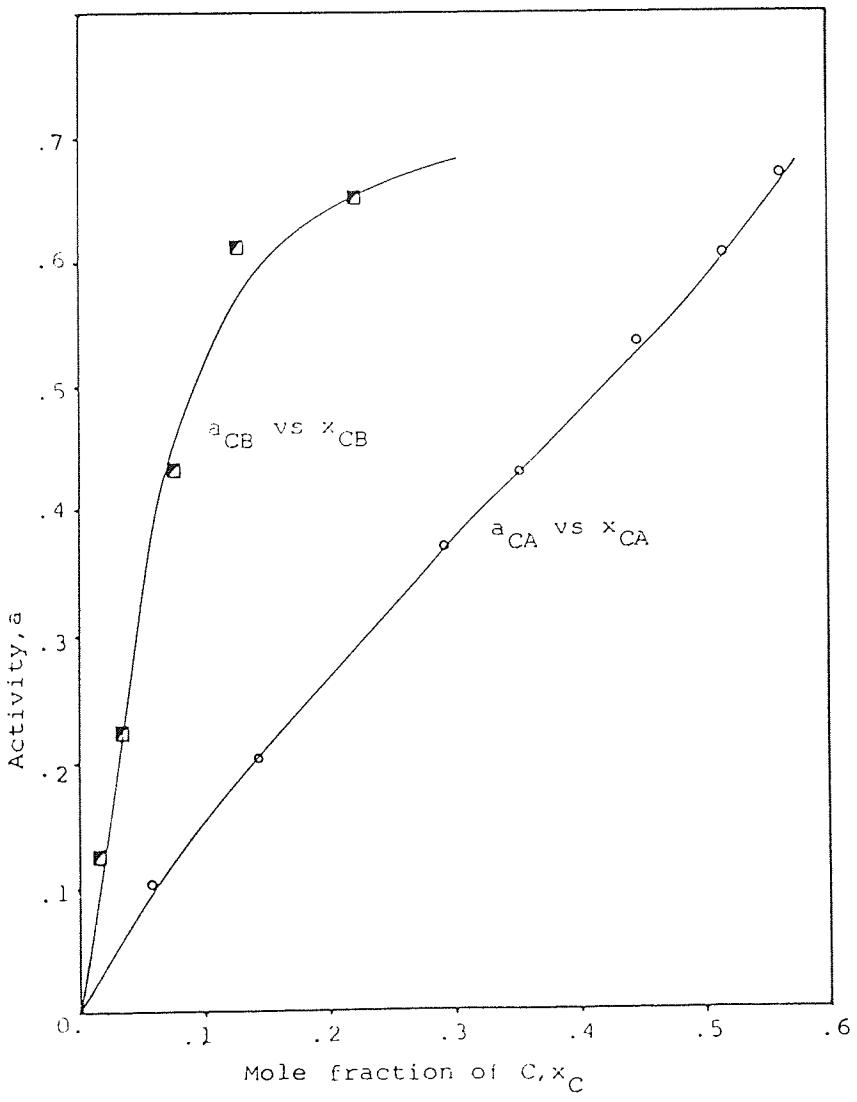

Figure V.2 : Activity vs Solute Concentration.

Table V.1 Values of

System : Acetone (C) - Water (B) - Toluene (A) at $20^{o}C$

$$\log \gamma_C = \frac{0.4536\ x_B^{\,2} + 0.1618\ x_A^{\,2} + 0.6078\ x_A\ x_C}{x_C + 0.7407\ x_B + 0.7211\ x_A^{\,2}}$$

Binary System	End Value Constant	Binary System	End Value Constant
Acetone in Water	$A_{CB} = 0.8268$	Water in Acetone	$A_{BC} = 0.6124$
Acetone in Toluene	$A_{CA} = 0.3112$	Toluene in Acetone	$A_{AC} = 0.2244$
Toluene in Water	$A_{AB} = 0.0$	Water in Toluene	$A_{BA} = 0.0$

Table V.2

System : Isopropanol (C) - Water (B) - Cyclohexane (A)

at $20^{o}C$

$$\log \gamma_C = \frac{0.2652\ x_B^{\,2} + 0.3459\ x_A^{\,2} + 0.6081\ x_A\ x_C}{x_C + 0.442\ x_B + 0.5512\ x_A^{\,2}}$$

Binary System	End Value Constant	Binary System	End Value Constant
Isopropanol in Water	$A_{CB} = 1.3575$	Water in Isopropanol	$A_{BC} = 0.6$
Isopropanol in Cyclohexane	$A_{CA} = 1.1384$	Cyclohexane in Isopropanol	$A_{AC} = 0.6275$
Cyclohexane in Water	$A_{AB} = 0.0$	Water in Cyclohexane	$A_{BA} = 0.0$

Table V.3 CALCULATION OF ACTIVITY COEFFICIENTS.

TOLUENE (A) ACETONE (C)

$$\gamma_C \text{ (at } x_C \to 0) = \frac{P_t - P_A}{x_C P_C}$$

$$= \frac{P_t - 74.2\, x_A}{511.8\, x_C}$$

$$\gamma_C \text{ (at } x_C \to 0) = \frac{P_t - P_C}{x_A P_A}$$

$$= \frac{P_t - 511.8\, x_C}{74.2\, x_A}$$

x_C	x_A	$-\gamma_{CA}$	$-\gamma_A$
.125	.9875	1.5361	1.04681
.034	.966	1.8690	1.2110
.0495	.9505	1.8818	1.3167
.0935	.9065	1.7311	1.5201
.1185	.8815	1.6933	1.6428
.2015	.7985	1.5306	1.9236
.2615	.7385	1.4690	2.1455
.508	.492	1.1969	2.4025
.6245	.3755	1.1243	2.4256
.777	.223	1.0588	2.4133
.872	.128	1.0245	2.1490
.961	.039	1.0046	1.7832

Table V.4 : CALCULATION FOR ACTIVITY VALUES.

x_{CA}	γ_{CA}	a_{CA}	x_{CB}	γ_{CB}	a_{CB}
0.0194	7.4903	0.1453	0.057	3.7688	0.2148
0.0369	7.3604	0.2715	0.1427	2.9648	0.4231
0.0792	7.0275	0.5566	0.2940	2.0663	0.6075
0.0937	6.8992	0.6465	0.3540	1.8134	0.6420
0.1299	6.5826	0.8551	0.4483	1.5424	0.6915
0.1586	6.2806	0.9961	0.5163	1.4302	0.7384
0.1682	6.1787	1.0393	0.5631	1.4077	0.7927

Table V.5 : PREDICTED EQUILIBRIUM DATA

x_{CA}	.013	.048	.053	.069	.077	.085	.098	.116	.127
x_{CB}	.025	.108	.125	.194	.235	.287	.462	.517	.59

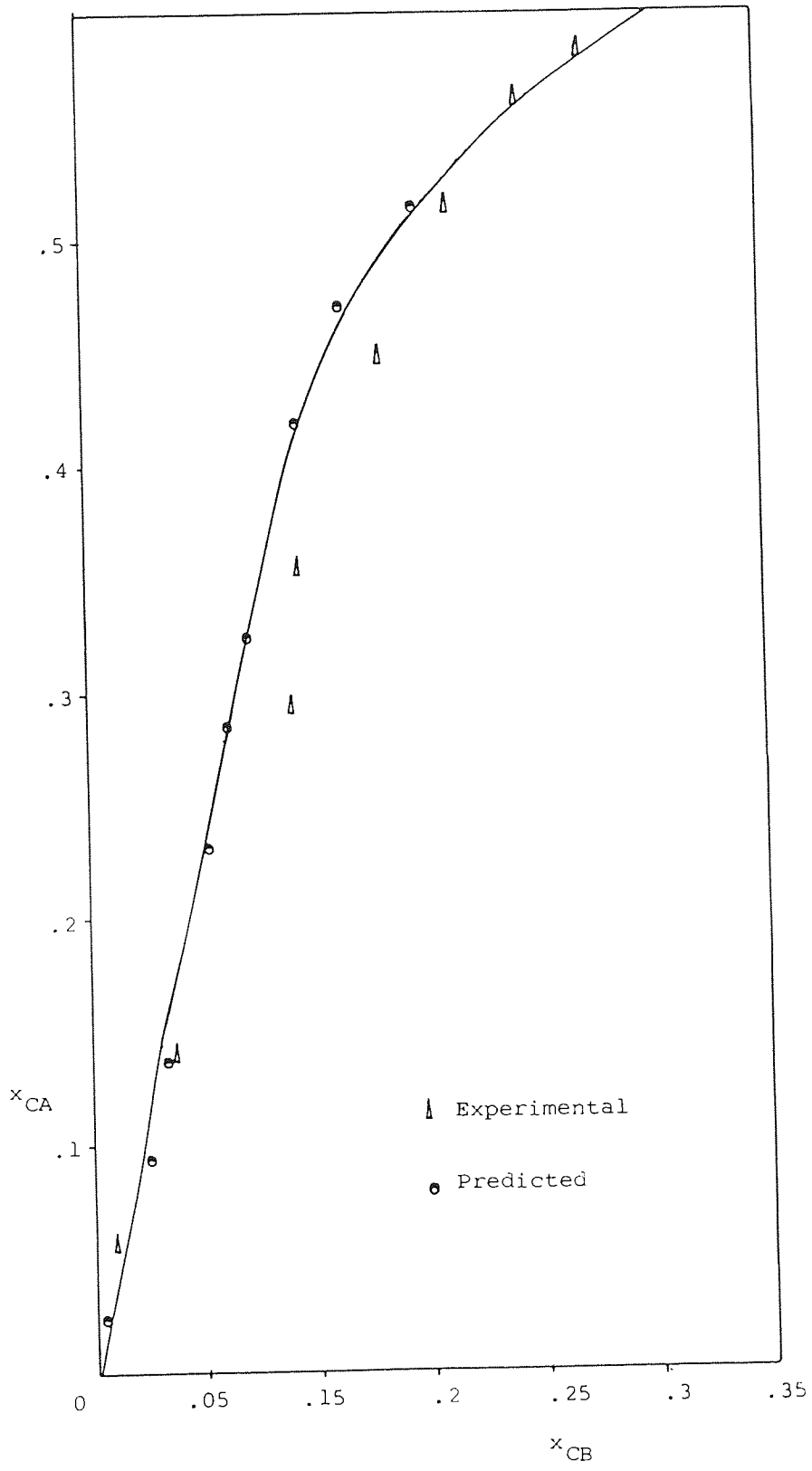

Figure V.3 : Comparison of Experimental and Predicted Equilibrium Data for System: Acetone-Toluene-Water at 20°C.

APPENDIX VI

Sample Calculation of Drop Size and Drop Size Distribution.

APPENDIX VI.1

Sample Calculation of d_{32}

Rotor Speed: 700 r.p.m.

Magnification: 1.86

Phase ratio (C/D): 2/1

Drop size count:

$$d_{act} = \frac{d_{obs}}{\text{Magnification}}$$

Cumulative drops volume:

$$v_i = \Sigma n_i \frac{\pi}{6} d_i^3$$

% Cumulative drops volume:

$$\% \; v_i = \frac{v_i}{v_{total}} \times 100$$

$$\frac{dv}{dd} = \frac{v_{f,i} - v_{f,i-1}}{d_i - d_{i-1}}$$

where v_f is the fractional cumulative drop volume

$$v_{f,i} = \frac{v_i}{v_{total}}$$

From Figure IV.2

$d_{10} = 1.58$, $d_{50} = 2.99$, $d_{90} = 4.35$

$$\frac{d_m}{d_{50}} = \frac{d_{50}(d_{90}+d_{10}) - 2d_{90}d_{10}}{d_{50}^2 - d_{90}d_{10}}$$

$$\frac{d_m}{2.99} = \frac{2.99(1.58+4.35) - 2(1.58)(4.35)}{(2.99)^2 - (1.58)(4.35)}$$

$$d_m = 5.7638$$

$$\bar{a} = \frac{d_m - d_{50}}{d_{50}}$$

$$= \frac{5.7638 - 2.99}{2.99} = 0.9277$$

From Figure IV.3, $u_{90} = 3.16$, $u_{50} = 1.175$

$$\delta = \frac{0.394}{\log(U_{90}/U_{50})} = 0.917$$

$$d_{32} = d_m/(1+\bar{a}e^{\frac{1}{4\delta^2}}) = 2.708 \text{ mm}$$

$$\text{calculated } d_{32} = \frac{\Sigma n_i d_i^3}{\Sigma n_i d_i^2} = 2.688 \text{ mm}$$

correlated d_{32} (Equation 8.7) = 2.563 mm

Table VI.1 Drop Size Distribution Results

	d_{obs} (mm)	d_{act} (mm)	n	v (mm^3)	%v	u	$\frac{dv}{dd}$ (mm^{-1})
1	1.05	0.565	12	1.136	0.07	0.1087	
2	1.23	0.662	9	1.369	0.15	0.1298	0.0082
3	1.42	0.765	17	3.979	0.38	0.1529	0.0044
4	1.60	0.862	29	9.711	0.95	0.1758	0.0588
5	1.78	0.958	26	11.987	1.65	0.1995	0.0722
6	1.97	1.061	21	13.125	2.42	0.2256	0.0753
7	2.15	1.158	20	16.249	3.37	0.2513	0.0551
8	2.34	1.260	26	27.234	4.96	0.2798	0.1417
9	2.52	1.357	22	28.782	6.64	0.3079	0.1732
10	2.70	1.454	24	38.618	8.90	0.3374	0.2330
11	2.89	1.556	18	35.519	10.98	0.3698	0.2039
12	3.07	1.653	7	16.558	11.95	0.4021	0.1000
13	3.26	1.755	10	28.323	13.61	0.4378	0.1627
14	3.44	1.852	6	19.967	14.78	0.4734	0.1643
15	3.62	1.949	2	7.756	15.23	0.5109	0.1082
16	3.81	2.052	7	31.649	17.08	0.5528	0.1796
17	3.99	2.149	6	31.158	18.90	0.5945	0.1835
18	4.18	2.251	6	35.824	20.99	0.6408	0.2049
19	4.36	2.348	7	47.430	23.76	0.6874	0.2716
20	4.54	2.445	6	45.900	26.44	0.7367	0.2763
21	4.73	2.547	6	51.907	29.44	0.7918	0.2941
22	4.91	2.644	3	29.031	31.14	0.8475	0.1753
23	5.10	2.746	2	21.689	32.41	0.9099	0.1245
24	5.28	2.843	6	72.201	36.63	0.9734	0.4351
25	5.46	2.940	5	66.534	40.52	1.0412	0.4010
26	5.65	3.042	3	44.234	43.10	1.1176	0.2529
27	5.83	3.139	2	32.399	44.99	1.1959	0.1948
28	6.02	3.242	1	17.835	46.03	1.2856	0.1010
29	6.20	3.339	3	58.451	49.45	1.3770	0.3523

(Cont..)

Table VI.1 (Cont..)

	d_{obs} (mm)	d_{act} (mm)	n	v (mm^3)	%v	u	$\frac{dv}{dd}$ (mm^{-1})
30	6.38	3.435	6	127.381	56.89	1.475	0.7750
31	6.57	3.538	5	115.920	63.66	1.590	0.6573
32	6.75	3.635	4	100.569	69.54	1.708	0.6062
33	6.94	3.737	1	27.326	71.14	1.844	0.1569
34	7.12	3.834	3	88.523	76.31	1.987	0.5330
35	7.30	3.931	1	31.803	78.17	2.145	0.1917
36	7.49	4.033	1	34.351	80.18	2.330	0.1971
37	7.67	4.130	1	36.887	82.34	2.528	0.2227
38	8.22	4.426	1	45.405	84.99	3.308	0.0895
39	8.41	4.529	3	145.882	93.51	3.668	0.0325
40	8.78	4.728	2	110.664	99.98	4.565	0.0002
Σ	-	-	351	1711.266	-	-	-

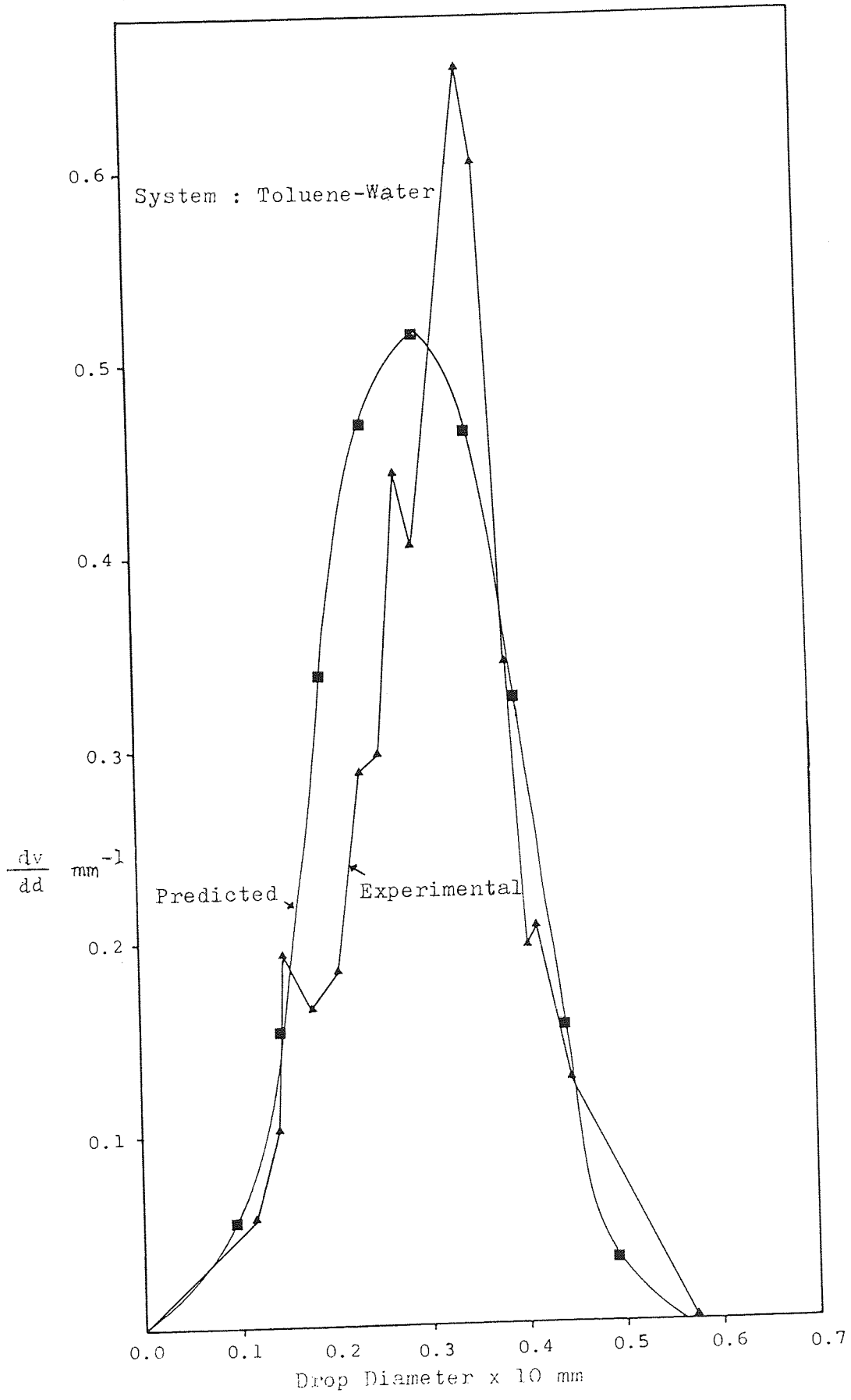

Figure VI. 1 : Comparison of Experimental and Predicted Upper-Limit Drop Size Distribution for Rotor Speed 700 r.p.m.

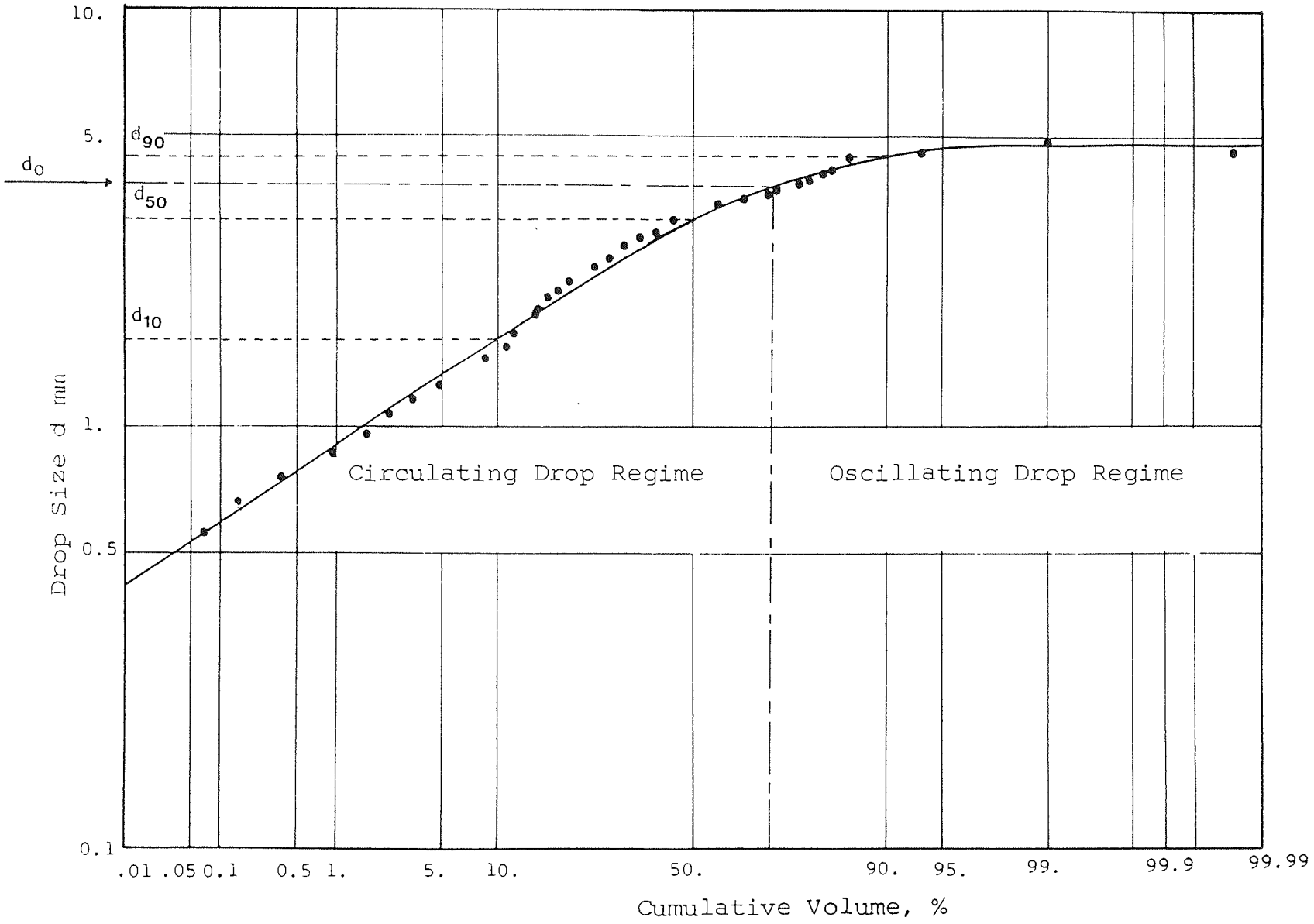

Figure IV.2 : Cumulative Drop Size Distribution for Rotor Speed 700 r.p.m. and Phase Ratio 2/1.

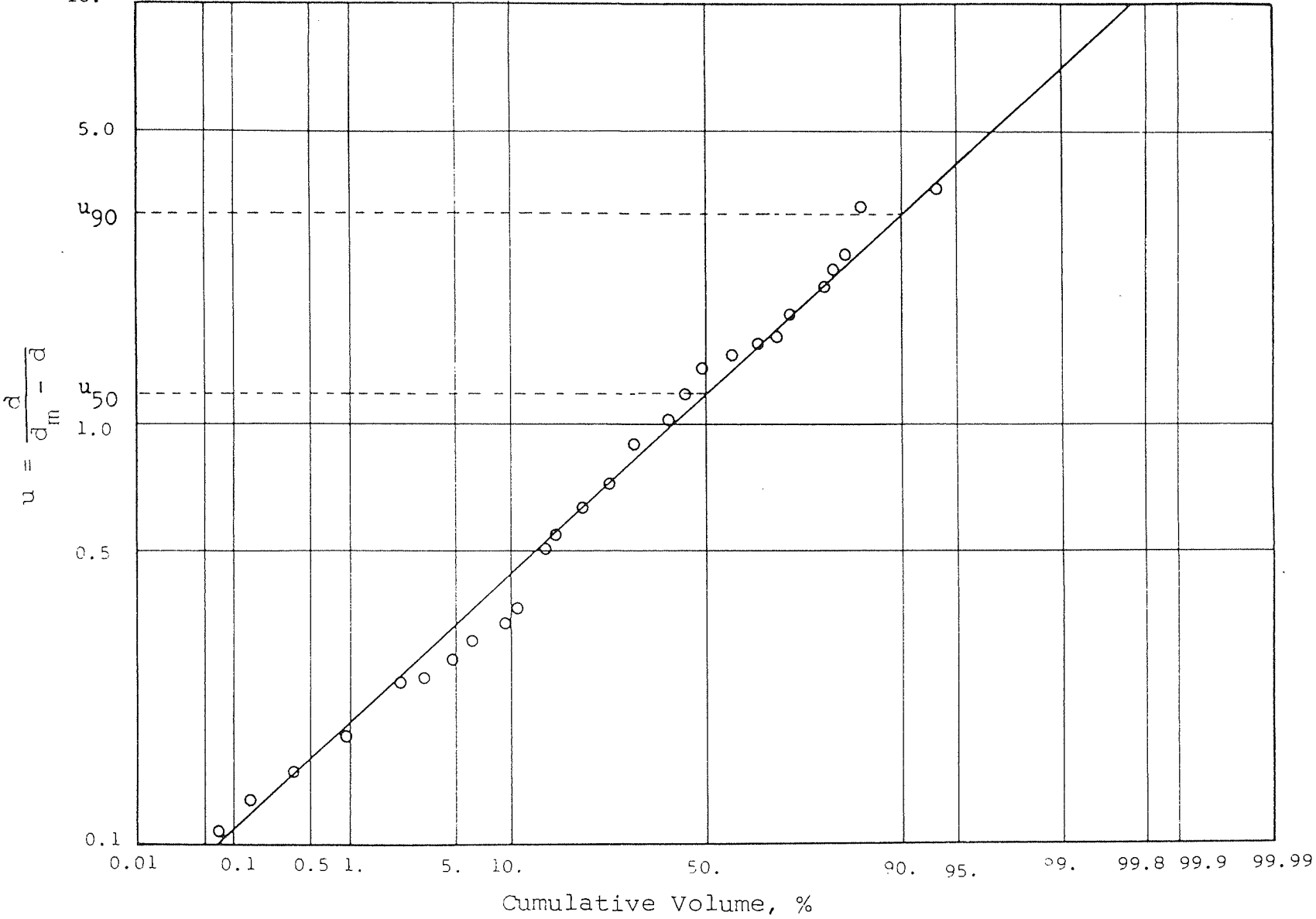

Figure IV.3 : Cumulative Drop Size Distribution for Rotor Speed 700 r.p.m. and Phase Ratio (C/D) = 2/1.

APPENDIX VI.2 Sample Calculation of d_{32}

Rotor Speed: 500 r.p.m.; Magnification: 2.5; Phase Ratio(C/D): 1/1

From Figure IV.4

$d_{10} = 1.86$, $d_{50} = 5.6$, $d_{90} = 7.95$

$$\frac{d_m}{d_{50}} = \frac{d_{50}(d_{90} + d_{10}) - 2d_{90}\, d_{10}}{d_{50}^2 - d_{90}\, d_{10}}$$

$$\frac{d_m}{5.6} = \frac{5.6(1.86 + 7.95) - 2(1.86)(7.95)}{(5.6)^2 - 1.86(7.95)}$$

$$d_m = 8.57$$

$$\bar{a} = \frac{d_m - d_{50}}{d_{50}} = \frac{8.57 - 5.6}{5.6} = 0.5304$$

From Figure IV.5

$u_{90} = 11.8 \quad u_{50} = 1.78$

$$\delta = \frac{0.394}{\log(u_{90}/u_{50})} = \frac{0.394}{\log(11.8/1.78)}$$

$$= 0.4796$$

$$d_{32} = d_m/(1 + \bar{a}\, e^{\frac{1}{4\delta^2}})$$

$$= 8.57/\left[1 + 0.5304\, e^{\frac{1}{4(0.4796)^2}}\right]$$

$$= 3.3312 \text{ mm}$$

Calculated $d_{32} = \frac{\Sigma n_i\, d_i^3}{\Sigma n_i\, d_i^2} = 3.284$ mm

Correlated (Equation 8.7) $d_{32} = 3.796$ mm

Table VI.2 Drop Size Distribution Results

	d_{obs} (mm)	d_{act} (mm)	n	v (mm^3)	v%	u	$\frac{dv}{dd}$ mm^{-1}
1	1.49	0.596	74	8.203	0.32	.0747	
2	2.04	0.816	120	34.139	1.32	.1052	.045
3	2.59	1.036	73	42.500	2.97	.1375	.075
4	3.14	1.256	36	37.350	4.42	.1717	.0659
5	3.70	1.48	36	61.110	6.79	.2088	.1058
6	4.25	1.7	28	72.030	9.58	.2475	.1268
7	4.8	1.92	16	59.300	11.88	.2887	.1086
8	5.35	2.14	12	61.577	14.27	.3328	.1332
9	5.90	2.36	11	75.705	17.20	.3800	.0477
10	6.46	2.58	3	27.102	18.25	.4317	.0814
11	7.01	2.80	4	46.173	20.04	.4863	.1532
12	7.56	3.02	6	86.875	23.41	.5453	.0314
13	8.11	3.24	1	17.875	24.10	.6091	.0382
14	8.66	3.46	1	21.764	24.94	.6784	.0927
15	9.22	3.69	2	52.529	26.98	.7554	.055
16	9.77	3.91	1	31.251	28.19	.8383	.1945
17	10.32	4.13	3	110.494	32.47	.9294	.1518
18	10.87	4.35	2	86.080	35.81	1.0299	.0877
19	11.42	4.57	1	49.909	37.74	1.1415	.2032
20	11.98	4.79	2	115.230	42.21	1.2685	.1159
21	12.53	5.01	1	65.922	44.76	1.4087	.3388
22	15.84	6.34	1	133.180	49.92	2.8364	.1434
23	16.94	6.78	1	162.900	56.23	3.7774	.3473
24	18.05	7.22	2	394.130	71.51	5.3489	.4145
25	19.15	7.66	2	470.670	89.75	8.4194	.0145
26	19.70	7.88	1	256.200	99.68	11.424	
					100.00		
Σ	-	-	-	476	2580.19	-	-	

* The corresponding drop size distribution curve has already been given on page 211 as Figure 8.13.

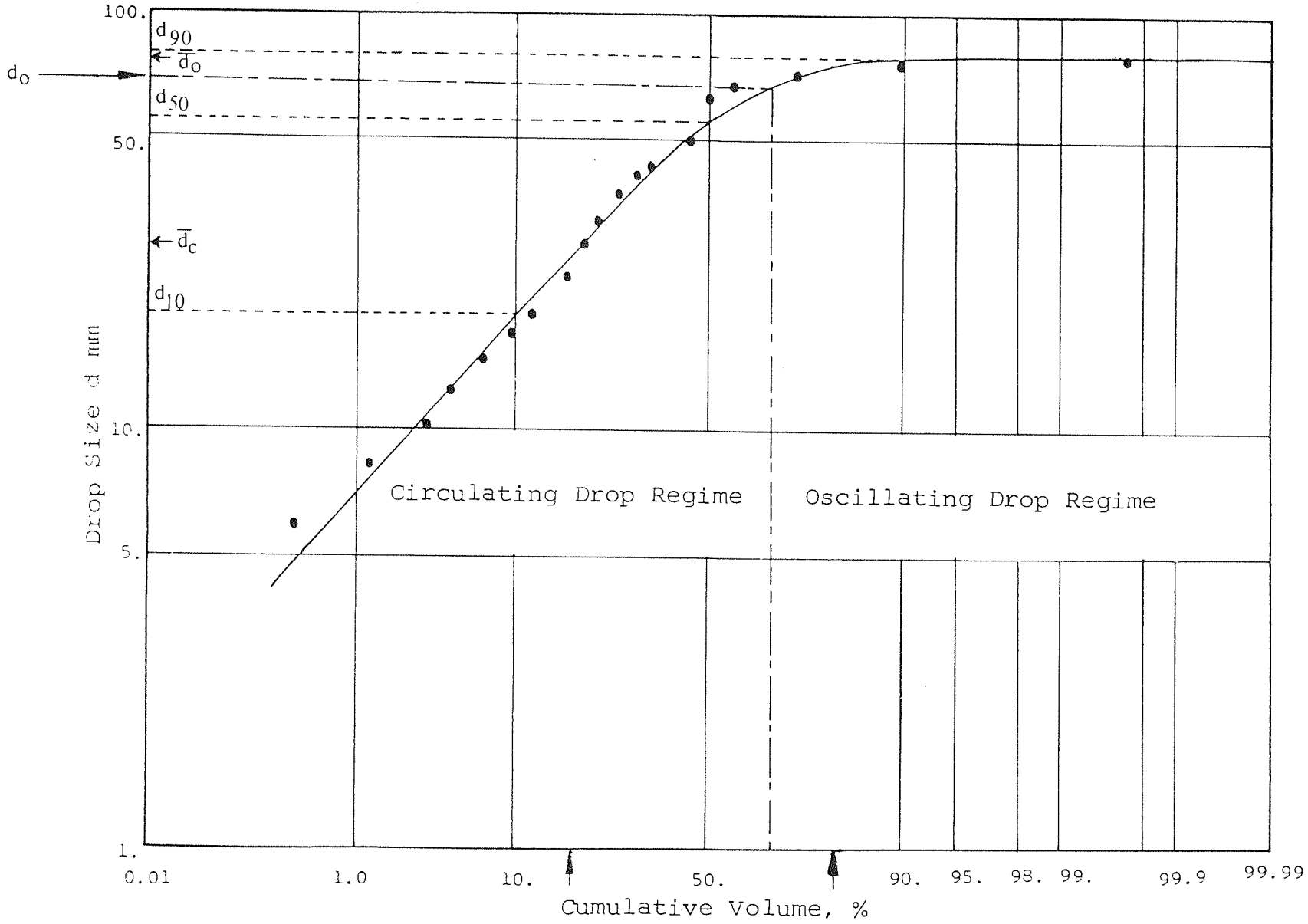

Figure IV.4: Cumulative Drop Size Distribution for Rotor Speed 500 r.p.m. and Phase Ratio 1/1.

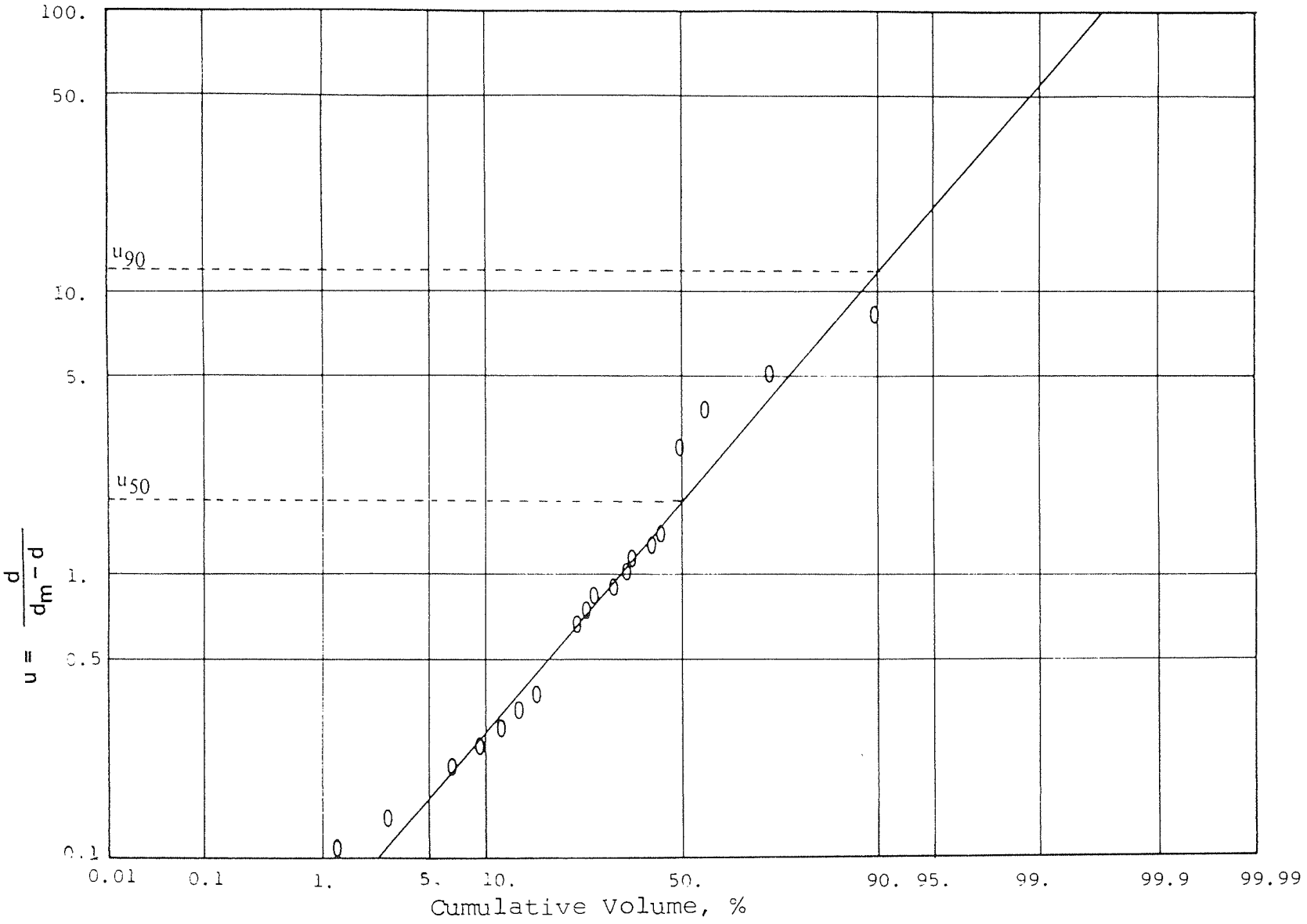

Figure VI.5 : Cumulative Drop Size Distribution for Rotor Speed 500 r.p.m. and Phase Ratio 1/1.

APPENDIX VII

Sample Calculation of i) Experimental Mass Transfer Coefficient

ii) Theoretical Mass Transfer Coefficient.

APPENDIX VII

a) Experimental mass transfer coefficient

The overall experimental dispersed phase mass transfer coefficient under each set of operating conditions was calculated using Equation:

$$N = K\ A\ \Delta C_m$$

Hold-up, X = 0.102

Sauter mean diameter = 0.3660 cm

Continuous phase velocity, V_c = 0.2759 cm/s

Dispersed phase velocity, V_d = 0.2759 cm/s

Rotor speed, N = 500 r.p.m.

Column cross-sectional area, A = 19.635 cm^2

Effective column height, H_E = 110 cm

The specific interfacial area, $a = \frac{6X}{d_{32}}$

$$a = \frac{6 \times 0.102}{0.3660}$$

$$= 1.6721\ cm^2/cm^3$$

Total interfacial area, A = a x V

where V is the effective column volume.

$$A = 1.6721 \times 110 \times 19.635$$

$$= 3611.49\ cm^2$$

Rate of mass transfer, $N = Q_c \rho_c (y_{out} - y_{in})$

$= Q_d \rho_d (x_{in} - x_{out})$

$N = 19.635 \times 0.2759 \times 0.998 \times (0.008 - 0.0)$

$= 0.0433$ gm/s

The mean driving force Δy_m was estimated by applying Simpson's rule as:

$$\Delta y_m = \frac{1}{18}\left[\Delta y_1 + 4\Delta y_2 + 2\Delta y_3 + 4y_4 + 2\Delta y_5 + 4\Delta y_6 + \Delta y_7\right]$$

$\Delta y_1 = .008$

$\Delta y_2 = .025$

$\Delta y_3 = .025$

$\Delta y_4 = .016$

$\Delta y_5 = .0080$

$\Delta y_6 = .0140$

$\Delta y_7 = .0065$

$$\Delta y_m = \frac{1}{18}\left[0.171\right] = .0095$$

$$\Delta C_m = \frac{0.0095}{\rho_c} = \frac{0.0095}{0.998} = .0095$$

$$\therefore K_{exp} = \frac{N}{A\Delta C_m}$$

$$= \frac{.0433}{3611.49 \times .0095}$$

$$= 1.26 \times 10^{-3} \text{ cm/s}$$

b) Theoretical overall mass transfer coefficient

The vertical relative velocity of drops of V_o in the R.D.C. was determined by applying Misek's equation (152):

$$V_o = \left[\frac{V_d}{X} + \frac{V_c}{(1-X)} \right]$$

$$= \left[\frac{0.276}{0.102} + \frac{0.276}{(1-0.102)} \right]$$

$$= 3.013 \text{ cm/s}$$

The maximum diameter of the stagnant drops in the whole drop population when droplet Reynold number, Re = 10 was found from.

$$\frac{d_s \rho_c V_o}{\mu_c} = 10$$

$$\therefore \quad d_s = \frac{10 \times 0.01003}{0.998 \times 3.013} = 0.033 \text{ cm}$$

The maximum diameter of the oscillating drops regime when Re = 200 was

$$d_o = \frac{200 \times 0.01003}{0.998 \times 3.013} = 0.667 \text{ cm}$$

The drop size distribution diagram of Figure VI.4 shows that d_s is too small to be included in the calculation. Hence the drop population is considered to contain only circulating and oscillating drops, with d_o the boundary between the two regimes. Therefore, from the drop size distribution diagram, the fractional proportion of circulating drops $\nu = 0.63$, and the oscillating drops fractional proportion = $(1-\nu) = 0.37$.

1) Circulating drops regime

a) A dispersed phase mass transfer coefficient was estimated by the Kronig and Brink (129) equation

$$k_{d.c} \cong \frac{17.9\ Dd}{\bar{d}_c}$$

where $\bar{d}_c$ is the circulating drop mid-sector diameter and D_d is the molecular diffusion of acetone in the dispersed phase.

$$k_{d.c} = \frac{17.9 \times 2.70 \times 10^{-5}}{0.38} = 1.27 \times 10^{-3}\ cm/s$$

b) Continuous phase mass transfer coefficient was estimated by Garner et al (133) correlation

$$\frac{k_{c.c}\ \bar{d}_c}{D_c} = -126 + 1.8\ Re^{0.5}\ Sc^{0.42}$$

$D_c = 1.11 \times 10^{-5}\ cm^2/s$ for diffusion of acetone in water.

$$k_{c.c} = \frac{1.11 \times 10^{-5}}{0.38}\left[-126+1.8\left(\frac{0.38\times0.998\times3.013}{0.01003}\right)^{0.5}\left(\frac{0.01003}{0.998\times1.11\times10^{-5}}\right)^{0.42}\right]$$

$$k_{c.c} = 6.12 \times 10^{-3} \text{ cm/s}$$

c) Overall mass transfer coefficient of the circulating drops.

$$\frac{1}{K_{o.c}} = \frac{1}{k_{d.c}} + \frac{m}{k_{c.c}}$$

$$= \frac{1}{1.27 \times 10^{-3}} + \frac{1.11}{6.12 \times 10^{-3}}$$

$$K_{o.c} = 1.032 \times 10^{-3} \text{ cm/s}$$

2) Oscillating drop regime

a) Dispersed phase mass transfer was firstly estimated by Rose and Kintner (131) equation.

$$k_{d.o} = 0.45 (D_d \omega)^{0.5}$$

where

$$\omega^2 = \frac{\sigma b}{r^3} \left[\frac{n(n-1)(n+1)(n+2)}{(n+1)\rho_d + n \rho_c} \right]$$

$$n = 2 \text{ and } b = \frac{\bar{d}_o^{\,0.225}}{1.242}$$

$\bar{d}_o = 0.7$ cm from drop size distribution diagram Figure Vl.4

$$b = \frac{(0.7)^{0.225}}{1.242} = 0.743$$

$$r = \frac{0.7}{2} = 0.35 \text{ cm}$$

σ = 28.4 dyne/cm or mN/m

$$\omega^2 = \frac{28.4 \times 0.743}{(0.35)^3} \left[\frac{2(2-1)(2+1)(2+2)}{(2+1)0.867+(2x0.998)}\right]$$

$$\omega^2 = 2569.4 \text{ 1/s}$$

$$\omega = 50.69 \text{ 1/s}$$

$$\therefore k_{d.o} = 0.45 (2.70 \times 10^{-5} \times 50.69)^{0.5}$$

$$= 1.665 \times 10^{-2} \text{ cm/s}$$

Secondly, by Angelo et al (115) Equation

$$k_{d.o} = \sqrt{\frac{4D_d\omega(1+\varepsilon+\frac{3}{8}\varepsilon^2)}{\pi}}$$

where $\varepsilon = 0.434 \left[(\frac{\omega\bar{d}_o}{V_o})^{-0.46} (\frac{\bar{d}_o V_o^3 \rho_c}{\sigma})^{-0.53} (\frac{\mu V_o}{\sigma})^{-0.11}\right]$

$$= 0.434 \left[(\frac{50.69x0.7}{3.013})^{-0.46} (\frac{0.7x(3.013)^3x0.998}{28.4})^{-0.53} (\frac{0.01003x3.013}{28.4})^{-0.11}\right]$$

$$= 0.3656$$

$$k_{d.o} = \sqrt{\frac{4x2.7x10^{-5}x50.69(1+0.366+\frac{3}{8}x(0.366)^2}{\pi}}$$

$$= 4.968 \times 10^{-2} \text{ cm/s}$$

b) Continuous phase mass transfer coefficient was estimated by Garner et al (133) correlation:

$$\frac{k_{c.o}\bar{d}_o}{D_c} = 50 + 0.0085 \text{ Re } Sc^{0.7}$$

$$k_{c.o} = \frac{1.11x10^{-5}}{0.7}\left[50 + 0.0085\left(\frac{0.7x0.998x3.013}{0.1003}\right)\left(\frac{0.01003}{0.998 \times 1.11 \times 10^{-5}}\right)^{0.7}\right]$$

$$= 4.11 \times 10^{-3} \text{ cm/s}$$

c) The overall mass transfer coefficient of oscillating drops:

Firstly, for Rose and Kintner (131) and Garner et al (133):

$$\frac{1}{K_{o.o}} = \frac{1}{k_{d.o}} + \frac{m}{k_{c.o}}$$

$$= \frac{1}{4.968 \times 10^{-2}} + \frac{1.11}{4.11 \times 10^{-3}}$$

$$K_{o.o} = 3.446 \times 10^{-3} \text{ cm/s}$$

Secondly, by Angelo et al (115) equation:

$$K_{o.o} = k_{d.o} \left[\frac{1}{1+m \sqrt{\frac{D_d}{D_c}}} \right]$$

$$= 4.968 \times 10^{-2} \left[\frac{1}{1+1.11 \sqrt{\frac{2.70 \times 10^{-5}}{1.11 \times 10^{-5}}}} \right]$$

$$= 1.819 \times 10^{-2} \text{ cm/s}$$

So, the theoretical overall mass transfer coefficient for the whole drop population:

$$K_{cal} = K_{o.c} \, \nu + k_{o.o} \, (1-\nu)$$

1) $K_{cal} = 1.032 \times 10^{-3} \, (0.63) + 3.45 \times 10^{-3} \times (1-0.63)$

$$= 1.927 \times 10^{-3} \text{ cm/s}$$

2) $K_{cal} = 1.032 \times 10^{-3} \, (0.63) + 1.819 \times 10^{-2} \, (1-0.63)$

$$= 1.32 \times 10^{-3} \text{ cm/s}$$

This compares favourably with 1.26×10^{-3} cm/s obtained experimentally.

NOMENCLATURE

A	Parameter for general activity coefficient equation and the various excess Gibbs energy
A	Total interfacial area, cm^2
A	Surface area of an oscillating drop, cm^2
A_n	Eigenvalue in Equation (5.12) and (5.15)
A_o	Initial surface area of an oscillating drop, cm^2
a	Interacting parameters of the components as given in Equation (5.11)
a	Activity referred to pure component
a	Interfacial area per unit column volume, (cm^2/cm^3)
a_o	Initial radius or half axis length
a'	Distribution parameter
a_p	Amplitude
a',b'	Constants in Equation (4.11)
B	Constant as defined in the various excess Gibbs energy and activity coefficient relationships
ΔC	Concentration driving force, gm/cm^3
C	Solute concentrations, gm/cm^3
C_1, C_2	Constants
C_R	Constriction factor
CST	Critical solution temperature
D	Molecular Diffusivity, cm^2/sec
D_c	Column diameter, cm

D_s	Stator ring opening, cm
D_R	Rotor disc opening, cm
ΔD	Distance between agitator and column wall $D_C - D_R/2$, cm
d	Diameter of drop, cm
d_{gm}	Geometric mean diameter, cm
d_{max}, d_m	Diameter of maximum stable drop size, cm
d_o	Mean drop diameter, cm
d_{vs}	Diameter of fictitious spheres, cm
d_{12}	Surface mean diameter, cm
d_{32}	Sauter mean diameter, cm
d_{10}	Drop diameter at 10% cumulative drops volume, cm
d_{50}	Drop diameter at 50% cumulative drop volume, cm
d_{90}	Drop diameter at 90% cumulative drop volume, cm
E	Extract phase volumetric flowrate
E	Eddy diffusivity
E	Energy
E	Axial mixing coefficients, cm^2/s
E_f	Mass transfer efficiency
E_m	Extraction efficiency
e	Exponential
F	Feed volumetric flowrate
F	Harkins Brown correction factor in Equation (5.9)
F	Objective function or residual
F_B	Superficial flowrate of interstage mixing per unit cross sectional area of column, cm/s
f	Fugacity
f	Mean actual interstage mixing per unit area of stator opening

G	Flowrate of the phase, gm mol/cm^2h
G	Molar Gibbs energy
ΔG	Molar Gibbs energy of mixing
G^E	Excess Gibbs energy
g, g_c	Acceleration due to gravity, cm/sec^2
H	Compartment height, cm
H_c	Overall column height, cm
H_E	Effective column height, cm
H.T.U.	Height of transfer unit, cm
h	Column height at certain point, cm
h_f	Dispersed phase hold-up at flooding
K	Distributuion coefficient
K	Overall mass transfer coefficient, cm/s
K_{cal}	Overall theoretical mass transfer coefficient, cm/s
K_{df}	Mass tranfser coefficient during drop formation, cm/s
K_{exp}	Overall experimental mass transfer coefficient, cm/s
$K_{o.c}$	Overall mass transfer coefficient of circulating drop, cm/s
$K_{o.o}$	Overall mass transfer coefficient of oscillating drop, cm/s
K_a	Overall mass volumetric mass transfer coefficient, l/s
K_1, K_2, K_3, K_4	Geometric factor (constants)
k	Individual mass transfer coefficient, cm/s
k_c	Continuous phase mass transfer coefficient, cm/s
$k_{c.c}$	Continuous mass transfer coefficient of circulating drop, cm/s

$k_{c.o}$	Continuous mass transfer coefficient of oscillating drop, cm/s
k_d	Dispersed phase mass transfer coefficient, cm/s
$k_{d.c}$	Dispersed phase mass transfer coefficient of circulating drop, cm/s
$k_{d.o}$	Dispersed phase mass transfer coefficient of oscillating drop, cm/s
L	$\frac{V_d}{V_c}$ ratio of the superficial velocity of dispersed phase to superficial velocity of continuous phase under flooding condition
L	Characteristic dimension of turbulence, cm
m	Distribution coefficient of a solute between two liquid phases
N	Speed of rotation of the central disc, r.p.m.
N	Rate of mass transfer, gm/s
N_c	Total number of compartment
N.T.U.	Number of transfer unit
n	Number of moles
n	Compartment number
P	Total pressure, atm
Pe	Peclet number
P_n	Power input per compartment
P_i^o	Pure component vapour pressure
p	Partial pressure of a component of a solution, atm
p	Plait point
Q	Volumetric flow rate, cm^3/s
Q	Excess free energy of mixing
R	Raffinate volumetric flowrate, cm^3/s
R	Disc diameter, cm

	Universal gas constant
	Parameter for general activity coefficient equation
	Radius of sphere of volume equal to that of a drop, cm
	Initial radius of a drop
	Stable drop radius, cm
	Reynold's number
	Stator ring opening, cm
	Solvent volumetric flowrate
	Distance between the centres of the drops in Equation (5.7)
	Fractional rate of renewal
	Parameter for general activity coefficient equation
Sc	Schidmt number
Sh	Sherwood number
S_w	Specific surface, cm
$\bar{S}_w$	Average specific surface, cm
T	Absolute temperature, ^oC
t	Time, second
t_c	Penetration time, second
t_f	Formation time, second
t_1, t_2, t_3, t_4	Temperatures at which isothermals are indicated
	NRTL or UNIQUAC parameter
U_N	Dispersed phase average velocity through the nozzle in Equation (5.10), cm/s
V	Molar volume
V	Parameter for general activity coefficient equation

V	Phase superficial velocity, cm/s
V_F	Drop volume after break off from the nozzle in Equation (5.14), cm^3
$V_N, \bar{V}_N$	Characteristic velocity, cm/s
V_o	Vertical relative velocity of drops, cm/s
V_s	Slip velocity, cm/s
V_t	Terminal velocity, cm/s
W	Objective function weighting factor
X	Composition of components expressed in weight fraction units
X	Dispersed phase hold-up
X_f	Dispersed phase hold-up at flooding point
x'	Point hold-up
x	Distance, cm
$x, \bar{x}, x, y$	Mole fraction of a component in the two non-consolute phases
Y, y	Solute concentration in the extract phase, gm/100 g
Δy_m	Actual mean concentration driving force, gm/100 gm
y_i	Weight fraction of particles with diameter, d_i
y_o	Phase boundary
Z	Effective volume fraction of the individual component
Z	Coalescence component
z	Overall composition, mole fraction
Σ	Power input per unit mass

Greek Letters

α	Constant in Equation (5.14)
α	Back mixing correlation factor
α	Back flow coefficient
α	Parameter for NRTL equation
β	Selectivity or separation factor
γ	Activity coefficient referred to pure component
γ	Surface tension, dyne/cm
δ	Uniformity distribution parameter
∂	Partial differential
$\varepsilon, \bar{\varepsilon}$	Energy input per unit mass and time, erg/gms
π	Total pressure
τ	Parameter for NRTL equation
ε	Amplitude of oscillation
ε_o	Function of amplitude of oscillation defined by Equation (5.14)
λ_n	Eigen value in Equation (5.12) and (5.13)
μ	Viscosity, gm/cms
μ	Chemical potential
ν	Kinematic viscosity, cm^2/s
ν	Cumulative volume of drops, cm^3
ρ	Density, gm/cm^3
ρ_m	Mean density = $\rho_d x + \rho_c (1-x)$, gm/cm^3
$\Delta\rho$	Density difference, gm/cm^3
σ	Interfacial tension, dyne/cm
τ	NRTL or UNIQUAC parameter
τ	Dimensionless time
τ	Parameter for NRTL equation

ψ	Coalescence frequency
ψ	Fractional hold-up of dispersed phase in Equation (5.17)
ω	Frequency of oscillation, 1/s
π	Constant = 3.1416

Subscripts

A	refers to phase A
A,B,C	Components, i.e. diluent, solvent, solute respectively
AA	Diluent A in diluent-phase A
AB	Diluent A in solvent-phase B
a	Apparent
av	Average
BA	SOlvent B in diluent-phase A
BB	solvent B in solvent-phase B
C	Column
c	Continuous phase
c	Circulating drop
CA	solute C in diluent-phase A
cri	Critical
cal	Calculated or theoretical
CB	solute C in solvent- phase B
d	Drop
d	Dispersed phase
E	Effective
E	Extract phase
E	Efficiency
Exp	Experimental

F	Feed
f	Flooding condition
f	Drop formation
i	Initial
i	ith stage
i,j,k	Any component of a mixture
m	Measured
m,max	maximum
mix	Mixture of the consolute phase
N	Nozzle
n	Nth stage
o	Initial
o	Oscillating drop
o	Overall
p	Plug flow condition
R	Raffinate phase
R	Drop release
r	Rotating disc
s	Stagnant drop
s	Stator opening
s	Slip
s.d	Stable drop
T	Top of column
T	Total
t	true
T,P	At conditions of constant temperature and pressure
v_g	Geometric mean
vs	Sauter mean volume to surface ratio of droplets

∞	Infinite dilution property
1,2,3	Pure components 1,2,3 respectively
11,12,13	Interaction of component 1 in 1, 1 in 2 and 1 in 3
111,112,113	Interaction parameter suffixes to represent the component species taking part in the interaction

Superscripts

E	Excess
E	Extract phase
R	Raffinate phase
o	Standard state
'	Compositions expressed on binary basis
-	Mean or average
I,II	Phases

Dimensionless Groups

Fr	Froude number $\frac{V_c^2}{g_c D_c}$
Fr	Modified Froude number $\frac{V_d^2}{g_c D_c X^2}$
G_a	Galiko number $\frac{d^3 \rho^2 g}{\mu^2}$
N_p	Power number $\frac{p}{N^3 D^5 \rho}$
$(Pe)_c$	Peclet number $\frac{V_c H}{E_c}$ for continuous phase
$(Pe)_d$	Peclet number $\frac{V_d H}{E_d}$ for dispersed phase
Re	Disc Reynolds number $\frac{D_r^2 N \rho}{\mu}$

Re	Droplet Reynolds number $\frac{dV_o\rho}{\mu}$
Re	Column Reynolds number $\frac{V_d H\rho_c}{\mu_x}$
Sc	Schmidt number $\frac{\mu}{\rho D}$
Sh	Sherwood number $\frac{kd}{D}$
We	Disc Weber number $\frac{N^2 Dr^3 \rho_c}{\sigma}$
We	Droplet Weber number $\frac{dV_o^2 \rho_c}{\sigma}$

REFERENCES

AL AL-SAADI,A.N.,'Study of liquid-liquid extraction with
si simultaneous chemical reaction',Ph.D Thesis,University
of of Aston in Birmingham,U.K(1978).

CH CH. 6,TecQuipment Ltd.(1980).

SM SMITH,S.A. and FUNK,J.E.,Petroleum Refiner,30 (9),(1951).

SM SMITH,S.A. and FUNK,J.E.,Petroleum Refiner,39 (9),(1960).

VC VON BERG,R.L. and WIEGANT,H.F.,Chemical Engineering
Re Report,59(6),189(1952).

6) DAVIES,G.A.,'Choices of Solvents in Liquid-Liquid Extraction'
2nd Solvent Symposium (held at) UMIST,Manchester(1977).

7) OBERG,T.,Chem. Eng.,70(7),119(1963).

8) FRANCIS,A.W.,J.Phys. Chem.,58,1099(1954).

9) SAAL,R.N.J. and VAN DYCK,W.J.D.,Proc. World Petroleum
Cong.(London),11,352(1933).

10) a) SMITH,J.C.,J. Phys. Chem.,46,376(1942).
b) SMITH,J.C.,Industr. Engng. Chem.,42,1206(1950).

11) CUMMING,A.P.C. and MORTON,F.,J. Appl. Chem.,3,358(1953).

12) CREMER,H.W. and DAVIES,T.,Chemical Engineering Practice,
Vol. 5,Butterworths Scientific Publications,London(1958).

13) FRANCIS,A.W.,Industr. Engng. Chem.,45(12),2789(1953).

4) FRANCIS,A.W.,Industr. Engng. Chem.,45(12),2789(1953).

5) FRANCIS,A.W.,Industr. Engng. Chem.,46(1),205(1954).

6) BENEDICT,M.,Chem. Engng. Prog.,43,41(1947).

7) VARTERESSIAN,K.A. and FENSKE,M.R.,Industr. Engng. Chem., 28(11),1352(1936).

8) FERRIS,S.W.,Science of Petroleum,Vol. III,Oxford University Press(1938).

9) HUNTER,T.G.,Pet. Refiner,34,963(1942).

20) ALDERS,L.,Appl. Sci. Res.,the Hague,A4,171(1954).

21) CARLSON,H.C. and COLBURN,A.P.,Industr. Engng. Chem. (Industr.),32,581(1942).

22) TREYBAL,R.E.,Industr. Engng. Chem.,36,875(1944).

23) EERBECK,C.D.F.,Rec. Trav. Chim. Pays-Bas,72,5(1953).

24) TREYBAL,R.E.,'Liquid-Liquid Extraction',1st. Edn.,McGraw Hill Inc.,New York(1951).

25) GLASSTONE,S.,'Physical Chemistry',2nd. Edn.,van Nostrand, New York(1947).

26) SMITH,J.M.,'Introduction to Chemical Engineering Thermodynamics',McGraw Hill Inc.,New York(1949).

27) STRICKLAND - CONSTABLE,R.F.,Chem. Engng. Practice,Vol. IV, Butterworth,London (1957).

28) SETSCHENOV,J.,Z. Physik Chem.,4,117(1889).

29) SWABB,L.E. and MORGAN,E.L.,Chem. Eng. Progr. Symp. Ser., 48(3),40(1954).

30) WHITEHEAD,K.E. and GEANKOPLIS,C.J.,Ind. Eng. Chem., 47,2114(1955).

31) LUMB,E.C. and WINDSOR,P.A.,Ind. Eng. Chem.,45,1086(1953).

32) PAULING,L.,'The Nature of the Chemical Bond',Oxford University Press(1948).

33) EWELL,R.H.,HARRISON,J.M. and BERG,L.,Industr. Engng. Chem. (Industr.),36,871(1944).

34) PARIS,A.,Industr. chim.,40,97(1953).

35) SAUNDERS,K.W.,Industr. Engng. Chem.,43(1),121(1951).

36) PERRY,R.H.,'Chemical Engineering Handbook',5th. Edn., McGraw Hill Inc.,New York(1973).

37) KOBE,K.A. and MCKETTLE,J.,'Advances in Petroleum Chemistr and Refining',Vol. 1,p. 475,Interscience Pub. Inc.,New York(1958).

38) Oil Gas Journal,No. 45,20(1952).

39) GILMONT,R.,ZUDKEVICH,D. and OTHMER,D.F.,Ind. Eng. Chem., 53,223(1961).

40) ROBBINS,L.A. in 'Handbook of Separation Techniques for Chemical Engineers',(Section 1.9),Edited by Schweitzer,P McGraw Hill Inc.(1979).

41) HORSLEY,L.H.,'Azeotropic Data III',American Chemical Soc Washington D.C (1973).

42) LEO,A.,HANSCH,C. and ELKINS,D.,Chem. Rev.,71(6),525(1971

43) FRANCIS,A.W.,'Liquid - Liquid Equilibriums',Wiley-Inters New York(1963).

44) HILDEBRAND,J.H.,'Solubility of Non-Electrolytes',Ch. IX, Reinhold Publishing Corp.(1936).

45) MIYAUCHI,T.,A.I.Ch. E. Jl.,12.508 (1966).

46) MUMFORD,C.J.,Brit. Chem. Eng.,13(7),981(1968).

47) LOGSDAIL,D.H. and LOWES,L.,Ch. 5,'Recent Advances in Liquid - Liquid Extraction',Ed. HANSON,C.,Pergamon Press (1971).

48) MORELLO,V.S. and POFFENBERGER,N.,Ind. Eng. Chem.,42, 1021(1950).

49) SHERWOOD,T.K. and PIGFORD,R.L.,'Absorption and Extraction' 2nd. edn.,McGraw Hill Inc.,New York (1952).

50) TREYBAL,R.E.,Ind. Eng. Chem.,44,53-63(1952).

51) SARKAR,S.,'Liquid -Liquid Extraction with Chemical Reactic in Agitated Columns',Ph.D Thesis,University of Aston in Birmingham,U.K(1976).

52) YACU,W.A.,' Purification of Phosphoric Acid by Solvent Extraction',Ph.D Thesis,University of Aston in Birmingham U.K(1977).

53) HANSON,C.,Chem. Eng.,26(8),76(1968).

54) SKELLAND,A.H.P.,Ind. Eng. Chem.,53(10),799(1961).

55) WEHNER,J.F.,A.I.Ch.E.Jl.,9,406(1959).

56) CORNISH,R.E.,Ind. Eng. Chem.,26,397(1934).

57) HUNTER,T.G. and NASH,A.W.,Ind. Eng. Chem.,27,836(1935).

58) HUNTER,T.G. and NASH,A.W.,Soc. Chem. Ind.,53,95T(1934).

59) MALONEY,J.O. and SCHUBERT,A.E.,Trans. Am. Inst. Chem. Eng., 36,741(1940).

60) SHERWOOD,T.K.,Ind. Eng. Chem.,31,1114(1939).

61) VARTERESSIAN,K.A.,Ind. Eng. Chem.,29,270 (1937).

62) HIXSON,A.W.,Trans. Am. Inst. Chem. Eng.,37,927 (1941).

63) CANNON,M.R.,Ind. Eng. Chem.,28,1035 (1936).

64) ALDERS,L.,'Liquid-Liquid Extraction',Elsevier Publishing Company (1959).

65) THIELE,E.W.,Ind. Eng. Chem.,27,392 (1935).

66) PROCESS HANDBOOK,Petroleum Refiner,39 (9),2333(1960).

67) PASSINO,H.J.,Ind. Eng. Chem.,41,280 (1949).

68) HANSON,D.N.,DUFFIN,J.H. and SOMERVILLE,G.F.,'Computation of Multistage Separation Processes',p. 333,Reinhold Pub. Co.,New York (1962).

69) KIRK,R.E. and OTHMER,D.F.,'Encyclopaedia of Chemical Technology',Vol. 6,p. 138,Interscience Encyclopaedia Publisher,New York.

70) BRANCKER,A.V. and HUNTER,T.G.,Ind. Eng. Chem.,33,880(1941).

71) WOOD,J.T.,Trans. Inst. Chem. Eng.,36,382(1958).

72) JAMRACK,W.D.,'Rare Metal Extraction by Chemical Engineering Techniques',Pergamon Press Inc.,New York (1963).

73) AOYAMA,K.,Shoseki Giho,3,106-114(1959).

74) SOMEKH,G.S.,Hydrocarbon Proc. & Petr. Ref.,42(7)161(1963), 42(8)123(1963),42(9)201(1963),42(10)157(1963).

75) BIRAY,S.,'The Design of a High Pressure Solvent Extraction Process Using Liquid Ammonia as Solvent',Ph.D Thesis, University of Aston in Birmingham,U.K(1979).

76) SMITH,S.,Brit. Chem. Eng.,12(9),1361-3(1967).

77) SORENSON,J.M.,MAGNUSSEN,T.,RASMUSSEN,P. and FREDENSLUND,A., Fluid Phase Equilibria,3,47(1979).

78) HAND,D.B.,J. Phys. Chem.,34,1961 (1930).

79) BRANCKER,A.V.,HUNTER,T.G. and NASH,A.W.,Ind. Eng. Chem. Anal. Ed.,12(3),35(1940).

80) VOLD,R.D. and VOLD,M.J.,'Techniques of Organic Chemistry', (Ed. WEISSBERGER,A.),2nd. edn.,Vol.1,Interscience Publishers,New York(1949).

81) ZIMMERMAN,H.K.,Chem. Rev.,51,52(1952).

82) GLADEL,Y.L. and DURANDET,J.,J. Rev. Inst. Petrol.,9,221(195

83) PIEROTTI,G.J.,DEAL,C.H. and DERR,E.L.,Ind. Eng. Chem., 51(1),95-102(1959).

84) HILDEBRAND,J.H.,PRAUSNITZ,J.M. and SCOTT,R.L.,'Regular and Related Solutions',van Nostrand Reinhold,New York(1970)

85) REDLICH,O. and KISTER,A.T.,Ind. Eng. Chem.,40,341-345, (1948) & J. Chem. Phys.,15,849(1947).

86) RENON,H.M. and PRAUSNITZ,J.M.,J. Am. Inst. Chem. Engrs., 14(1),135(1968).

87) HIRANUMA,M.,J. Chem. Eng., Japan,8,69(1975).

88) SCHULTE,H.W.,Ph.D Thesis,University of Dartmund,Germany(196

89) ABRAMS,D.S. and PRAUSNITZ,J.M.,A.I.Ch.E.Jl.,21,116(1975).

90) WILSON,G.M. and DEAL,C.H.,Ind. Eng. Chem. Fundamentals, 1,20(1962).

91) SCHELLER,W.A.,Ind. Eng. Chem. Fundamentals,4,459 (1965).

92) RATCLIFFE,G.A. and CHAO,K.C.,Can. J. Chem. Eng.,47,148(1969

93) DERR,E.L. and DEAL,C.H.,'Distillation 1969',Sec. 3,p. 37, Brighton,U.K.,Int. Conf. Distillation(Sept. 1969).

94) FREDENSLUND,A.,JONES,R.L. and PRAUSNITZ,J.M.,A.I.Ch.E.Jl., 21,1086(1975).

95) LEE,T.W.,GREENKORN,R.A. and CHAO,K.C.,Ind. Eng. Chem. Fundamebtals,11,293(1972).

96) LO,H.S. and PAULAITIS,M.E.,A.I.Ch.E.Jl.,27(5),842-4(1981).

97) ECKERT,C.A.,HSIEH,C.K. and MCCABE,J.R.,A.I.Ch.E.Jl., 20(1),20(1974).

98) TARASENKOV,D.N. and PAULSEN,I.A.,Acta Physicochim.,USSR, 11,75(1939).

99) PILLOTON,R.L.,A.S.T.M. Spec. Tech. Pub..,238,5(1958).

100) CAMPBELL,J.A.,Ind. Eng. Chem.,36,1158(1944).

101) BRANCKER,A.V.,HUNTER,T.G. and NASH,A.W.,J. Inst. Pet., 28,15-26(1942).

102) BACHMAN,I.,Ind. Eng. Anal. Ed.,12(3)38(1940).

103) OTHMER,D.F. and TOBIAS,P.E.,Ind. Eng. Chem.,34(6)693(1942)

104) ISHIDA,K.,Bull. Chem. Soc. Japan,33,393 (1960).

105) WHITMAN,W.G.,Chem. Met. Engr.,29.146 (1923).

106) NERNST,W.,Z. Phys. Chem.,47,52(1904).

107) HIGBIE,R.,Trans. Am. Inst. Chem. Eng. J.,31,365 (1935).

108) DANCKWERTS,P.V.,Ind. Eng. Chem.,43,1460 (1951).

109) LAMONT,J.C. and SCOTT,D.S.,A.I.Ch.E.Jl.,16,513(1970).

110) SHERWOOD,T.K.,PIGFORD,R.L. and WILKE,C.R.,'Mass Transfer', McGraw Hill Inc. (1975).

111) SKELLAND,A.H.P.,'Diffusional Mass Transfer',John Wiley Int. (1974).

112) SCRIVEN,L.E.,Chem. Engr. Educ.,2,150(Fall 1968),26(Winter 1969),94(Spring 1969).

113) WEST,F.P.,Ind. Eng. Chem.,43,234(1951) & 44,625(1952).

114) STRAND,C.P.,OLNEY,R.B. and ACKERMAN,G.H.,A.I.Ch.E.Jl., 8 (5) ,252-261 (1962).

115) ANGELO,J.B.,LIGHTFOOT,E.N. and HOWARD,D.W.,A.I.Ch.E.Jl., 12,751 (1966).

116) LITCHT,W. and PENSING,W.F.,Ind. Eng. Chem.,45,1885 (1953).

117) HEERTJES,P.M. and HOLVE,W.A.,Chem. Eng. Sci.,3,122 (1954).

118) SKELLAND,A.H.P. and MINHAS,S.S.,A.L.Ch.E.Jl.,17,1316(1971).

119) OLNEY,R.B.,A.I.Ch.E.Jl.,10(6),827(1964).

120) HEERTJES,P.M. and de NIE,L.H.,Chem. Eng. Sci.,26,697(1971).

121) JOHNSON,A.I. and HAMIELEC,A.E.,A.I.Ch.E.Jl.,6,145(1960).

122) MARSH,B.D. and HEIDEGER,W.J.,Ind. Eng. Chem. Fundamentals 4,129 (1965).

123) POPOVICH,A.T.,Chem. Eng. Sci.,19,357 (1964).

124) LICHT,W. and CONWAY,J.B.,Ind. Eng. Chem.,47,1151 (1950).

125) HEERTJS,P.M. and de NIE,L.H.,Chem. Eng. Sci.,21,755 (1966).

126) GARNER,F.H. and SKELLAND,A.H.P.,I.E.C.,48,51 (1956).

127) LINTON,M. and SUTHERLAND,K.I.,Proc. 2nd. International Conference of Surface Technology.

128) NEWMAN,A.B.,Trans. Am. Inst. Chem. Engrs.,27,310 (1931).

129) KRONIG,R. and BRINK,J.C.,Appl. Sci. Res.,A2,142 (1960).

130) HANDLOS,A.E. and BARON,T.,A.I.Ch.E.Jl.,3,127(1957).

131) ROSE,P.M. and KINTER,R.C.,A.I. Ch.E.Jl.,12(5),530-4(1966).

132) BOUSSINESQU,J.J.,Math. Pure-appl.,60,285(1965).

133) GARNER,F.H. and TAYEBAN,M.,Anal. Renl. Soc. Estan. Fix. Quinn (Madrid),1356,479 (1960).

134) HARRIOT,P.,Can. J. Chem. Engng.,40,60 (1952).

135) HUGHMARK,G.A.,Ind. Engng. Chem. Funds.,6,408(1967).

136) GARNER,F.H.,FOORD,A.,TAYEBAN,M.,J. Appl. Chem.,9,313 (1959).

137) GAL - OR,B. and HOELSCHER,H.E.,A.I.Ch.E.Jl.,12,499 (1966).

138) COULSON,J.H. and SKINNER,S.J.,Chem. Eng. Sci.,1,1976(1951).

139) AL -GHABBAN,M.R.,'Solvent Extraction in Phosphoric Acid', Ph.D Thesis,University of Aston in Birmingham,U.K.(1981).

140) TRICE,V.C.Jr. and RODGER,W.A.,A.I.Ch.E.Jl.,2(2),205(1956).

141) ROOIJ-ABRAHM,H. and JAN-ELMENDORD,B.,U.S.Patent 3,363,978 (Jan. 16,1968).

142) SEIDLOVA,B. and MISEK,T.,Proceedings International Solvent Extraction Conference,Vol. 3,p. 2365 (1974).

143) SULLIVANCE,D.M. and LINDSEY,E.E.,Ind. Eng. Chem. Fund., 1,87 (1962).

144) HONEKAMP,J.R., Ph. D Dissertation,Iowa State University(1960)

145) MLYNEK,Y. and RESNICK,W.,A.I.Ch.E.Jl.,18(1).122(1972).

146) DALLAVALLE,J.M.,'Micrometrics,the Technology of Fine Particles',2nd. Edn.,Pitman Publishing Co.,New York (1948).

147) MUMFORD,C.J. and AL-HEMERI,A.A.,Proceed,ISEC,Lyon,2,1591 (1974).

148) MISEK,T. and MAREK,J.,Brit, Chem. Eng.,15,202 (1970).

149) MISEK,T.,Coll. Czech. Chem. Comm.,32,4018 (1967).

150) ROD,V.,Brit. Chem. Eng.,11 (6),483 (1966).

151) CHARTRES,R.H. and KORCHINSKY,W.J.,Trans. Inst. Chem. Engrs.,53,247 (1975).

152) MISEK,T.,'Rotating Disc Contactor',Statni Nakadatelstri Technicke Literatury,Prague (1964).

153) MUMFORD,C.J.,'Droplet Break - up and Coalescence in Rotary Agitated Column Extractors',Ph. D Thesis,University of Aston in Birmingham,U.K (1970).

154) JEFFREYS,G.V. and MUMFORD,C.J.,Proc. Int. Solvent Extn. Conf.,the Hague (ISEC),1,667 (1971).

155) THORNTON,J.D.,Ind. Chemist, (12),632-637(1963).

156) BLAZEJ,L.,VAJDA,M.,BAFRNCOVA,S. and HAVALDA,J.,Chem. Zvesti,32 (3),341 (1978).

157) AL - ASWAD,K.K.M.,'Liquid - Liquid Extraction in a Pilot Scale Rotating Disc Contactor',Ph. D Thesis,University of Aston in Birmingham,U.K (1982).

158) BOUYATIOTIS,B.A. and THORNTON,J.D.,Instn. Chem. Engrs. Symp. Series,No. 26 (1967).

159) CHEN,H.T. and MIDDLEMAN,S.,A.I.Ch.E.Jl.,13,989 (1967).

160) SPROW,F.B.,Chem. Eng. Sci.,22,435 (1967).

161) BROWN,D.E. and PITT,K.,Proc. Chemece '70,Butterworth, Australia (1970).

162) PEBALK,V.L. and MISHEW,V.M.,Tear. Osnovy. Khim. Tekhnol., 3,418 (1969).

163) GILES,J.G.,HANSON,C. and MARSLAND,J.,Proc. ISEC '74, the HAGUE (1971).

164) KORCHINSKY,W.J. and AZIMZADEH - KHATAYLO,S.,Chem. Eng. Sci., 31,871 (1976).

165) MUGELE,R.A. and EVANS,H.D.,Ind. Engng. Chem.,43,1317 (1951).

166) VERMIJS,H.J.A. and KRAMERS,H.,Chem. Eng. Sci.,3,55 (1954).

167) LEE,J.C. and LEWIS,G.,Instn. of Chem. Eng. Symposium on Extraction (1967).

168) LOGSDAIL,D.H.,THORNTON,J.D. and PRATT,H.R.C.,Trans. Instn. Chem. Eng.,35,301 (1957).

169) PIPER,H.B.,MSc Thesis,University of Manchester (1966).

170) SLATTER,M.A.,MSc Thesis,University of Aston in Birmingham, (October 1968).

171) 'Phase Separation Mechanisms in Continuous Flow Systems', Chem. Eng. Lab. Report,University of Aston in Birmingham, 1969.

172) de NIE,L.H.,Chem. & Proc. Eng.,50 (4),133 (1969).

173) DUNN,I.,LAPIDUS,L. and ELGIN,J.C.,A.I.Ch.E.Jl.,11(1),158 (1965).

174) DAVIES,J.T.,RITCHIE,J.M. and SOUTHWARD,D.C.,Trans. Instn. Chem. Eng.,38,331 (1960).

175) WILSON,M.P. - Private Communication,University of Aston in Birmingham (1981).

176) VERMUELEN,T.,WILLIAMS,G.M. and LANGLOIS,G.E.,Chem. Eng. Prog. 51 (2),85F (1955).

177) Discussion of Papers at 2nd. Session,Symposium on Surface Effects and Liquid Behaviour,Trans. Instn. Chem. Eng., 38,343 (1960).

178) REMAN,G.H. and VAN DER VUSSE,J.G.,Pet. Refiner,34 (9), 129 (1955).

179) MISEK,T. and ROZKOS,B.,Chem. Prum.,15 (8),450 (1965).

180) KOMOSAWA,I. and INGHAM,J.,Chem. Eng. Sci.,33,341 (1978).

181) KUNG,E.Y. and BECKMANN,R.G.,A.I.Ch.E.Jl.,7,319 (1961).

182) CHARTRES,R.H. and KORCHINSKY,W.J.,Trans. Inst. Chem. Eng., 56,91 (1978).

183) LADDHA,G.S.,DEGALEESAN,T.E. and KANNAPPAN,R.,Can. J. Chem. Eng.,56,137 (1978).

184) REMAN,G.H.,Proc. 3rd. World Petroleum Congress,the Hague, Section III,121 (1951),U.S. Patents 2,601,674 (1952), 2729 (1956) & 2,912,310 (1959).

185) BRINK,A.A. and GERICKE,J.J.,S.African Ind. Chemist, 18 (11),152 (1964).

186) KAGAN,S.Z.,TRUKHANOV,L.G.,KOSTIN,P.A. and KUDRYANSTEV,E.W., Int. Chem. Eng.,4,473 (1964).

187) THEYZE,V.G.,WALL,R.J.,TRAIN,K.E. and OLNEY,R.B.,Oil Gas Jl.,59,70 (1961).

188) CRONAN,C.S.,Chem. Eng.,65,54 (1958).

189) MARPLE,S.,TRAIN,K.E. and FOSTER,P.D.,Chem. Eng. Prog., 57,44 (1961).

190) MISEK,T. and ROZKOS,B.,Int. Chem. Eng.,6,130 (1966).

191) REMAN,G.H.,Joint Symposium - The Scaling-up of Chemical Plant and Processes,Instn. Chem. Engrs.,26, (1957), and Pet. Ref.,36 (9),269 (1967).

192) REMAN,G.H. and OLNEY,R.B.,Chem. Eng. Prog.,51,141 (1955).

193) Anon.,Pet. Processes,10,230 (1955).

194) MAREK,J.,MISEK,T. and WIDMER,F.,Paper presented at Soc. Chem. Ind. Symp.,Bradford,U.K. (1967).

195) REMAN,G.H.,Dutch Patent 70,866 (1952).

196) KRISHNAIAH,N.M.,Chem. Eng.,12,719 (1967).

197) GOUROJI,I.C.,NARULA,A.S. and PA,M.V.,Brit. Chem. Eng., 5,67 (1971).

198) SOKOV,Y.F. and PUTILOVA,A.S.,Trans. Vses. Nouchn. Tech. Soveshch Protsessy Zhidkostnoi Electraktsii i Khemostbtsii, 2nd. edn.,p. 228,Leinengrad (1966).

199) INGHAM,J.,Proc. ISEC (Soc. of Chem. Ind.,London(1974)), Vol. 3,p. 2365.

200) KUHNI,A.G.,VERFAHRENS,K.A.,Technik and Apparateban CH-4123, Allschwil - Basel,Switzerland.

201) THORNTON,J.D.,Chem. Eng. Prog. Symp. Ser. Nuclear Engineering,13,39 (1954),Chem. Eng. Sci.,5,201(1956).

202) REMAN,G.H.,Pet. Pro.,10 (2),230-2 (1955).

203) MISEK,T. ,Coll. Czech. Chem. Comm.,29,2086 (1964).

204) RESNICK,W.,Paper presentad at 3rd. Int. Congr. on Chem. Eng.,Marianske Lanze (1969).

205) ROD,V.,Brit. Chem. Eng.,16,617 (1971).

206) MURAKAMI,A.,MISONOV,A. and INOUE,E.L.,Int. Chem. Eng., 18,16 (1978).

207) JEFFREYS,G.V.,AL - ASWAD,K.K.M. and MUMFORD,C.J.,Paper presented in the 2nd. Symposium on Separation Science and Technology for Energy Application,Gatlinburg,Tenn.,USA, (May,1981).

208) WESTERTERP,K.R. and LANDSMAN,P.,Chem Eng. Sci.,17,363 (1962).

209) INGHAM,J.,'Recent Advances in Liquid - Liquid Extraction', Ch. 8,Ed. HANSON,C.,Pergamon Press (1971).

210) STAINTHORP,F.P. and SUDALL,N.,Trans. Int. Chem. Engrs., 42,T198 (1964).

211) MURAKAMI,A. and MISONUO,A.,Int. Chem. Engrs.,18(1),22(1978).

212) HINZE,J.O.,A.I.Ch.E.Jl.,1 (9),289 (1955).

213) OLIVER,E.D.,'Diffusional Separation Processes - Theory, Design and Evaluation',p. 383,John Wiley,New York (1966).

214) SCHLEICHER,C.A.,A.I.Ch.E.Jl.,5,145 (1959).

215) AL - HEMERI,A.A.A., 'The Effect of Surface Renewal on Mass Transfer in Agitated Contactor',Ph.D Thesis,University of Aston in Birmingham,U.K(1973).

216) GROOTHUIS,H. and KRAMERS,H.,Chem Eng. Sci.,4,17 (1955).

217) MIYAUCHI,T.,A.I.Ch.E.Jl.,12,508 (1966).

218) BRUIN,J.S.,Paper 100,ISEC '74,Lyon (1974).

219) STEMERDING,S.,Chemie Ingr. Tech.,35,844 (1963).

220) BORREL,A.,Paper 140,ISEC '74,Lyon (1974).

221) SAX,N.I.,'Dangerous Properties of Industrial Materials', van Nostrand,Reinhold (1979).

222) MUIR,G.D.,'Hazards in the Chemical Laboratory',2nd. edn., Royal Institute of Chemistry,London (1977).

223) HANDBOOK OF CHEMISTRY AND PHYSICS,53rd. edn.,CRC Press (197

224) SMITH,T.E. and BONNER,R.F.,Industr. Engng. Chem.,42 (5), 896 (1950),CH. 12,TecQuipment Ltd. (1980).

225) HONEKAMP,J.R. and BURKHART,L.E.,Ind. Eng. Chem.,Proc. Design and Dev.,1 (3),177 (1962).

226) HACKL,A.,SOLAR,W.,ZIEBLAND,G.,Institution fur Verfahrens-technik und Technologie der Brennstoffe,TH Wien (1975).

227) PANASONIC,V.,Chemical Dynamics Laboratory,B. Kidric Institute,Vinca - Beogard (1974).

228) BRANDT,H.W.,SCHROETER,J. and STRAUSS,G.,Ferbenfabriken Bayer,Leverkusen (1975),Bericht No. VT -40324.

229) 'Recommended Systems for Liquid Extraction Studies', ed. Misek,T.,European Federation of Chemical Engineering Working Party on Distillation,Absorption and Extraction, The Institution of Chemical Engineers (1978).

230) DAUPHIN,J., Bull. Soc. Chim., France,53 (1954).

231) WALTON,J.H. and JENKINS,J.D.,J. Am. Chem. Soc.,45,2555-6, (1923).

232) VERHOEYE,L.A., J. Chem. & Engng. Data,13,462 (1968).

233) KASATKIN,A.G., KAGAN,S.Z. and TRUKHANOV,V.E., J. Appl. Chem., (USSR),35,1903 (1962).

234) WASHBURN,E.R.,BROCKWAY,C.E.,GRAHAM,C.L. and DEMING,P.,J.Am. Chem. Soc.,64,1886 (1942).

235) HARTLEY,J.,J. S. C. I.,69 (2),60-61 (1950).

236) SORENSEN,J.M. and ARLT,W., 'Liquid-liquid Equilibrium Data Collection',Chemistry Data Series, Vol. V, Part 2, Published by DECHEMA (1978).

237) DANCKWERTS,P.V., Trans. Faraday Soc., 46,300 (1950).

238) CALDERBANK,P.H. and KORCHINSKI,I.J.O., Chem. Eng. Sci., 6 (6), 65-78 (1958).

239) ORYE,R.V ,Trans. Faraday Soc., 61,1338 (1965).

240) BEARE,W.G.,MC VICAR,G.A. and FERGUSON,J.B., J. Phys. Chem.,34,1310 (1930).

241) HALA, E., Ind. Eng. Chem, Process Des. Develop.,11,638 (1972)

242) AL-HASSAN,T.S.,'A Study of Mass Transfer from Large Oscillating Drops',Ph.D Thesis,University of Aston in Birmingham UK (1979).

Original References for Table 4.1.

MARGULES,M. ,Sitzber. Akad. Wiss. Wien. Math. Naturw. Klass(II), 104,1243 (1895).

VAN LAAR,J.J., Z. Physik. Chem., 72,723 (1910).

REDLICH,O. and KISTER,A.T., Ind. Eng. Chem., 40,345 (1948).

KRETSCHMER,C.B. and WIEBE,R., J. Chem. Phys., 22,1697 (1954).

BLACK,C., A.I.Ch.E.J., 5,249 (1959).

WILSON,G.M., J. Am. Chem. Soc., 86,127 (1964).

RENON,H. and PRAUSNITZ,J.M., A. I. Ch. E. J.,14,135 (1966).

HEIL,J.F. and PRAUSNITZ,J.M., A. I. Ch. E. J.,12,678 (1966).

ABRAMS,D.S. and PRAUSNITZ,J.M., A.I.Ch.E.J.,21,116 (1975).